



UCL

**THE BIOCHEMICAL INVESTIGATION OF GENETIC
DISORDERS RESPONSIVE TO VITAMIN B₆
SUPPLEMENTATION**

Thesis submitted for the degree of Doctor of Philosophy (PhD)

Matthew Wilson

University College London

March 2019

DECLARATION

I, Matthew Wilson confirm that the work presented in this thesis is my own. Where information has been derived from other sources, I confirm that this has been indicated in the thesis.

Signed.....

Date.....

ABSTRACT

The active form of vitamin B₆, pyridoxal 5'-phosphate (PLP), is a cofactor required for many essential functions such as the metabolism of amino acids and neurotransmitters, the one-carbon cycle, haem biosynthesis, glycogenolysis, and sphingolipid metabolism. Humans are not capable of *de novo* PLP synthesis but do have a pathway for the interconversion of B₆ vitamers. Several inborn errors of metabolism (IEMs) can lead to an insufficient supply of available PLP (e.g. pyridox(am)ine 5'-phosphate oxidase [PNPO], aldehyde dehydrogenase 7 family member A1 [ALDH7A1] and pyridoxal 5'-phosphate homeostasis protein [PLPHP] deficiencies). These disorders are typically characterised by neonatal/infantile-onset seizures refractive to standard anti-epileptic drugs but responsive to vitamin B₆ supplementation.

This thesis describes the investigation of B₆ vitamer measurement from dried blood spots (DBS) as a diagnostic method for the B₆-responsive epilepsies with a focus on PNPO deficiency. In addition, a diagnostic LC-MS/MS-based enzyme assay was developed for the measurement of PNPO activity from DBS. The biochemical effect of a novel IEM leading to pyridoxal kinase deficiency was also characterised using LC-MS/MS-based enzyme assays.

Some PNPO deficient individuals receiving high-dose PLP for seizure treatment develop signs of liver damage leading eventually to cirrhosis. The photodegradation profile of PLP was characterised in order to help elucidate the mechanism causing liver damage in these patients; hypotheses as to the cause of this phenomenon are discussed.

Vitamin B₆ has been reported as an effective anticonvulsant in genetic epilepsies other than those known to directly affect vitamin B₆ metabolism. Whole exome and whole genome sequencing data was used in order to investigate a genetic basis for vitamin B₆-responsive seizures in 5 children. In two of these individuals, variants affecting the ion channel KCNQ2 were identified. A response to B₆ supplementation in cases of KCNQ2-related epilepsy has also been documented in the literature. The mechanism behind this was investigated using electrophysiological techniques.

IMPACT STATEMENT

This thesis has developed new strategies for the diagnosis of vitamin B₆-responsive disorders and has further elucidated their biochemical mechanisms; this will aid clinical management and hence disease outcome. An emphasis was placed on the development of methods utilising mass spectrometry for the quantification of analytes of interest.

Firstly, the measurement of B₆ vitamers from dried blood spots (DBS) was assessed as an analytical method for the diagnosis of vitamin B₆-dependent disorders, in particular pyridox(am)ine 5'-phosphate oxidase (PNPO) deficiency. An enzyme assay for measuring PNPO activity from DBS was also developed. This will give clinicians a tool in order to rapidly diagnose patients with PNPO deficiency; a disorder associated with an improved outcome upon prompt and appropriate treatment with vitamin B₆ supplementation. Each of these methods were enabled by the availability of more sensitive modern LC-MS/MS instrumentation and this thesis is a good example of the application of this technology towards the diagnosis of inborn errors of metabolism.

We were also able to confirm the pathogenicity of a variant in the *PDXK* gene encoding pyridoxal kinase (PK) found in three siblings with childhood-onset peripheral neuropathy. This aided in the development of a successful treatment regime for two of these individuals. More broadly, this has implications within the field of genetic neuropathies if variants affecting PK are found to be a more common cause of this disorder.

As well as the diagnosis of patients with these disorders, the development of rapid LC-MS/MS-based enzyme assays for both pyridoxal kinase and PNPO activity from DBS will allow the screening of larger cohorts to detect treatable disorders at a pre-symptomatic or very early symptomatic stage. These could include neuropathy caused by *PDXK* mutations or a less severe presentation of PNPO deficiency caused by, for example, homozygosity for the p.R116Q variant in *PNPO*.

The photodegradation profiles and rates of photolysis were characterised from PLP preparations mimicking those given to B₆-dependent epilepsy patients receiving high dose PLP for seizure treatment. This was important in order to investigate the mechanism causing hepatic cirrhosis in these patients and to work towards a

formulation of pyridoxal 5'-phosphate that treats the seizure disorder effectively but does not cause liver damage.

Investigation was also carried out on the effect of B₆ vitamers upon KCNQ2/3 channels in a cell model. This work was valuable in order to investigate the anticonvulsant effect of vitamin B₆ in epilepsy caused by *KCNQ2* mutations and opens opportunities for further work in this field.

Away from the direct clinical implications of this thesis, important insight can be gained into the homeostasis of the B₆ vitamers. An example of this is the additional evidence that, in the blood, the phosphorylated B₆ vitamers are sequestered in red blood cells. This leads to further questions as to the transport of B₆ vitamers across the cell membrane. In addition, the discovery that a variant in *PDXK* leading to reduced PK activity causes neuropathy but not epilepsy raises several questions as to the mechanisms protecting the brain from PLP deficiency; for example, how the B₆ metabolic enzymes are regulated both pre and post-transcriptionally in a tissue-specific manner.

PUBLICATIONS

Some ideas, methodologies and figures appear in the following publications:

1. Darin N, Reid E, Prunetti L, Samuelsson L, Husain RA, **Wilson MP**, El Yacoubi B, Footitt E, Chong WK, Wilson LC, Prunty H, Pope S, Heales S, Lascelles K, Champion M, Wassmer E, Veggiotti P, de Crécy-Lagard V, Mills PB, Clayton PT (2016). Mutations in PROSC Disrupt Cellular Pyridoxal Phosphate Homeostasis and Cause Vitamin-B₆-Dependent Epilepsy. *Am J Hum Genet* 99(6): 1325-1337.
2. Mohamed-Ahmed AH*, **Wilson MP***, Albuera M, Chen T, Mills PB, Footitt EJ, Clayton PT, Tuleu C (2017). Quality and stability of extemporaneous pyridoxal phosphate preparations used in the treatment of paediatric epilepsy. *J Pharm Pharmacol* 69(4): 480-488. ***Joint first authors**
3. **Wilson MP**, Footitt EJ, Papandreou A, Uudelepp ML, Pressler R, Stevenson DC, Gabriel C, McSweeney M, Baggot M, Burke D, Stödberg T, Riney K, Schiff M, Heales SJR, Mills KA, Gissen P, Clayton PT, Mills PB (2017). An LC-MS/MS-Based Method for the Quantification of Pyridox(am)ine 5'-Phosphate Oxidase Activity in Dried Blood Spots from Patients with Epilepsy. *Anal Chem* 89(17): 8892-8900.
4. Scott TA, Quintaneiro LM, Norvaisas P, Lui PP, **Wilson MP**, Leung KY, Herrera-Dominguez L, Sudiwala S, Pessia A, Clayton PT, Bryson K, Velagapudi V, Mills PB, Typas A, Greene NDE, Cabreiro F (2017). Host-Microbe Co-metabolism Dictates Cancer Drug Efficacy in *C. elegans*. *Cell* 169(3): 442-456 e418.
5. **Wilson MP**, Plecko B, Mills PB, Clayton PT (2019) Disorders Affecting Vitamin B6 metabolism. *J Inherit Metab Dis*. doi: 10.1002/jimd.12060.
6. Chelban V, **Wilson MP**, Chardon JW, Vandrovcova J, Zanetti MN, Zamba-Papanicolaou E, Efthymiou S, Pope S, Conte MR, Abis G, Liu Y-T, Tribollet E, Haridy NA, Botía JA, Ryten M, Nicolaou P, Minaidou A, Christodoulou K, Kernohan K, Eaton A, Osmond M, Ito Y, Bourque P, Jepson JEC, Bello O, Bremner F, Cordivari C, Reilly MM, Foiani M, Heslegrave A, Zetterberg H, Heales SJR, Wood NW, Rothman JE, Boycott KM, Mills PB, Clayton PT and Houlden H (2019) *PDXK* mutations cause polyneuropathy responsive to PLP supplementation. *Ann Neurol* (Article accepted pending publication).

ACKNOWLEDGEMENTS

Firstly I want to thank my primary supervisor, Philippa Mills, for her endless support throughout my PhD. With her help I have developed as both a scientist and as a person and I will be forever grateful to her for providing me with the opportunities I have had over the past four years. Equally I would like to thank Peter Clayton for providing regular sparks of inspiration and encouragement whenever they were required.

During my PhD it has become ever clearer that, in terms of modern scientific discovery, we truly are 'standing on the shoulders of giants'. It is a great source of pride that I have been able, in my own small way, to reach a little higher. Furthermore, I feel fortunate to have been given the opportunity to perform research that will have a direct impact on the care of individuals suffering from rare and debilitating diseases. For this I have to thank Great Ormond Street Hospital Children's Charity for providing funding aimed at research into extremely rare disorders that are often not seen as a priority.

In addition, this research would have been impossible without a worldwide network of patients, parents, clinicians and carers who have been generous with their time and donation of samples without the expectation of any personal benefit. It is an example of the international community coming together in a world that, at the time of writing, seems to be drifting further apart.

I am also fortunate to have received the help and assistance of a great many colleagues and collaborators. These include, but are not limited to, Kevin Mills for his mass spectrometry expertise, Emma Footitt for being perhaps the most enthusiastic clinical proponent on this project, Paul Gissen and Simon Heales for providing funding and for giving me the time to complete my research, Abeer Mohamed-Ahmed, Sabrina MacKinnon, Wyatt Yue, Viorica Chelban, David Brown, my colleagues at the BMSC and the team over in the GOSH chemical pathology department. In the laboratory, colleagues such as Emma Reid, Youssef Khalil and David Benton deserve a special mention for their technical and moral support. Finally, I'd like to thank my wife Lore and the rest of my family for giving me their support whenever I needed it.

CONTENTS

1. BACKGROUND	28
1.1 Vitamin B₆	29
1.1.1 Vitamin B ₆ metabolism and homeostasis	30
1.1.2 Reactions catalysed by PLP-dependent enzymes	33
1.1.3 Non-enzymatic roles of the B ₆ vitamers	38
1.1.4 The reactivity of pyridoxal 5'-phosphate – a mixed blessing.....	39
1.2 Inborn errors affecting vitamin B₆ metabolism	40
1.2.1 Diagnosis and treatment of vitamin B ₆ -responsive seizure disorders	47
1.2.2 Vitamin B ₆ for the treatment of genetic epilepsies	49
1.3 LC-MS/MS for the diagnosis of inborn errors of metabolism.	51
1.4 Aims and scope of this thesis.....	54
2. MATERIALS AND METHODS.....	55
2.1 Materials	56
2.2 Ethics statement.....	58
2.3 Collection and storage of dried blood spots.....	58
2.4 Quantification of B₆ vitamers and 4-pyridoxic acid using LC-MS/MS	58
2.4.1 Identification of B ₆ vitamers and pyridoxic acid	58
2.4.2 Identification and quantification of FMN	61
2.4.3 Sample preparation for measurement of B ₆ vitamers and pyridoxic acid.....	62
2.4.3.1 <i>Dried blood spots</i>	62
2.4.3.2 <i>Cell Lysates</i>	63
2.4.3.3 <i>Cell culture medium</i>	63
2.5 Enzyme assay for the quantification of PNPO activity from dried blood spots.....	64
2.5.1 Measurement of the haemoglobin concentration of whole blood stored in DBS	65
2.6 Enzyme assay for the study of recombinant PNPO enzyme	66
2.6.1 Quantification of FMN associated with the recombinant PNPO protein	66
2.7 LC-MS/MS detection of PNPO-derived tryptic digest peptides	67
2.7.1 Selection of peptides	67
2.7.2 LC-MS/MS analysis of PNPO-derived peptides.....	67
2.7.3 Sample preparation	70
2.8 Enzyme assay for the study of recombinant pyridoxal kinase enzyme.....	72
2.9 Enzyme assay for quantification of pyridoxal kinase activity from dried blood spots	73
2.10 Characterisation of the photodegradation profile of PLP.....	74

2.10.1	Photodegradation protocol & sample preparation	74
2.10.2	LC-MS/MS for the assessment of photodegradants	75
2.10.2.1	<i>Investigation of PLP photodegradation products</i>	75
2.10.2.2	<i>Quantification of pyridoxic acid 5'-phosphate</i>	75
2.11	Whole exome and whole genome sequencing	76
2.11.1	Interpretation of variants using bioinformatics tools	77
2.12	DNA Extraction and Sanger sequencing	78
2.12.1	DNA extraction from DBS	78
2.12.2	Primer design	78
2.12.3	Amplification of target genes from genomic DNA using the Polymerase Chain Reaction (PCR)	79
2.12.3.1	<i>PCR conditions</i>	79
2.12.3.2	<i>Visualisation of PCR products by agarose gel electrophoresis</i>	80
2.12.4	Sanger sequencing	80
2.12.4.1	<i>Purification of PCR products</i>	80
2.12.4.2	<i>Sanger sequencing preparation</i>	80
2.12.4.3	<i>DNA precipitation</i>	81
2.13	Cell culture of CHO cells	81
2.13.1	Cell culture conditions	81
2.13.2	Protein assay	82
2.14	Patch recording of the M-current from CHO cells	83
2.14.1	Preparation of solutions	83
2.14.2	Data acquisition and analysis	84
3.	DRIED BLOOD SPOTS AS A TOOL TO PROFILE THE B₆ VITAMERS; USEFULNESS FOR THE DIAGNOSIS OF PNPO DEFICIENCY	86
3.1	Method validation	89
3.1.1	Assessment of recovery of the B ₆ vitamers and pyridoxic acid from DBS	89
3.1.2	Assessment of the measurement precision of B ₆ vitamers and pyridoxic acid from dried blood spots	91
3.2	Analysis of B₆ vitamer profiles of patient samples	94
3.3	Kinetics of oral pyridoxal 5'-phosphate supplementation	104
3.3.1	Long-term PLP treatment of an adolescent	104
3.3.2	Neonatal prophylactic PLP treatment	107
3.4	Discussion and future work	112
4.	DEVELOPMENT OF LC-MS/MS-BASED ENZYME ASSAYS FOR THE MEASUREMENT OF PNPO ACTIVITY	114
4.1	Investigation and development of an LC-MS/MS-based Enzyme assay using dried blood spots for the diagnosis of PNPO deficiency	117
4.1.1	Investigation and development of a coupled enzyme assay	118

4.1.1.1	Comparison of single-step and coupled assays - Preliminary investigation of substrates and stable isotope internal standards	118
4.1.1.2	Optimisation of coupled PK and PNPO enzyme assay conditions.....	125
4.1.1.3	Validation of coupled enzyme assay and stability of PK and PNPO in DBS upon storage ..	129
4.1.1.4	Effects of high dose PLP supplementation on the accuracy of analysis of dried blood spot PNPO activity.	131
4.1.2	Investigation and optimisation of a single-step PNPO enzyme assay from DBS	139
4.1.2.1	Development of PNPO assay using pyridoxine 5'-phosphate as substrate	139
4.1.2.2	Further optimisation of single-step assay conditions	146
4.1.2.3	Effect of supraphysiological B ₆ vitamer concentrations found in patients on supplementation	151
4.1.2.4	Validation of single-step assay	154
4.1.2.5	Stability of dried blood spot PNPO activity	155
4.1.2.6	Investigation of blood haemoglobin measurement from dried blood spots	157
4.1.2.7	Analysis of patient samples	161
4.2	The effect of the p.R116Q variant on PNPO activity and expression	166
4.2.1	Preliminary development of a method to measure activity from bacterially-prepared recombinant PNPO enzyme	168
4.2.2	Effect of flavin mononucleotide concentration on the kinetics of recombinant wild-type and p.R116Q PNPO activity	168
4.2.3	Development of an LC-MS/MS method for the quantification of PNPO protein in DBS ..	175
4.2.3.1	Selection of PNPO-derived tryptic peptides and LC-MS/MS method development	176
4.2.3.2	Analysis of PNPO peptides in dried blood spots	180
4.3	Discussion & future work.....	185
5.	BIOCHEMICAL CHARACTERISATION OF A NOVEL NEUROPATHY CAUSED BY DEFICIENCY OF PYRIDOXAL KINASE.....	187
5.1	Investigation of the <i>in vitro</i> effect of p.A228T on the enzyme kinetics of recombinant pyridoxal kinase	190
5.1.1	The effect of pyridoxal concentration on enzyme activity	191
5.1.2	Effect of adenosine 5'-triphosphate on enzyme activity	192
5.2	The effect of p.A228T on the activity of pyridoxal kinase in red blood cells.....	197
5.2.1	Method development.....	197
5.2.2	Analysis of patient samples	199
5.3	Effect of the c.(-306_-305insGCGGCGG) insertion in the PK promoter region on enzymatic activity of pyridoxal kinase in red blood cells.....	204
5.3.1	Optimisation of the amplification of the <i>PDXK</i> promoter region.	204
5.3.2	Dried blood spot pyridoxal kinase activity does not correlate with the presence of the c.(-306_-305insGCGGCGG) insertion in the promoter region of <i>PDXK</i>	210
5.4	Discussion & future work.....	212
5.4.1	Implications of the association between vitamin B ₆ metabolism and peripheral neuropathy	212
5.4.2	Further biochemical characterisation of pyridoxal kinase and activity variation in the general population.....	215

6. STABILITY AND SUITABILITY OF PYRIDOXAL 5'-PHOSPHATE FOR THE TREATMENT OF VITAMIN B₆-RESPONSIVE DISORDERS	218
6.1 Characterisation of the pyridoxal 5'-phosphate photodegradation profile	222
6.1.1 Investigation and identification of pyridoxal 5'-phosphate photodegradants	222
6.1.2 The effect of light irradiation on the rate of pyridoxal 5'-phosphate degradation and 4-pyridoxic acid 5'-phosphate formation	230
6.2 Confirmation of a diketone pyridoxal 5'-phosphate dimer as a pyridoxal 5'-phosphate photodegradation product.....	231
6.3 Assessment of commercially available pyridoxal 5'-phosphate dietary supplements	233
6.4 Discussion & future work.....	236
7. THE IDENTIFICATION OF NOVEL GENETIC CAUSES OF VITAMIN B₆-RESPONSIVE EPILEPSY.....	238
7.1 Investigation of individuals with B₆-responsive epilepsy using next generation sequencing technology	240
7.1.1 Assessment of variants identified using NGS technology that could lead to B ₆ -dependent epilepsy	241
7.1.1.1 <i>Subject NGS1</i>	243
7.1.1.2 <i>Subject NGS2</i>	249
7.1.1.3 <i>Subject NGS3</i>	252
7.1.2 Subjects NGS4 & NGS5	258
7.2 Investigation of the effect of B₆ vitamers on the M-current facilitated by KCNQ2 channels	259
7.2.1 The effect of PL and PLP on the M-current in CHO cells overexpressing KCNQ2/3.....	260
7.2.2 The effect of growth in B ₆ -depleted medium upon the M-current in CHO cells overexpressing KCNQ2/3	263
7.3 Discussion & future work.....	267
7.3.1 Investigation of patients with vitamin B ₆ -dependent epilepsy using NGS data	267
7.3.2 The mechanism of response to vitamin B ₆ supplementation in patients with mutations in <i>KCNQ2</i>	268
8. SUMMARY AND FUTURE WORK	270
9. APPENDIX.....	275
9.1 Conditions used for PCR amplification of candidate variants identified by next generation sequencing.....	276
9.2 Gene lists used as biological context filters during analysis of next generation sequencing data using Ingenuity Variant Analysis	277

LIST OF FIGURES

Figure 1.1: The B ₆ vitamers and 4-Pyridoxic acid	29
Figure 1.2: Enzymes and transporters responsible for human PLP synthesis and homeostasis.	31
Figure 1.3: Overview of the symptoms reported in the literature for patients with ATQ deficiency.	41
Figure 1.4: Overview of the symptoms reported in the literature for patients with PNPO deficiency.	42
Figure 1.5: Liquid chromatography-tandem mass spectrometry.	52
Figure 2.1: LC-MS/MS detection of the B ₆ vitamers and pyridoxic acid.	59
Figure 3.1: B ₆ vitamer and pyridoxic acid concentrations in DBS.	98
Figure 3.2: PM/PA and PNP/PLP ratios in DBS.	101
Figure 3.3: Subject 11 - Concentrations of B ₆ vitamers and pyridoxic acid prior to and after oral supplementation with 75 mg PLP.	105
Figure 3.4: Subject 11 – PM/PA and PNP/PLP ratios prior to and after oral supplementation with 75 mg PLP.	106
Figure 3.5: Subject 2 – Concentration of B ₆ vitamers and pyridoxic acid prior to and after oral supplementation with 35 mg PLP.	107
Figure 3.6: Subject 2 – PM/PA and PNP/PLP ratios prior to and after oral supplementation with 35 mg PLP.	108
Figure 4.1: Coupled and single-step PNPO assays using d ₂ -PN and PMP as substrates.	117
Figure 4.2: Summary of the protocol used for the development of a PNPO activity assay from DBS.	118
Figure 4.3: Linearity of calibration curves using 500 nmol/L d ₂ -PA as internal standard.	120
Figure 4.4: Initial comparison of coupled and single-step enzyme assays.	121

Figure 4.5: Assessment of the matrix effect on LC-MS/MS signal intensity of the B ₆ vitamers and their isotopically-labelled analogues.	122
Figure 4.6: Coupled pyridoxal kinase and pyridox(am)ine 5'-phosphate oxidase assay using PN as substrate.	124
Figure 4.7: Coupled pyridoxal kinase and pyridox(am)ine 5'-phosphate oxidase activity in a 3 mm punch from a healthy adult control.	124
Figure 4.8: Effect of FMN concentration on PNPO activity in a 3 mm DBS punch from a healthy adult control.	125
Figure 4.9: Pyridoxal 5'-phosphate chromatography on LC-MS/MS analysis.	127
Figure 4.10: PNPO activity between pH 6.6 - 8.6.	128
Figure 4.11: Repeatability of PLP formation after a 2 hour incubation with a 3 mm DBS from a healthy adult.	129
Figure 4.12: Effect of (a) short and (b) long-term storage on PNPO activity measured in a 3 mm DBS from a healthy adult.	130
Figure 4.13: Comparison of the B ₆ vitamers concentrations upon incubation of a 3 mm DBS from a healthy adult control and a PNPO deficient subject.	132
Figure 4.14: Comparison of the B ₆ vitamers concentrations upon incubation of a 3 mm DBS from a healthy adult with exogenous B ₆ vitamers.	133
Figure 4.15: PLP formation after the 2 hour incubation of a 3 mm DBS with exogenous B ₆ vitamers.	134
Figure 4.16: Concentrations of B ₆ vitamers during incubation of a 3 mm DBS with varying buffer compositions.	135
Figure 4.17: Concentrations of B ₆ vitamers during incubation of a 3 mm DBS with varying buffer compositions.	136
Figure 4.18: Formation of pyridoxal 5'-phosphate after incubation of a 3 mm DBS with varying PL and PLP concentrations.	137
Figure 4.19: Single-step PNPO assay using PNP as substrate.	139
Figure 4.20: Concentrations of B ₆ vitamers after incubation of a 3 mm DBS with varying initial B ₆ concentrations and different buffers.	140

Figure 4.21: Comparison of coupled and single-step PNPO enzyme assay in DBS from a PNPO deficient patient and an adult control.	142
Figure 4.22: Effect of sonication on PNP and PLP concentrations measured prior to incubation with a 3 mm DBS from a PNPO deficient child or adult control.	143
Figure 4.23: Effect of sonication on DBS PNPO activity.	144
Figure 4.24: Conversion of PNP to PLP by control and PNPO deficient DBS when using optimised sonication protocol.	145
Figure 4.25: PNPO activity as a function of DBS weight.	146
Figure 4.26: PNPO activity as a function of PLP formation from 0-120 min.	147
Figure 4.27: Effect of substrate on PNPO activity.	148
Figure 4.28: Lineweaver-Burk plot showing the effect of substrate concentration on PLP formation.	149
Figure 4.29: Effect of FMN concentration on PLP formation.	150
Figure 4.30: Effect of exogenous PMP on PNPO activity measured as PLP formation.	153
Figure 4.31: Intra and inter-assay validation of a single-step DBS PNPO assay.	154
Figure 4.32: Effect of humidity on the short-term stability of the PNPO enzyme in dried blood spots.	156
Figure 4.33: Effect of storage temperature on the long-term stability of the PNPO enzyme in dried blood spots.	156
Figure 4.34: Haemoglobin calibration curve.	158
Figure 4.35: Haemoglobin concentration (gHb/dL) measured in 3 mm DBS.	159
Figure 4.36: Correlation of Haemoglobin concentration (gHb/dL) measured from whole blood and DBS.	160
Figure 4.37: Haemoglobin concentration (gHb/dL) measured from 3 mm DBS after a 10 minute sonication step.	160
Figure 4.38: DBS PNPO activities of patients with PNPO deficiency relative to control individuals.	164
Figure 4.39: Effect of the p.R116Q variant on the activity of recombinant PNPO.	168

Figure 4.40: Effect of FMN concentration on activity of recombinant wild-type and p.R116Q PNPO enzymes.	169
Figure 4.41: FMN concentration in T0 time points of the recombinant PNPO enzyme assay.	170
Figure 4.42: Kinetics of PNPO protein when varying concentrations of substrates PNP and PMP.	171
Figure 4.43: Kinetics of the PNPO protein when varying concentrations of FMN.	173
Figure 4.44: Measurement of FMN bound to recombinant PNPO protein using a $^{13}\text{C}_4^{15}\text{N}_2$ riboflavin internal standard.	173
Figure 4.45: Predicted structure of the PNPO active site.	174
Figure 4.46: Predicted exonic splicing enhancers in exon 3 of the PNPO gene.	176
Figure 4.47: Predicted disruption of exonic splicing enhancer sites by the c.347G>A (p.R116Q) variant in PNPO.	176
Figure 4.48: Amino acid sequence of the PNPO protein.	177
Figure 4.49: Chromatographic separation of peptides selected for UPLC-MS/MS detection from trypsin digested PNPO protein.	179
Figure 4.50: Examples of chromatograms obtained upon LC-MS/MS analysis of DBS digests spiked with a) wild-type and b) p.R116Q recombinant PNPO protein.	183
Figure 5.1: (a) Structures of the amino acids alanine and threonine (b) Predicted structure of the PK active site.	190
Figure 5.2: Effect of pyridoxal concentration on pyridoxal kinase activity.	191
Figure 5.3: Kinetics of recombinant PK protein when varying ATP concentration.	193
Figure 5.4: Kinetics of recombinant PK protein when varying ATP concentration in the presence of an excess of MgCl_2 and PL.	194
Figure 5.5: Sigmoidal kinetics of recombinant PK protein using MgATP as substrate.	195
Figure 5.6: Pyridoxal kinase activity in a 3 mm DBS.	198
Figure 5.7: Preliminary pyridoxal kinase assay from DBS indicated reduced PK activity in p.A228T individuals.	199
Figure 5.8: Pyridoxal kinase activities in controls and subjects PKHET1, PK1 and PK2.	201

Figure 5.9: Age does not affect erythrocyte pyridoxal kinase activity.	202
Figure 5.10: Effect of gender on pyridoxal kinase activity.	203
Figure 5.11: Annealing temperature optimisation of primers Prom F & Prom R.	206
Figure 5.12: Effect of DMSO on the amplification of the PDXK 5'-promoter region.	207
Figure 5.13: Amplification of the PDXK 5'-promoter region using genomic DNA extracted from DBS taken from PK-deficient individuals and controls.	208
Figure 5.14: Representative electropherograms of the wild-type, heterozygous and homozygous c.(-306_-305InsGCGCGGCG) alleles from DBS extracts.	208
Figure 5.15: Comparison of pyridoxal kinase activity with genotype data for c.(-306_-305InsGCGCGGCG).	210
Figure 5.16: The PDXK 5'-promoter region showing common variants with a minor allele frequency (MAF) greater than 0.1 in GnomAD.	216
Figure 6.1: MS1 Scan acquisitions after (a) 0 and (b) 72 h light irradiation of a 1 mmol/L PLP solution.	223
Figure 6.2: Neutral loss (- 98) acquisitions after (a) 0 and (b) 72 h light irradiation of a 1 mmol/L PLP solution.	224
Figure 6.3: Postulated PLP photodegradation products.	225
Figure 6.4: Formation of PLP photodegradation products.	227
Figure 6.5: Postulated structures of MS fragments derived from m/z 264, identified as pyridoxic acid 5'-phosphate.	229
Figure 6.6: Percentage PLP and PAP levels after light irradiation.	230
Figure 6.7: Absorbance spectrum of the HPLC eluent likely to be a PLP diketone dimer.	231
Figure 6.8: Mass spectrum of the eluent fraction thought to correspond to a PLP diketone dimer.	232
Figure 7.1: Summary of the filter cascade used for variant analysis.	242
Figure 7.2: M-Current measured in CHO cells overexpressing KCNQ2/3 channels.	261

Figure 7.3: The effect of 10 $\mu\text{mol/L}$ PLP on the M-current in CHO cells over-expressing KCNQ2/3 channels.	262
Figure 7.4: The B ₆ vitamer concentrations in media used for the culture of normal and B ₆ -depleted CHO cells.	264
Figure 7.5: The concentration of the B ₆ vitamers in normal and B ₆ -depleted CHO cells.	265
Figure 7.6: The M-current amplitude of normal and B ₆ -depleted CHO cells.	266

LIST OF TABLES

Table 1.1: Human PLP-dependent enzymes.	34
Table 1.2: Clinical and biochemical features of inborn errors leading to B ₆ -responsive seizures.	43
Table 1.3: Clinical and biochemical presentations caused by perturbed function of PLP-dependent enzymes in a PLP deficient state.	46
Table 2.1: Gradient profile for separation of B ₆ vitamers and pyridoxic acid by LC-MS/MS.	59
Table 2.2: Parameters used for the MRM-based identification of the B ₆ vitamers and pyridoxic acid and their stable isotope internal standards.	60
Table 2.3: Parameters used for the MRM-based identification of FMN and ¹³ C ₄ ¹⁵ N ₂ -Riboflavin.	61
Table 2.4: Selected peptides for LC-MS/MS analysis of trypsin digested PNPO protein.	67
Table 2.5: MRM transitions for LC-MS/MS analysis of trypsin digested PNPO protein.	68
Table 2.6: Gradient profile for separation of tryptic digest peptides.	69
Table 2.7: MRM transitions for LC-MS/MS detection of peptides derived from trypsin digested human albumin and yeast enolase proteins.	70
Table 2.8: Extended gradient profile for separation of tryptic digest peptides.	70
Table 2.9: Ingenuity Variant Analysis parameters for filtering variants identified in VCF files derived from whole exome or genome data.	77
Table 2.10: Standard conditions for targeted PCR amplification of genomic DNA.	79
Table 2.11: Standard thermal cycling parameters for PCR amplification of genomic DNA.	79
Table 2.12: Thermal cycling parameters for Sanger Sequencing of PCR products.	81
Table 2.13: Composition of extracellular patching solution.	83
Table 2.14: Composition of pipette solution.	84
Table 3.1: Recovery of the B ₆ vitamers and pyridoxic acid from DBS.	90
Table 3.2: Precision validation of B ₆ vitamer and pyridoxic acid measurement from DBS.	92
Table 3.3: Precision validation of LC-MS/MS measurement of B ₆ vitamers and pyridoxic acid.	93

Table 3.4: Concentrations of B₆ vitamers and pyridoxic acid measured in DBS from PNPO deficient patients, p.R116Q heterozygotes and other patients with epilepsy responding to B₆ supplementation.

96

Table 4.1: Effect of pH on PNPO activity using a coupled assay. **127**

Table 4.2: Composition of reaction buffers for the measurement of PNPO activity from DBS. **140**

Table 4.3: Effect of pH on PNPO Activity using a single step assay. **151**

Table 4.4: Effect of exogenous PLP on PNPO activity. **152**

Table 4.5: Summary of subjects with mutations identified in PNPO. **162**

Table 4.6: Peptides selected for LC-MS/MS detection of trypsin digested PNPO protein. **177**

Table 4.7: Peptides detected from tryptic digests of DBS and spiked standards. **182**

Table 5.1: Summary of control and affected subjects collected for DBS pyridoxal kinase activity analysis. **200**

Table 5.2: Optimal parameters for PCR primer design and primer sequences for amplification of the PDXK 5' promoter region. **205**

Table 5.3: Presence of the PDXK variant c.(-306_-305InsGCGCGGCG) in subjects collected for DBS pyridoxal kinase activity analysis. **209**

Table 6.1: Parameters used for the MRM-based identification of PLP, PL, PA and photodegradants of PLP. **226**

Table 6.2: Quantification of PLP contained in 50 mg nutraceutical formulations. **234**

Table 6.3: Proportion of PLP lost and PAP formed on light irradiation of 5 mg/mL PLP formulations. **235**

Table 7.1: CSF B₆ Vitamers and pyridoxic acid concentrations in Subject 1. **244**

Table 7.2: Candidate variants that may be causative for the B₆-responsive seizures of Subject NGS1. **246**

Table 7.3: Candidate variants that may be causative for the B ₆ -responsive seizures of Subject NGS2.	250
Table 7.4: Candidate variants that may be causative for the B ₆ -responsive seizures of Subject NGS3.	254
Table 7.5: Genes linked to early infantile epileptic encephalopathy and developmental delay in the isodisomic region of chromosome X in Subject 3.	257
Table 9.1: Primers and conditions used to amplify the regions containing pathogenic variants of unknown significance identified using NGS analysis.	276
Table 9.2: Genes encoding PLP-dependent proteins or proteins implicated in the metabolism of vitamin B ₆ .	277
Table 9.3: Genes on the early infantile epileptic encephalopathy gene panel at Great Ormond Street Hospital.	278
Table 9.4: Genes in the human genome known to encode ion channels.	279

LIST OF ABBREVIATIONS

3-OMD	3-Ortho-methyldopa
5-HIAA	5-Hydroxyindoleacetic Acid
5-HT	5-Hydroxytryptamine
5-HTP	5-Hydroxytryptophan
6-oxo-PIP	6-oxo-pipecolic acid
α -AASA	α -aminoadipic semialdehyde
ACN	Acetonitrile
ADHD	Attention deficit hyperactivity disorder
AED	Anti-epileptic drug
ALAS	Aminolevulinic acid synthase
ALG13	UDP-N-acetylglucosaminyltransferase subunit
ALDH7A1	Aldehyde dehydrogenase 7 family member A1
AMCG	American college of medical genetics and genomics
AOX	Aldehyde oxidase
ATP	Adenosine 5'-triphosphate
AUC	Area under the curve
BCA	Bicinchoninic acid
Bsu1 ⁺	Vitamin B ₆ uptake protein
CACNA1A	Calcium voltage-gated channel subunit alpha1 A
CC	Corpus callosum
cDNA	Complementary deoxyribonucleic acid
CHO	Chinese hamster ovary
CID	Collision induced dissociation
CMT	Charcot-Marie-Tooth

CNV	Copy number variation
CoA	Coenzyme A
CP	Choroid plexus
CPBP	Core promoter binding protein
CSF	Cerebrospinal fluid
CU	Concentration units
DBS	Dried blood spot
DBP	Albumin D-site-binding protein
DEPDC5	DEP domain-containing protein 5
DMSO	Dimethyl sulphoxide
DNA	Deoxyribonucleic acid
dsDNA	Double stranded deoxyribonucleic acid
DXP	Deoxyxylulose 5-phosphate
E-PMP	Enzyme-pyridoxamine 5'-phosphate complex
E-PLP	Enzyme-pyridoxal 5'-phosphate complex
EC	Enzyme Commission
ECM	Extracellular matrix
EDTA	Ethylenediamine-tetra-acetic acid
EEG	Electroencephalogram
EGTA	Ethylene glycol-bis(β -aminoethyl ether)-N,N,N',N'-tetra-acetic acid
EIEE	Early infantile epileptic encephalopathy
EMA	European Medicines Agency
ESI	Electrospray ionisation
ExAC	Exome aggregation consortium
FA	Formic acid
FBS	Foetal bovine serum

FMN	Flavin mononucleotide
GABA	γ -aminobutyric acid
GABRD	γ -aminobutyric acid type A receptor delta subunit
gnomAD	Genome Aggregation Database
GOSH	Great Ormond Street Hospital
GPI	Glycosylphosphatidylinositol
HEPES	4-(2-hydroxyethyl)-1-piperazineethanesulfonic acid
HFBA	Heptafluorobutyric acid
HGMD	Human Gene Mutation Database
HLF	Hepatic leukaemia factor
HPLC	High performance liquid chromatography
HPH	Hyperprolinaemia type 2
HPLC-UV/VIS	High-performance liquid chromatography-ultraviolet/visible spectroscopy
HVA	Homovanillic acid
IGV	Integrated genomics viewer
IS	Internal standard
IVA	Ingenuity variant analysis
KCNAB2	Potassium channel, voltage-gated, subunit beta-2
KCNQ2	Potassium channel, voltage-gated, subfamily Q, member 2
KCNQ3	Potassium channel, voltage-gated, subfamily Q, member 3
L-DOPA	L-3,4-dihydroxyphenylalanine
LC	Liquid chromatography
LC-MS/MS	Liquid chromatography-tandem mass spectrometry
LFT	Liver function test
LLOQ	Lower limit of quantification

m/z	Mass/charge ratio
MCADD	Medium-chain acyl-CoA dehydrogenase deficiency
mGOT	Mitochondrial glutamic-oxaloacetic transaminase
MRI	Magnetic resonance imaging
MRM	Multiple reaction monitoring
mSHMT	Mitochondrial serine hydroxymethyltransferase
MSUD	Maple syrup urine disease
MTM1p	Manganese trafficking factor for mitochondrial sod2 protein
NMDA	N-methyl-D-aspartate
NAD	Nicotinamide adenine dinucleotide
NADH	Nicotinamide adenine dinucleotide (reduced)
NADP	Nicotinamide adenine dinucleotide phosphate
NADPH	Nicotinamide adenine dinucleotide phosphate (reduced)
NEE	Neonatal epileptic encephalopathy
NGS	Next generation sequencing
NHLBI ESP	National heart, lung, and blood institute exome sequencing project
OCD	Obsessive–compulsive disorder
OMIM	Online mendelian inheritance in man
P2X7R	P2 purinoceptor 7 receptors
P5C	Δ^1 -pyrroline-5-carboxylate
P6C	L- Δ^1 -piperidine-6 carboxylate
PA	4-pyridoxic acid
PAP	4-pyridoxic acid 5'-phosphate
PAR bZip	Proline and acidic amino acid-rich basic leucine zipper
PCDH19	Protocadherin 19
PCR	Polymerase chain reaction

PDE	Pyridoxine-dependent epilepsy
PIP	Phosphatidylinositol phosphate
PIP ₂	Phosphatidylinositol 4,5-bisphosphate
PK	Pyridoxal kinase
PKU	Phenylketonuria
PL	Pyridoxal
PLP	Pyridoxal 5'-phosphate
PLPase	Pyridoxal 5'-phosphate phosphatase
PLPBP	Pyridoxal 5'-phosphate binding protein
PLPHP	Pyridoxal 5'-phosphate homeostasis protein
PLR	Pyridoxal reductase
PM	Pyridoxamine
PMP	Pyridoxamine 5'-phosphate
PN	Pyridoxine
PNG	Pyridoxine-5'- β -D-glucoside
PNP	Pyridoxine 5'-phosphate
PNPO	Pyridox(am)ine 5'-phosphate oxidase
PPI	Inorganic pyrophosphate
PROSC	Proline synthetase co-transcribed bacterial homolog protein
Pup1	Phosphorus uptake 1 protein
QC	Quality control
R5P	Ribose 5-phosphate
RDA	Recommended daily allowance
RF	Radio frequency
ROS	Reactive oxygen species
rpm	Revolutions per minute

RT	Retention time
SCN1A	Sodium voltage-gated channel alpha subunit 1
SD	Standard deviation
SEM	Standard error of the mean
S/N	Signal/noise ratio
SLC4A3	Solute carrier family 4 member 3
SLC15A5	Solute carrier family 15 member 5
SLC25A39	Solute carrier family 25 member 39
SLC25A40	Solute carrier family 25 member 40
SNP	Single nucleotide polymorphism
SPE	Solid phase extraction
T1	Postulated plasma membrane vitamin B ₆ transporter
T2	Postulated mitochondrial membrane vitamin B ₆ transporter
TAE	Tris-acetate-EDTA
TCA	Trichloroacetic acid
TCEP	Tris(2-carboxyethyl)phosphine
TEF	Thyrotroph embryonic factor
TFA	Trifluoroacetic acid
TGF- β	Transforming growth factor beta
TNSALP	Tissue nonspecific alkaline phosphatase
Tpn1p	Transport of pyridoxine protein 1
Tris	Tris(hydroxymethyl)aminomethane
ULOQ	Upper limit of quantification
UPLC	Ultra performance liquid chromatography
VA	Vanillic acid
VLA	Vanillactic acid / vanillyl lactic acid

UMCG	Universitair Medisch Centrum Groningen
UCSC	University of California Santa Cruz
WES	Whole exome sequencing
WGS	Whole genome sequencing
WT	Wild-type

1. BACKGROUND

1.1 Vitamin B₆

Vitamin B₆ was first described in 1934 by György as a 'rat pellagra preventative factor'. Over the next few decades the structures of the B₆ vitamers were determined as several closely related 2-methyl-3-hydroxypyridine analogues differing only at the 4' and 5' positions (**Figure 1.1**).¹ Substitution at the 4' position leads to pyridoxine (PN - CH₂OH), pyridoxal (PL - CHO) and pyridoxamine (PM - CH₂NH₂). At the 5' position each of these vitamers can have either a hydroxymethyl (CH₂OH), phosphomethyl (CH₂PO₄H₂) or methoxyglucosyl (C₇H₁₃O₆) moiety. The phosphorylated forms are known as pyridoxine 5'-phosphate (PNP), pyridoxal 5'-phosphate (PLP) and pyridoxamine 5'-phosphate (PMP). In humans, excess vitamin B₆ is excreted as 4-pyridoxic acid (PA – COOH at the 4' position). PLP is the active coenzyme form of vitamin B₆. In humans, PLP is a cofactor for more than 50 diverse enzymes required for many essential metabolic functions (**Section 1.1.2**).²⁻⁴

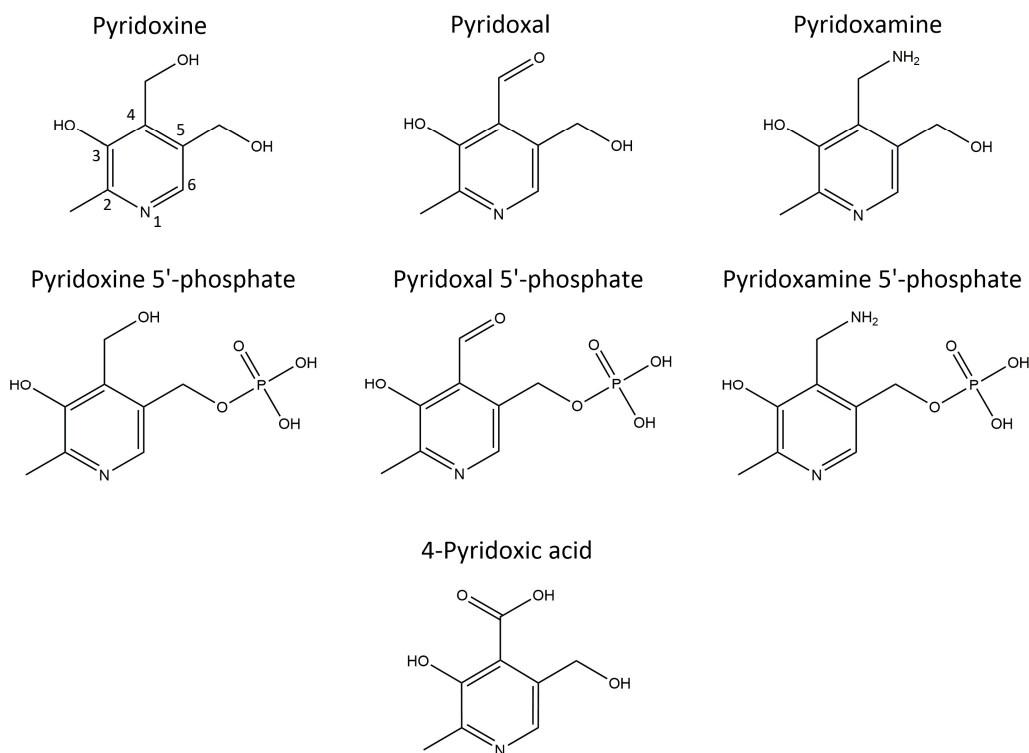


Figure 1.1: The B₆ vitamers and 4-Pyridoxic acid. The B₆ vitamers: Pyridoxine (PN); Pyridoxal (PL); Pyridoxamine (PM); Pyridoxine 5'-phosphate (PNP); Pyridoxal 5'-phosphate (PLP); Pyridoxamine 5'-phosphate (PMP). Human urinary excretion product: 4-Pyridoxic acid (PA).

1.1.1 Vitamin B₆ metabolism and homeostasis

The use of PLP as a cofactor is widespread across all domains of life. Indeed, PLP is thought to be a prebiotic compound (i.e. a compound that existed prior to the emergence of life).⁵ In lower organisms there are two major pathways for the biosynthesis of vitamin B₆, the deoxyxylulose 5-phosphate (DXP)-dependent and DXP-independent pathways.⁶ However, in man the body's needs must largely be met from dietary sources (despite a contribution from gut microbiota).⁷ The ubiquitous use of B₆ as a cofactor means it is prevalent in most components of the human diet. In food derived from plant matter it is present mostly in the form of pyridoxine, pyridoxine 5'-phosphate or pyridoxine 5'-glucoside.⁸ In meat it is more prevalent as pyridoxal and pyridoxal 5'-phosphate, this is also true for human breast milk.⁹ Vitamin B₆ derived from meat is also present as pyridoxamine 5'-phosphate.¹⁰⁻¹¹

The prevalence of vitamin B₆ in most foods as well as its synthesis by gut microbiota may be why dietary B₆ deficiency is rare. A deficiency is however more likely to occur early in life when the gut microbiota is not fully established; in the 1950's, infants fed a heat-treated milk formula developed seizures due to B₆ deficiency, the vitamin B₆ in this milk formula having been thermally degraded.¹² Seizures due to B₆ deficiency have also been reported in an autistic child with a severely self-restricted diet¹³ and in adults with impaired liver function.¹⁴

Whilst humans are not capable of *de novo* synthesis of pyridoxal 5'-phosphate, they do have a pathway for the interconversion and regulation of the B₆ vitamers (**Figure 1.2**). The 5'-phosphorylated B₆ vitamers present in the diet must first be hydrolysed by intestinal phosphatases before absorption across the gut barrier. The absorbed non-phosphorylated vitamers (PN, PL and PM) are then rapidly taken up into the liver before rephosphorylation to PNP, PLP and PMP by pyridoxal kinase (PK). Conversion of PNP and PMP to active PLP is carried out by pyridox(am)ine 5'-phosphate oxidase (PNPO).¹⁵ In addition, it has recently been shown that the B₆ metabolic pathway is intact in a Caco-2 (enterocyte) cell model. It is possible that at least some dietary B₆ is metabolised to PL or PLP before basolateral excretion into the blood and thus transport around the body¹⁶, removing the requirement for hepatic conversion of PL to PLP. Excess B₆ is excreted in the urine as PA after the hepatic conversion of PL to PA by aldehyde oxidase or aldehyde dehydrogenases.¹⁷⁻¹⁸

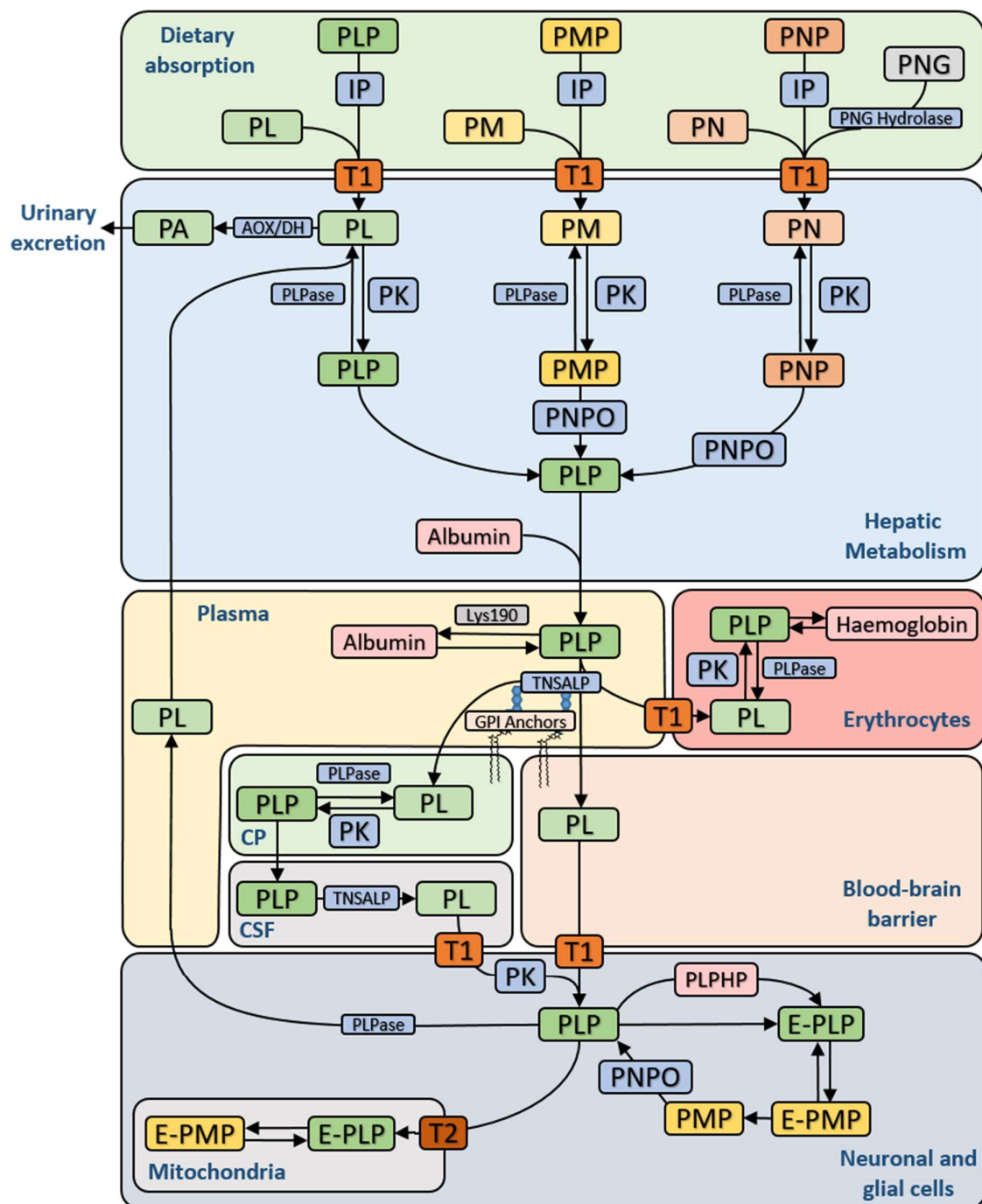


Figure 1.2: Enzymes and transporters responsible for human PLP synthesis and homeostasis.

Pyridoxal 5'-phosphate (PLP); pyridoxal (PL); pyridoxamine 5'-phosphate (PMP); pyridoxamine (PM); pyridoxine 5'-phosphate (PNP); pyridoxine (PN); pyridoxine-5'- β -D-glucoside (PNG); 4-pyridoxic acid (PA); intestinal phosphatases (IP); plasma membrane transporter (identity unknown; T1); mitochondrial membrane transporter (postulated to be encoded by the *SLC25A39/40* genes; T2); pyridoxal kinase (PK); pyridox(am)ine 5'-phosphate oxidase (PNPO); tissue non-specific alkaline phosphatase (TNSALP); pyridoxal-phosphatase (PLPase); aldehyde oxidase (Mo cofactor)/ β -NAD dehydrogenase (AOX/DH); glycosylphosphatidylinositol (GPI) anchor; pyridoxal 5'-phosphate binding protein (PLPHP/PROSC or PLBPB); cerebrospinal fluid (CSF); choroid plexus (CP). This figure shows the homeostasis and supply of PLP to the brain, other cells such as hepatocytes derive their B₆ from the plasma directly.

PLP is exported from the liver bound to lysine-190 of albumin.¹⁹ The removal of the 5' phosphate is then required in order for the vitamin to cross cell membranes and be delivered to the tissues that require it (e.g. across the blood-brain barrier). This is carried out by TNSALP, an ecto-enzyme encoded by the *ALPL* gene. TNSALP is bound to the cell surface by a glycosylphosphatidylinositol anchor.²⁰ PL and PLP are the two major forms of B₆ found in human plasma and CSF when subjects are not receiving high-dose B₆ supplementation.²¹⁻²²

Whilst there is evidence from a Caco-2 cell model of a transporter for dephosphorylated B₆ vitamers on the plasma membrane facilitating, in particular, intestinal absorption²³, a B₆ transporter has yet to be identified in mammals. However, one has been reported in *Saccharomyces cerevisiae* (Tpn1p)²⁴, *Arabidopsis thaliana* (PUP1)²⁵ and *Saccharomyces pombe* (bsu1+).²⁶ Intracellular trafficking of PLP has been postulated to rely on the pyridoxal 5'-phosphate homeostasis protein (PLPHP/PLBP/PROSC), perhaps between subcellular compartments.²⁷

Cytoplasmic rephosphorylation of PL to PLP by PK provides intracellular enzymes with active cofactor. Typically, this is bound to a lysine residue at the active site of PLP-dependent enzymes. These enzymes are present in multiple intracellular compartments such as the mitochondrion (e.g. mitochondrial glutamic oxaloacetic transaminase [mGOT], mitochondrial serine hydroxymethyltransferase [mSHMT], and aminolevulinic acid synthase [ALAS]) and peroxisome (e.g. alanine-glyoxylate aminotransferase [AGXT]). This presents a biological challenge with regards to the intracellular trafficking of PLP to the compartments in which it is required. The B₆ metabolic enzymes are thought to be primarily localised to the cytoplasm²⁸ with the exception of PLPHP, recently localised mostly to the mitochondria of human and yeast cell models.²⁹ The trafficking and homeostasis of PLP is discussed further in **Section 1.1.4.**

Recently the Mtm1p carrier has been identified as a mitochondrial PLP transporter in *Saccharomyces cerevisiae*.³⁰ In humans the mechanism by which PLP is transported into the mitochondrion is currently unknown, the SLC25A39 and SLC25A40 proteins are good candidates due to their homology with Mtm1p but have yet to be characterised.³⁰⁻³¹ Indeed, silencing of *slc25a39* in murine erythroleukaemia cells impaired iron incorporation into protoporphyrin IX, potentially indicative of reduced PLP-dependent mitochondrial δ -aminolevulinate synthase activity.³²

PLP-dependent half-transamination reactions can produce an apo-enzyme with bound PMP. This can then be recycled to PLP by PNPO. The pyridoxal 5'-phosphate phosphatase (PLPase) enzyme is thought to be responsible for subsequent intracellular hydrolysis of pyridoxal 5'-phosphate when it is surplus to requirements.³³ PLPase deficiency induced by knockout of the *pdxp* gene in a mouse model leads to raised PLP and GABA in the brain alongside neurological changes such as improved cognition, mild anxiety and decreased motor performance.³⁴

Unsurprisingly given the importance of PLP-dependent enzymes to human metabolism, PK, PNPO and PLPase are present in most human tissues.³⁵ The regulation of human B₆ metabolic enzymes has been partially characterised. The enzymatic activities of PK and PNPO are subject to feedback inhibition by their product, PLP.³⁶ In addition, recent work in an epithelial ovarian cancer cell line has indicated that PNPO expression is regulated by TGF- β . In this model, PNPO expression was suppressed by PLP administration and enhanced by PN administration.³⁷

There are population differences in the red blood cell activities of both PK³⁸ and PNPO.³⁹ In PK these differences have been ascribed to an erythroid specific promoter.⁴⁰ PK is also known to be under the control of temporally regulated PAR bZip transcription factors. Knockout of these transcription factors in mice leads to seizures and low brain concentrations of dopamine, serotonin and PLP.⁴¹ In *Salmonella typhimurium*, the PtsJ protein has been identified as a MocR-like transcriptional repressor that binds PLP as an effector and regulates the expression of PK, providing feedback regulation.⁴²

In humans, a genome-wide association study indicated that the C allele of a common SNP (rs4654748; T>C) close to the *ALPL* gene (encoding TNSALP) is associated with lower plasma PLP concentrations.⁴³

1.1.2 Reactions catalysed by PLP-dependent enzymes

According to the Enzyme Commission, pyridoxal 5'-phosphate is a cofactor for approximately 140 enzymatic activities (greater than 50 in man). In total, this is 4% of all enzymatic activities (<http://www.chem.qmul.ac.uk/iubmb/enzyme>). These include many critical for amino acid and neurotransmitter metabolism, as well as those important for gluconeogenesis from amino acids, glycogenolysis and one-carbon

metabolism. **Table 1.1** summarises all currently characterised PLP-dependent enzymes in humans, as described by Percudani and Peracchi³, as well as a summary of their main activities and any known inborn errors of metabolism caused by their aberrant function.

In humans, the cofactor activity of PLP is facilitated by the formation of a covalent Schiff base linkage to the ϵ -amino group of an active site lysine residue. The vast majority of subsequently catalysed reactions include the formation of a new Schiff base with an amino group on an amino acid substrate. This allows for increased reactivity of α , β and γ -carbons of the amino acid and subsequent transamination, decarboxylation, racemisation, replacement or elimination activities. The specific reaction depends upon the enzyme.⁴⁴

One notable exception to this mode of catalytic action is that of the glycogen phosphorylase enzyme (EC 2.4.1.1). In this case, although a Schiff base is formed with the Lys680 residue of glycogen phosphorylase, the next step instead results in the cleavage of the terminal α 1,4 glycosidic bond in a linear glycogen chain and transfer of a phosphate group onto a newly liberated glucose monosaccharide.⁴⁵

Table 1.1: Human PLP-dependent enzymes. Abbreviations: pyridoxal 5'-phosphate (PLP); nicotinamide adenine dinucleotide (NAD); γ -aminobutyric acid (GABA); L-3,4-dihydroxyphenylalanine (L-DOPA); 5-hydroxytryptophan (5-HTP); 5-hydroxytryptamine (5-HT, serotonin); cerebrospinal fluid (CSF); homovanillic acid (HVA); 5-hydroxyindoleacetic acid (5-HIAA); 3-O-methyldopa (3-OMD, 3-methoxytyrosine); coenzyme A (CoA).

Pathway	PLP-dependent enzyme	Main catalytic activities	Biological and biochemical function	Known disorders related to enzyme deficiency
Amino acid and neurotransmitter metabolism	Histidine decarboxylase (HDC; EC 4.1.1.22)	The decarboxylation of histidine to form histamine	Histamine is important as a neurotransmitter and for inflammatory responses	
	Aspartate transaminase (AST or GOT; EC 2.6.1.1)	The reversible transfer of an α -amino group from aspartate to glutamate	Important for the recycling of amino acids, the malate-aspartate shuttle and gluconeogenesis	Mutations in mitochondrial GOT2 cause serine and B ₆ -responsive epileptic encephalopathy, developmental delay and spastic paraparesis ⁴⁶

	Alanine transaminase (ALT or GPT1 + 2; EC 2.6.1.2)	Reversible conversion of L-alanine + α -ketoglutarate to pyruvate + L-glutamate		GPT2 (mitochondrial) deficiency leads to developmental delay and neurological disease (MIM: 616281). Severe PLP deficiency can cause hypoglycaemia.
	Kynureninase (KYNU; EC 3.7.1.3)	Conversion of L-kynurenine to anthranilic acid and alanine	Degradation of kynurenine, part of the tryptophan catabolic pathway	KYNU deficiency leads to congenital abnormalities, increased xanthurenic acid excretion and NAD deficiency (MIM: 617661). High xanthurenic acid excretion is a marker of systemic B ₆ deficiency.
	Kynurenine aminotransferase (KYAT1 & 2; EC 2.6.1.7)	Conversion of L-kynurenine + 2-oxoglutarate to kynurenic acid + L-glutamate		
	Cystathionine- β -synthase (CBS; 4.2.1.22)	The formation of L-cystathionine from L-serine + L-homocysteine	Regulation of homocysteine levels and the removal of excess sulphur-containing amino acids	Homocystinuria due to CBS deficiency (MIM: 236200). May be pyridoxine-responsive
	Cystathionine- γ -lyase (CTH; EC 4.4.1.1)	The conversion of L-cystathionine to cysteine, α -ketobutyrate and ammonia	Important for glutathione production and has an alternate activity that produces H ₂ S, a neuromodulator	Cystathioninuria; thought to be a benign biochemical abnormality (MIM: 219500)
	Glutamate decarboxylase (GAD1 + 2; EC 4.1.1.15)	The decarboxylation of glutamate to GABA	The regulation of GABA-glutamate interconversion. Low GABA has been found in <i>ALDH7A1</i> ^{-/-} zebrafish and in a mouse model of hypophosphatasia with epilepsy	
	GABA-transaminase (GABA-T; EC 2.6.1.19)	The conversion of GABA + 2-oxoglutarate to succinate semialdehyde + L-glutamate	Amongst other pathways, important for the neuronal recycling of GABA to glutamate	GABA-transaminase deficiency causes developmental delay and neurological abnormalities (MIM: 613163)

	Aromatic L-amino acid decarboxylase (AADC; EC 4.1.1.28)	Among other activities, the conversion of L-DOPA to dopamine; 5-HTP to 5-HT; L-phenylalanine to phenethylamine and L-tyrosine to <i>p</i> -tyramine.	Synthesis of monoamine central and peripheral neurotransmitters including dopamine, adrenaline, noradrenaline and 5-HT	AADC deficiency causes serotonin/catecholamine deficiencies leading to hypotonia and other features of neurological dysfunction (MIM: 608643). Biochemically this is indicated by low CSF HVA & 5-HIAA and high CSF 3-OMD & 5-HTP, features of B ₆ metabolic disorders such as PNPO deficiency; these cause a secondary lack of AADC activity due to PLP deficiency
	Branched-chain amino acid aminotransferase (BCAT1 + 2; EC 2.6.1.42)	Conversion of branched-chain amino acids to branched chain α -keto acids and glutamate	Important for the regulation of glutamate production in the brain	
	L-Serine racemase (SRR; EC 5.1.1.18)	Racemisation of L-serine to D-serine	D-serine is important for neuronal migration and as a neurotransmitter	
	Alanine-glyoxylate aminotransferase (AGXT; EC 2.6.1.44)	Conversion of L-alanine + glyoxylate into pyruvate + glycine	Prevents the overproduction of oxalate and consequent renal stones	Deficiency causes primary hyperoxaluria, type 1 (MIM: 259900). May be pyridoxine-responsive
	Ornithine δ -aminotransferase (OAT; EC 2.6.1.13)	Reversibly transaminates ornithine to L-glutamate 5-semialdehyde	Important for the formation of glutamate/GABA, arginine and proline.	Deficiency causes gyrate atrophy of choroid and retina and hyperammonaemia in infancy (MIM: 258870). May be pyridoxine-responsive
	Phosphoserine aminotransferase (PSAT1; EC 2.6.1.52)	Reversible conversion of O-phospho-L-serine + 2-oxoglutarate to 3-phosphonooxypyruvate + L-glutamate.	Important for the biosynthesis of serine and glycine	Deficiency causes low plasma and CSF serine and glycine leading to intractable seizures, microcephaly, craniofacial dysmorphism, hypertonia and developmental delay (MIM: 610992; 616038)
	Tyrosine aminotransferase (TAT; EC 2.6.1.5)	Reversible liver-specific conversion of L-tyrosine + 2-oxoglutarate to 4-hydroxyphenylpyruvate + L-glutamate	Important for tyrosine catabolism	Deficiency causes tyrosinaemia type 2 (MIM: 276600) characterised by lesions of the cornea/skin and developmental delay

	Glycine C-acetyltransferase (GCAT; EC 2.3.1.29)	Responsible for the second step of L-threonine conversion to glycine, converting 2-amino-3-ketobutyrate + CoA to glycine + acetyl-CoA	Important for threonine catabolism	
	2-Aminoadipate aminotransferase (EC 2.6.1.39)	Reversibly converts L-2-aminoadipate + 2-oxoglutarate to 2-oxoadipate + L-glutamate	Important for lysine catabolism	
	Serine/threonine deaminase (SDS; EC 4.3.1.17)	Deamination of L-serine or L-threonine to form pyruvate or 2-oxobutanoate + ammonia/ammonium	Important for the formation of pyruvate and hence gluconeogenesis from amino acids	
Folate cycle and one-carbon metabolism	Serine hydroxyl methyltransferase (SHMT1 + 2; EC 2.1.2.1)	Reversible conversion of L-serine + tetrahydrofolate to glycine and 5,10-methylenetetrahydrofolate	Essential part of the folate cycle; neuronal cells deprived of B ₆ have low 5-methyltetrahydrofolate ⁴⁷	
	Glycine dehydrogenase (decarboxylating) (GLDC; EC 1.4.4.2)	The cleavage of glycine into CO ₂ + a protein-bound methylamine group	Essential part of the glycine cleavage system	Deficiency of GLDC and other enzymes in the glycine cleavage system cause glycine encephalopathy (MIM: 605899). High CSF glycine can be a feature of PLP deficiency
Protein Synthesis	O-phosphoserine-tRNA(Sec) selenium transferase (SEPSECS; EC 2.9.1.21)	Transfers selenium from a selenophosphate to O-phospho-L-seryl-tRNA(Sec) forming L-selenocysteinyl-tRNA(Sec)	Selenocysteinyl-tRNA(Sec) is the tRNA required for synthesis of selenoproteins	Deficiency causes pontocerebellar hypoplasia type 2D characterised by progressive microcephaly and developmental delay (MIM: 613811)
Carbohydrate metabolism	Glycogen phosphorylase (PYG(M[uscle],L[liver],B[brain])); EC 2.4.1.1)	Liberation of glucose-1-phosphate from the terminal 1,4-glycosidic bond of glycogen	The rate-limiting step in glycogenolysis	Deficiency of PYGM + PYGL cause glycogen storage disease types V + VI, respectively (MIM: 232600 + 232700). Severe PLP deficiency can cause hypoglycaemia
	Various - see amino acid and neurotransmitter metabolism (AST, ALT, AGXT, KYAT, GABA-T, BCAT, TAT, SDS)	Various – see amino acid and neurotransmitter metabolism	Gluconeogenesis from amino acids	Severe PLP deficiency can cause hypoglycaemia.

Lipid Metabolism	Serine palmitoyltransferase (SPT; EC 2.3.1.50)	Conversion of palmitoyl-CoA + L-serine into CoA, 3-dehydro-D-sphinganine and CO ₂	A step in the synthesis of sphingosine and therefore many additional sphingolipids	Mutations cause hereditary sensory neuropathy type IA (MIM: 162400)
	Sphingosine-1-phosphate lyase (SGPL1; EC 4.1.2.27)	Converts sphingosine 1-phosphate to phosphoethanolamine + palmitaldehyde	Important for the regulation of phospholipid signalling through S1P	Deficiency causes a nephrotic syndrome with systemic manifestations (MIM: 617575)
Mitochondrial Function and Erythropoiesis	Δ-Aminolevulinic acid synthase (ALAS1 + 2; EC 2.3.1.37)	Conversion of succinyl-CoA + glycine into CoA, Δ-Aminolevulinic acid and CO ₂	Required for haem biosynthesis	ALAS2 (erythroid-specific) deficiency causes sideroblastic anaemia (MIM: 300751). Anaemia and lactic acidosis are common features of severe PLP-deficiency
	Cysteine desulfurase (NFS1; EC 2.8.1.7)	The conversion of L-cysteine to L-alanine by transferring the sulfur-group of free cysteine onto a cysteine residue of the NFS enzyme	Part of the Fe-S core complex, essential for Fe-S cluster formation	Deficiency causes myopathy with lactic acidosis (MIM: 255125)
Molybdenum cofactor synthesis	Molybdenum cofactor sulfurase (MOCOS; EC 2.8.1.9)	Sulphuration of the molybdenum cofactor of xanthine dehydrogenase (XDH; 607633) and aldehyde oxidase (AOX1; 602841)	XDH activity is required for purine metabolism and AOX1 is an promiscuous oxidase with several important activities	Deficiency causes xanthinuria type II (MIM: 603592). Can lead to urinary tract calculi, renal failure and myositis due to xanthine deposition
Synthesis of Polyamines	Ornithine decarboxylase (ODC1; EC 4.1.1.17)	Decarboxylation of ornithine to form putrescine	Polyamines are involved in cell signalling, growth and programmed death	

1.1.3 Non-enzymatic roles of the B₆ vitamers

Reports suggest that the B₆ vitamers may have important activities unrelated to their action as a cofactor. PLP is known to interact with P2 purinoceptor 7 receptors (P2X7R), thought to be linked to neuronal ATP-mediated inflammation⁴⁸ and recently identified as a potential target for the treatment of AED-resistant epilepsy.⁴⁹⁻⁵⁰ B₆ vitamers are also antioxidants and can quench singlet oxygen effectively.⁵¹ PLP has been shown to affect gene expression in mammals through modulation of the transcription and activity of steroid hormone receptors.⁵²⁻⁵³

1.1.4 The reactivity of pyridoxal 5'-phosphate – a mixed blessing

Pyridoxal 5'-phosphate contains a reactive aldehyde at the 4' position. This reactivity is essential for its role as a cofactor and, as mentioned previously (**Section 1.1.2**), leads to the formation of covalent Schiff bases with ϵ -amino groups of active site lysines in PLP-dependent enzymes.⁵⁴ However, PLP can also react non-specifically with compounds containing an amine group.^{28, 55} This provides the cell with a very specific problem; how to supply PLP to the apoenzymes that require it as a cofactor, while simultaneously keeping free PLP low enough to avoid unwanted side reactions with both small molecules and proteins.²⁸ These side reactions can result in the inhibition of enzymatic activity through the alteration of protein structure.⁵⁶⁻⁵⁷ Aldehydes can also directly damage DNA.⁵⁸

There are several known mechanisms by which the human body maintains free PLP concentrations. Firstly, as mentioned previously (**Section 1.1.1**), PNPO is subject to product inhibition by PLP.^{36, 59} Evidence *in vitro* also suggests that PNPO helps to protect newly synthesised PLP; it has been proposed that PNPO contains a secondary PLP binding site, enabling it to function as a chaperone, directly delivering PLP to the target apoenzymes.⁶⁰ Additionally, PLP in blood is found mostly bound to albumin (ϵ Lys190) in plasma, or haemoglobin (ϵ Lys82 or α Val1) in red blood cells;^{19, 61} this protects it from degradation by the phosphatases (such as TNSALP) present in blood and also from reacting with other nucleophilic compounds in plasma or red blood cells. Similarly, pyridoxal 5'-phosphate homeostasis protein (PLPHP; previously known as PROSC or PLPBP) has recently been proposed as an intracellular chaperone of PLP.^{27, 62} Homologues of PLPHP are highly conserved across species, in *E. Coli* as YggS and yeast as YBL036C, suggesting an important cellular function.

1.2 Inborn errors affecting vitamin B₆ metabolism

Although vitamin B₆ deficiency is uncommon due to the prevalence of dietary B₆, there are several disorders which can lead to a specific deficiency of bioavailable PLP. These include inborn errors which affect the B₆ metabolic pathway i.e. PNPO deficiency [MIM: 610090]⁶³, those which result in the inactivation of free PLP (e.g. Pyridoxine Dependent Epilepsy [PDE] due to mutations in *ALDH7A1*) [MIM: 266100]⁶⁴ and a disorder which is thought to cause aberrant intracellular regulation and trafficking of PLP (i.e. PLPHP deficiency [MIM: 617290]).²⁷ These disorders are typically characterised by neonatal/infantile-onset seizures refractive to standard AEDs but responsive to vitamin B₆ supplementation^{2, 27}.

Although B₆-responsive seizures dominate the clinical pictures of PNPO, PLPHP and *ALDH7A1* deficiencies, in the neonate systemic features such as lactic acidosis and anaemia may also be present. In all three disorders developmental delay is common in patients that survive into infancy. However, when treated promptly and appropriately, some individuals can have a normal developmental outcome. This is particularly evident in cases of PLPHP and PNPO deficiency.⁶⁵⁻⁶⁶ A summary of the clinical and biochemical features of pyridoxine-dependent epilepsy due to mutations in *ALDH7A1* and PNPO deficiency can be found in **Figures 1.3 and 1.4**, respectively. To date, 27 individuals have been reported with PLPHP deficiency. The clinical spectrum of this disorder appears broad, ranging from severe seizures immediately after birth alongside profound microcephaly and intellectual disability to seizure onset after 9 days of life and a normal developmental outcome at 30 years of age.^{27, 29, 67-68}

Other inborn errors of metabolism which can result in B₆-responsive epilepsy include hypophosphatasia (MIM: 241500), glycosylphosphatidylinositol (GPI) anchor defects (MIM: 239300; 614749) and hyperprolinaemia type 2 (HPH [MIM: 239510]). These can cause B₆-responsive seizures but are either clinically distinct from PNPO/PLPHP deficiency and PDE (in the cases of hypophosphatasia and GPI anchor defects) or very rare and leading to seizures only infrequently, in the case of HPH (**Table 1.2**).⁶⁹⁻⁷¹ Recently, compound heterozygous variants were identified in the *GOT2* gene encoding mitochondrial glutamate oxaloacetate transaminase (mGOT) in a child with acquired microcephaly, severe seizures and spasticity alongside low plasma and CSF serine. Treatment with pyridoxine and serine supplements was effective for seizure resolution.⁴⁶

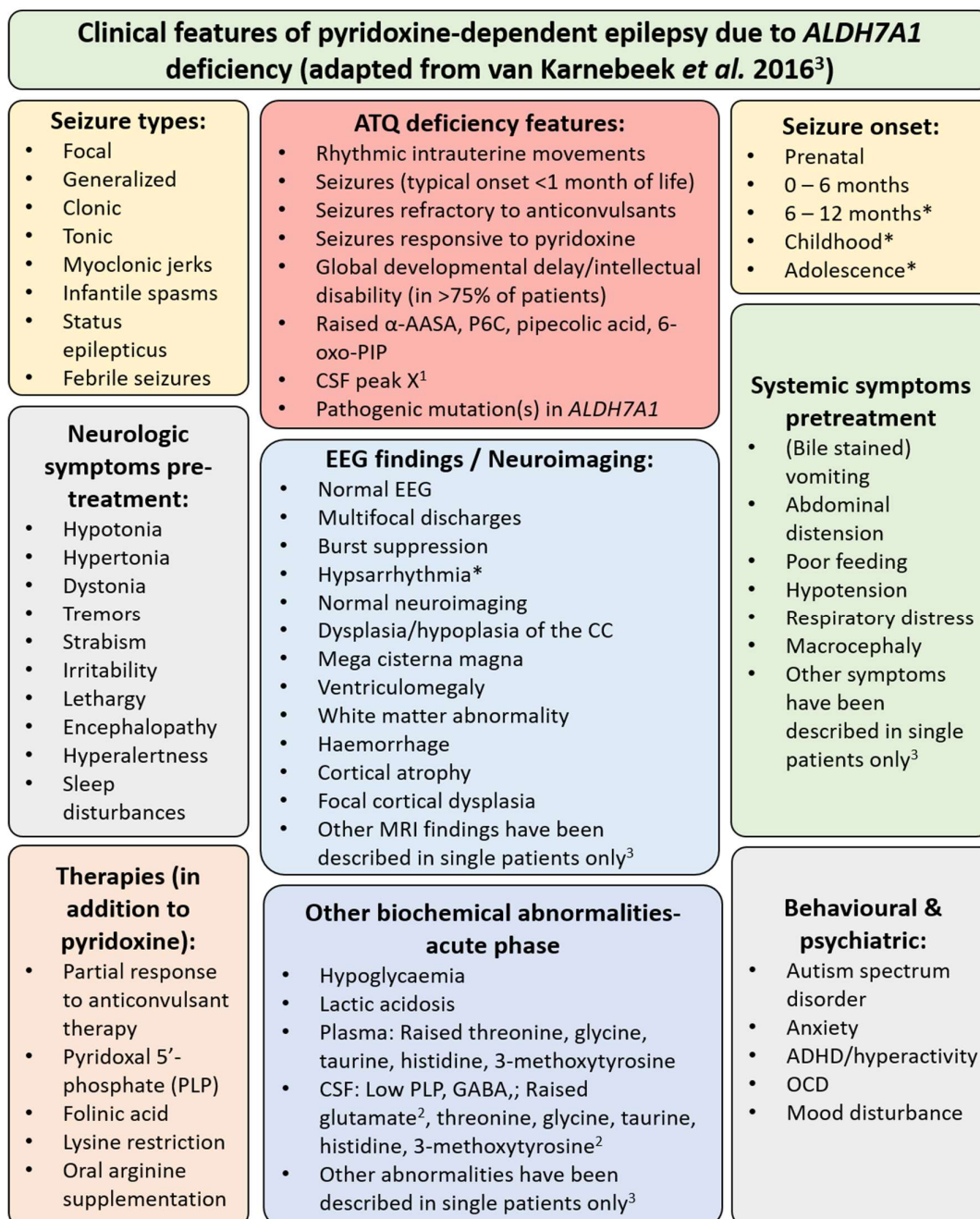


Figure 1.3: Overview of the symptoms reported in the literature for patients with ATQ deficiency. Red box: symptoms or biochemical features present in the majority of patients. All other boxes: symptoms present in the minority of patients. *Ultra-rare symptoms, reported in eight literature patients or fewer. ¹Unidentified peak in the HPLC chromatogram for CSF monoamine neurotransmitter analysis in ATQ deficiency patients. ²Can normalise on pyridoxine therapy. ³See van Karnebeek *et al.* 2016. 6-oxo-PIP, 6-oxo-pipecolic acid; α -AASA, α -amino adipic semialdehyde; ADHD, attention deficit hyperactivity disorder; ATQ, antequitin; CC, corpus callosum; CSF, cerebrospinal fluid; GABA, gamma-aminobutyric acid; OCD, obsessive-compulsive disorder; P6C, L- Δ 1-piperidine-6 carboxylate.

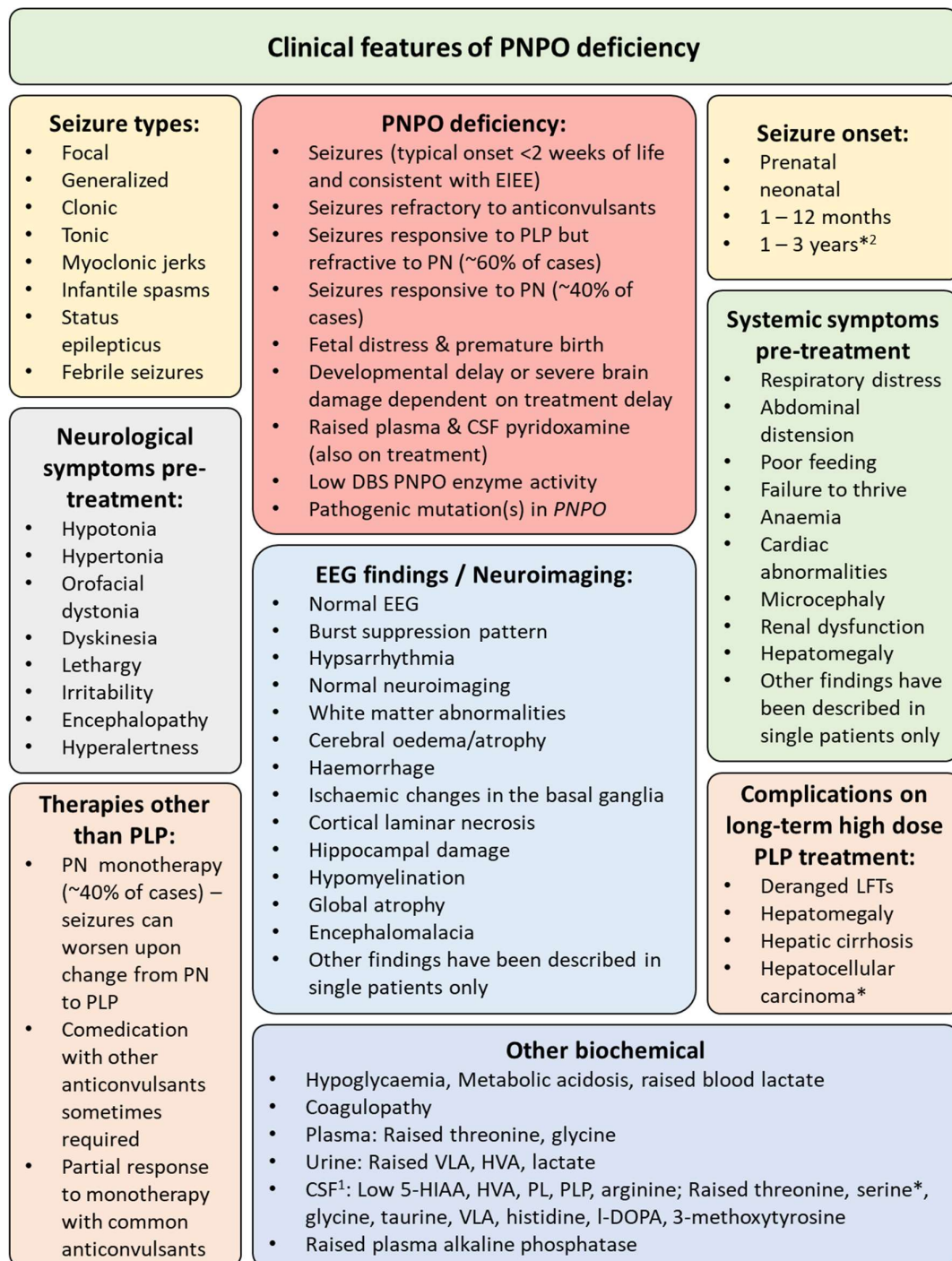


Figure 1.4: Overview of the symptoms reported in the literature for patients with PNPO deficiency. Red box: symptoms or biochemical features present in the majority of patients. All other boxes: symptoms present in the minority of patients. *Ultra-rare symptoms, reported in three literature patients or fewer. ¹Can normalise on effective treatment with PLP/PN. ²Seizure onset after 1 year seen with patients homozygous for the p.R116Q variant in PNPO. α -AASA, α -aminoadipic semialdehyde; ADHD, attention deficit hyperactivity disorder; ATQ, antitiquitin; CSF, cerebrospinal fluid; GABA, gamma-aminobutyric acid; OCD, obsessive-compulsive disorder; P6C, L- Δ 1-piperidine-6 carboxylate; DBS, dried blood spot; VLA, vanillactic acid; HVA, homovanillic acid; 5-HIAA, 5-hydroxyindoleacetic acid; PL, pyridoxal; PLP, pyridoxal 5'-phosphate; L-DOPA, L-3,4-dihydroxyphenylalanine; EIEE, early infantile epileptic encephalopathy; LFT, liver function test; PN, pyridoxine.

Table 1.2: Clinical and biochemical features of inborn errors leading to B₆-responsive seizures. α-AASA = α-aminoadipic semialdehyde; NEE = neonatal epileptic encephalopathy; P5C = Δ¹-pyrroline-5-carboxylate; GPI = glycosylphosphatidylinositol; DBS = dried blood spot. Presentation of B₆-responsive seizure disorders is often dependent upon prompt and appropriate treatment e.g. MRI abnormalities can be a consequence of NEE and are usually present only in patients with a more severe form of the disorder or those with delayed treatment. + Usually present; ± Variably present; - Not present.

Inborn Error	ALDH7A1/ATQ deficiency	PNPO deficiency	PLPHP deficiency	Hyperprolinaemia type II	Hypophosphatasia	GPI anchor defects	Molybdenum cofactor deficiency
Genetic locus	<i>ALDH7A1</i>	<i>PNPO</i>	<i>PLPBP (PROSC)</i>	<i>ALDH4A1</i>	<i>ALPL</i>	<i>PIGO</i> ; <i>PIGV</i> (+ others)	<i>MOCS1</i> ; <i>MOCS2</i> ; <i>GPHN</i>
Neonatal/infantile B ₆ -responsive seizures	± A few patients have presented with onset after the 1 st year of life ⁷² and as late as adolescence ⁷³	± A few patients have presented with onset after 1 st year of life ⁷⁴	+	± (~50% of cases; seizure onset usually in infancy or childhood) ⁷⁵	± Only 7.5% of hypophosphatasia cases are infantile – not all of these present with seizures ⁷⁶	± Variable presentation according to specific GPI defect ⁷⁷	± Only isolated cases reported to respond to pyridoxine ⁷⁸
Prevalence of Developmental delay	± 75% have developmental abnormalities ⁷⁹	± Can be developmentally normal – linked to early treatment (13/41 Guerin <i>et al.</i>) ⁸⁰	+	± Asymptomatic individuals described ⁸¹ but in the absence of developmental delay behavioural problems/psychosis/anxiety are usually present ⁸²	± Not in milder cases ⁸³	+	+

Some cases resistant to pyridoxine	- Ambiguous initial response is seen in about 15% ⁶⁶	± ~60% of cases ⁸⁰	-	-	± ⁸⁵	± Proportion unknown ⁷⁷	± Only isolated cases reported to respond to pyridoxine ⁷⁸
Skeletal abnormalities	± Macrocephaly, facial dysmorphism in rare cases ⁸⁶	± Microcephaly in severe, untreated cases	± Microcephaly at birth 4/14; acquired microcephaly in an additional 4/14 ^{27, 67-68}	-	+ Similar to rickets; less pronounced in mild cases – some only dental ⁸³	+ Brachytelephalangy	± Microcephaly common ⁸⁴
Abnormal MRI (including white matter changes)	± Including narrow corpus callosum (especially posterior), dilated ventricles, small cerebellum ⁷²	± May have changes (including white matter oedema) as a result of untreated NEE ⁸⁷ Normal in 37% (5/15) ⁸⁰	± Global underdevelopment (Coarse gyri shallow sulci) + underdeveloped white matter ²⁷	-	-	± In one case of PIGO: Hypomyelination; Lesions in the bilateral basal ganglia and brainstem ⁷¹	+ Delayed myelination, enlarged ventricles, cerebral atrophy in >40%; corpus callosum & cerebellar atrophy in >20% ⁸⁴
Parental history of infertility, miscarriage or prematurity	-	± 8/22 families ⁸⁷	-	-	-	-	-
Unique biochemical features (Among B₆-responsive seizure disorders)	Raised plasma + urinary α-AASA ⁷² but normal urinary S-sulphocysteine	Raised plasma pyridoxamine/pyridoxic acid ratio ⁸⁸ ; low DBS PNPO enzyme activity (<40% below the normal range) ⁸⁹	N/A	Raised plasma proline and P5C; Raised urinary P5C and N-(pyrrole-2-carboxyl) glycine ^{2, 90}	Low plasma alkaline phosphatase; high plasma phosphate, urine phosphoserine & phosphoethanolamine	Raised plasma alkaline phosphatase	Raised plasma + urinary α-AASA AND raised urinary S-sulfocysteine/xanthine/taurine ⁹¹

The mechanism causing PLP deficiency in cases of PNPO deficiency is the inability to convert PNP and PMP to PLP; this is important in the synthesis of PLP from dietary precursors and also for the recycling (salvage) pathway.⁶³ The mechanism behind the PLP deficiency seen in patients with mutations in *ALDH7A1* is related to the reactive nature of PLP. Low ALDH7A1 activity leads to a block in the lysine catabolic pathway, resulting in high concentrations of alpha-amino adipic semialdehyde (α -AASA) and its cyclic analogue, Δ^1 -piperidine-6-carboxylate, the latter of which reacts with and inactivates PLP.⁶⁴ Very recently, 6-oxo-pipecolic acid has been tentatively identified as a novel biomarker for ALDH7A1 deficiency but further work is required in order to confirm this finding.⁹² Less clear is the mechanism behind PLPHP deficiency. This is not fully understood as the function of PLPHP has yet to be fully elucidated. However, it has been hypothesised that the absence of three postulated aspects of PLPHP function lead to pathogenesis: i) PLPHP protects PLP from intracellular phosphatases; ii) PLPHP directly supplies PLP to apoenzymes; iii) PLPHP acts as a carrier, preventing PLP from reacting with other molecules.²⁷

In HPIL, the mechanism involved in decreased PLP bioavailability is similar to that which occurs in ALDH7A1 deficiency, namely inactivation of PLP by a metabolite (i.e. Δ^1 -pyrroline-5-carboxylate) which accumulates due to a metabolic block in the proline catabolic pathway.² The B₆-responsive epilepsy seen in hypophosphatasia and GPI anchor defects is caused by the inability to hydrolyse plasma PLP, sequestering it in the circulatory system.

The mechanism behind the seizures and other features of neurological dysfunction that result from PLP deficiency in the brain are not entirely understood. There is however direct evidence of alterations in the activity of PLP-dependent enzymes involved in neurotransmitter metabolism. Imbalances in GABA, glutamate, serotonin and dopamine are postulated to lead to the epilepsy seen in PLP deficiency.⁹³ High glutamate and/or low GABA in particular could provide potentially excitotoxic conditions leading to seizures⁹⁴⁻⁹⁶; this hypothesis has been explored on various occasions and in different models^{47, 97} but results have sometimes been inconclusive, in part due to the difficulties encountered equating CSF neurotransmitter metabolite concentrations with those in the brain itself.

Several of the other features of severe PLP deficiency such as lactic acidosis and hypoglycaemia can be explained by deficient activity of PLP-dependent enzymes. These enzymes are summarised in **Table 1.3**, alongside the postulated biochemical

mechanisms leading to the clinical phenotypes caused by the deficiency of PLP-dependent enzymes.

Table 1.3: Clinical and biochemical presentations caused by perturbed function of PLP-dependent enzymes in a PLP deficient state. Abbreviations: pyridoxal 5'-phosphate (PLP); γ -aminobutyric acid (GABA); 5-hydroxytryptophan (5-HTP); 5-hydroxytryptamine (5-HT, serotonin); cerebrospinal fluid (CSF); vanillic acid (VA); homovallinic acid (HVA); 5-hydroxyindoleacetic acid (5-HIAA); 3-O-methyldopa (3-OMD, 3-methoxytyrosine); N-methyl-D-aspartate (NMDA).

Clinical or biochemical features identified in individuals with impaired vitamin B ₆ metabolism	Implicated PLP-dependent enzymes	Mechanism
Seizures	Branched-chain amino acid aminotransferase (BCAT1 + 2; EC 2.6.1.42)	Major source of glutamate in the brain
	Glutamate decarboxylase (GAD1 + 2; EC 4.1.1.15)	GAD produces GABA from glutamate; GABA-T produces glutamate from GABA. Both are therefore important for the regulation of neuronal GABA/glutamate interconversion and therefore neuronal excitability. Imbalances of these neurotransmitters are thought to explain the seizures caused by PLP deficiency. Low GABA has been found in <i>ALDH7A1</i> ^{-/-} zebrafish and in a mouse model of hypophosphatasia with epilepsy.
	GABA-transaminase (GABA-T; EC 2.6.1.19)	
Dystonic movements	Aromatic L-amino acid decarboxylase (AADC; EC 4.1.1.28)	Deranged regulation of serotonin and catecholamine neurotransmitters leads to dystonia and a characteristic CSF neurotransmitter profile seen in both primary AADC deficiency and that which is secondary to severe PLP deficiency.
Low CSF HVA & 5-HIAA; raised VA & 3-OMD		
Neuronal migration defects	L-Serine racemase (SRR; EC 5.1.1.18)	Deficiency leads to an inability to form D-serine, implicated in neuronal migration & neurotransmission through NMDA receptors. Although rare, neuronal migration defects and dysplasia have been identified in individuals with perturbed vitamin B ₆ metabolism
Anaemia & lactic acidosis	Δ -Aminolevulinic acid synthase (ALAS1 + 2; EC 2.3.1.37)	Disordered haem and Fe-S cluster synthesis due to severe PLP deficiency leads to haematological abnormalities and lactic acidosis.
	Cysteine desulfurase (NFS1; EC 2.8.1.7)	

Hypoglycaemia	Aspartate transaminase (AST or GOT; EC 2.6.1.1)	Important for the formation of pyruvate and therefore gluconeogenesis from amino acids. Mitochondrial GOT important for the malate-aspartate shuttle.
	Alanine transaminase (ALT or GPT1 + 2; EC 2.6.1.2)	
	Serine/threonine deaminase (SDS; EC 4.3.1.17)	
	Glycogen phosphorylase (PYG(M[uscle],L[iver],B[rain])); EC 2.4.1.1)	The rate-limiting step in glycogenolysis. Severe PLP deficiency leads to the inability to liberate sufficient glucose from stored glycogen through the action of hepatic phosphorylase
Disordered plasma & CSF serine, threonine and glycine	Serine hydroxymethyltransferase (SHMT1 + 2; EC 2.1.2.1)	These enzymes are important for the biosynthesis and catabolism of serine, threonine, glycine and for the folate cycle. Recently, an <i>in vitro</i> study of neuronal cells has reported reduced synthesis of serine and glycine cultured in B ₆ -deficient medium; the homeostasis of these amino acids is complex and tissue-specific. This manifests in severely PLP deficient humans as high concentrations of threonine, serine and glycine in plasma and CSF. Neuronal cells deprived of B ₆ have low 5-methyltetrahydrofolate due to SHMT deficiency.
	Glycine dehydrogenase (decarboxylating) (GLDC; EC 1.4.4.2; component of the glycine cleavage system)	
	Serine/threonine deaminase (SDS; EC 4.3.1.17)	
	Phosphoserine aminotransferase (PSAT1; EC 2.6.1.52)	
	Glycine C-acetyltransferase (GCAT; EC 2.3.1.29)	
Elevated urinary xanthurenic acid	Kynureninase (KYNU; EC 3.7.1.3)	Impaired tryptophan catabolism leads to elevated urinary xanthurenic acid excretion in cases of PLP deficiency
	Kynurenine aminotransferase (KYAT1 & 2; EC 2.6.1.7)	

1.2.1 Diagnosis and treatment of vitamin B₆-responsive seizure disorders

In a neonate presenting with seizures, a challenge for the treating clinician is to diagnose a B₆-responsive disorder alongside much commoner causes of neonatal seizures. Within these disorders, once a response to B₆ supplementation is identified, the similarity seen in the clinical pictures of PNPO, PLPHP and ALDH7A1 deficiencies means they are often difficult to distinguish diagnostically. It was previously thought possible to differentiate between PNPO and ALDH7A1 deficiencies by identifying an anticonvulsant effect of PLP, but resistance to PN, in PNPO deficiency. However,

more recently it has been shown that approximately 40% of PNPO deficient individuals respond to PN supplementation.^{80, 87, 98}

After the identification of a specific anti-epileptic response to either PLP or PN, differential diagnosis of these three disorders is currently performed by sequencing of candidate genes or, in the case of PDE, detection of a raised urinary α -AASA concentration.⁶⁴ Sequencing is performed either on a single gene basis or as part of a gene panel. This genetic analysis is often not requested until after α -AASA measurement. It can therefore take several months to achieve a diagnosis. Prompt and appropriate treatment of PNPO deficiency is extremely important for prognosis; reports suggest that this is a major factor in facilitating a normal developmental outcome.^{65, 99}

Several methods have been proposed for the diagnosis of PNPO deficiency but have proven unreliable. Indeed, no specific biomarker exists for its diagnosis. Low CSF PLP prior to treatment is characteristic of the disorder and was previously considered a consistent biomarker.¹⁰⁰ However, recently a patient in whom CSF PLP levels were normal has been reported.¹⁰¹ Equally, deficiency of ALDH7A1¹⁰² and PLPHP²⁷ can also lead to low CSF PLP. Initially, Darin *et al.*²⁷ reported that, in PLPHP deficiency, plasma PLP concentrations were higher, on treatment, than that seen in PNPO and ALDH7A1 deficiencies. However, this finding was recently shown to be inconsistent.⁶⁷

The CSF neurotransmitter metabolite profiles of PNPO deficient children have also been used in the diagnostic workup of this disorder. Although some patterns characteristic of low PLP-dependent enzyme activity such as high 3-O-methyldopa (3-OMD) or threonine and low homovanillic acid (HVA) or 5-hydroxyindoleacetic acid (5-HIAA) have emerged, these are not present in all patients or may only be transient. They can also be found in the other B₆-responsive seizure disorders and are likely suggestive of PLP deficiency rather than PNPO deficiency itself.²⁷

A raised plasma pyridoxamine/pyridoxic acid ratio has recently been suggested as a specific biomarker of PNPO deficiency, seemingly due to an accumulation of pyridoxamine caused by low PNPO activity.⁸⁸ However, this study included only six PNPO deficient patients, four of whom were homozygous for the same p.R225H variant. Whether this finding is consistent in more patients with a wide range of mutations and in samples taken prior to high-dose B₆ supplementation remains to be seen.

Typically, oral supplements of either PN or PLP are used for the long term treatment of B₆-dependent seizure disorders. High dose PLP is unpalatable and can lead to emesis; compliance can be problematic, particularly in infants.^(personal communication) Intravenous infusion preparations of both compounds exist but for PLP this is available only in Japan.

Recently there have been reports of raised liver function tests (LFTs) and hepatic cirrhosis in patients receiving high-dose PLP supplementation (> 30 mg/kg/d).^{99, 103} Hepatotoxicity has not been identified in individuals receiving PN for seizure control. In aqueous solution some B₆ vitamers, particularly PLP, are photolabile.¹⁰⁴⁻¹⁰⁶ It is possible that photodegradation products of PLP are hepatotoxic. Another hypothesis is that supraphysiological concentrations of one or more of the B₆ vitamers cause liver damage. The plasma concentrations of PLP and PL in those receiving PLP for seizure control can be 10-1000 times higher than the normal range.²² In the liver of a PNPO deficient patient receiving 50 mg/kg/d PLP, the pyridoxal concentration measured after hydrolysis of phosphate esters was approximately 40 times higher than that of a control. However, this patient had also presented with hepatic cirrhosis, the effect of this upon B₆ vitamer concentrations is unknown.¹⁰³

Patients receiving high-dose long-term PN supplementation do not develop liver damage but a side effect of PN supplementation is peripheral neuropathy.¹⁰⁷ This is thought to be due to inhibition of PLP-dependent enzymes in peripheral nerves and is similar to that seen upon PLP deficiency induced by high doses of isoniazid or theophylline.¹⁰⁸⁻¹¹¹

1.2.2 Vitamin B₆ for the treatment of genetic epilepsies

Although in Europe and the United States, PN and PLP are occasionally used as second-line treatment options for patients with drug-resistant epilepsy, in Japan B₆ supplementation is often used as a first-line treatment option.¹¹² Indeed, there is an increasing body of evidence that epilepsies other than those that directly affect B₆ metabolism can benefit from PN/PLP supplementation.

Wang *et al.* reported that 11/94 children with idiopathic intractable epilepsy showed a dramatic and sustained response to PLP supplementation. In these patients PLP was more effective than PN for seizure control.¹¹³ Ohtahara *et al.* found high-dose vitamin B₆ supplementation was effective for seizure control in 13.9% of West syndrome

cases, including 11.5% of those with identifiable brain pathologies.¹¹⁴ Recent research in mice has shown that B₆ is a modifier of seizure severity in a model of SCN1A (Dravet syndrome) epilepsy^{113,115}, another indication that vitamin B₆ supplementation of affected individuals could be important in the management of a number of epilepsies with varying aetiologies.

It has also been reported that epilepsy caused by dominant mutations in the *KCNQ2* gene are particularly amenable to treatment with PLP.¹¹⁶⁻¹¹⁷ The *KCNQ2* protein is a major constituent of the KCNQ or 'M'-channels, these modulate the M-current, responsible for maintaining the resting potential of neurons and thus regulating neuronal excitability.¹¹⁸ M-channel openers such as retigabine can be used to treat epilepsy.¹¹⁹ Preservation of the M-current is also linked to the antiepileptic effect of valproate.¹²⁰ The mechanism behind a response to vitamin B₆ supplementation in individuals with *KCNQ2* mutations has yet to be characterised.

The concentration of PLP in the CSF of children with epilepsy has recently been shown to be lower than controls.¹²¹ Although this finding has not been consistent¹⁰², it is possible that the low CSF PLP seen in these patients is due to a secondary B₆ deficiency caused by poor nutrition of these often severely ill children. Another hypothesis however is that the seizures are causing a depletion of PLP through the creation of reactive oxygen species (ROS) or increased neurotransmitter turnover due to neuronal excitotoxicity. ROS and oxidative stress are hypothesised to be epileptogenic factors¹²² and PLP is protective against oxidative stress.¹²³

Supplementation with vitamin B₆ could result in improved seizure control either by attenuating oxidative stress or simply replacing the PLP lost to reaction with ROS, or increased neurotransmitter turnover, hence rescuing a relative PLP-deficient state.¹²⁴ Currently however, it is unknown whether this seizure control conveyed by vitamin B₆ is due to a rescuing of relative PLP deficiency or whether PLP itself is having a direct anti-convulsant effect.¹²⁵

The identification of existing and novel genetic epilepsies amenable to vitamin B₆ supplementation is a priority in order to aid the treatment of individuals with these disorders. In addition, there are several genes encoding proteins linked to vitamin B₆ metabolism in which pathogenic variants have not been identified, but disorders caused by mutations in these genes could be amenable to treatment. These include the *PDXK* and *PDXP* genes encoding PK and PLPase, respectively, and the *SLC25A39/40* genes, predicted to encode mitochondrial B₆ transporters.

1.3 LC-MS/MS for the diagnosis of inborn errors of metabolism.

In the last 20 years, the importance of tandem mass spectrometry (MS/MS) for the diagnosis of inborn errors of metabolism has been steadily growing, particularly when coupled with an additional liquid chromatography (LC) separation step prior to MS/MS analysis.¹²⁶⁻¹²⁸ Although traditionally more expensive and requiring greater technical expertise than other methods¹²⁹, LC-MS/MS provides unrivalled specificity and sensitivity in the field of clinical biochemistry, particularly for the analysis of small to medium biomolecules.¹³⁰⁻¹³¹

Liquid chromatography separates molecules of interest according to their variable affinity for a stationary phase when dissolved in a mobile (liquid) phase. This affinity depends on the chemistry of each individual compound as well as the composition of the mobile and stationary phases. By varying these parameters, a wide range of biomolecules can be separated from one another by the time it takes for them to elute from the column and reach a detector (the retention time). Prior to recent years, the length of time taken for LC separation was a concern with regards to clinical utility. However, the introduction of instrumentation capable of maintaining a higher mobile phase pressure, usually up to 15,000 psi¹³², has enabled the use of smaller stationary phase particle sizes of 1.6 – 1.8 μm . This has reduced a typical LC method length from > 20 to < 5 minutes¹³³ while maintaining chromatographic separation, thereby enhancing practicability in the clinical diagnostic arena.

The commonest type of tandem mass spectrometry used clinically is electrospray ionisation (ESI)-MS/MS analysis. This utilises two mass analysis steps, separated by a fragmentation step, typically colliding the ions of interest with an inert gas such as argon. This type of fragmentation is termed collision-induced dissociation (CID) and the process as a whole can be called 'triple quadrupole mass spectrometry', referring to the two mass analyser quadrupoles separated by a radio frequency (RF)-only quadrupole acting as the collision cell.

In brief, MS/MS analysis is performed as follows: firstly, ions pertaining to the molecule of interest are formed in an ion source and selected according to their mass-to-charge (m/z) ratio at the first quadrupole (Q_1). 'Precursor ions' selected for analysis are then fragmented in the collision cell (q_2) via CID, before proceeding to the second mass analyser (Q_3) where 'product ions' are analysed, again according to their m/z

ratio (**Figure 1.5**). The use of CID allows for an increased level of selectivity as isobaric ions can be separated according to their fragmentation into specific product ions. Modern tandem mass spectrometers are capable of the analysis of many precursor and product ions simultaneously, by rapidly switching between the monitoring of different m/z ratios. This is termed multiple reaction monitoring (MRM) and enables the quantification of many compounds from one LC injection.¹³⁰

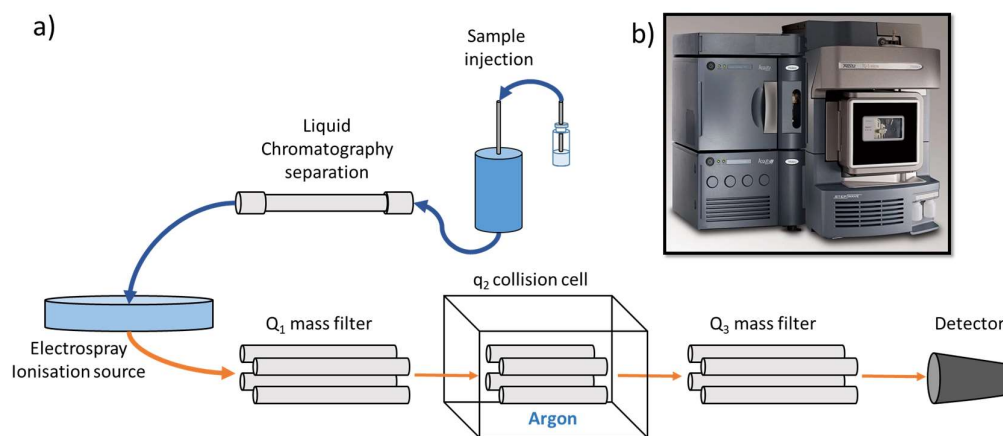


Figure 1.5: Liquid chromatography-tandem mass spectrometry. a) Schematic of a typical LC-MS/MS system. b) Waters Acquity I-Class LC coupled to a Xevo TQ-S mass spectrometer, a modern LC-MS/MS system used in clinical laboratories.

LC-MS/MS analysis is rendered quantitative by the use of isotopically labelled internal standards. Typically, this internal standard is identical to the molecule of interest apart from being labelled with several ^{15}N , ^{13}C or ^2H atoms. By using the ratio of the non-labelled analyte against that of the isotope-labelled internal standard, more accurate quantification is enabled and the effect of sample matrix minimised and often eliminated. In addition, analytical error introduced during sample preparation is reduced.¹³⁴

With regards to clinical application, the use of LC coupled with MS/MS allows for improved specificity, as compounds are separated according to both affinity for the stationary phase, molecular weight (as an m/z ratio), and fragmentation via CID. MS/MS analysis is also enhanced by LC separation as this step reduces the number of co-eluting compounds, enhancing sensitivity.¹³⁵

Within the field of inborn errors of metabolism, applications of LC-MS/MS (or other MS-based techniques) include newborn screening for the detection of, amongst other disorders, phenylketonuria (PKU)¹³⁶, maple syrup urine disease (MSUD)¹³⁷, medium-chain acyl-CoA dehydrogenase deficiency (MCADD)¹³⁸ and isovaleric acidaemia.¹³⁹

LC-MS/MS methods are also widely used for the diagnosis of a wide variety of lysosomal storage disorders such as the mucopolysaccharidoses¹⁴⁰, Gaucher, Pompe, Krabbe and Fabry diseases¹⁴¹ and Niemann-Pick disease types A/B¹⁴² and C.¹⁴³ Clinical diagnostic laboratories are also moving towards LC-MS/MS for more routine analyses such as the quantification of amino acids from plasma, useful for the diagnosis of a wide variety of metabolic disorders.¹⁴⁴ Specific to disorders causing vitamin B₆ dependent epilepsy, LC-MS/MS methods exist for the quantification of α -AASA and P6C, important for the diagnosis of pyridoxine-dependent epilepsy due to mutations in *ALDH7A1*.⁶⁴ LC-MS/MS is also useful for the measurement of B₆ vitamers in plasma and CSF.²²

Many of the recently developed methods mentioned above utilise dried blood spots (DBS) as a sample matrix. The application of a small amount of venous or capillary blood to filter paper is a convenient way to collect samples, particularly from infants. Storage of blood samples as DBS improves the stability of many analytes, including proteins, and often removes the need for freezing of the sample on storage.¹⁴⁵⁻¹⁴⁸

DBS were first developed by Dr. Robert Guthrie for the neonatal detection of PKU in the 1960s.¹⁴⁹ Their use has since expanded to newborn screening programs around the world. The enhanced sensitivity of LC-MS/MS equipment allows the detection of less abundant analytes from the small sample volumes found in DBS. This often requires only an elution step and subsequent analysis of this eluent.¹⁴⁵ In recent years, diagnostic DBS tests have also been developed using the protein contained in a DBS sample to quantify the activity of a specific enzyme within the blood. Currently these are mostly limited to the diagnosis of lysosomal storage disorders.¹⁵⁰⁻¹⁵⁴

1.4 Aims and scope of this thesis

The aims of this thesis are to:

- Develop an LC-MS/MS-based method to profile the B₆ vitamers in dried blood spots from individuals with vitamin B₆-dependent seizure disorders and, using this method, identify metabolite patterns that could aid the diagnosis or treatment of these individuals.
- Develop an LC-MS/MS-based method for the measurement of PNPO activity from dried blood spots and determine if this method is a useful tool for the diagnosis of PNPO deficiency.
- Characterise the biochemical abnormalities in a family with peripheral neuropathy thought to be caused by a pathogenic variant in the *PDXK* gene encoding pyridoxal kinase.
- Characterise the photodegradation profile of PLP in aqueous solution in order to advise the treatment of individuals receiving PLP supplementation.
- Use next generation sequencing technology to identify novel candidate gene loci responsible for seizures in undiagnosed B₆-dependent epilepsy patients.
- Determine the mechanism behind a response to vitamin B₆ supplementation identified in some individuals with seizures caused by mutations in *KCNQ2*.

In summary, this thesis aims to identify new strategies for the diagnosis of vitamin B₆-dependent disorders and elucidate further their biochemical mechanisms in order to aid their clinical management and hence disease outcome. This will also provide insights into the homeostasis of the B₆ vitamers as well as other metabolic pathways in which vitamin B₆ is important.

2. MATERIALS AND METHODS

2.1 Materials

The following were purchased from Sigma Aldrich (Poole, UK):

Acetic Acid (LC-MS Grade), Adenosine 5'-Triphosphate disodium salt, Amidosulphobetaine-14 (ASB-14), Amphotericin B, Dimethyl sulfoxide (DMSO), 1,4-Dithiothreitol (DTE), 100% Ethanol, Ethylene glycol-bis(β -aminoethyl ether)-N,N,N',N'-tetraacetic acid (EGTA), Glucose, Glycerol, Hank's Balanced Salt Solution (HBSS), 4-(2-hydroxyethyl)-1-piperazine-ethanesulfonic acid (HEPES), Heptafluorobutyric Acid (LC-MS grade) (HFBA), Iodoacetamide (IAA), Linopirdine, Magnesium Chloride (MgCl_2), Magnesium-Adenosine 5'-Triphosphate (MgATP), Potassium Chloride, Potassium Gluconate, Potassium Phosphate, Pyridoxal (PL), d_3 -Pyridoxal, Pyridoxal 5'-phosphate (PLP), Pyridoxamine (PM), d_3 -Pyridoxamine, Pyridoxamine 5'-phosphate (PMP), 4-Pyridoxic acid (PA), d_2 -4-Pyridoxic acid, Pyridoxine (PN), d_2 -pyridoxine, $^{13}\text{C}_4^{15}\text{N}_2$ -Riboflavin, Sodium Acetate, Sodium Chloride, Sylgard 184, Thiourea, Trifluoroacetic Acid, Tris Base, Tris-EDTA buffer, Tris(2-carboxyethyl)phosphine (TCEP), Urea.

The following were purchased from Thermo Fisher Scientific (Waltham, MA, US):

0.3ml Screw Top Fixed Insert Vials & Lids, BigDye Terminator v1.1 Cycle Sequencing Kit, B_6 -depleted Ham's F-12 Medium, Dialysed Fetal Bovine Serum (FBS), DNA oligonucleotides used as primers for PCR amplification, dNTP solutions set (100 mmol/L), Exonuclease I, Fetal Bovine Serum (FBS), Formic Acid (LC-MS Grade), Ham's F-12 Medium, Methanol (LC-MS Grade), Nuclease-Free Water, Orange DNA Loading Dye, Pierce BCA Protein Assay Kit, Taq DNA Polymerase (including MgCl_2 and PCR reaction mix), Tris-acetate-EDTA (TEA), Trypsin-EDTA (0.25%), Shrimp Alkaline Phosphatase (SAP), UltraPure Agarose

The following were purchased from Genscript (Piscataway, NJ, US):

Custom synthesized peptides (desalted): DGKPSAR; FFTNFESR; FFTNFESQK; SSQIGAVVSHQSSVIPDR.

The following were purchased from VWR (Lutterworth, UK):

Acetone, Acetonitrile (LC-MS Grade), Calcium Chloride, Sodium Hydroxide.

The following were purchased from Instruchemie B.V. (Delfzijl, The Netherlands):

Alkaline D-575 Reagent, Haemoglobin standard

The following were purchased from Toronto Research Chemicals (North York, Canada): d₅-Pyridoxal 5'-phosphate, Pyridoxine 5'-phosphate

1 kb DNA Ladder was purchased from New England Biolabs (Ipswich, MA, US). 6.1 N Trichloroacetic Acid (TCA) was purchased from MP Biomedicals (Santa Ana, CA, US), 8.5% Orthophosphoric Acid was purchased from BDH Chemicals (Poole, UK), Flavin mononucleotide (FMN) was purchased from Applichem (Darmstadt, Germany), GC150 TF-15 borosilicate capillary tubes were purchased from Warner Instruments (Hamden, CT, US), Isolute C18 Solid-Phase Extraction Columns were purchased from Biotage (Ystrad Mynach, UK), d₃-Pyridoxal Phosphate was purchased from Buchem B.V. (Apeldoorn, Netherlands), 4-Pyridoxic Acid 5'-Phosphate (PAP) was purchased from the Vrije Universiteit Medical Centre (Amsterdam, The Netherlands), QIAamp DNA Micro Kit was purchased from Qiagen (Hilden, Germany), d₂-pyridoxal 5'-phosphate was kindly provided as a gift by Dr. Coburn (Indiana University, Fort Wayne), Whatman 903 Protein Saver Cards were purchased from GE Healthcare (Little Chalfont, UK), Yeast Enolase standard protein was purchased from Waters (Milford, MA, US).

Unless specified, all H₂O used was purified using a Millipore Milli-Q Direct 8 system with a 0.22 µm filter.

2.2 Ethics statement

Where appropriate, this study was approved by the National Research Ethics Service (NRES) Committee (London, Bloomsbury [RED ref. no. 3/LO/0168]). Written informed consent was obtained from all subjects before sample collection.

2.3 Collection and storage of dried blood spots

DBS from PNPO deficient patients and subjects with other/undiagnosed vitamin B₆-responsive epilepsies were collected from centres across Europe. Child control DBS were collected from patients attending Great Ormond Street Hospital for Children, London, UK.

Whatman 903 Protein Saver cards were used for the collection of samples from either venous or capillary blood. Sample collection from individuals that had received a blood transfusion in the preceding 100 days was avoided. Blood was spotted in the centre of the printed circle and allowed to dry for 16-24 hours prior to storage in a zip-lock bag with silica desiccant, protecting from both humidity and light. Cards were kept at 22 °C for a maximum of 7 days prior to storage at either -20 °C or -80 °C until analysis. Those with poor quality sampling were rejected after visual inspection.

2.4 Quantification of B₆ vitamers and 4-pyridoxic acid using LC-MS/MS

2.4.1 Identification of B₆ vitamers and pyridoxic acid

PLP, PNP, PMP, PL, PN, PM and PA were quantified using a protocol similar to that of Footitt *et al.*²² with some modifications. A flow-through needle H-Class UPLC system coupled to a Xevo TQ-S triple quadrupole mass spectrometer using electrospray ionisation (ESI) and multiple reaction monitoring (MRM) was used for UPLC-MS/MS analysis (Waters, MA, US). Positive ion mode was used for compound detection. Injection volume was 8 µL and the samples were flow-injected onto a Waters Acquity UPLC HSS T3 column (1.8 µm, 2.1 x 50 mm) protected by a 1.8 µm Acquity UPLC HSS T3 guard column. The mobile phase constituents and gradient used for reversed-phase separation can be found in **Table 2.1**. Mass spectrometry

settings were as follows: capillary 2.50 kV, source temperature 150°C, desolvation temperature 600°C, cone gas flow rate 150 L/h and desolvation gas flow rate 1200 L/h. The wash solvents used were: Purge Solvent = 95% dH₂O; 5% Methanol; Seal Wash and Sample Manager Wash = 5% dH₂O; 95% Methanol.

Table 2.1: Gradient profile for separation of B₆ vitamers and pyridoxic acid by LC-MS/MS.

(A) = 3.7% acetic acid, 0.02% HFBA; (B) = 100% Methanol.

Time (min)	% mobile phase		Flow rate (mL/min)	Gradient curve
	A	B		
0.00	97.5	2.5	0.40	N/A
0.40	97.5	2.5	0.40	6
3.75	50.0	50.0	0.40	6
4.25	0.1	99.9	0.40	11
5.00	97.5	2.5	0.40	11
6.50	97.5	2.5	0.40	6

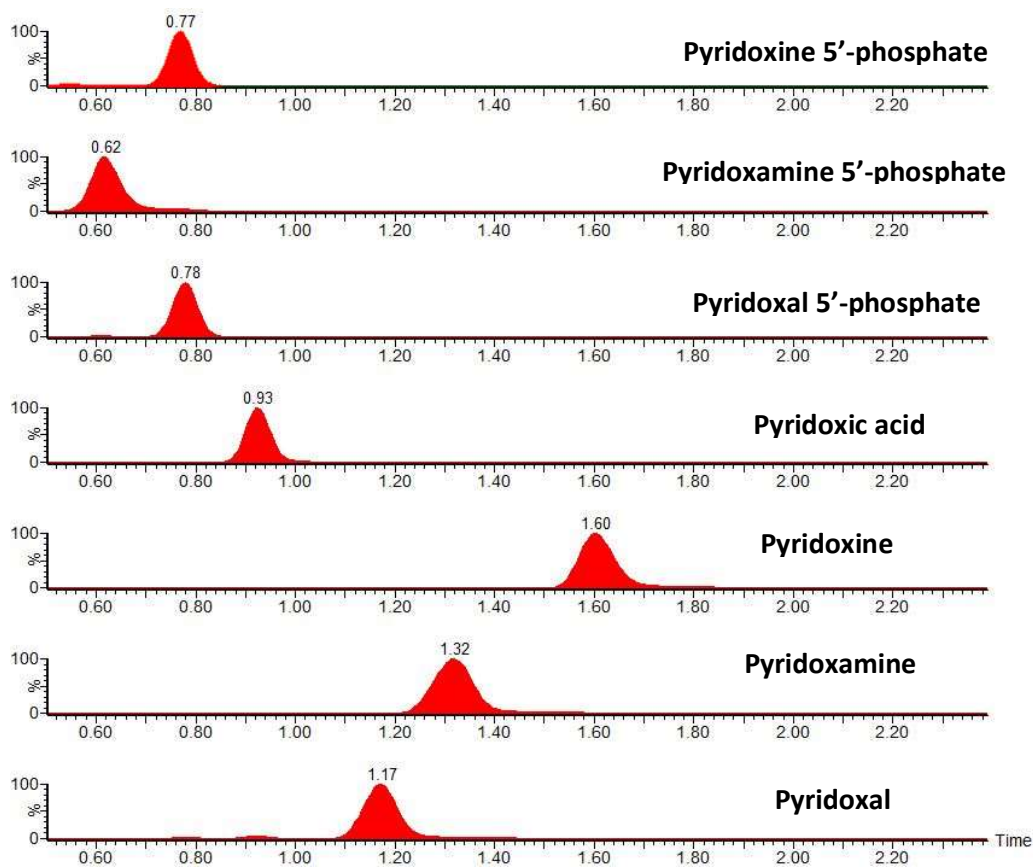


Figure 2.1: LC-MS/MS detection of the B₆ vitamers and pyridoxic acid. X-axis = mins.

The precursor and product ions used for B₆ vitamers detection are as detailed in **Table 2.2**, as well as the optimised cone voltage and collision energy for each compound. All vitamers could be specifically identified according to the m/z ratios of their precursor and product ions and retention times. All compounds were detected in ES+ mode. An example chromatogram can be found in **Figure 2.1**.

Table 2.2: Parameters used for the MRM-based identification of the B₆ vitamers and pyridoxic acid and their stable isotope internal standards. V = voltage; m/z = mass/charge ratio. Several internal standards were used for pyridoxal 5'-phosphate quantification during method developed. The MRM transitions for each of these are shown individually.

Analyte	Retention time (min)	Precursor ion (m/z)	Product ion (m/z)	Cone voltage (V)	Collision energy (V)	Loss upon Fragmentation
Pyridoxamine 5'-phosphate	0.62	249.04	134.05	27	22	H ₃ PO ₄ + NH ₃
Pyridoxine 5'-phosphate	0.77	250.16	134.13	58	20	H ₃ PO ₄ + H ₂ O
d ₅ -Pyridoxal 5'-phosphate	0.78	253.16	155.18	30	18	H ₃ PO ₄
d ₃ -Pyridoxal 5'-phosphate	0.78	251.16	153.18	30	18	H ₃ PO ₄
d ₂ -Pyridoxal 5'-phosphate	0.78	250.10	152.10	30	18	H ₃ PO ₄
Pyridoxal 5'-phosphate	0.78	248.00	150.01	30	18	H ₃ PO ₄
d ₂ -Pyridoxic acid	0.92	186.06	149.99	18	18	2H ₂ O
Pyridoxic acid	0.92	184.06	147.99	18	18	2H ₂ O
d ₃ -Pyridoxal	1.17	171.10	153.05	21	12	H ₂ O
Pyridoxal	1.17	168.10	150.05	21	12	H ₂ O
d ₃ -Pyridoxamine	1.32	172.12	137.04	22	20	H ₂ O + NH ₃
Pyridoxamine	1.32	169.12	134.04	22	20	H ₂ O + NH ₃
d ₂ -Pyridoxine	1.60	172.09	136.04	27	19	2H ₂ O
Pyridoxine	1.60	170.09	134.04	27	19	2H ₂ O

Stock solutions of the vitamers and internal standards were stored individually in H₂O at -80 °C for long-term storage. During experimentation, vitamer solutions were kept in the dark and on ice when possible. Calibration curves were created using the ratios of vitamers against a known concentration of their deuterated internal standard with the exception of PMP and PNP as stable isotopes of these compounds were not available. These vitamers were ratioed against d₃-PLP or d₅-PLP for quantification.

The LLOQ for B₆ vitamer quantification was determined as the lowest point on the calibration curve. On each occasion the signal/noise (S/N) ratio was above 10. The S/N ratio is calculated by dividing the peak height of the analyte by the background signal before and after the peak of interest.

In all cases, data was collected using the Waters MassLynx software package and quantification was carried out by interpolating the ratio of each vitamer/internal standard combination to its respective calibration curve.

2.4.2 Identification and quantification of FMN

Flavin mononucleotide (FMN) was quantified using methodology similar to that described in **Section 2.4.1**. Apart from those detailed in **Table 2.3**, the liquid chromatography conditions and mass spectrometry parameters were identical. No deuterated standard of FMN was available so a B₂ analogue (¹³C₄¹⁵N₂-riboflavin) was used instead. MRM transitions for both compounds were determined by direct infusion into the Xevo TQ-S mass spectrometer and using the Waters Intellistart software package for optimisation. A calibration curve was established using differing concentrations of FMN and a fixed concentration of ¹³C₄¹⁵N₂-riboflavin, FMN was quantified as described for the B₆ vitamers in **Section 2.4.1**.

Table 2.3: Parameters used for the MRM-based identification of FMN and ¹³C₄¹⁵N₂-Riboflavin

Analyte	Retention time (min)	Precursor ion (m/z)	Product ion (m/z)	Cone voltage (V)	Collision energy (V)
Flavin mononucleotide	1.88	475.2	359.3	4	22
¹³ C ₄ ¹⁵ N ₂ -Riboflavin	3.12	383.2	249.1	84	38

2.4.3 Sample preparation for measurement of B₆ vitamers and pyridoxic acid

2.4.3.1 *Dried blood spots*

Two duplicate 3 mm punches were taken from each DBS sample and placed in separate 1.5 ml polypropylene tubes; one for low and one for high concentration quantification (see below). 120 µL H₂O was then added to each tube prior to sonication in an XUBA3 Ultrasonic Bath (Grant Instruments Ltd., Royston, UK) for 10 minutes at 22 °C. 120 µl of 0.3 N TCA containing deuterated internal standards (d₅-PLP, d₃-PL, d₂-PN, d₃-PM and d₂-PA) at 50 or 5 nmol/L was then added to each tube. This gave final concentrations of 0.15 N TCA and 25 or 2.5 nmol/L. Samples were incubated for 45 min on ice, prior to centrifugation at 16,000 x *g* for 10 minutes at 4 °C. The supernatant was then taken and stored at -20 °C until analysis. On the day of LC-MS/MS analysis samples were again centrifuged at 16,000 x *g* for 10 minutes at 4 °C and the supernatant was transferred into a 300 µl insert vial.

It was necessary to create two calibration curves, one for quantifying low concentrations of 0.0675 – 5 nmol/L and another for high concentrations of 5 – 200 nmol/L. A final stable isotope internal standard concentration of 2.5 nmol/L was used for quantifying lower concentrations, whereas a concentration of 25 nmol/L was used for higher concentrations. This method using two calibration curves allowed linearity of all vitamers across both measurement ranges ($R^2 > 0.99$) and therefore more accurate quantification of lower concentrations than would otherwise be possible. Due to the high doses of B₆ supplements taken by B₆-responsive epilepsy subjects, the vitamer concentrations found in these samples can be up to four orders of magnitude greater than controls – this made the creation of two calibration curves necessary.

Calibration standards were created by spiking an aqueous 0.15 N TCA mix with known concentrations of the B₆ vitamers to the final concentrations required (0.0675 – 200 nmol/L). These concentrations upon analysis (0.0675 – 200 nmol/L) are equivalent to 5 – 15,000 nmol/L in whole blood, once a x 75 dilution factor is taken into account. This corresponds to a 3 mm DBS containing 3.2 µL blood¹⁵⁵ being placed into a total volume of 240 µL for analysis. The amount of blood contained within a 3 mm DBS punch is affected by factors such as the amount of blood spotted on the card on the card and the haematocrit of the subject. This is discussed further in

Sections 3.1.1 and 4.1.2.6. Quantification of the B₆ vitamers and pyridoxic acid was carried out using the LC-MS/MS method described in **Section 2.4.1**.

2.4.3.2 Cell Lysates

Chinese Hamster Ovary (CHO) cell pellets were stored at -80°C after being harvested as described in **Section 2.13.1**. After removal from storage, they were resuspended in 50 µL dH₂O and mixed by vortexing. Each pellet was then lysed by freeze-thawing five times. This was carried out by alternating the samples between methanol cooled to -79°C using dry ice, and a 37°C water bath. The sample was pelleted by centrifuging at 4,500 x g for 10 minutes; the cell lysate supernatant was then collected for analysis. This cell lysate was used for the determination of protein concentration using a Pierce BCA Protein Assay Kit (see **Section 2.13.2**).

The cell lysate was prepared for quantification of B₆ vitamers and pyridoxic acid by adding 10 µL cell lysate to 50 µL dH₂O and 60 µL 0.3 N TCA containing deuterated internal standards (d₅-PLP, d₃-PL, d₂-PN, d₃-PM and d₂-PA) at 50 nmol/L each (25 nmol/L final concentration). Each sample was subsequently vortexed and incubated for 45 minutes on ice in order to ensure precipitation of protein in the sample. The sample was then centrifuged for 10 minutes at 16,000 x g (at 4°C) and the supernatant was transferred into a 300 µl insert vial. Calibration curves from 0.5 – 200 nmol/L were prepared in parallel for each B₆ vitamer and pyridoxic acid. LC-MS/MS analysis for quantification of these analytes was carried out using the method described in **Section 2.4.1**.

2.4.3.3 Cell culture medium

The B₆ vitamers and pyridoxic acid were quantified in Ham's F-12 medium, B₆-depleted Ham's F-12 medium, Fetal Bovine Serum (FBS) and dialysed FBS. 120 µL 0.3 N TCA containing deuterated internal standards (d₅-PLP, d₃-PL, d₂-PN, d₃-PM and d₂-PA) at 50 nmol/L (25 nmol/L final concentration) was added to 120 µL of media. Samples were vortexed and incubated for 45 minutes on ice in order to precipitate protein prior to centrifugation for 10 minutes at 16,000 x g, 4°C. The supernatant was transferred to a 300 µL glass insert vial for analysis. A calibration curve from 0.5 – 200 nmol/L was prepared for each B₆ vitamer and pyridoxic acid. Quantification was performed using the LC-MS/MS protocol detailed in **Section 2.4.1**.

2.5 Enzyme assay for the quantification of PNPO activity from dried blood spots

The protocol described below is the optimised method for a single step PNPO enzyme assay using PNP as substrate, the development of which is described in **Section 3.1**.

Two 3 mm punches (T0 and T30) were taken for each patient sample from a spotted blood card and placed in a 1.5 ml polypropylene tube. Each punch was first rehydrated in 60 μ L 40 mmol/L TrisPO₄ and then sonicated in an XUBA3 Ultrasonic Bath (Grant Instruments Ltd., Royston, UK) at 22 °C for 2 min. 60 μ L reaction buffer containing 800 nmol/L PNP substrate and 3 μ mol/L FMN was then added to each tube. The final concentrations of PNP and FMN were 400 nmol/L and 1.5 μ mol/L, respectively. A reaction stop solution of 120 μ L 0.3 N TCA (containing 50 nmol/L internal standard d₅-PLP) was then added immediately to the T0 punch. Final concentrations of TCA and d₅-PLP for analysis were 0.15 N and 25 nmol/L, respectively.

The TrisPO₄ buffer was prepared by adjusting a 40 mmol/L Tris solution to pH 7.6 using 8.5% orthophosphoric acid. Potassium phosphate and Tris-Cl buffers were prepared in a similar manner during method development, with the pH adjusted according to requirements using HCl or 85% orthophosphoric acid.

The T30 punch was incubated with rotary shaking at 300 rpm at 37 °C for 30 min in a Thermomixer C (Eppendorf, Hamburg, Germany) before addition of 120 μ L reaction stop solution. Both the T0 and T30 punches were incubated for 45 mins on ice, in the dark, prior to sonicating for 5 minutes at 22 °C. The addition of TCA was required for protein precipitation as well as the release of protein-bound PLP into solution and cessation of enzyme activity. Subsequent centrifugation at 16,000 x g for 10 min at 4 °C resulted in pelleting of the punches and precipitated blood proteins. The supernatant containing B₆ vitamers was then taken and stored at -20 °C until analysis. After thawing, each sample was re-centrifuged at 16,000 x g for 10 min at 4 °C and transferred to a 300 μ L insert vial.

Quantification of PLP formation was used to calculate PNPO activity. Endogenous PLP was measured at 0 min in the T0 DBS punch and subtracted from that measured after 30 min incubation with substrate in the T30 punch. Enzyme activity was expressed as pmol PLP/3 mm DBS/h. PNP concentrations were also monitored but

not used for quantification of PNPO activity. Calibration curves were used to quantify PLP and PNP from 1.25 to 200 nmol/L using the analyte/internal standard ratio (PLP/PNP to d₅-PLP). Apart from where specified in **Section 3.1**, the other B₆ vitamers and pyridoxic acid were not monitored during this experimentation. All LC-MS/MS data acquisition and analysis was performed using Masslynx software (Waters, Milford, USA) as described in **Section 2.4.1**.

2.5.1 Measurement of the haemoglobin concentration of whole blood stored in DBS

Haemoglobin quantification was carried out using the Alkaline Haematin D-575 Reagent according to the manufacturer's specification, with minor modifications made in order to analyse the volumes of blood in a 3 mm DBS punch. 1 x 3 mm DBS was placed into a 1.5 mL microcentrifuge tube alongside 310 µL Alkaline Haematin D-575 Reagent and 10 µL dH₂O. Each sample was then either agitated for 30 minutes at 22°C in a Thermomixer C (Eppendorf, Hamburg, Germany) or sonicated in a XUBA3 Ultrasonic Bath (Grant Instruments Ltd., Royston, UK) for varying times according to the experimentation detailed in **Section 3.1.2.6**. After incubation, microcentrifuge tubes were centrifuged for 5 minutes at 16,000 x g before the supernatant was placed into a 96-well microplate. A calibration curve was created in parallel by the addition of appropriately diluted 0 – 0.25 g/dL haemoglobin standards to adjacent wells with 310 µL Alkaline Haematin D-575 Reagent. This allowed the creation of a calibration curve and extrapolation of haemoglobin concentrations in the 3.2 µL blood contained in a 3 mm DBS¹⁵⁵, diluted in 320 µL reagent to those in whole blood by using a 100 x dilution factor. Final concentrations of haemoglobin were expressed at gHb/dL in whole blood. Samples were analysed at 595 nm on a Tecan Infinite 200 Microplate Reader (Tecan, Männedorf, Switzerland) and the absorbance of standards were plotted against their known concentrations. The haemoglobin concentration of the eluted DBS blood samples was calculated using this calibration curve.

2.6 Enzyme assay for the study of recombinant PNPO enzyme

Bacterially prepared recombinant human PNPO enzyme was a kind gift from Dr. Wyatt Yue (Structural Genomics Consortium, The University of Oxford). The PNPO enzyme was stored at -80 °C in 50 mmol/L HEPES, 500 mmol/L NaCl, 5% glycerol, 0.5 mmol/L TCEP.

For all experiments, 100 ng of recombinant protein was used per reaction. Protein was diluted to 20 ng/μl in dH₂O and 5 μL was added to each well of a 96-well plate. 115 μL reaction buffer containing 20 mmol/L pH 7.6 TrisPO₄, substrates and cofactors was added to each well. TrisPO₄ was prepared as described in **Section 2.5**. Substrate type, cofactor concentration and incubation time were varied according to experimentation (0 - 10 μmol/L PNP or PMP, 0 – 3 μmol/L FMN, 0 – 60 minutes). As described in **Section 2.5**, after gentle vortexing, a reaction stop mixture of 120 μl 0.3 N TCA containing internal standard (d₃-PLP – 50 nmol/L) was immediately added to the T0 wells. The other wells were incubated at 37 °C with agitation at 300 rpm for their allotted times before addition of the reaction stop mixture. After incubation on ice for 45 min, samples vortexed and analysed by LC-MS/MS using the method described in **Section 2.4.1**. PNPO activity was calculated by quantifying PLP formed during the incubation and expressed as nmol PLP/L/h. This can be converted to pmol/mg protein/h using a conversion factor of x 2.4 (e.g. 1 nmol/L/h = 2.4 pmol/mg/h). Subtraction of PLP at T0 was required not as no endogenous PLP was measured from T0 time points. Kinetic parameters were calculated using the Graphpad Prism software package.

2.6.1 Quantification of FMN associated with the recombinant PNPO protein

FMN was measured from the same reaction mix used for the T0 time point during experimentation with p.R116Q and wild-type PNPO enzymes, prepared as described above. FMN was quantified using the LC-MS/MS method detailed in **Section 2.4.2**.

2.7 LC-MS/MS detection of PNPO-derived tryptic digest peptides

2.7.1 Selection of peptides

Peptides predicted to be formed upon tryptic digest of the PNPO protein were identified using the Skyline software package (MacCoss Lab Software, University of Washington, US). The specificity of these peptides to the PNPO protein was determined using the BLASTp online tool (www.blast.ncbi.nlm.nih.gov). Peptides that were not specific to PNPO were discarded, 4 peptides were selected for analysis (Peptides 1-4, **Table 2.4**). Additional rationale for the selection of these peptides can be found in **Section 3.2.3.1**.

Table 2.4: Selected peptides for LC-MS/MS analysis of trypsin digested PNPO protein. AA = amino acid.

Peptide	AA position in PNPO protein	Monoisotopic mass (daltons)	Notes
1: DGKPSAR	89 - 95	729.37	Upstream of p.R116Q
2: FFTNFESR	109 - 116	1046.47	Only present in wild-type PNPO protein
3: FFTNFESQK	109 - 117	1146.52	Only present in wild-type p.R116Q protein
4: SSQIGAVVS HQSSVIPDR	164 - 181	1865.95	Downstream of p.R116Q

2.7.2 LC-MS/MS analysis of PNPO-derived peptides

Custom synthesised peptides 1-4 were resuspended in 50:50 dH₂O:acetonitrile (ACN) to a concentration of 10 µmol/L and stored at -20°C. For LC-MS/MS tuning, each peptide was diluted to a working stock at 10 nmol/L in 1 mL 97% dH₂O, 3% ACN, 0.1 % trifluoroacetic acid (TFA). Tuning was carried out using direct infusion (DI) of each working stock at 10 µL/min into a Xevo TQ-S mass spectrometer (Waters, MA, US) with a carrier stream of 50:50 dH₂O:ACN, 0.1% FA at 0.4 mL/min. An MS1 scan (Cone voltage ramp = 0 – 80V) was performed for each peptide in order to identify the most abundant ion produced from each peptide. All experimentation was carried out using positive ion mode. Instrument tuning parameters for this and subsequent analyses were as follows: capillary 2.70 kV, source temperature 150°C,

desolvation temperature 600°C, cone gas flow rate 150 L/h and desolvation gas flow rate 1000 L/h.

The most abundant precursor ions were selected from each peptide, optimal multiple reaction monitoring (MRM) transitions were determined by infusing each peptide, as above, using the Intellistart software package (Waters, MA, US) to automatically adjust the ionisation and collision energies in order to select the most abundant daughter ions. The resulting MRM transitions and ionisation conditions are shown in **Table 2.5**. These were used for all further analysis of peptides 1-4.

Table 2.5: MRM transitions for LC-MS/MS analysis of trypsin digested PNPO protein. V = voltage; m/z = mass/charge ratio

Peptide	Precursor ion (m/z)	Product ion (m/z)	Cone voltage (V)	Collision Energy (V)
1: DGKPSAR	365.94	430.42	2	10
2: FFTNFESR	524.31	753.65	32	16
3: FFTNFESQK	574.43	267.27	52	18
4: SSQIGAVVS HQSSVIPDR	623.22	726.81	2	18

In order to optimise the liquid chromatography conditions, each of the peptide working stocks were pooled and diluted to a concentration of 100 pmol/L in 300 μ L 97% dH₂O, 3% ACN, 0.1 % FA. 10 μ L of this pooled peptide mix was injected using an flow-through needle H-Class UPLC system (Waters, MA, US) coupled to a Xevo TQ-S triple quadrupole mass spectrometer.

During initial experimentation, samples were injected onto a CORTECS UPLC C18+ column (1.6 μ m, 2.1 x 50 mm; Waters, MA, US) protected by a CORTECS UPLC C18 VanGuard Pre-column (1.6 μ m; Waters, MA, US). As detailed in **Section 3.2.3.1**, this column was later changed to an Acquity UPLC HSS T3 column (1.8 μ m, 2.1 x 50 mm; Waters, MA, US) protected by an Acquity UPLC HSS T3 guard column; (1.8 μ m; Waters, MA, US). The final mobile phase composition and gradient profile used for liquid chromatography analysis can be found in **Table 2.6**. The column and precolumn heaters were operated at 45°C. Wash solvents were as follows: Purge solvent = 97% dH₂O, 3% ACN, 0.1 % FA; Seal wash: 3% dH₂O, 97% ACN; Sample manager wash: 3% dH₂O, 97% ACN. The retention time (RT) of each peptide was monitored by

MS/MS analysis using the MRM transitions in **Table 2.5**. Each peptide could be identified according to their RT and the m/z ratio of their corresponding precursor and product ions. Where appropriate, alterations made to the protocol during method development are detailed in **Section 3.2.3.1**.

Table 2.6: Gradient profile for separation of tryptic digest peptides. Conditions of Mobile phase A: 0.2% FA in H₂O, 0.01% HFBA; Mobile Phase B: 0.2% FA in acetonitrile, 0.01% HFBA. N/A = not applicable.

Time (min)	% mobile phase		Flow rate (ml/min)	Gradient curve
	A	B		
0.00	97.0	3.0	0.80	N/A
0.40	97.0	3.0	0.80	6
7.00	60.0	40.0	0.80	6
7.01	0.1	99.9	0.80	6
8.50	0.1	99.9	0.80	6
8.51	97.0	3.0	0.80	1
10.00	97.0	3.0	0.80	1

MRM transitions for the detection of two peptides derived from human albumin and yeast enolase were also monitored during method development (**Table 2.7**). These were analysed using the same LC-MS/MS conditions used for analysis of peptides 1-4 and could be separated from the other peptides according to their retention time and respective m/z ratios of their precursor and product ions. For quantification, the relative abundance of all peptides was calculated by measuring the area of their respective peaks identified on LC-MS/MS analysis.

A longer 45 minute gradient profile was also used in order to improve the sensitivity of LC-MS/MS detection of the target peptides. This can be found in **Table 2.8**. All other LC-MS/MS conditions were identical for this analysis.

Table 2.7: MRM transitions for LC-MS/MS detection of peptides derived from trypsin digested human albumin and yeast enolase proteins. V = voltage; m/z = mass/charge ratio

Peptide	Parent protein	Precursor ion (m/z)	Product ion (m/z)	Cone voltage (V)	Collision Energy (V)
AVMDDFAAFVEK DGKPSAR	Albumin	671.99	578.02	54	18
SIVPSGASTGVHEALEMR	Yeast enolase	614.60	547.90	46	12

Table 2.8: Extended gradient profile for separation of tryptic digest peptides. Mobile phase A: 0.1% FA in H₂O; Mobile Phase B: 0.1% FA in acetonitrile.

Time (min)	% mobile phase		Flow rate (mL/min)	Gradient curve
	A	B		
0.00	97.0	3.0	0.80	N/A
0.20	97.0	3.0	0.80	6
40.00	60.0	40.0	0.80	6
41.00	0.1	99.9	0.80	6
42.00	0.1	99.9	0.80	6
44.00	97.0	3.0	0.80	1
45.00	97.0	3.0	0.80	1

2.7.3 Sample preparation

Trypsin digestion of proteins from dried blood spots (DBS) following disruption of disulphide bonds and blocking of sulphhydryl groups with iodoacetamide was performed as follows: 1, 2 or 4 x 3 mm punches from healthy control DBS were first placed into a 1.5 mL microcentrifuge tube and sonicated for 5 minutes in a XUBA3 Ultrasonic Bath (Grant Instruments Ltd., Royston, UK) at 22°C after the addition of 60 µL digestion buffer containing 100 mmol/L Tris-HCl, 6 mol/L urea, 2 mol/L thiourea and 2% amidosulphobetaine-14 (pH 7.8). Subsequently, 4.5 µL of 200 mmol/L dithiothreitol (DTE) in 100 mmol/L Tris-HCl (pH 7.8) was added before shaking at 1500 rpm, 22°C for one hour. 9 µL iodoacetamide (IAA) was added thereafter, samples were then protected from light, shaken for 5 minutes at 1500 rpm and then incubated at 22°C for 45 minutes. 497 µL dH₂O was added to each sample prior to vortexing and the 3 mm DBS was then removed. 30 µL of 0.1 µg/µL mass

spectrometry grade trypsin gold was added and each sample was incubated at 37°C for 16 hours in a Thermomixer C (Eppendorf, Hamburg, Germany).

After digestion, samples were 'cleaned' using C18 solid phase extraction (SPE) in order to remove the salts, detergents and reagents used. Digested samples were diluted 1:1 in 0.2% TFA in order to facilitate interaction with the SPE column. The C18 columns were first primed with 2 x 1 mL washes of 30:70% H₂O:ACN, 0.1% TFA and then 2 x 1 mL H₂O, 0.1% TFA. The prepared sample was then applied to the C18 SPE column. The eluent was collected in a 1.5 mL microcentrifuge tube and reapplied to ensure binding to the column. After this second application 1 mL H₂O, 0.1% TFA was applied to the column in order to wash away residual salts. The column-bound peptides were then eluted using 1 mL 30:70 H₂O:ACN, 0.1% TFA. The eluent was collected in a clean 1.5 mL microcentrifuge tube and lyophilised overnight. The resulting pellets were resuspended in 100 µL 97%:3% H₂O:ACN, 0.1% TFA, vortexed for 10 seconds and centrifuged at 16,000 x g for 10 minutes. The supernatant was transferred to 300 µL insert vials for LC-MS/MS analysis.

TCA acetone precipitation was added to the protocol in order to further clean samples by removing proteins of extremely high abundance such as albumin. Samples were prepared for this by first adding 300 µL dH₂O containing 500 ng yeast enolase protein to DBS in a 1.5 mL microcentrifuge tube. This was sonicated in a XUBA3 Ultrasonic Bath (Grant Instruments Ltd., Royston, UK) at 22°C for 5 minutes. TCA acetone precipitation was then performed by adding the supernatant to 1.2 mL -20°C 10% TCA in acetone. Samples were vortexed then incubated for 16 hours at -20°C. Thereafter, each tube was centrifuged for 10 minutes at 16,000 x g, 4°C and the supernatant discarded. 1 mL 100% acetone was added to the remaining pellet, samples were vortexed and centrifuged again for 10 minutes at 16,000 x g, 4°C. The supernatant was discarded and the pellet dried in a fume hood at 22°C for two hours before digestion.

2.8 Enzyme assay for the study of recombinant pyridoxal kinase enzyme

Bacterially prepared recombinant pyridoxal kinase enzyme was a gift from collaborators (Dr. Viorica Chelban, UCL Institute of Neurology). The purified recombinant protein was stored in 25 mmol/L HEPES (pH 7.4), 100 mmol/L KCl and 1mmol/L DTT.

100 ng protein was used for each reaction after diluting the protein in dH₂O to 20 ng/μL. A round-bottomed 96-well plate was heated to 37°C in a Thermomixer C (Eppendorf, Hamburg, Germany). 5 μL of diluted protein at 20 ng/μL was added to each well before the subsequent addition of 115 μL reaction buffer containing 20 mmol/L potassium phosphate adjusted to pH 6.1 with 8.5% orthophosphoric acid. This reaction buffer also contained substrate (pyridoxal; 0 – 100 μmol/L) and cofactors (MgCl₂; 0 – 3 mmol/L, Na₂ATP; 0 – 500 μmol/L, MgATP; 0 – 500 μmol/L) at concentrations as described in **Section 5.1**. Plates were covered and the reaction in each well proceeded at 37°C with agitation at 300 rpm before being stopped with the addition of 120 μL 0.3 N TCA containing 50 nmol/L d₅-PLP internal standard after 10 minutes. The 96-well plate was subsequently covered and briefly vortexed before being placed on ice for 45 minutes. The plate was again vortexed before the reaction mixture from each well was transferred to 300 μL insert vials for LC-MS/MS analysis.

Pyridoxal kinase activity was measured by calculating the PLP formed from PL substrate after the 10 minute incubation period at 37°C. Activity was expressed as μmol PLP/L/h. Activity can be converted to nmol/mg protein/h using a conversion factor of x 2.4 (e.g. 1 μmol/L/h = 2.4 nmol/mg/h). Subtraction of PLP at T₀ was not required as no endogenous PLP was detectable. PLP quantification was carried out using the LC-MS/MS protocol detailed in **Section 2.4.1** and elsewhere. Kinetic parameters were calculated using the GraphPad Prism software package.

2.9 Enzyme assay for quantification of pyridoxal kinase activity from dried blood spots

Two 3 mm punches (T0 and T10) from each sample source were placed into separate 1.5 mL microcentrifuge tubes. 60 μ L 40 mmol/L potassium phosphate pH 6.1 was added to each tube. Potassium phosphate buffer was prepared by adjusting the pH of a 40 mmol/L potassium phosphate buffer with 8.5% orthophosphoric acid. Each DBS was then sonicated in an XUBA3 Ultrasonic Bath (Grant Instruments Ltd., Royston, UK) for 2 minutes at 22°C. Subsequently, 60 μ L of a reaction buffer containing 20 μ mol/L pyridoxal and 600 μ mol/L MgATP in dH₂O was added. The final concentrations of substrate (pyridoxal) and cofactor (MgATP) were therefore 10 μ mol/L and 300 μ mol/L, respectively. Next, the reaction in the T0 DBS punch was stopped by the addition of 120 μ L 0.3 N TCA containing 50 nmol/L of d₅-PLP as internal standard. The T10 DBS punch was incubated in a Thermomixer C (Eppendorf, Hamburg, Germany) at 37°C for 10 minutes with agitation at 300 rpm.

Each of the T0 and T10 DBS punches were, after the addition of the TCA reaction stop solution, incubated for 45 minutes on ice in order to precipitate blood protein. Each sample was then sonicated again for 5 minutes at 22°C before centrifugation at 16,000 x g to pellet precipitated protein. The supernatant was transferred to a 300 μ L insert vial and taken for analysis.

LC-MS/MS-based quantification of pyridoxal kinase activity was carried out by measuring PLP formed over the 10 minute incubation period. PLP was measured in each of the T0 and T10 with the PLP measured at T0 subtracted from that in the T10 punch. Quantification of PLP was carried out using a PLP:d₅-PLP calibration curve from 0.5 – 200 nmol/L, this was prepared as discussed in **Section 2.4.1**. Pyridoxal kinase activity was expressed as pmol PLP 3 mm DBS/h. All LC-MS/MS data acquisition and analysis was performed using Masslynx software (Waters, Milford, USA) as described in **Section 2.4.1**.

2.10 Characterisation of the photodegradation profile of PLP

2.10.1 Photodegradation protocol & sample preparation

For the initial investigation of PLP degradation, 1 mmol/L solutions of > 99.8% PLP were, after mixing to solubilise PLP, prepared in 2 mL dH₂O and left at 22 °C in sealed transparent glass vials on a sunny window ledge for 1 h, 5 h, 72 h and 144 h before freezing at -20 °C until analysis. Another 0 h sample was frozen at -20°C immediately after preparation.

For the further characterisation of PLP degradation and PAP formation, samples were prepared by incubation in a custom-made enclosed wooden box containing 2 Philips TL 8W/35 fluorescent lamps and a 240 V AC cooling fan running at a speed of 50 - 60 Hz at 23 W; this was necessary to maintain a consistent temperature of 22 °C. 2 mL 20.24 mmol/L solutions of PLP in dH₂O were, after stirring for 45 min in order to solubilise the high concentrations of PLP, incubated for 0 h, 1 h, 4 h and 24 h before being frozen at -20 °C until analysis.

Commercially available PLP nutraceutical products were also assessed by the dissolution of samples in 10 mL dH₂O at 5 mg/mL (20.24 mmol/L). In order to facilitate dissolution, tablets were crushed using a mortar and pestle prior to preparation. Capsules were emptied directly into dH₂O, ensuring they were fully dispensed. After preparation, each sample was agitated in the dark for 1 hour to ensure the dissolution of all PLP. After this, samples were split into equal volumes at 0 h and 24 h time points and incubated under the same conditions used for pure PLP. Samples were frozen at -20°C until analysis.

The postulated diketone dimer of PLP was investigated using a Uvikon XL spectrophotometer (NorthStar Scientific, Leeds, UK). A sample believed to correspond to this dimer was collected by collaborators (Dr. A Mohamed-Ahmed, School of Pharmacy, UCL) from the eluent of a single peak seen using HPLC-UV/VIS. The absorbance of each this sample was measured over the range of 226 – 400 nm. A sample containing 90% dH₂O, 10% methanol, 0.2% formic acid was also measured (blank sample). This is the mobile phase that was used for separation of the PLP degradation products by HPLC. The absorbance measured at each wavelength in this blank was subtracted from that calculated over the same range upon analysis of

the peak seen by HPLC-UV/VIS analysis postulated to correspond to a diketone dimer of PLP.

2.10.2 LC-MS/MS for the assessment of photodegradants

2.10.2.1 Investigation of PLP photodegradation products

Initial investigation of the potential degradation products of PLP was performed by flow injection analysis-mass spectrometry. The carrier stream was 97.5% A (3.7% acetic acid, 0.01% HFBA) and 2.5% B (100% methanol). Before infusion, all samples were diluted in dH₂O to a concentration of 10 µmol/L. All compounds were detected in ES⁺ mode. Analyses were performed with full MS scans using either the MS1 or MS2 quadrupoles. Product scans were performed according to a loss of H₃PO₄ (-98) upon fragmentation in order to investigate phosphorylated compounds. Exact parameters used for analysis (i.e. cone voltages, collision energies) are described in **Section 6**. The mass spectrometry tuning parameters used for analysis can be found in **Section 2.4.1**.

After the identification of several unidentified compounds of interest, MRM transitions for these potential photodegradants were created as described in **Section 6**. The area under the curve (AUC) was used to semi-quantitatively calculate the relative abundancy of these compounds at each specified time point. The levels of PLP, PL and PA were assessed similarly. For LC-MS/MS analysis, samples were first diluted to 200 nmol/L in dH₂O and then acidified with an equal amount of 0.3 N TCA (final concentration 0.15 N TCA; nominal 100 nmol/L PLP), the injection volume was 8 µl. The gradient profile in **Table 2.1** was used for chromatographic separation.

2.10.2.2 Quantification of pyridoxic acid 5'-phosphate

PAP formation and PLP degradation were quantified from the solutions described above by the creation of a calibration curve from 1.25 – 200 nmol/L in a solution of H₂O with 0.15 N TCA and 25 nmol/L d₃-PLP as internal standard. 4-Pyridoxic acid 5'-phosphate (PAP) was purchased from the VU Medical Centre, Amsterdam, The Netherlands. PLP and PAP to d₃-PLP calibration curves were linear ($R^2 > 0.99$) between 1.25 – 200 nmol/L. PLP and PAP were distinguishable according to both their retention time and m/z ratio. The MRM transition used for quantification of PAP was 264.07 > 166.07 with a cone voltage and collision energy of 27 and 16,

respectively. This corresponded to the loss of H_3PO_4 (-98) upon fragmentation. PAP eluted at 0.82 minutes from the HSS T3 column used for analysis. Experimentation was performed using the LC-MS/MS method described in **Section 2.4.1**.

2.11 Whole exome and whole genome sequencing

Whole exome sequencing (WES) and whole genome sequencing (WGS) was performed by GOSgene, UCL GOS Institute of Child Health, London, UK or the Universitair Medisch Centrum Groningen (UMCG), Groningen, The Netherlands. The processing of raw data and creation of VCF files was performed by Dr. Hywel Williams of GOSgene or Drs. Erica Gerkes and Roan Kanninga of the UMCG.

VCF files were uploaded to the Ingenuity Variant Analysis software package (IVA; Ingenuity, Redwood City, CA, US). Filtering of variants was carried out using parameters that differed according to each patient analysed and were adjusted as appropriate during analysis. The default parameters can be found in **Table 2.9**.

2.11.1 Interpretation of variants using bioinformatics tools

Variants that were considered potentially pathogenic were assessed using a variety of tools. These included those for assessment of amino acid substitutions in affected proteins such as SIFT (www.sift.bii.a-star.edu.sg) and PolyPhen-2 (www.genetics.bwh.harvard.edu/pph2). These online tools assign pathogenicity scores to identified variants according to the impact on protein structure and evolutionary conservation. The biological function of proteins encoded by the genes in which variants were identified were assessed using the UniProt (www.uniprot.org), OMIM (www.omim.org) and proteinatlas (www.proteinatlas.org) databases. This was used in order to assess whether the proteins identified could be implicated in the phenotypes of each patient.

Table 2.9: Ingenuity Variant Analysis parameters for filtering variants identified in VCF files derived from whole exome or genome data. *Unless the variant is established as a pathogenic common variant. ExAC = Exome Aggregation Consortium (www.exac.broadinstitute.org); gnomAD = genome Aggregation Database (www.gnomad.broadinstitute.org); NHLBI ESP = National Heart, Lung, and Blood Institute Exome Sequencing Project); AMCG = American College of Medical Genetics and Genomics; HGMD = Human Gene Mutation Database (www.hgmd.cf.ac.uk); ClinVar = Clinical Variance (www.ncbi.nlm.nih.gov/clinvar).

Filter	Parameter
Confidence (keep only variants which satisfy these criteria)	Call Quality is at least 20 in any case and at least 20 in each control
	Read depth is at least 10 in any case and 10 in any control
	Variant is outside the top 1% of most exonically variable genes (defined by the 1000 genomes project)
Common variants (Exclude variants that have an allele frequency greater than)*	1% prevalence in the 1000 genomes project
	1% prevalence in the ExAC database
	1% prevalence in the gnomAD database
	1% prevalence in the NHLBI ESP exomes
Predicted Deleterious (Keep only variants no more than 20 bases into an intron that satisfy these criteria)	Experimentally observed to be associated with a pathogenic or likely pathogenic phenotype according to computed AMCG guidelines classification
	Listed in HGMD or ClinVar
	Associated with a Frameshift, in-frame indel or start/stop codon change
	Associated with a missense change
	Associated with a splice site loss up to 7 bases into an intron

2.12 DNA Extraction and Sanger sequencing

2.12.1 DNA extraction from DBS

Genomic DNA was extracted from dried blood spots using the QIAamp DNA Micro Kit as specified by the manufacturer. Three 3 mm DBS punches were placed into a 1.5 mL microcentrifuge tube. 180 μ L Buffer ATL was then mixed with 20 μ L proteinase K by vortexing. The microcentrifuge tube was incubated for 1 hour with 900 rpm shaking at 56°C. After this incubation, 200 μ L of Buffer AL was added and the solution was mixed again by pulse vortexing. The mixture was then incubated again at 70°C for 10 minutes, with shaking at 900 rpm. This lysate was placed into a MinElute column inside a 2 mL collection tube and centrifuged at 6,000 x *g* for 1 minute. The flow-through was discarded and the MinElute column was placed inside another 2 mL collection tube before the addition of 500 μ L Buffer AW1. The tube was again centrifuged for 1 minute at 6,000 x *g* before this process was repeated, this time with the addition of 500 μ L Buffer AW2. The MinElute column was then placed into a fresh 1.5 mL microcentrifuge tube before the addition of 50 μ L Buffer AE (elution buffer). This was incubated for 5 minutes at room temperature before centrifugation at 20,000 x *g* for 1 minute to elute the genomic DNA. The resulting DNA samples were stored at -20°C until analysis. The concentration and purity of extracted DNA was determined using a NanoDrop 100 (Thermo Scientific).

2.12.2 Primer design

In order to design primers for the amplification of target areas of genomic DNA using the Polymerase Chain Reaction (PCR), the gene sequence was downloaded from the Ensembl database (www.ensembl.org). The sequence was then imported into the Thermo Fisher Primer Designer tool (Thermo Fisher, Loughborough, UK) and primers were selected according to the parameters detailed in **Section 5.3.1, Table 5.2**. The Primer-BLAST tool (www.ncbi.nlm.nih.gov/tools/primer-blast) was used to ensure specificity of the primers chosen to the region of interest.

2.12.3 Amplification of target genes from genomic DNA using the Polymerase Chain Reaction (PCR)

2.12.3.1 PCR conditions

Standard PCR reactions were carried out using the conditions detailed in **Table 2.10**. For each reaction, negative controls were prepared simultaneously using nuclease-free water in order to ensure the PCR reaction mix had not been contaminated. A Veriti 96-well Thermal Cycler (Thermo Fisher, Loughborough, UK) was used for PCR amplification. The cycling parameters can be found in **Table 2.11**.

Table 2.10: Standard conditions for targeted PCR amplification of genomic DNA. T_m = melting temperature; bp = base pairs

Parameter/Reagent	Condition
MgCl ₂ concentration	1.5 mmol/L
Primer concentration	0.5 μ mol/L
Taq Polymerase per reaction	1 U
Template genomic dsDNA	~50 ng
dNTP concentrations	200 μ mol/L
Annealing temperature	Variable (50°C – 65°C) but approx. 2°C lower than T_m of primer pair
Extension time	30 s for ~500 bp amplicons (1 min per 1000 bases)

Table 2.11: Standard thermal cycling parameters for PCR amplification of genomic DNA. * varies according to primer pair. **Extension time can vary according to amplicon length. *** Number of cycles can be extended, this will increase the final yield of PCR product DNA but can induce errors.

Step	Conditions
1	96°C; 5 minutes
2	96°C; 30 seconds
3	Specified annealing temperature*; 30 seconds
4	72°C; 30 seconds**
5	Repeat steps 2-4 34 times for 35 cycles***
6	72°C; 10 minutes

2.12.3.2 Visualisation of PCR products by agarose gel electrophoresis

In order to assess whether PCR amplification had been effective and specific to the target region, products were visualized using agarose gel electrophoresis. A 1% (w/v) agarose gel was prepared using 1 g of UltraPure Agarose in 100 mL 1X Tris-acetate-EDTA (TAE) buffer. After heating to allow dissolution of the agarose into the TAE buffer, the gel was decanted into a sealed tray containing a comb; this was allowed to set at room temperature. This gel was then placed into a tank containing 1X TAE buffer and the comb removed.

Before loading the DNA of interest into each well, 5 µL of PCR product was combined with 3 µL Orange DNA Loading Dye. 5 µL of 1 kb DNA Ladder was also placed into the first well to allow size quantification of the PCR products. Conditions of electrophoresis varied according to the size of the PCR products visualised, but was usually carried out at 100 V for 30 – 60 minutes. Visualisation of bands was achieved using a ChemiDoc MP System (Bio-Rad, Hemel-Hempstead, UK) and the Image Lab software package.

2.12.4 Sanger sequencing

2.12.4.1 Purification of PCR products

Purification of PCR products was carried out using the ExoSAP protocol; 10 µL PCR product was added to 1 µL of shrimp alkaline phosphatase (SAP), 0.75 µL dH₂O, 0.5 µL of exonuclease I and 0.25 µL of a SAP dilution buffer. Using the Veriti 96-well Thermal Cycler (Thermo Fisher), the sample was mixed and incubated at 37°C for 15 minutes, then 80°C for 15 minutes.

2.12.4.2 Sanger sequencing preparation

Cleaned PCR products were prepared for Sanger sequencing using the Big Dye Terminator v1.1 Cycle Sequencing Kit. 1.5 µL of sequencing buffer, 0.5 µL of Big Dye Terminator v1.1, 4 µL dH₂O and 1 µL of forward or reverse primer was added to 3 µL cleaned PCR product. The parameters in **Table 2.12** were then used for amplification.

Table 2.12: Thermal cycling parameters for Sanger Sequencing of PCR products.

Step	Conditions
1	95°C; 2 minutes
2	95°C; 20 seconds
3	50°C; 10 seconds
4	60°C; 3 minutes
5	Repeat steps 2-4 34 times for 35 cycles

2.12.4.3 DNA precipitation

Sequencing products prepared using the protocol in **Section 2.12.4.2** were incubated at room temperature for 20 minutes with 50 µL pure ethanol and 2 µL 3 M sodium acetate. Centrifugation at 20,000 x *g* was carried out for 40 minutes before discarding the supernatant. The resulting DNA pellet was washed using 50 µL 70% ethanol and centrifuged again for 10 minutes at 20,000 x *g*. The supernatant was discarded and plates were inverted before pulse centrifugation for 10 – 20 seconds. The sequencing products were then suspended in 10 µL 0.1X Tris-EDTA buffer before sequencing at the North East Thames Regional Genetics Service Laboratories, Great Ormond Street Hospital, London on an ABI DNA Sequencer (Applied Biosystems, Foster City, CA, US). Resulting electropherograms were visualised using the Sequencher software package (v4.10.1; Gene Codes, Ann Arbor, MI, US).

2.13 Cell culture of CHO cells

2.13.1 Cell culture conditions

Chinese Hamster Ovary (CHO) cells, were cultured in Ham's F-12 medium supplemented with 10% fetal bovine serum (FBS). Cultures were grown in 75 cm² sterile flasks, at 37°C in 5% CO₂. When cells were approximately 75% confluent the media was removed and cells were washed with 8 mL Hank's Balanced Salt Solution (HBSS) prior to the addition of 3 mL 0.25% trypsin-EDTA at 37°C for 2 minutes to help detach the cells. Detachment was performed by gently banging the flasks. 13 mL Ham's F-12 medium was then added and the resulting mixture split between two new flasks. Cells were transfected by collaborators with KCNQ2/3 cDNA as per the

protocol detailed by Selyanko *et al.*¹⁵⁶ and split into several 35 x 10 mm culture dishes. M-current recording was performed 2 days after transfection.

When cells were harvested for measurement of B₆ vitamers (**Section 2.4.3.3**) or total protein quantification (**Section 2.13.2**), confluence was first achieved and the media was removed. Cells were then subjected to trypsin digestion as described above before addition of 10 mL medium and were then decanted into a 15 mL falcon tube. The resulting cell suspension was centrifuged at 4,500 x *g* for 5 minutes before removal of the supernatant and storage of the pellet at -80°C until analysis.

The B₆ depletion protocol referenced in **Section 7.2** was carried out by transitioning cells from Ham's F-12 with 10% normal FBS, as described above, to B₆-depleted Ham's F-12 with 10% dialysed FBS (DFBS). Initially, cells were placed in B₆-depleted Ham's F-12 with 10% normal FBS and grown for three weeks, with regular splitting as above. The 10% FBS fraction of this culture medium was then changed on a weekly basis as follows: Week 1: (20:80 DFBS:FBS); Week 2: (50:50 DFBS:FBS); Week 3 (80:20 DFBS:FBS); Week 4 (100:0 DFBS:FBS). This resulting B₆ depleted CHO cell culture was used for experimentation.

2.13.2 Protein assay

The concentration of protein in CHO cell lysates was measured according to manufacturer's instructions for the Pierce BCA Protein Assay Kit; analysis was performed in a 96-well plate. The working reagent mix was prepared by mixing reagents A and B at a 50:1 ratio. 10 µL of the Pierce BCA Protein Assay Kit calibration standards were added to consecutive wells of a 96-well plate, alongside 10 µL of each cell lysate. Cell lysates were prepared using the protocol detailed in **Section 2.4.3.3**. 200 µL BCA reagent was added to each cell lysate before mixing and incubation for 30 minutes at 37°C. Absorbance was measured at 555 nm for each sample using a Tecan Infinite 200 Microplate Reader (Tecan, Männedorf, Switzerland). For standards, the absorbances were plotted against their known concentrations in order to create a calibration curve (0 – 2000 µg/mL) from which the protein concentration of the cell lysate samples was calculated.

2.14 Patch recording of the M-current from CHO cells

Formed of a KCNQ2/3 tetramer, the M-channels mediate the M-current; this carries K^+ ions and is of importance for the regulation of neuronal excitability. Electrophysiology experimentation using CHO cells for the measurement of the M-current was carried out with the kind assistance of collaborators at the UCL department of Neuroscience, Physiology & Pharmacology.

2.14.1 Preparation of solutions

The extracellular bath solution (**Table 2.13**) was prepared on the day of analysis. Additional solutions containing PLP, PL and Linopirdine (an M-channel blocker) were prepared identically with the addition of these components at a final concentration of 10 $\mu\text{mol/L}$, as required.

Table 2.13: Composition of extracellular patching solution.

Component	Concentration (mmol/L)
NaCl	144
KCl	2.5
CaCl ₂	2
MgCl ₂	0.5
HEPES	5
Glucose	10
Tris base	Adjusted to pH 7.4

The internal pipette solution (**Table 2.14**) was also prepared on the day of analysis. The pipette solution was filtered using a 0.22 μm filter prior to filling pipettes. When performing perforated patches, the pipette solution also contained 100 $\mu\text{g/mL}$ Amphotericin B.

Table 2.14: Composition of pipette solution.

Component	Concentration (mmol/L)
K Gluconate	90
KCl	20
CaCl ₂	1
MgCl ₂	3
HEPES	40
EGTA	3
NaOH	Adjusted to pH 7.4

2.14.2 Data acquisition and analysis

Chinese Hamster Ovary (CHO) cells transfected with KCNQ2/3 were prepared as described in **Section 2.13.1**. 35 x 10 mm cell culture dishes containing the cells were placed onto a custom-adapted Eclipse TE200 Microscope (Nikon, Tokyo, Japan). This allowed visualisation of CHO cells and manual micromanipulation of the pipette containing the electrode used to determine the M-current parameters. The cells were allowed to stand for 10 minutes to allow equilibration to 22°C and for the cell culture medium to be replaced by the extracellular bath solution (**Table 2.13**). This was continuously replenished throughout experimentation using a Reciprocating Piston Air Pump (Medcalf Bros., Potters Bar, UK).

Pipettes were pulled from 150 mm borosilicate capillaries (GC150 TF-15) to a resistance of 3.0 – 5.0 MΩ. The tip of each pipette was coated in Sylgard and heated in order to reduce capacitance. For perforated patching, each pipette was filled with pipette solution (**Table 2.14**) containing 100 µg/mL Amphotericin B before the tip was held for 30 seconds in pipette solution containing no Amphotericin B; this was in order to avoid contaminating the extracellular bath solution with Amphotericin B.

Subsequently, the pipette was fitted over the 'internal' electrode and lowered rapidly to the CHO cell of interest. Each electrode was coated in silver chloride on the day of analysis. The resistance of each pipette was monitored using a test pulse of +10 mV for 10 ms at 100 ms intervals, this was to check for damaged pipettes. Once close to the target cell (identified both visually and by a raised resistance), negative pressure

was applied manually in order to facilitate a seal on the cell membrane. When a 'gigaseal' (resistance > 1 GΩ) was achieved, the test pulse was terminated and a holding potential of -60mV was initiated. 10 minutes was taken in order for the cell membrane to permeabilise – this was required to achieve a perforated patch. A further summary of this technique is described in **Section 7.2.1**.

The M-current was activated according to a step protocol from -60 to +20 mV, in 10mV steps, at 5 second intervals for 500 ms. M-currents were quantified by measuring the current amplitude, in picoamperes (pA), when the membrane potential was 0 mV. In order to determine the effect of exogenous compound addition to the extracellular bath solution, recordings were initiated in 1 minute intervals around bath solution exchange. The mean of 3-5 recordings prior to and 3-5 recordings after were taken and compared to one another in order to determine the effect of the exogenous compound.

Data was acquired using a HEKA EPC 9 and analysed using the PULSE Software package v8.8 (HEKA Elektronik, Lambrecht, Germany). Currents were filtered at >0.5 kHz and sampled at 5–10 kHz.

3.DRIED BLOOD SPOTS AS A TOOL TO PROFILE THE B₆ VITAMERS; USEFULNESS FOR THE DIAGNOSIS OF PNPO DEFICIENCY

Pyridox(am)ine 5'-phosphate oxidase (PNPO) deficiency is a genetic disorder of vitamin B₆ metabolism that results in seizures caused by a deficiency of the active form of B₆, pyridoxal 5'-phosphate (PLP). Treatment includes supplementation with high doses of vitamin B₆ in the form of PLP or pyridoxine (PN). Since most cases present in the newborn period, the challenge is to distinguish this rare cause of seizures from common causes of neonatal seizures such as hypoxic ischaemic encephalopathy. Sometimes the neonatologist will get a strong indication of a B₆ responsive disorder from the cessation of fits in response to administration of PN or PLP (if this is carried out), however, this does not distinguish between deficiencies of ALDH7A1, PLPHP and PNPO.¹⁵⁷ Currently, diagnosis of PNPO deficiency is carried out by sequencing of the PNPO gene. This is, however, often delayed until after ALDH7A1 deficiency is excluded by urinary α -AASA analysis. Prompt diagnosis and appropriate treatment of PNPO deficiency is associated with a good neurodevelopmental outcome. There is therefore a need for a rapid and reliable diagnostic test for PNPO deficiency.

Using LC-MS/MS techniques, concentrations of the B₆ vitamers and pyridoxic acid have been characterised in plasma and CSF from controls and patients with B₆-responsive epilepsies. However, these cohorts have been relatively small and have included a limited number of PNPO-deficient patients.^{21-22, 88} It was hoped that, by measuring the B₆ vitamers in dried blood spots (DBS), diagnostic information could be obtained from each individual. If patterns diagnostically specific to PNPO deficiency (or another B₆-dependent seizure disorder) could be identified, this would be useful as an adjunct to other assays (i.e. urinary α -AASA) or in its own right as a diagnostic test. This could include studying ratios of B₆ vitamer concentrations between CSF and the blood.⁴ In addition, it would be an advantage to quantify the B₆ vitamers from an easily obtained sample source such as DBS, particularly as many analytes are more stable when stored in a DBS card, compared to other sample sources (i.e. plasma). This could be particularly important for the labile B₆ vitamers (**Section 1.1.4**).

This chapter describes the assessment of LC-MS/MS as a method to measure the B₆ vitamer concentrations in dried blood spots (DBS) from individuals with PNPO deficiency and other B₆-dependent seizure disorders. This method also allowed an assessment of the pharmacokinetics of the PLP supplementation of two PNPO-deficient individuals. This could have implications for the treatment of these individuals who require lifelong supplementation with supraphysiological PLP doses,

particularly as some patients with PNPO deficiency develop liver damage, potentially caused by high levels of some B₆ vitamers (**Section 6**).

3.1 Method validation

The LC-MS/MS-based method for the quantification of the B₆ vitamers and pyridoxic acid is based on that previously published by Footitt *et al.*²² Parameters for detection and quantification can be found in **Section 2.4**.

Due to the supraphysiological B₆ doses received by individuals with B₆-dependent epilepsy, it was expected that concentrations would vary by several orders of magnitude compared to controls. Two calibration curves were therefore created and the duplicate analysis of DBS from each individual was performed, one at each concentration range. One calibration curve ranged from 5 nmol/L to 750 nmol/L and used an internal standard (IS) concentration of 187.5 nmol/L, the other from 750 to 15,000 nmol/L with an IS concentration of 1,875 nmol/L.

The dynamic range of the Xevo TQ-S MS/MS instrumentation used was not linear for all B₆ vitamers above 15,000 nmol/L. Measurement of concentrations higher than 15,000 nmol/L required reanalysis after dilution of the DBS extract prior to the addition of the TCA internal standard mix.

3.1.1 Assessment of recovery of the B₆ vitamers and pyridoxic acid from DBS

The recovery of B₆ vitamers from DBS was assessed by spiking whole blood from a control individual with 0.75, 3.75 and 7.5 µmol/L (final concentrations) of each of the B₆ vitamers and pyridoxic acid. 50 µL of whole blood was spotted onto Whatman 903 protein saver cards and dried overnight before analysis. Endogenous concentrations (i.e. from samples that had not been spiked) were also measured and subtracted from the calculated final concentrations. In each case, measurement was carried out in triplicate from three 3 mm DBS punches. Recovery was calculated as a percentage of the nominal (spiked) concentrations. Whilst haematocrit can affect the amount of blood in a 3 mm punch¹⁵⁸, as discussed in **Section 4.1.1.2**, this had not been measured prior to spotting for our subjects or controls. The assumption was therefore made that each 3 mm DBS contained 3.2 µL blood.¹⁵⁵ Recoveries of the B₆ vitamers and pyridoxic acid are presented in **Table 3.1**.

Table 3.1: Recovery of the B₆ vitamers and pyridoxic acid from DBS. Combined = Mean % recovery of all vitamers at that concentration.

Spiked conc. ($\mu\text{mol/L}$)	Recovery (%)							
	PLP	PNP	PMP	PL	PN	PM	PA	Combined
0.75	249.6	50.3	58.6	177.1	31.2	17.0	103.5	98.2
3.75	113.6	77.6	64.6	138.0	79.5	45.0	89.8	86.8
7.5	103.6	76.9	48.8	143.5	106.3	65.9	97.2	91.7

Recovery greater than 100% was observed for PLP and PL at each concentration. At 0.75 $\mu\text{mol/L}$ extremely high recoveries of >150% were identified for these vitamers. For PNP, PMP, PN and PM, with one exception (PN; 7.5 $\mu\text{mol/L}$), recoveries were lower than 100%. In blood, PN and PM can be phosphorylated to PNP and PMP by PK and subsequently converted to PLP by PNPO. PLP can also be hydrolysed to PL by several phosphatase enzymes. These results indicate that PN, PM, PNP and PMP are converted to PLP and PL when spiked into whole blood and spotted onto a DBS card. This hypothesis is further supported by the accurate (<11% deviation from nominal) recovery of PA at all concentrations; as a urinary excretion product, PA is not subject to enzymatic degradation. The accurate recovery of PA also indicates that the enzymes responsible for conversion of PL to PA (aldehyde oxidase and aldehyde dehydrogenases) in humans are not active in the blood. This correlates with the current understanding of vitamin B₆ metabolism.⁴

During these experiments, the whole blood was stored on ice prior to the addition of exogenous B₆ vitamers and PA. After this, the blood was immediately spotted onto DBS cards. Enzymatic interconversion of the B₆ vitamers was therefore likely occurring while the whole blood was briefly on ice or during the drying step. This step is required for the accurate assessment of recovery from DBS.

To address this, the B₆ vitamers were prepared in a 0.3 N TCA solution (instead of H₂O) prior to their addition to whole blood. It was hypothesised that this would halt interconversion of the spiked B₆ vitamers by denaturing the enzymes responsible (PK and PNPO). However, the addition of TCA dramatically increased the viscosity of the blood, which did not then spread in a manner representative of normal whole blood. When calculating the recovery of analytes from DBS the spreading of blood across the card is important as it is necessary to know the exact quantity of blood contained within the 3 mm punch retrieved from a DBS card.

Despite being unable to further validate the recovery of B₆ vitamers from DBS, the accurate recovery of PA (90 – 104%) was encouraging. This meant that the correction factor applied in order to extrapolate to whole blood concentrations was accurate and that PA, at least, was fully liberated from the DBS.

If enzymatic interconversion was the reason behind the inaccurate recoveries of individual B₆ vitamers, an average recovery of all vitamers combined of close to 100% would still be expected. Indeed this was the case, with mean recoveries of 98.2, 86.8 and 91.7% at 0.75, 3.75 and 7.5 µmol/L, respectively. This indicated that the recovery of each of the individual vitamers was close to complete.

3.1.2 Assessment of the measurement precision of B₆ vitamers and pyridoxic acid from dried blood spots

In order to validate the intra assay precision of measurement for all six B₆ vitamers and pyridoxic acid from DBS of patients receiving high doses of vitamin B₆, eight 3 mm punches were analysed from a single DBS card derived from a patient receiving 42 mg/kg/d PLP for the management of their seizures. A summary of these results and statistical analyses performed can be found in **Table 3.2**. An acceptable % coefficient of variation (CV) is defined as <10% by the European Medicines Agency. The calculated %CV was < 10% for all vitamers except for PMP for which the %CV was 10.80%.

Table 3.2: Precision validation of B₆ vitamer and pyridoxic acid measurement from DBS. All concentrations $\mu\text{mol/L}$.

DBS punch no.	B ₆ vitamer concentration ($\mu\text{mol/L}$)						
	PLP	PNP	PMP	PL	PN	PM	PA
1	9.06	6.19	2.71	157.00	4.59	1.11	8.06
2	8.47	6.33	2.07	156.86	4.85	1.23	8.19
3	10.60	7.26	2.94	186.33	5.25	1.39	9.30
4	9.16	6.74	2.50	163.12	4.72	1.13	7.72
5	8.91	6.42	2.50	156.41	4.92	1.06	7.96
6	9.25	6.54	2.48	164.59	5.08	1.24	8.73
7	9.49	7.24	2.91	178.84	4.49	1.15	8.31
8	9.33	7.11	2.64	165.60	4.45	1.05	8.02
Mean	9.28	6.73	2.59	166.09	4.79	1.17	8.29
Coefficient of variation	6.63%	6.33%	10.80%	6.61%	5.93%	9.60%	6.09%

According to European Medicines Agency (EMA) guidelines, quality control (QC) standards were created by spiking blank vials with four concentration levels (Lower limit of quantification-QC (LLOQ-QC): $0.005 \mu\text{mol/L}$, Low-QC: $0.075 \mu\text{mol/L}$, Medium-QC: $7.5 \mu\text{mol/L}$ and High-QC: $15 \mu\text{mol/L}$) of each of the B₆ vitamers. Each sample was injected three times, at the beginning, middle and end of an analytical run and the mean concentration calculated. EMA guidelines state that the mean calculated concentrations of these QC standards should deviate by less than 20% of their nominal values at the LLOQ and less than 15% at values higher than this. The majority of samples were found to have acceptable deviation with four exceptions. These were LLOQ-QC for the measurement of PMP; LLOQ-QC and L-QC for PM and LLOQ-QC for PL. Full details of this analysis can be found in **Table 3.3**.

Table 3.3: Precision validation of LC-MS/MS measurement of B₆ vitamers and pyridoxic acid. % deviation calculated by comparing mean calculated concentrations to nominal spiked concentrations. All values $\mu\text{mol/L}$. Nominal values are 0.005, 0.75, 7.5 and 15 $\mu\text{mol/L}$ for LLOQ-QC, L-QC, M-QC and H-QC respectively. Acceptable values: < 20% deviation at LLOQ-QC; < 15% above this. nd = not detected.

LLOQ-QC (0.005 $\mu\text{mol/L}$)	Calculated B₆ vitamer concentration ($\mu\text{mol/L}$)						
	PLP	PNP	PMP	PL	PN	PM	PA
Injection 1	0.0039	0.0053	0.0070	nd	0.0043	0.0062	0.0055
Injection 2	0.0042	0.0049	0.0070	nd	0.0057	0.0071	0.0051
Injection 3	0.0047	0.0048	0.0053	nd	0.0043	0.0062	0.0048
Mean	0.0043	0.0050	0.0064	nd	0.0048	0.0065	0.0051
% deviation	-15.822	+1.593	+25.829		-5.88	+28.645	+1.287
L-QC (0.075 $\mu\text{mol/L}$)	PLP	PNP	PMP	PL	PN	PM	PA
Injection 1	0.070	0.076	0.068	0.063	0.073	0.059	0.074
Injection 2	0.070	0.075	0.071	0.049	0.071	0.050	0.075
Injection 3	0.077	0.075	0.076	0.083	0.080	0.076	0.076
Mean	0.072	0.075	0.072	0.065	0.075	0.062	0.075
% deviation	-3.516	+0.031	-4.078	-13.315	-0.139	-17.664	+0.136
M-QC (7.5 $\mu\text{mol/L}$)	PLP	PNP	PMP	PL	PN	PM	PA
Injection 1	7.87	8.09	7.16	8.66	7.87	8.09	7.76
Injection 2	7.96	7.64	7.10	7.82	7.96	7.64	7.48
Injection 3	8.02	8.08	7.24	7.31	8.02	8.08	7.50
Mean	7.95	7.94	7.17	7.93	7.95	7.94	7.58
% deviation	+5.96	+5.85	-4.452	+5.776	+5.96	+5.85	+1.078
H-QC (15 $\mu\text{mol/L}$)	PLP	PNP	PMP	PL	PN	PM	PA
Injection 1	16.20	16.55	14.83	16.50	16.20	16.55	15.25
Injection 2	16.36	15.65	14.91	16.40	16.36	15.65	15.14
Injection 3	15.96	16.40	14.75	15.31	15.96	16.40	14.99
Mean	16.17	16.20	14.83	16.07	16.17	16.20	15.12
% deviation	+7.816	+8.006	-1.124	+7.147	+7.816	+8.006	+0.832

3.2 Analysis of B₆ vitamer profiles of patient samples

The B₆ vitamer profiles of 19 patients with mutations identified in PNPO and 11 subjects receiving vitamin B₆ for their seizure control in whom PNPO deficiency had been excluded genetically or diagnostically are shown in **Table 3.4**. Preliminary control ranges were established using six healthy adult controls not receiving vitamin B₆ supplementation (also shown in **Table 3.4**).

Whilst control ranges of B₆ vitamers in DBS have not been published previously, values have been reported for plasma. Midtunn *et al.*¹⁵⁹ have reported that the only detectable B₆ vitamers in plasma were PLP, PL and PA (n = 94 healthy adult controls); reference ranges: 17 - 102 (PLP), 6 - 28 (PL) and 11 - 88 (PA) nmol/L. Other studies using plasma from both children and adults show similar ranges.^{22, 88} In this study of B₆ vitamers from DBS, comparable ranges of 41 - 110 (PLP), 7 - 24 (PL) and 7-13 (PA) nmol/L were found.

Similarly to plasma, no PM, PN or PNP were detectable in our adult DBS controls, however PMP was present at concentrations similar to that of PLP (range: 30 - 71 nmol/L). In humans, PMP is thought to be found mostly inside the cell and protein-bound, resulting from intracellular half-transamination enzymatic reactions. This, coupled with the fact that the phosphorylated B₆ vitamers are not thought to effectively cross the plasma membrane, could account for intracellular PMP compartmentalisation and hence its presence in DBS but not plasma.

Comparison of the patient samples (PNPO deficient and those with other epilepsies) with the control range revealed that concentrations of PLP, PL and PA are raised in all individuals known to be receiving vitamin B₆ supplementation. In those individuals receiving high doses of PLP, concentrations of this vitamer were 10 - 100 times the control range. PL and PA were raised still further, with concentrations of up to 4,000 times the upper limit of the control range established. PLP concentrations from 137 - 17,307 nmol/L, PL concentrations from 266 - 102,524 nmol/L and PA concentrations from 83 - 22,931 nmol/L were measured. This wide range of concentrations is likely indicative of the range of doses (shown in **Table 3.4**); type of supplementation (PLP or PN) and also the timing of dosage relative to sample collection. Data with regards to timing of the most recent dose received was not collected.

The DBS concentrations of PA are comparable to plasma concentrations identified by Mathis *et al.* (PA = 245 - 13,200) and Footitt *et al.* (PA = 144 - 7,926) in patients receiving B₆ supplementation, the cohorts of patients reported in those papers are

comparable to that used in this study, with a mixture of children with diagnosed and undiagnosed B₆-dependent epilepsies, including PNPO deficiency and ALDH7A1 deficiency.

In this study, PL and PLP concentrations of individuals on B₆ supplementation are increased compared to the previous studies (For example, maximum plasma PL and PLP concentration in individuals receiving supplementation measured by Mathis *et al.* were 16,300 and 2,930, respectively, compared to 102,524 and 17,307 nmol/L in this study). However, when comparing to the plasma results of Mathis *et al.*, it should also be noted that in their study almost all individuals for whom the type of supplementation was known were receiving PN monotherapy (35/37). In this study of DBS, however, only 4/26 were receiving PN monotherapy, with 22/26 receiving PLP supplementation for the treatment of their seizures. Hence, higher PLP or PL concentrations would be expected in our cohort. In addition, as was discussed with regard to PMP above, PLP may be compartmentalised within red blood cells, leading to higher concentrations in DBS samples compared to plasma. This will be discussed further below, particularly with regard to the B₆ vitamers concentrations found in PNPO-deficient individuals.

Table 3.4: Concentrations of B₆ vitamers and pyridoxic acid measured in DBS from PNPO deficient patients, p.R116Q heterozygotes and other patients with epilepsy responding to B₆ supplementation. *homozygous unless denoted as heterozygous (het). **Sibling of Subject 10, has not presented with seizures or received B₆ supplementation. ***no second variant identified. All concentrations shown as nmol/L. Control ranges are derived from 6 healthy adult controls not receiving B₆ supplementation. Values shown are means of the duplicate analysis of 2 x 3 mm DBS from each subject. Time of supplementation unknown except for Subject 2 and Subject 11; Subject 2 = 4 h after initial PLP dose; Subject 11 = 30 min before dose, 3h 30 min after last dose. PNPO deficient subject numbers also correspond to those in **Table 4.5**. Diagnosis = gene in which a disease causing mutation was identified. PNPO activity measured using the DBS assay developed in **Section 3.1** N/A = not available.

Subject	Diagnosis	B ₆ Therapy; Dose	PNPO variant*	PLP	PNP	PMP	PL	PN	PM	PA	PM/PA ratio	PNP/PLP ratio
Control range (nmol/L)	-	-	-	41.2 – 110.0	<5.0	29.6 – 70.7	6.7 – 24.3	<5.0	<5.0	6.5 -12.7	<0.01	<0.01
1	PNPO	PLP; 53 mg kg ⁻¹ d ⁻¹	p.R95H (het) + p.E50K; c.[364-1G>A] (het)	16812.3	10303.4	3532.4	94653.3	6550.7	1751.2	3952.8	0.44	0.61
2	PNPO	PLP; 50 mg kg ⁻¹ d ⁻¹	c.[364-1G>C]	17307.4	9301.0	5134.3	84784.3	2775.2	765.0	5932.7	0.13	0.54
3	PNPO	PLP; 50 mg kg ⁻¹ d ⁻¹	p.P213S	8538.9	6692.4	4405.3	64565.4	3893.6	2250.2	3062.8	0.74	0.78
4	PNPO	PLP; 50 mg kg ⁻¹ d ⁻¹	p.P213S	11758.8	10107.4	5157.1	48979.7	2313.2	1349.1	1929.2	0.70	0.86
5	PNPO	PLP; 40 mg kg ⁻¹ d ⁻¹	c.[263+2T>C]	2845.6	731.2	2377.7	34351.6	1264.9	1284.3	9942.7	0.13	0.26
6	PNPO	PLP; 38 mg kg ⁻¹ d ⁻¹	p.R229Q (het) + p.L136P (het)	557.5	42.5	705.4	1377.7	45.1	193.6	429.0	0.45	0.08
7	PNPO	PLP; 30 mg kg ⁻¹ d ⁻¹	c.[363+5G>A]	11777.3	937.7	187.3	102524	940.6	208.1	22930.6	0.01	0.08
8	PNPO	PLP; 30 mg kg ⁻¹ d ⁻¹	c.[363+5G>A]	296.4	6.3	103.4	266.6	<5.0	<5.0	82.8	0.00	0.02
9	PNPO	PLP; 30 mg kg ⁻¹ d ⁻¹	p.R225C	3596.8	2732.4	6795.1	8487.7	1078.4	1327.8	5411.5	0.24	0.76
10	PNPO	PLP; 10 mg kg ⁻¹ d ⁻¹	p.R116Q	1854.6	<5.0	495.2	2294.1	<5.0	<5.0	447.3	0.00	0.00
11	PNPO	PLP; 75 mg x 6 doses	p.E50K; c.[364-1G>A]	5927.9	2239.6	8169.8	12956.7	722.7	1551.4	3957.2	0.39	0.38
12	PNPO	PLP; Unknown	c.264-21_264-1delinsC (het) + p.D33V (het)	3600.1	8952.5	2304.4	38538.4	3752.7	377.5	3596.0	0.10	2.49
13	PNPO	PLP; Unknown	p.Q214fs(het) + ? ***	10385.7	5374.2	2634.3	94787.3	6290.8	1408.5	8876.4	0.16	0.52
14	PNPO	PLP; unknown	p.D33V (het) + p.Y157X (het)	2681.4	700.4	4962.1	3882.6	245.8	643.5	1443.2	0.45	0.26
15	PNPO	PLP; Unknown	p.W65L	4540.5	7485.6	1159.1	50589.3	8922.3	585.0	5332.4	0.11	1.64
16	PNPO	PN; 123 mg kg ⁻¹ d ⁻¹	p.R116Q;p.R225H	865.6	6715.6	1589.5	4926.3	4171.0	474.0	868.0	0.55	7.76
17	PNPO	PN; 30 mg kg ⁻¹ d ⁻¹	p.D33V	136.9	8763.8	1322.7	680.6	3031.2	428.8	450.8	0.95	63.87
18	PNPO	PN; 100 mg x 2 doses	p.R116Q	4059.4	8307.1	495.2	16477.8	5705.8	160.9	2860.5	0.02	2.04
19	PNPO	None; N/A	p.R116Q**	146.9	<5.0	86.1	29.5	<5.0	<5.0	25.0	0.00	0.00

Subject	Diagnosis	B ₆ Therapy; Dose	PLP	PNP	PMP	PL	PN	PM	PA	PM/PA ratio	PNP/PLP ratio
Control range (nmol/L)	-	-	41.2 – 110.0	<5.0	29.6 – 70.7	6.7 – 24.3	<5.0	<5.0	6.5 - 12.7	<0.01	<0.01
C1	?	PLP; 30 mg kg ⁻¹ d ⁻¹	9109.3	<5.0	501.5	83314.2	79.5	225.7	2774.9	0.08	0.00
C2	TRMT11	PLP; 30 mg kg ⁻¹ d ⁻¹	9633.8	41.6	172.1	20733.3	<5.0	<5.0	5994.7	0.00	0.00
C3	?	PLP; 10 mg kg ⁻¹ d ⁻¹	3930.6	<5.0	17.6	7732.3	<5.0	18.9	4668.6	0.00	0.00
C4	KCNQ2	PLP; Unknown	794.4	23.4	123.5	1357.8	81.40	108.0	298.10	0.36	0.03
C5	?	PLP; Unknown	542.8	<5.0	244.1	861.8	<5.0	26.8	356.4	0.08	0.01
C6	?	PLP; Unknown	1974.5	9.7	85.6	1702.6	<5.0	<5.0	235.5	0.00	0.00
C7	?	PLP; Unknown	2997.4	13.1	<5.0	2993.6	<5.0	<5.0	481.4	0.00	0.00
C8	PROSC	PN; 250 mg d ⁻¹	973.1	<5.0	<5.0	918.1	<5.0	<5.0	165.9	0.00	0.00
C9	?	Unknown	127.8	<5.0	38.4	100.9	<5.0	14.4	18.3	0.75	0.06
C10	ALDH7A1	Unknown	7683.8	<5.0	<5.0	17854.9	<5.0	<5.0	2085.1	0.00	0.00
C11	STX1B	Unknown	1338.0	<5.0	<5.0	4341.2	<5.0	<5.0	750.5	0.00	0.00

The most striking observation upon examination of the DBS vitamer profiles is that, with a few exceptions, the concentrations of PNP, PMP, PN and PM are higher in DBS from PNPO deficient patients compared to the 'other epilepsy' cohort (**Figure 3.1**). Although not exclusive to PNPO deficiency, this shows that raised concentrations of these vitamers can be indicative of PNPO deficiency. This is due to substrate accumulation caused by a deficiency of PNPO which catalyses PNP and PMP conversion to PLP.

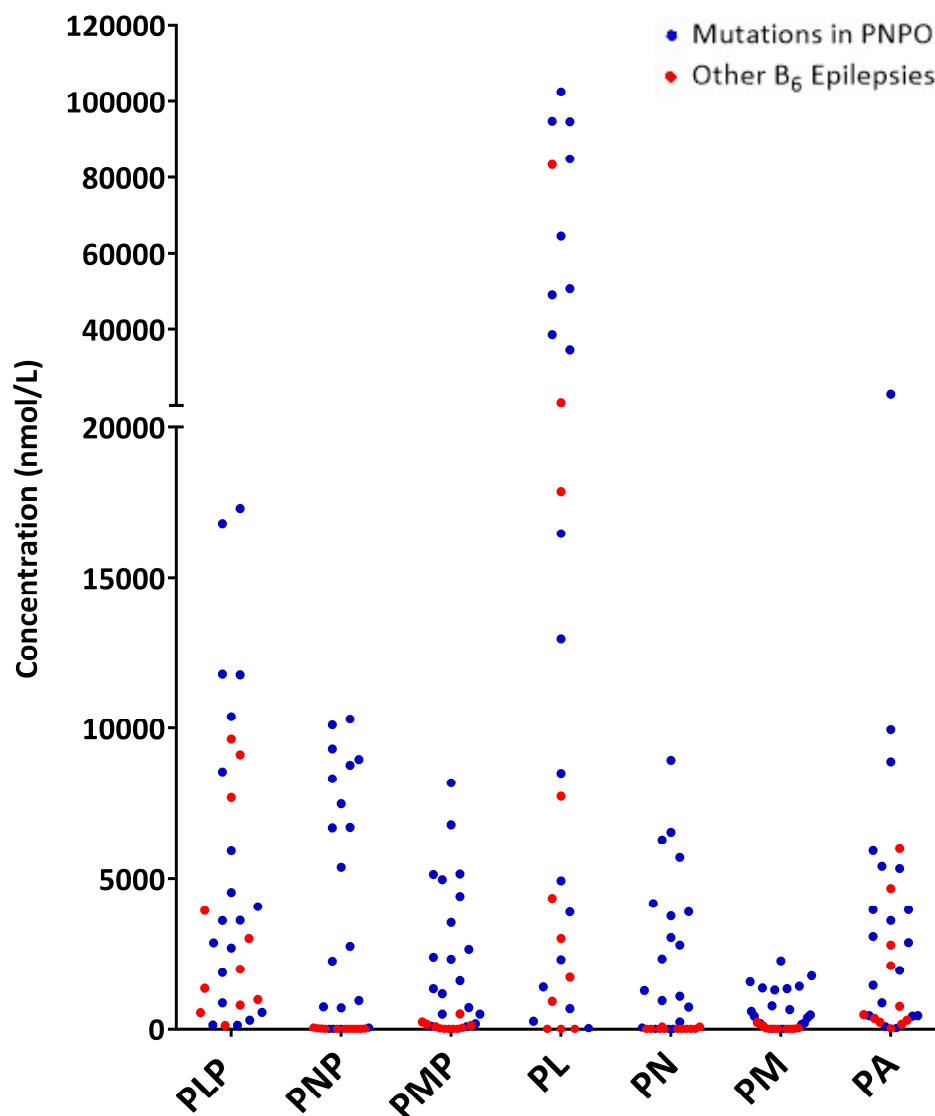


Figure 3.1: B₆ vitamer and pyridoxic acid concentrations in DBS. Data points shown are the mean from duplicate analysis of each DBS punch.

There are however three cases (**Subjects 10, 19 and 8**) within the PNPO cohort for whom PNP, PN and PM were not raised. **Subject 10**, who is homozygous for the p.R116Q PNPO variant, had a B₆ vitamer profile similar to that seen in patients with normal PNPO activity receiving B₆ supplementation (except for raised PMP). However, residual or tissue-specific p.R116Q activity cannot explain the dissimilarity of **Subject 10**'s vitamer profile to that of other PNPO-deficient subjects: **Subject 18**, also homozygous for p.R116Q, has raised levels of PNP, PMP, PN and PM. **Subject 19**, the p.R116Q homozygous sibling of **Subject 10**, who has never been supplemented with B₆ and has not presented with seizures, has a vitamer profile similar to controls. **Subject 8** also appears to have only mildly raised vitamer concentrations compared to controls despite apparently receiving 30 mg/kg/d PLP; this raises questions with regards to the treatment compliance of this patient.

In the remaining PNPO deficient patients, PNP concentrations were higher than those of individuals with other epilepsies receiving B₆ supplementation. Previously it has not been possible to accurately quantify the concentration of PNP. However, a PNP standard has recently become commercially available and this allowed accurate quantification of PNP for the first time. In previous studies PNP concentrations were either expressed as 'concentration units' (CU)²² or excluded completely.^{21, 88} The assumption that Footitt *et al.* made with regard to their PNP 'concentration units' relied on the signals of PLP and PNP upon LC-MS/MS analysis being similar. We found this to be the case, with the raw signals of each vitamer being within 10% at the same concentration; this means an approximate comparison to the data of Footitt *et al.* can be made. If the PNP concentrations measured from DBS are compared with the 'concentration units' (assumed to approximate to nmol/L) measured by Footitt *et al.* in plasma (43 and 77 CU in PNPO deficient patients; (n = 2)) those reported here in DBS are usually far higher (42.5 – 10,303 nmol/L; mean = 4,705 nmol/L).

This is possibly due to PNP being compartmentalised in erythrocytes (as discussed above with regards to PLP and PMP), a hypothesis supported by results for the two subjects for whom we have PNP concentration measurements for paired DBS and plasma samples; **Subject 17** (DBS: 8,764 nmol/L, plasma: 30 nmol/L) and **Subject 11** (DBS: 2,240 nmol/L, plasma 17 nmol/L). Similarly, a comparison of PMP concentrations measured from DBS of PNPO deficient patients (187.3 – 8170 nmol/L; mean = 2717 nmol/L; (n = 19)) to those measured in plasma by Footitt *et al.* (18 and 101 nmol/L; (n = 2)) show higher concentrations in DBS.

A previous study (Mathis *et al.*)⁸⁸ has suggested that a raised PM/PA ratio in plasma is diagnostic for PNPO deficiency. However, the cohort of PNPO deficient patients included in that study was small (n = 6) and one subject homozygous for the p.R116Q mutation was excluded (not referred to as PNPO deficient). 4/6 of these patients had the same pathogenic homozygous PNPO variant (p.R225H). We did not see the same clear distinction when PM/PA ratios were measured in DBS in a larger cohort of PNPO deficient patients. Although a significant difference was identified between groups using a Mann-Whitney U test ($P < 0.01$), no diagnostic cut-off could be created using this data. 4/19 PNPO deficient individuals had a PM/PA ratio (≤ 0.01) similar to that seen in the adult control range (n = 6). 4/11 subjects receiving B₆ supplementation who were not PNPO deficient (no mutations found in *PNPO*) had a raised PM/PA ratio (> 0.01) (**Figure 3.2**). It was not possible to obtain paired plasma samples from these individuals in order to make a direct comparison between DBS and plasma PM/PA ratios. However, it is unlikely that the sample type will affect the discrepancy between our results and those of Mathis *et al.* as the four PNPO deficient patients with PM/PA ratios less than 0.01 had PM concentrations of less than 5 nmol/L. Concentrations would not conceivably be high enough in matched plasma samples from each of these to provide PM/PA values raised enough to delineate these patients from the subjects receiving B₆ supplementation who were not PNPO deficient.

We hypothesise that the lack of diagnostic utility of PM/PA ratios, in our cohort, contrary to the findings of Mathis *et al.*, is due to the expanded variety of genotypes or different types of supplementation. In total, our cohort included 19 subjects with 15 different genotypes. The PNPO deficient cohort published by Mathis *et al.* included 6 subjects with only 3 different homozygous mutations (4 x c.674G > A; 1 x 263+2T>C; 1 x c.416A>C). Mathis *et al.* also excluded one individual homozygous for p.R116Q as being PNPO deficient; this patient had a normal PM/PA ratio.

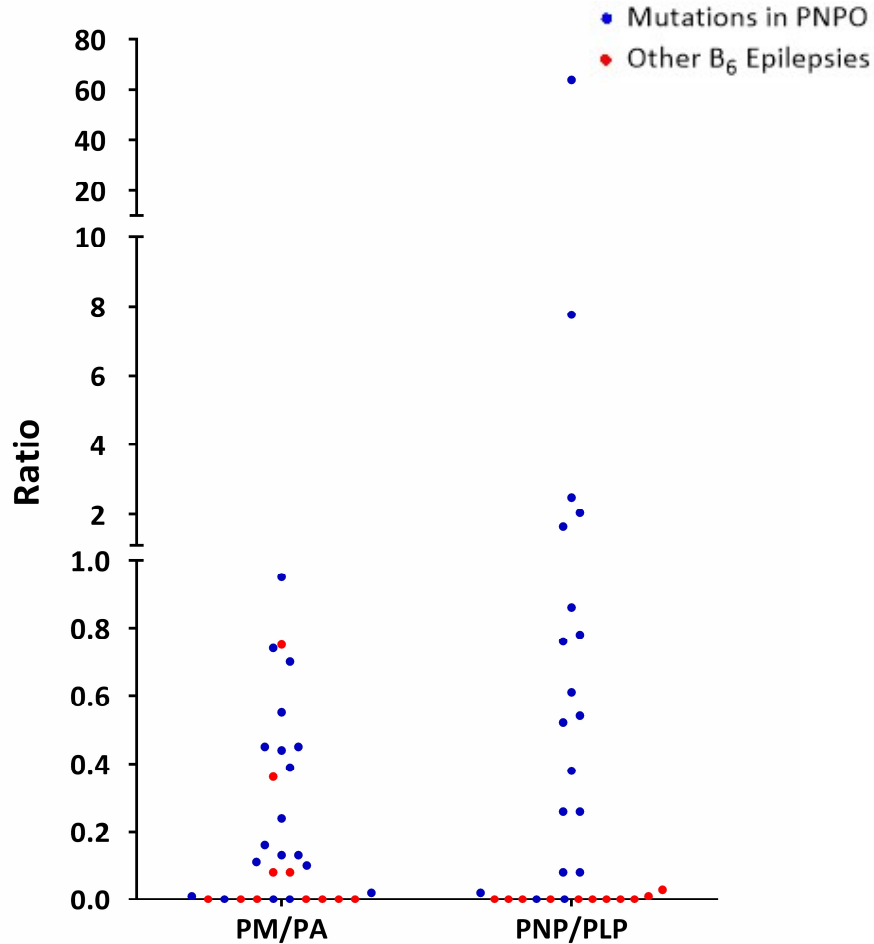


Figure 3.2: PM/PA and PNP/PLP ratios in DBS. Note split Y axis. Data points shown are the mean of the ratios calculated (n=2).

There has been some discussion as to the potential pathogenicity of the p.R116Q variant in *PNPO*.⁸⁷ Of the *PNPO* deficient patients in our cohort for whom the PM/PA ratio was <0.01 , 2/3 were homozygous for p.R116Q. This data agrees with the findings of Mathis *et al.* and would suggest that p.R116Q is not pathogenic. However, the response of p.R116Q patients to PLP and the lack of other mutations found in these patients indicate that this variant can be pathogenic. Equally, studies have recently shown that p.R116Q affects the structure of *PNPO*.⁷⁴ The effect of the p.R116Q variant will be discussed further in **Section 4.2**.

Of the 7 *PNPO* deficient patients Mathis *et al.* measured PM/PA ratios for, only one *PNPO* deficient individual was receiving vitamin B₆ exclusively in the form of PLP, with 6 receiving either a mixture of PN and PLP or PN monotherapy. 15/19 patients in our cohort received PLP supplementation for their seizures, with 3 of the remaining

4 receiving PN (one individual was not receiving supplementation). It is possible that PM/PA ratios are dependent upon type of B₆ supplementation as well as genotype; it may be that, for some genotypes, PLP supplementation is less likely to lead to a raised PM/PA ratio than PN supplementation. For example, in our cohort, **Subject 18** is the only p.R116Q homozygote with a PM/PA ratio > 0.01, and also the only p.R116Q homozygote receiving PN monotherapy. This warrants further investigation.

The raised PNP concentrations identified in DBS samples from PNPO deficient patients gave rise to the hypothesis that a raised PNP/PLP ratio could be a better indicator of PNPO deficiency than a raised PM/PA ratio (**Figure 3.2**). A Mann-Whitney U test was performed and a significant difference was identified between cohorts ($P < 0.0001$). Although some overlap is seen between controls and **Subjects 10, 19 & 8** when using PNP/PLP ratios, there appears to be a greater distinction of the PNPO-deficient patients from controls than when PM/PA is used. Given the wide variety of supplementation type (PN or PLP), dosage and the variation in vitamer concentrations prior to and after supplementation (see **Section 3.3.2**), it is likely a PNP/PLP ratio will prove more indicative of PNPO deficiency.

The p.R116Q homozygous **Patients 10 & 19** did not have raised PNP/PLP ratios. As mentioned above, **Patient 19** is not receiving B₆ supplementation. **Patient 10** receives 10 mg/kg/d PLP. The other p.R116Q homozygote in this study (**Patient 18**) had a raised PNP/PLP ratio of 2.04; this patient was receiving 200 mg/d PN. This disparity within the same genotype could be due to difference in supplementation type. Indeed, this data allows a broader comparison of B₆ vitamer profiles between PNPO deficient individuals receiving PLP ($n = 15$) and PN ($n = 3$) for seizure control. As has previously been reported in studies from plasma^{22, 88}, little distinction could be made based solely on supplementation type. As mentioned above, in these prior studies PNP had not been quantified. It was predicted that PNP concentrations would be higher in patients receiving PN supplementation due to the metabolic block at the PNPO enzyme. The mean PNP concentration of PNPO deficient patients receiving PN supplementation was approximately twice that of those receiving PLP (PN sup. = 7928 nmol/L PLP sup. = 4373 nmol/L). A similar pattern was seen when comparing the PNP/PLP ratios of patients receiving PN with those receiving PLP: (PN; range = 2.04 – 63.87, $n=3$); (PLP; range = 0.00 – 2.49; $n=15$). However, in both cases the groups were not clearly delineated, with some overlap seen. When PN is used for treatment, there must be some residual PNPO activity, unless gut flora bacteria or another process is capable of converting PL or PLP to PN or PNP.

Subject 17, who receives 30 mg/kg/d PN supplementation for treatment of their PNPO deficiency, is particularly interesting. Their PLP concentration (137 nmol/L), unlike most other patients on B₆ supplementation, is only slightly above the adult control range but the concentrations of other vitamers are raised dramatically (all at least ten times the upper limit of the control ranges established). Plasma and CSF PLP concentrations from this patient were within the normal range (data not shown). That this concentration of PLP is enough to provide seizure control in **Subject 17** raises the question of whether other PNPO deficient patients are receiving doses higher than required, an important factor when high doses of PLP have been suggested to be the cause of hepatic dysfunction in some of these patients (see **Section 6**).

Although samples were collected from 11 individuals with B₆-dependent seizures that were not due to PNPO deficiency, no more than one was collected from each of these disorders as defined genetically. This made it impossible to comment conclusively on whether a profile specific to each of these disorders could be identified.

3.3 Kinetics of oral pyridoxal 5'-phosphate supplementation

When developing a method for the measurement of B₆ vitamers from DBS, one potential variable that should be taken into account is the variation of vitamer concentrations before and after a dose of vitamin B₆. Patients usually receive PLP and PN orally. Mathis *et al.* have recently reported the plasma profile of PLP, PL, PA, PN and PM over a 24 hour period after a single 200 mg dose of PN in a healthy adult control.⁸⁸ This confirmed the findings in mice¹⁶⁰ that orally supplemented PN rapidly converts to pyridoxal; Mathis *et al.* showed that after 2 hours PN peaks at a concentration of ~2,000 nmol/L but returns to baseline concentrations after 4 hours. PLP concentrations increase steadily to ~800 nmol/L 12 hours after supplementation, before remaining steady at 24 hours. PL and PA concentrations increased to 4,000 – 5,000 nmol/L 2 hours after supplementation. At this point they were the most abundant B₆ metabolites, before declining to concentrations lower than that of PLP (<800 nmol/L) after 12 hours and continuing their gradual decline almost to baseline values after 24 hours.

In rats, the plasma concentrations of PLP and PL after oral and intravenous doses of PLP have been studied.¹⁶¹ This showed much higher plasma PLP upon intravenous dosing and helped confirm the hypothesis that most oral PLP is dephosphorylated before gut absorption. However, to date, a human profile of the B₆ vitamers immediately after oral PLP supplementation has not been measured. We report the DBS concentrations of B₆ vitamers and pyridoxic acid prior to and after a single PLP dose in two PNPO deficient patients; a 15 year old child receiving long-term PLP supplementation (**Subject 11**) and a neonate receiving their first dose of PLP shortly after birth (**Subject 2**).

3.3.1 Long-term PLP treatment of an adolescent

B₆ vitamer and pyridoxic acid concentrations, before and after supplementation with PLP, were measured in a DBS from one of the original PNPO-deficient patients described by Mills *et al.* in 2005 (**Patient J2**). Their first PLP dose was 50 mg, 3 weeks after birth. Thereafter, they have received PLP for the treatment of their seizures for their entire life. This patient is now 15 years old and requires 75 mg PLP (orally) 6 times a day to control their seizures. Compound heterozygous pathogenic *PNPO* variants are present in this individual (c.[148G> A]; c.[364-1G>A]).

Blood was taken from Subject 11 and spotted onto filter cards 30 minutes prior to PLP supplementation (T-30) and 10, 20, 30, 45, 60, 90 and 120 min (T10, T20, T30, T45, T60, T90 and T120) after oral supplementation with one 75 mg dose of PLP. Concentrations of the B₆ vitamers and pyridoxic acid over this time course were quantified (**Figure 3.3**) using the method described in **Section 3.2**.

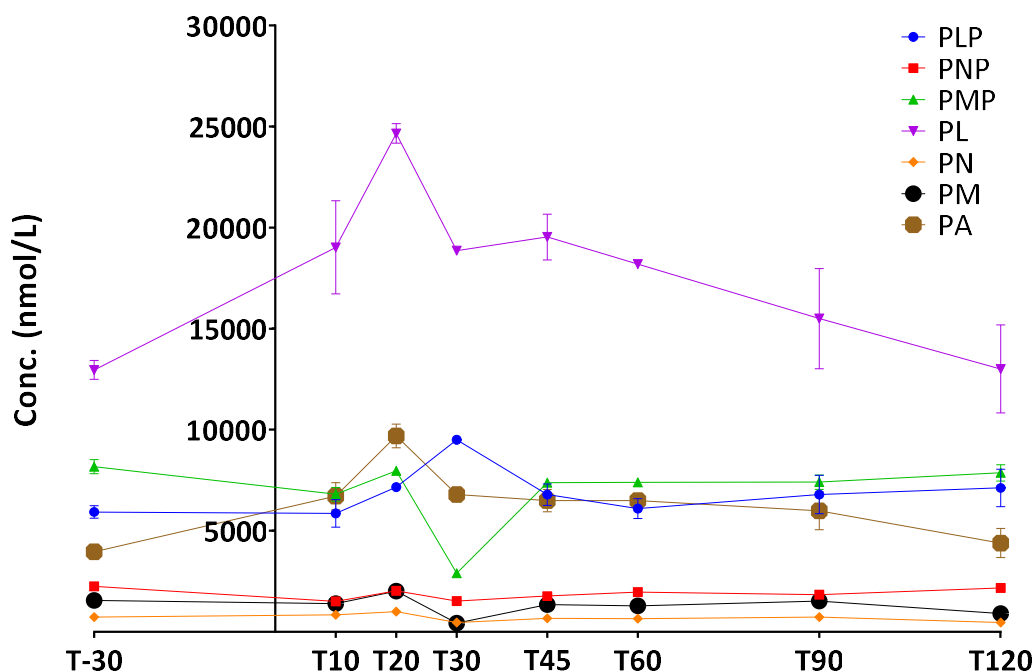


Figure 3.3: Subject 11 - Concentrations of B₆ vitamers and pyridoxic acid prior to and after oral supplementation with 75 mg PLP. Each point is the mean of 2 x 3 mm DBS punches and error bars indicate SEM.

Upon supplementation, concentrations of PL and PA show the most dramatic rise before returning to baseline after 120 min. This is similar to that seen in the plasma of healthy adult controls after PN supplementation (Mathis *et al.*). Unlike the studies of Mathis *et al.*, however, where PA was more abundant than PL after PN supplementation, PL concentrations were higher than PA in our patient. This is perhaps indicative of the differences between DBS and plasma samples, PLP and PN supplementation or the fact that our patient is receiving long-term supplementation. The increase in PA concentration suggests that PL is rapidly converted to PA by aldehyde oxidase and aldehyde dehydrogenases.

In the study by Mathis *et al.*, a steady and constant rise in PLP concentration was observed up to 12 h after PN supplementation of a healthy adult control, before

plateauing. However, no increase in PM concentration was seen. In our subject PLP rose initially, peaking at about 150% of baseline at T30, but values then decreased quickly (T60) to those seen before supplementation. Concentrations of the other vitamers (PNP, PMP, PN, PM) stayed relatively constant over the time course but were much higher than those seen in healthy controls (reference ranges in **Table 3.4**). These high concentrations were expected given the long term supplementation of this PNPO deficient patient; B₆ vitamer profiles typical of these patients were discussed in **Section 3.2**.

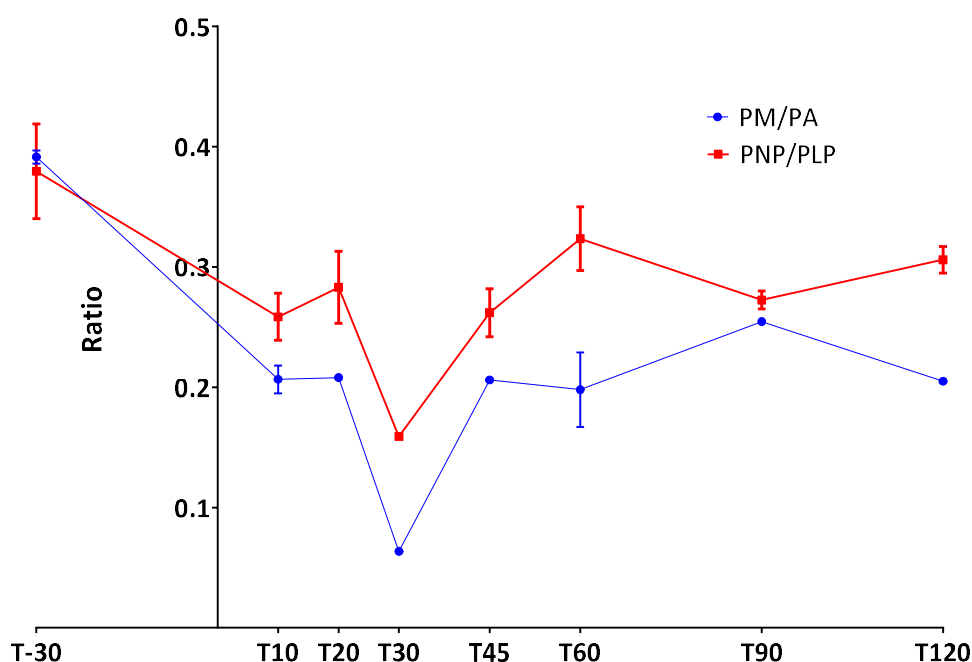


Figure 3.4: Subject 11 – PM/PA and PNP/PLP ratios prior to and after oral supplementation with 75 mg PLP. Each point is the mean of 2 x 3 mm DBS punches and error bars indicate SEM.

The ratios of PM/PA and PNP/PLP in the DBS of **Subject 11** prior to and after oral PLP supplementation are raised at each time point relative to those of healthy adult controls ($n = 6$; ref range <0.01 for both PM/PA and PNP/PLP) (**Figure 3.4**; reference ranges in **Table 3.4**). This suggests that when using PM/PA or PNP/PLP ratios to inform the diagnosis of PNPO deficiency (see **Section 3.2**) in a patient receiving long-term supraphysiological doses of PLP, the time of sampling around supplementation is not important. Although still raised, a reduction in both ratios is identified at each time point after supplementation when comparing to the dose 30 minutes before supplementation. This is unsurprising as PLP and PA concentrations appear to

increase after PLP supplementation whereas PNP and PM concentrations are relatively stable.

3.3.2 Neonatal prophylactic PLP treatment

Subject 2 was prenatally diagnosed with PNPO deficiency (homozygous c.364-1G>C) and a sibling was already receiving PLP for seizure control. Parents decided to continue with the pregnancy and steps were taken to avoid intrauterine seizures and neurological damage to the foetus. This included the mother taking daily dietary supplements containing 10 mg PN and prophylactically treating the child with PLP immediately after birth.

The child was born at term (3.6 kg) and treated with oral PLP. Samples were collected 10 mins prior to, and at three time points after a 36 mg dose of PLP given 15 mins after birth. The B₆ vitamers concentrations for these DBS samples are shown in **Figure 3.5**.

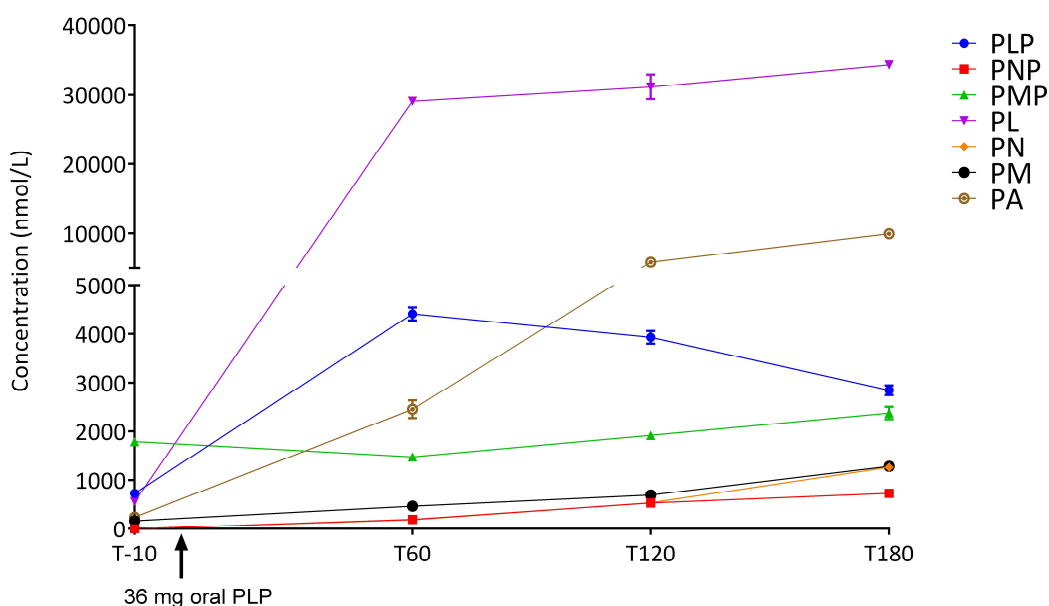


Figure 3.5: Subject 2 – Concentration of B₆ vitamers and pyridoxic acid prior to and after oral supplementation with 35 mg PLP. Note split Y axis. Error bars indicate SEM. (n=2)

Interestingly, at T-10, prior to supplementation, concentrations of PLP, PL and PA are already raised above those identified in the adult control range described in **Section 3.2**. This could be due to the mother receiving B₆ supplementation while pregnant and passing these vitamers to the foetus or simply reflective of differences between the blood B₆ vitamers concentrations of a neonate and adults. PMP and PM are also both

raised prior to supplementation, indicating that the metabolic block caused by PNPO deficiency has impaired the recycling of PMP after formation by half-transamination reactions in utero (see **Section 1.1.1**). PMP concentrations are relatively constant but those of PM increase over the time course. PN and PNP are not detectable at T-10, unlike most PNPO deficient individuals receiving long term supraphysiological PLP supplementation who often have concentrations orders of magnitude higher than those in controls.

The most dramatic increase in concentration after supplementation was seen for PL, reaching 29,087 nmol/L one hour after supplementation. This was expected given that PLP must be hydrolysed to PL before intestinal absorption. PLP concentrations also increased over the first 60 minutes, before falling again between T60 and T180, though not to original concentrations seen prior to supplementation. PA concentrations increased, although at a slower rate initially to those of PL.

The profile of the B₆ vitamers concentrations seen in **Subject 2** prior to supplementation is different to that described above for **Subject 11**. Although, as discussed, PLP, PL and PA concentrations are raised above the healthy adult control ranges described in **Section 3.2**, concentrations of most vitamers are approximately ten times lower in **Subject 2** than those in **Subject 11**. This is indicative of an accumulation of the B₆ vitamers and pyridoxic acid after long-term supplementation in **Subject 11**, a direct comparison is therefore impossible.

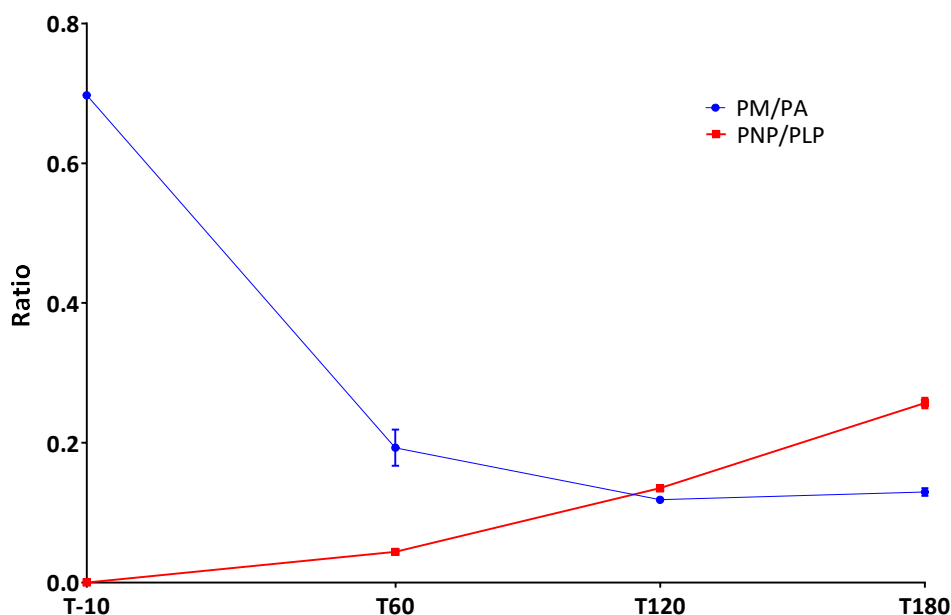


Figure 3.6: Subject 2 – PM/PA and PNP/PLP ratios prior to and after oral supplementation with 35 mg PLP. Error bars indicate SEM. (n=2)

The PM/PA ratios in the DBS prior to and after PLP supplementation in **Subject 2** show a reduction over the time course, from 0.7 before supplementation (at birth) to 0.1 three hours after the first 35 mg PLP dose (**Figure 3.6**). Hence an elevated PM/PA ratio was evident prior to the neonate presenting with seizures/receiving B₆ supplementation. However, the mother received oral supplementation with PN (10 mg daily). It is possible the PM/PA ratio would not be raised in a neonate whose mother was not in receipt of supplements during pregnancy.

PNP/PLP ratios are low before supplementation (within the adult control range of <0.01), and gradually increase over the time course studied. This is due to relatively low PNP concentrations present initially, unlike other PNPO deficient patients investigated previously. PL/PLP are the main B₆ vitamers present in the blood of a healthy adult and only PL would have crossed the placenta.¹⁶² For this reason the patient had likely not been exposed to significant amounts of PN or PNP *in utero*. By this reasoning, it seems likely that PNP/PLP ratios will only be raised after feeding and exposure to pyridoxine via the diet. The main B₆ vitamers in breast milk are PLP and PL.¹⁶³ This may provide complications for the use of PNP/PLP ratios for the diagnosis of PNPO deficiency in children that are exclusively breastfed, and means that DBS taken from these babies may be unsuitable for PNP/PLP analysis.

Since the patient received only PLP supplementation the gradual rise seen in concentrations of PN and PNP was at first puzzling. There are no known processes in the human body capable of the reduction of PL or PLP to PN or PNP, respectively. However, it is known that **Subject 2** received formula in place of breast milk immediately after birth. As mentioned, breast milk contains mostly PLP and PL, whereas baby formula usually contains PN. Ingestion of the PN present in formula could be another explanation for these gradually increasing concentrations of PN and PNP. It is also possible that the microbes constituting the neonatal gut microbiome¹⁶⁴ are capable of the conversion of PL or PLP to PN or PNP. However, an enzyme catalysing this reaction has not yet been characterised in bacteria or archaea.

An NADPH-dependent pyridoxal reductase (PLR) has however been characterised in *Saccharomyces cerevisiae*¹⁶⁵ and *Arabidopsis thaliana*¹⁶⁶; it was postulated that an enzyme capable of catalysing this reaction is also present in humans. In order to investigate whether human red blood cells are capable of the reduction of PLP or PL to PNP or PN, 3 mm healthy adult control DBS punches and 3 mm empty DBS card punches were incubated for 30 minutes with 1 µmol/L PLP and 1 mmol/L NADPH. Experimentation was carried out using a potassium phosphate buffer adjusted to pH 7.0. This pH is within the optimal range for yeast pyridoxal reductase and other conditions are similar to those previously used for the assay of pyridoxal reductase activity.^{165, 167} No decrease of PLP concentration or corresponding increase in PNP was identified (**Data not shown**).

Using a pBLAST search, the human protein most homologous to *A. Thaliana* PLR is KCNAB2 (E-value: 1.4e-24; 27.1% identity), homology is strong across the entire protein sequence. This is a beta subunit of a cytoplasmic potassium channel and is known to modulate activity of these channels.¹⁶⁸ KCNAB2 is an NADPH-dependent aldoketoreductase of broad substrate specificity¹⁶⁹, it is possible that it accepts PLP or PL as a substrate but is not expressed highly enough in the blood to provide detectable reductase activity by the methodology used in this study. This would also be important if the mechanism behind the anti-epileptic action of PLP supplementation (See **Section 7**) is related to a change in the conformation of the KCNAB2 subunit upon the binding and reduction of PLP to PNP. Important future work would be to fully investigate the presence of an enzyme in humans capable of the conversion of PL or PLP to PN or PNP. Depending on the function of this enzyme, this could be important for the treatment of epilepsy and, in particular, PNPO deficient

individuals treated with PLP (if accumulation of PNP was having an effect upon their seizure susceptibility or treatment).

Subject 2 is now 3 years of age, neurodevelopmentally normal and has not experienced any seizures. However, the subject has early stages of hepatic dysfunction on 40 mg/kg/d PLP. Specifically, the patient's liver is mildly enlarged with mild cytolysis and elasticity of 10.6 kPa (personal communication: Dr. Manuel Schiff). This shows the importance of identifying the mechanism behind liver damage in PNPO deficient patients on PLP supplementation (see **Section 6**).

3.4 Discussion and future work

This work demonstrates that measurement of B₆ vitamers from dried blood spots is a useful tool for the diagnosis of PNPO deficiency. Indeed, it appears that DBS are a more useful sample type than plasma due to the presence of higher PNP concentrations in DBS relative to plasma. This enables the use of a raised PNP/PLP ratio as a diagnostic indicator of PNPO deficiency.

Despite the collection of 11 samples from individuals with B₆-dependent seizures that were not due to PNPO deficiency, it was not possible to achieve numbers large enough to comment conclusively on whether a characteristic B₆ vitamer profile in DBS can be identified that assists in the diagnosis of these other B₆ dependent seizure disorders (e.g. PLPHP deficiency). The analysis of samples from a greater number of individuals with other disorders affecting B₆ metabolism would be important future work.

One potential limitation of the clinical and diagnostic utility of measuring B₆ vitamer concentrations from subjects on high-dose supplementation is the variation in concentrations prior to and after oral doses of B₆, which could be difficult to control for. This is described in more detail in **Section 3.3** where B₆ vitamer concentrations from two patients over a time course before and after doses of PLP are discussed. Similarly, it seems that the patterns identified (e.g. raised PNP/PLP and PM/PA ratios) are less pronounced or absent in patients receiving lower doses of PLP or PN (e.g. **Subject 8**), and in some patients homozygous for p.R116Q.

A useful addition to the pharmacokinetic studies in **Section 3.3** would be characterisation of the B₆ vitamer profile in the blood of normal control subjects with intact vitamin B₆ metabolism after receiving PLP supplementation.

The work carried out so far has been performed using a limited control range of 6 healthy adults. Since this method will be used mostly for the analysis of samples derived from children, age-matched control ranges should be established; these should include both children receiving B₆ supplementation and others without exposure to supraphysiological B₆ doses. Although control ranges have been published for plasma, we have shown that major differences are apparent when plasma profiles are compared to those of DBS (higher levels of PLP, PNP and PMP in DBS), thought to be due to the presence of erythrocytes.

In addition, it would be useful to look at whether there is any correlation between CSF and DBS B₆ vitamers concentrations – this could help titrate dosage to the minimum required for seizure control. Towards a similar end, future work on the kinetics of PLP/PN supplementation should also involve the supplementation of a healthy control with high dose PLP in order to characterise the differences between PNPO deficient individuals and controls.

With regards to the suitability of this method for clinical use, whilst the analysis of most B₆ vitamers was acceptable, PM, PL and PMP had unacceptably high variability at their LLOQs (>15%). Future work should involve the optimisation of either the LC-MS/MS method or sample preparation to enable the accurate quantitation of lower concentrations of these analytes.

In addition, validation of the recovery of B₆ vitamers and pyridoxic acid from DBS was unsuccessful due to enzymatic interconversion occurring when whole blood was spiked (**Section 3.1.1**). In the future, this experimentation should be repeated using, for example, inhibitors of the B₆ metabolic enzymes in order to minimise this effect and ensure that recoveries are accurate.

4.DEVELOPMENT OF LC-MS/MS-BASED ENZYME ASSAYS FOR THE MEASUREMENT OF PNPO ACTIVITY

A B₆-dependent seizure disorder, pyridox(am)ine 5'-phosphate oxidase (PNPO) deficiency results in the inability to interconvert the inactive forms of vitamin B₆ into the active cofactor, pyridoxal 5'-phosphate (PLP) (**Section 1.2.1**). PNPO deficiency is treatable with high doses of either PLP or pyridoxine (PN) and diagnosis is currently performed using genetic testing.

Section 3 describes the assessment of whether the measurement of B₆ vitamers and pyridoxic acid in dried blood spots (DBS) is a useful tool for the diagnosis of PNPO deficiency. It was discovered that raised PM/PA and PNP/PLP ratios may be important biomarkers for this disorder, with PNP/PLP proving the most useful. However, this still did not provide a conclusive diagnosis of PNPO deficiency; some PNPO deficient individuals had normal (≤ 0.01) PNP/PLP ratios. In particular, treatment naïve PNPO deficient individuals and/or those homozygous for the p.R116Q variant in PNPO may not have raised PNP/PLP ratios (**Section 3.2**). In addition, some individuals that had PNPO deficiency excluded genetically but were receiving B₆ supplementation had PNP/PLP ratios > 0.01 .

There is therefore still a requirement for a conclusive and rapid diagnostic test for PNPO deficiency. It was hypothesised that the development of an LC-MS/MS-based enzyme assay for the measurement of PNPO activity using DBS could meet this need. Several enzymatic assays for measuring PNPO activity have been described in the literature. However, these are not suitable for routine clinical diagnostic use, they require large sample volumes, radiolabelled substrates or are simply too laborious.^{39, 59, 170-174} This chapter describes the development of an LC-MS/MS-based PNPO enzyme assay using DBS.

The use of DBS from a heel or finger-prick is an established method for sample collection which was developed initially for the measurement of phenylalanine levels in the diagnosis of phenylketonuria in the 1960s.¹⁴⁹ Subsequently the use of DBS to assay enzymes present in the circulating blood has been reported for various metabolic disorders.¹⁷⁵ The non-invasive collection and simple transport/storage are a major advantage of DBS.

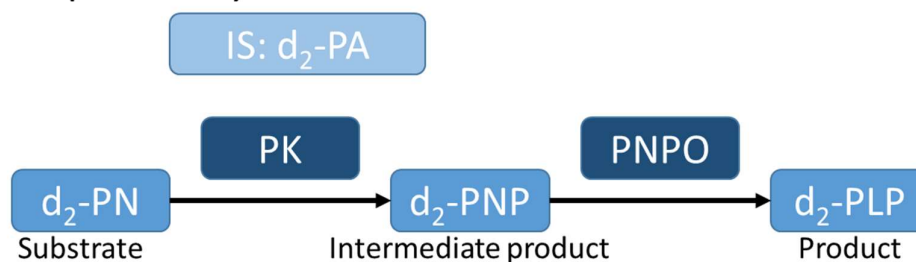
In addition to measuring PNPO activity from patient DBS, the assay was also adapted for analysis of the kinetics of recombinant PNPO enzyme. This is useful for the *in vitro* assessment of potentially pathogenic variants in the PNPO protein. This form of PNPO assay was used to determine the effect of the p.R116Q substitution. Individuals homozygous for the p.R116Q variant have a variable phenotype, some

presenting with the B₆-responsive seizures typical of PNPO deficiency and others seemingly healthy.⁸⁷ It was hoped that by studying the kinetics of recombinant p.R116Q protein, the reason behind this variable phenotype could be elucidated.

4.1 Investigation and development of an LC-MS/MS-based Enzyme assay using dried blood spots for the diagnosis of PNPO deficiency

Several protocols for the measurement of PNPO activity from dried blood spots were investigated. This included the comparison of single-step and coupled enzyme assays (**Figure 4.1**; **Section 4.1.1.1**); the coupled assay was optimised and validated for clinical use (**Sections 4.1.1.2 – 4.1.1.3**). In contrast to a single-step enzyme assay this type of assay requires an additional enzymatic conversion step prior to that which is of interest. Measurement of the rate of this second step is used to quantify enzyme activity. In this case, the first step of the coupled assay relied on pyridoxal kinase (PK), which phosphorylates the B₆ vitamer (in this case, PN) added as substrate prior to incubation. This results in PNP formation as an intermediate, the consumption and formation of which could be measured. The second step was conversion of PNP to PLP by the PNPO enzyme. The single-step assay investigated consisted of the conversion of PMP to PLP. Formation of PLP and the other B₆ vitamers, as required, were quantified using the LC-MS/MS method described in **Section 2.4**. Whilst conditions were varied throughout experimentation a summary of the protocol used throughout this section for measurement of PNPO activity can be found in **Figure 4.2**.

a) Coupled assay



b) Single-step assay

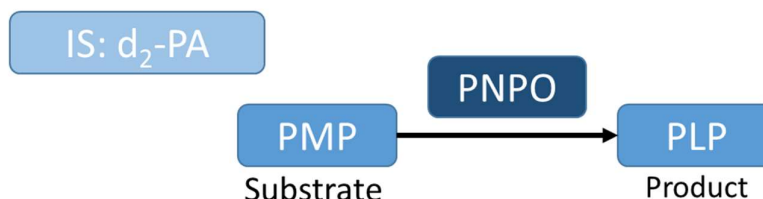


Figure 4.1: Coupled and single-step PNPO assays using d₂-PN and PMP as substrates. a) coupled PNPO assay; b) single-step PNPO assay; IS = internal standard used for quantification of each analyte; PA = 4-pyridoxic acid; PN = pyridoxine; PNP = pyridoxine 5'-phosphate; PLP = pyridoxal 5'-phosphate; PMP = Pyridoxamine 5'-phosphate; PNPO = pyridox(am)ine 5'-phosphate oxidase.

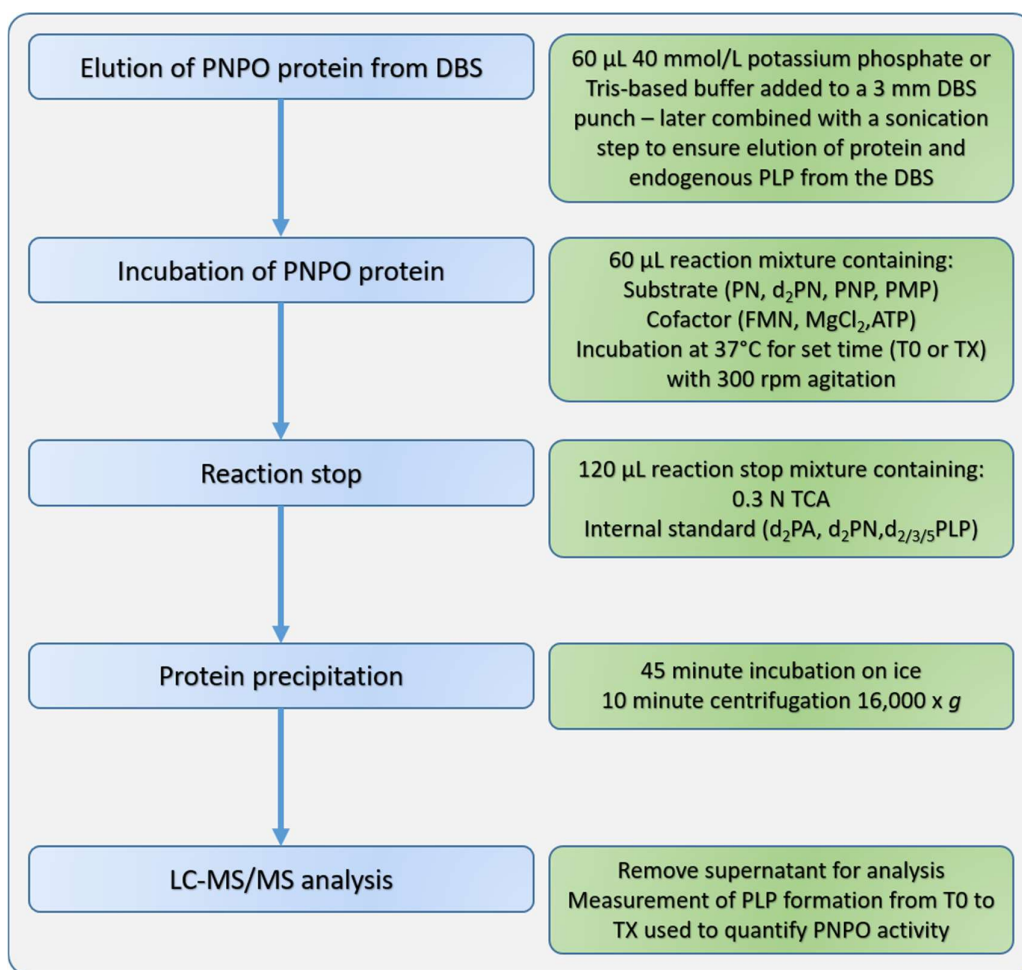


Figure 4.2: Summary of the protocol used for the development of a PNPO activity assay from DBS. Compositions of the elution buffer, reaction mixture and reaction stop solution were varied according to experimentation, as detailed in the text. FMN = Flavin mononucleotide; ATP = adenosine 5'-triphosphate; T0 = DBS to which the reaction stop mixture was added immediately after the reaction mixture; TX = DBS incubated at 37°C for time X.

4.1.1 Investigation and development of a coupled enzyme assay

4.1.1.1 Comparison of single-step and coupled assays - Preliminary investigation of substrates and stable isotope internal standards

Initial method development included comparison of d₂-pyridoxine (d₂-PN) and pyridoxamine 5'-phosphate (PMP) as substrates, the former as part of a coupled enzyme assay and the latter as a single-step assay (**Figure 4.1**). d₂-PN was chosen

as substrate for the coupled assay as, ideally, a deuterated substrate is used; this makes it possible to differentiate formation from the exogenous substrate from that already present in the sample. It was not possible to carry out a single-step assay with deuterated PNP or PMP as d_x-PNP was unavailable and d_x-PMP prohibitively expensive. PMP was used as PNP was not commercially available.

Conditions differed slightly between the coupled and single-step assays, as the requirements of PK in the coupled assay made necessary the addition of Mg²⁺ and ATP to the reaction mixture. Flavin Mononucleotide (FMN), the cofactor for PNPO, was required for both the single-step and coupled assays. The concentrations of these compounds in the final reaction mixture were 3 mmol/L MgCl₂, 0.3 mmol/L ATP and 1.5 μmol/L FMN. These cofactor concentrations had been used in prior studies for the in vitro analysis of PNPO activity (in the case of FMN)⁸⁷ or had been shown to saturate PK (in the cases of MgCl₂ and ATP).¹⁷⁶ d₂-PLP (for the coupled assay) or PLP (for the single-step assay) formation was measured over a four hour incubation period. Unless otherwise stated, all initial method development was carried out using 3 mm dried blood spots from healthy adult controls.

As shown in **Figure 4.1**, deuterated pyridoxic acid (d₂-PA) was used as an internal standard (IS) for the quantification of all analytes. Labelled internal standards are commonly used in LC-MS/MS methods. The addition of known concentrations to all calibration standards and samples of unknown concentration allows accurate quantification through the calculation of analyte/IS ratio in each sample. It is assumed that if there is any variation in recovery or MS performance the signal obtained from the IS will vary identically to the analyte of interest from sample to sample. This enables compensation for the variation in signal acquired between injections and samples upon LC-MS/MS analysis. Ideally, during LC-MS/MS analysis a labelled form of each individual analyte is used for quantification of that analyte; using an isotopically labelled analogue of the analyte itself is the best compensation for parameters that can affect quantification such as the matrix of the sample. These parameters include the recovery of the analyte upon sample preparation, or chromatography during analysis. The analyte/IS ratio provides an accurate measure of analyte concentration.

Whilst not an isotopically-labelled form of the analytes of interest, the use of d₂-PA as IS allowed its addition prior to incubation as activity of PK or PNPO should not be affected by its presence in the reaction buffer. The addition of other vitamers could affect measured PLP formation, for example, d₂-PLP could cause feedback inhibition

of PNPO activity.³⁶ It is preferable to add an IS at the earliest possible stage in a protocol as it then compensates for more steps of sample preparation.

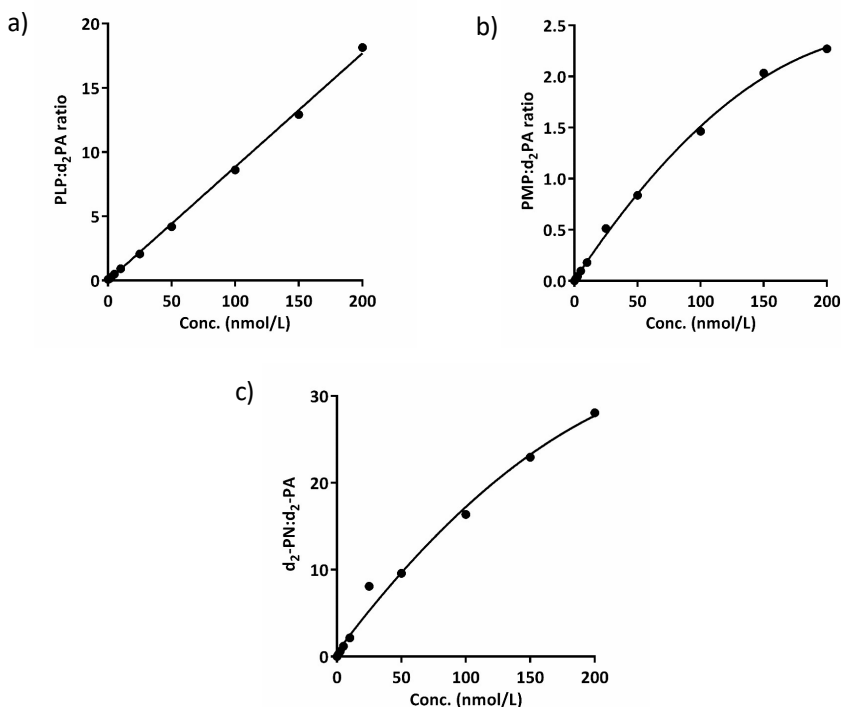


Figure 4.3: Linearity of calibration curves using 500 nmol/L d₂-PA as internal standard. Concentrations of a) PLP, b) d₂-PN and c) PMP from 0 – 200 nmol/L n=1 at each point. R² = PLP: 0.998 d₂-PN: 0.978 PMP: 0.977.

Preliminary experiments were carried out in order to determine the range of measurement for PLP using the LC-MS/MS equipment available. Linearity was achieved up to a concentration of 200 nmol/L when using d₂-PA as internal standard (**Figure 4.3a**). Above this concentration the calibration curve created for PLP quantification was non-linear. A lower injection volume was attempted but this led to poor retention and peak shape of PLP. This is due to an effect of the sample matrix pH on the interaction of PLP with the stationary phase.

The calibration curves for d₂-PN and PMP were non-linear over the same range investigated for PLP (i.e. 0 – 200 nmol/L) (**Figure 4.3b & c**). d₂-PLP linearity (product of the coupled d₂-PN > d₂-PNP > d₂-PLP assay) was identical to that of PLP (data not shown). Since the calibration curve created for the quantification of PLP was only linear to approximately 200 nmol/L, this was designated as the upper detection limit for this vitamer.

Concentrations of the substrates d_2 PN and PMP were therefore adjusted so their concentrations would result in a maximum of 200 nmol/L on analysis (400 nmol/L before addition of the TCA stop mix). This meant their concentrations, and the formation of product (d_2 PLP or PLP) could be accurately monitored over the incubation period of the enzyme assay. Concentrations of the d_2 -PA internal standard were reduced to 50 nmol/L from 500 nmol/L to ensure that the IS concentration was not at a saturating concentration and was within the range of the calibration curves used.

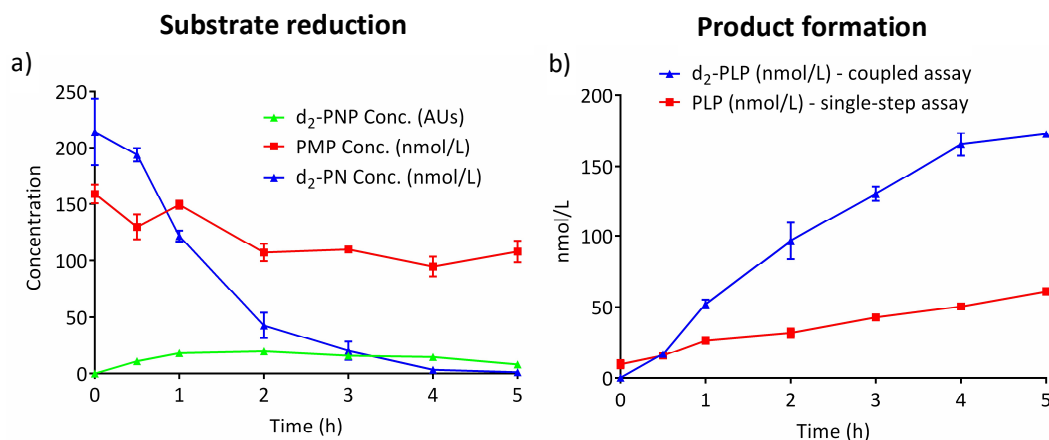


Figure 4.4: Initial comparison of coupled and single-step enzyme assays. Incubation conditions as follows: 20 mmol/L potassium phosphate buffer pH 7.6; 400nmol/L d_2 -PN or PMP; 0.3 mmol/L ATP; 3 mmol/L $MgCl_2$; FMN 1.5 μ mol/L; 37 °C; 300 rpm agitation; 0 – 5 h incubation; 1 x 3 mm DBS. AU = Arbitrary Units; calculated using the assumption that the d_2 PNP: d_2 PA ratio was identical to that of the d_2 PLP: d_2 PA calibration curve. Error bars = SEM. (n=2 at each data point).

When d_2 -PA was used as the IS for quantification of d_2 -PLP concentrations in the coupled enzyme assay, product formation was approximately linear over a four hour period. In the single-step enzyme assay using PMP as substrate, conversion to PLP was also linear over the incubation period (**Figure 4.4 (b)**). However, PMP > PLP conversion was only 29% of d_2 -PLP formed in the coupled assay over the five hour incubation period. Approximate d_2 -PN and PMP concentrations were quantified using the non-linear calibration curves shown in **Figure 4.3**. d_2 -PNP concentrations were calculated semi-quantitatively by using the calibration curve for d_2 -PLP and assuming the ratios were the same as for d_2 -PN quantification. Comparison of the coupled and single-step assays indicated that PLP was produced at a much faster rate by the coupled assay based on i) greater PLP than d_2 PLP formation and ii) rapid reduction of d_2 -PN substrate concentrations relative to PMP. A small amount of PLP at T = 0 can be seen in **Figure 4.4 (b)**, indicative of PLP contained in the PMP standard used

as substrate, or endogenous PLP found in the DBS analysed; these factors are discussed in **Sections 4.1.2.3** and **4.3.2.2**.

The use of d₂-PLP as an IS was also investigated for the quantification of PLP formation and PMP consumption in the single-step assay. Comparable PLP concentrations were calculated when using either d₂PA or d₂PLP as the internal standard. However, PMP concentrations varied from those calculated when using d₂-PA as the IS. The same pattern was seen for d₂-PN quantification (**data not shown**). This variability in the quantification when using different internal standards indicated that the difference in matrix (buffer composition and presence of DBS) between different samples could affect quantification of the B₆ vitamers. It was hypothesised that PLP (or d₂PLP) and d₂PA were suppressed by a similar amount according to the sample matrix, but PMP to a different extent. This would explain the discrepancy in PMP measurements when swapping d₂PA for d₂PLP as internal standard, but similarity for PLP measurement between the two internal standards.

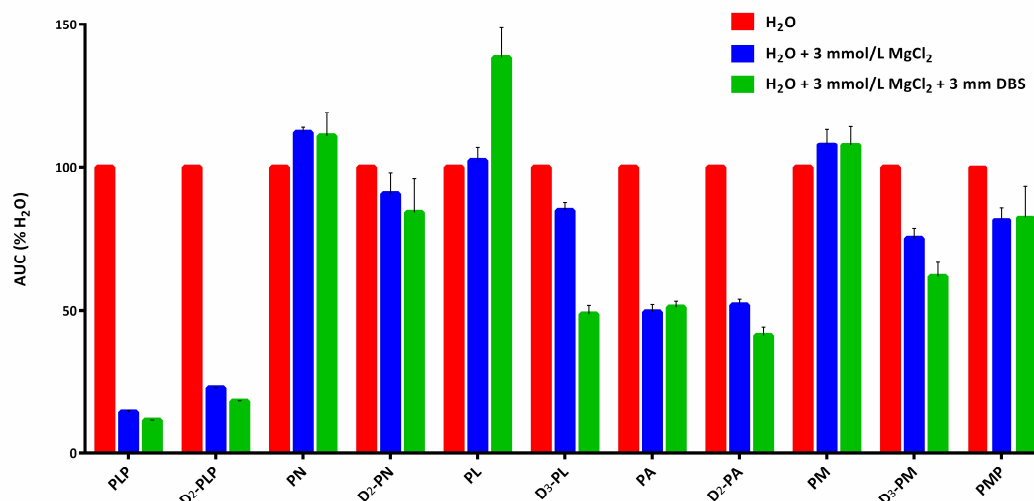


Figure 4.5: Assessment of the matrix effect on LC-MS/MS signal intensity of the B₆ vitamers and their isotopically-labelled analogues. Each sample contained a 100 nmol/L concentration of each vitamin in 0.15 N TCA with the matrix adjusted as specified in the figure legend. 100% = signal in H₂O + 0.15 N TCA. Error bars = SEM. n = 3. AUC = Area under curve.

Experiments were carried out in order to investigate which internal standards were suitable for the quantification of each B₆ vitamer. It was hypothesised that the exogenous MgCl₂ (3 mmol/L) added to samples undergoing incubation, but not to the calibration curve, could be introducing a matrix effect. In order to investigate this PLP, d₂-PLP, PN, d₂-PN, PL, d₃-PL, PA, d₂-PA, PM, d₃-PM and PMP were individually

spiked into 0.15 N TCA in the presence or absence of 3 mmol/L MgCl_2 . In addition, another set of samples were incubated with a 3 mm dried blood spot, as well as 0.15 N TCA and 3 mmol/L MgCl_2 . The peak area of each analyte upon LC-MS/MS analysis was evaluated (**Figure 4.5**). Substantial differences were identified in the level of ion suppression/enhancement for several vitamers. The signals obtained for some vitamers (PLP ~80% reduction and PA ~50% reduction) were predominantly affected by the presence of MgCl_2 where others were more dependent upon the matrix change found upon incubation with a 3 mm dried blood spot or showed little change irrespective of the sample matrix (e.g. PN; <10%).

This highlights the importance of using the deuterated form of each analyte as an IS, to minimise any analytical error due to matrix effect. Interestingly, PLP has the shortest retention time of the B₆ vitamers studied (0.9 minutes). The signal derived from this vitamer was most affected by sample matrix. It is possible that at the time of PLP elution, highly polar compounds and salts are co-eluting, forming adducts and reducing the detection of the protonated $[\text{PLP} + \text{H}]^+$ ion. In all subsequent experiments, an equal concentration of MgCl_2 to that added to the samples was added to calibration standards for those enzyme assays utilising MgCl_2 in the reaction buffer in order to minimise matrix effect.

The development of a coupled enzyme assay (PN > PNP > PLP) was initially pursued further, rather than monitoring PMP to PLP conversion in a single step assay. Several factors influenced this decision: i) A deuterated form of PMP for accurate quantification was unavailable ii) The chromatography and signal upon LC-MS/MS quantification of PMP was substantially worse than that of the other B₆ vitamers iii) PMP to PLP conversion appeared to be considerably slower than that measured when a coupled assay was employed (**Figure 4.4**). iv) The PMP standard used was found to contain approximately 1–2% PLP as evident in **Figure 4.4 (b)**; 9 nmol/L PLP is present at T0 in the single step assay, despite the fact that this DBS was not incubated with substrate before the TCA stop mix was added. This would interfere with measurement of endogenous PLP in the DBS and may also lead to feedback inhibition.

A coupled assay using PN (final concentration of 400 nmol/L on incubation) as the exogenous substrate rather than the deuterated d₂-PN was performed (**Figure 4.6**) thus allowing d₂PN to be used as the internal standard; the importance of using an isotopically labelled form of the analyte of interest is described above. All other conditions were kept the same. PLP formation was monitored over 5 hours, as were the concentrations of PNP and PN. d₂-PLP was used as the IS for PLP quantification and d₂-PN for PN quantification. The response of PNP was assumed to be the same as that for PLP and the ratio of PNP to d₂-PLP was used to quantitate PNP. This allowed relative and approximate quantification of PNP. Linear ($R^2 > 0.99$) formation of PLP was seen over a five hour incubation period (**Figure 4.7**).

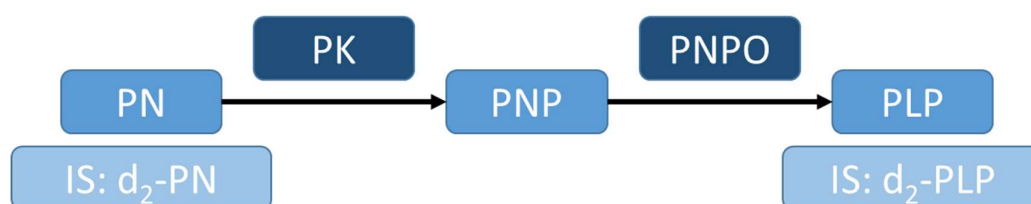


Figure 4.6: Coupled pyridoxal kinase and pyridox(am)ine 5'-phosphate oxidase assay using PN as substrate. IS = internal standard used for quantification of each analyte; PNP = pyridoxine 5'-phosphate; PLP = pyridoxal 5'-phosphate; PN = pyridoxine; PK = pyridoxal kinase; PNPO = pyridox(am)ine 5'-phosphate oxidase.

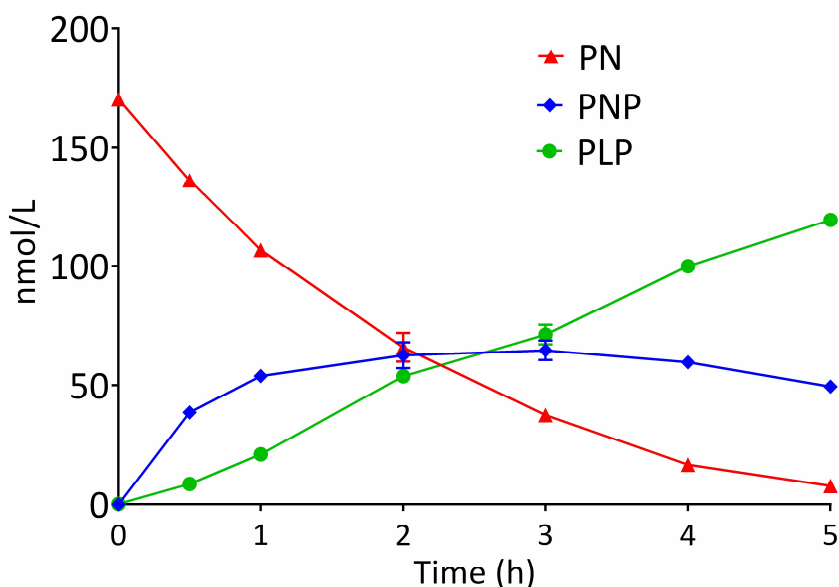


Figure 4.7: Coupled pyridoxal kinase and pyridox(am)ine 5'-phosphate oxidase activity in a 3 mm punch from a healthy adult control. Incubation conditions as follows: 20 mmol/L potassium phosphate buffer pH 7.6; 400nmol/L PN; 0.3 mmol/L ATP; 3 mmol/L MgCl₂; FMN 1.5 μmol/L; 37 °C; 300 rpm agitation; 0 – 5 h incubation; 1 x 3 mm DBS. Error bars = SEM. (n=9 at 2 h; n=3 at all other time points).

4.1.1.2 Optimisation of coupled PK and PNPO enzyme assay conditions

Proof of concept experiments described above showed that it was possible to measure PLP formation and therefore PNPO activity from DBS using a combined PK and PNPO enzyme assay. Subsequently, it was ensured that conditions for enzymatic PLP formation were optimal, providing suitable conditions for accurate quantification of PNPO activity.

Optimisation of Flavin mononucleotide concentration

Flavin mononucleotide (FMN; the active form of vitamin B₂) is the cofactor for PNPO.

Figure 4.8 shows the effect of increasing FMN concentration on PLP formation over a four hour incubation period, all other conditions were kept identical.

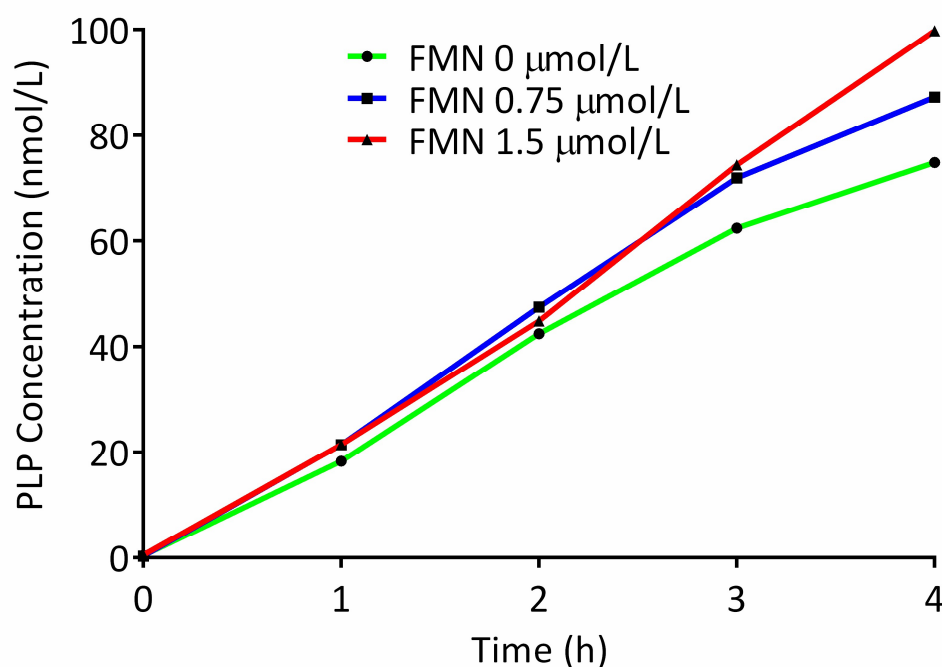


Figure 4.8: Effect of FMN concentration on PNPO activity in a 3 mm DBS punch from a healthy adult control. Incubation conditions as follows: 20 mmol/L potassium phosphate buffer pH 7.6; 400nmol/L PN; 0.3 mmol/L ATP; 3 mmol/L MgCl₂; FMN 0 - 1.5 μmol/L; 37 °C; 300 rpm agitation; 0 – 4 h incubation; 1 x 3 mm DBS. (n=1 at each data point).

An FMN concentration of 1.5 $\mu\text{mol/L}$ has been used previously in other published assays to study PNPO activity in mammalian tissues such as rabbit liver¹⁷⁷ and an *in vitro* over-expression system.⁸⁷ In the coupled assay described here, PLP formation was linear over the four hour incubation period in the presence of 1.5 $\mu\text{mol/L}$ FMN and 25% and 13% higher than at FMN concentrations of 0 and 0.75 $\mu\text{mol/L}$, respectively. The K_d for FMN binding to PNPO is in the low nanomolar range (13.1 nmol/L)⁷⁴ Concentrations in the $\mu\text{mol/L}$ range were expected to saturate the PNPO enzyme with FMN cofactor and higher concentrations would be unnecessary; they were therefore not investigated. The presence of exogenous FMN in the reaction mixture would ensure that any patients with a vitamin B₂ deficiency would not appear to have lower DBS PNPO activity.

Optimisation of reaction mixture pH

It has been reported that the red cell PNPO enzyme has optimal activity at pH 8.0.¹⁷⁰ Optimal pyridoxal kinase activity in erythrocytes occurs at pH 6 - 8.¹⁷⁸ A balance in pH must be found to provide adequate conditions for the activity of both enzymes. Little difference was seen in PLP formation between pH 7.2 and 8.0 when 20 mmol/L potassium phosphate was used as the incubation buffer (**Table 4.1**). This buffer had been used previously for the assessment of *in vitro* PNPO activity.⁸⁷ The buffering capacity of potassium phosphate is diminished above pH 8.0 hence higher pH ranges were not investigated. Additionally, above pH 7.8, peak splitting was observed during LC-MS/MS analysis (**Figure 4.9**).

Table 4.1: Effect of pH on PNPO activity using a coupled assay. Incubation conditions: 20 mmol/L potassium phosphate buffer (pH adjusted appropriately from 7.0 – 8.0); 1.5 $\mu\text{mol/L}$ FMN; 0.3 mmol/L ATP; 3mmol/L MgCl_2 ; 400 nmol/L PN; 37 °C; 300 rpm agitation; 1 x 3 mm DBS; 0-4 h incubation. DBS from a healthy adult control. Activity was quantified by PLP formation and was calculated from the slope of a linear regression performed upon PLP concentrations at time points of 0, 1, 2, 3 and 4 h at each pH. ANCOVA analysis was performed and no significant difference was identified between groups. (n=1)

pH	PNPO Activity ($\mu\text{mol/DBS/h}$)
7.0	4.01
7.2	4.78
7.4	5.47
7.6	4.94
7.8	5.29
8.0	5.13

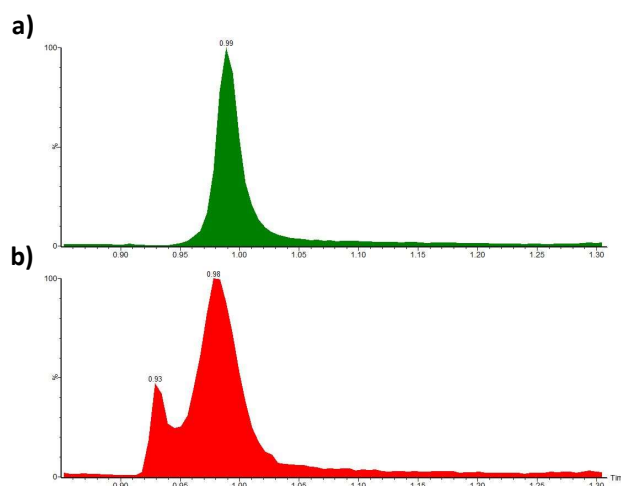


Figure 4.9: Pyridoxal 5'-phosphate chromatography on LC-MS/MS analysis. (a) Chromatography of PLP after samples incubated in a pH 7.6 potassium phosphate buffer. (b) Chromatography of PLP after samples incubated in a pH 8.0 potassium phosphate buffer.

This experiment was repeated and PNPO activity in a Tris-HCl buffer system was compared to that in a potassium phosphate buffer so that the activity of PNPO at a pH greater than 8 could be studied. Tris-HCl has an effective buffering capacity between pH 7 – 9. **Figures 4.10 (a), (b) and (c)** show the effect of potassium phosphate pH on PN depletion and the formation of PNP or PLP, respectively, at pH 6.6, 7.0 and 7.6. PNPO activity increases as the pH becomes more alkaline, this is consistent with a red blood cell optimal pH of 8.0, as reported previously.¹⁷⁰

Figure 4.10 (f) shows PLP formation on incubation of a DBS in a reaction mixture buffered to pH 7.6, 8.0 and 8.6 with Tris-HCl. PLP formed was approximately 30 – 50% that observed when using potassium phosphate at pH 7.6. Previous studies have shown that PK requires a monovalent cation such as K^+ for effective phosphorylation. Without the addition of exogenous K^+ in the reaction buffer, PK activity (measured as PNP formation), is reduced by at least 80% (**Figure 4.10 (e)**). A reaction buffer based solely on Tris-HCl is therefore unsuitable for a coupled PK and PNPO assay. Similar to the experiments using potassium phosphate as a buffer, peak splitting was evident at pH > 8.0. Subsequent experiments were therefore carried out at pH 7.6.

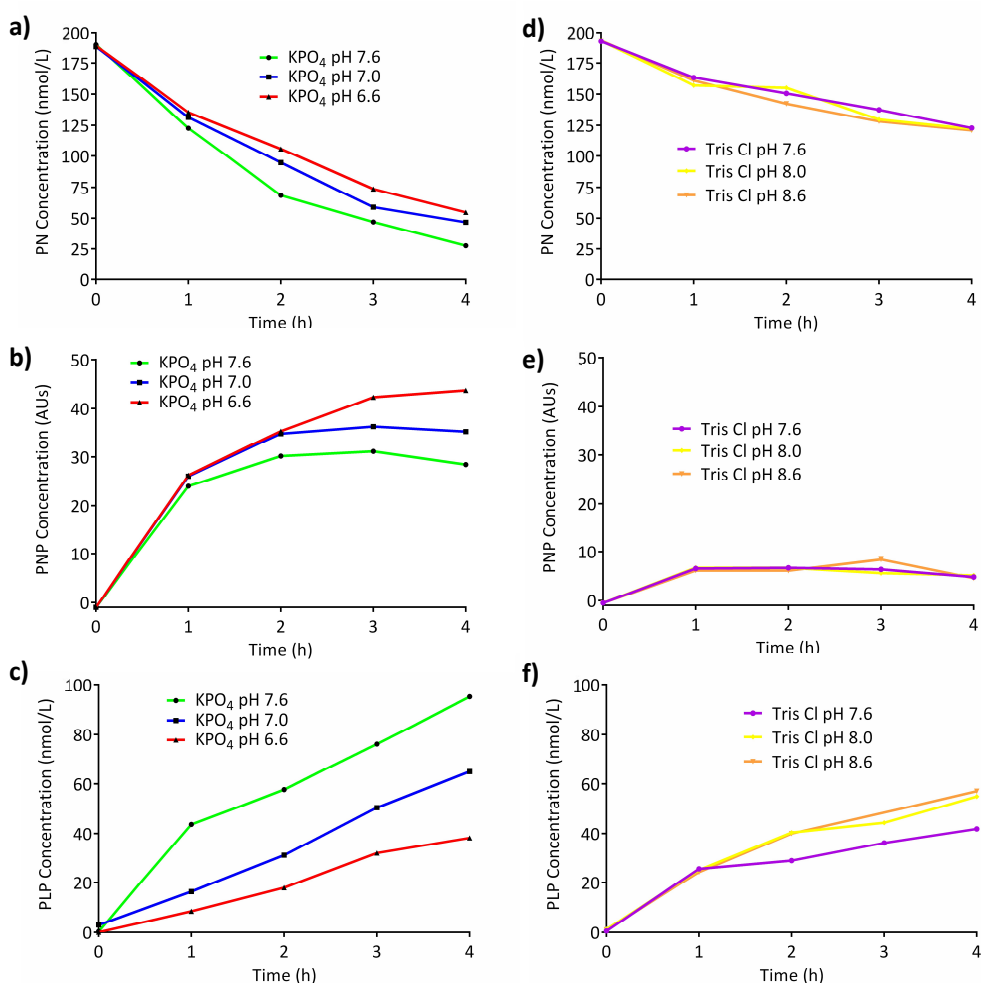


Figure 4.10: PNPO activity between pH 6.6 - 8.6. Incubation conditions: 20 mmol/L potassium phosphate buffer or Tris Cl (pH adjusted appropriately); 1.5 μ mol/L FMN; 0.3 mmol/L ATP; 3mmol/L $MgCl_2$; 400 nmol/L PN; 37 °C; 300 rpm agitation; 1 x 3 mm DBS; 0-4 h incubation. DBS from a healthy adult control. n=1 at each data point.

4.1.1.3 Validation of coupled enzyme assay and stability of PK and PNPO in DBS upon storage

In order to translate a research method into the clinical diagnostic arena, repeatability of analysis must be determined. Using the optimal conditions for PLP formation (Sections 4.1.1.1 and 4.1.1.2), the enzyme assay was repeated ten times, on four separate days, using 3 mm dried blood spots taken from a single healthy adult control. PLP formation was measured over a 2 h incubation period; PNPO activity had already been shown to be linear over this period (Section 4.1.1.1). Intra and inter-assay %CVs were 8.44% and 4.09%, respectively (Figure 4.11). Typically, %CVs of less than 15% are considered suitable for clinical diagnostic use.¹⁷⁹

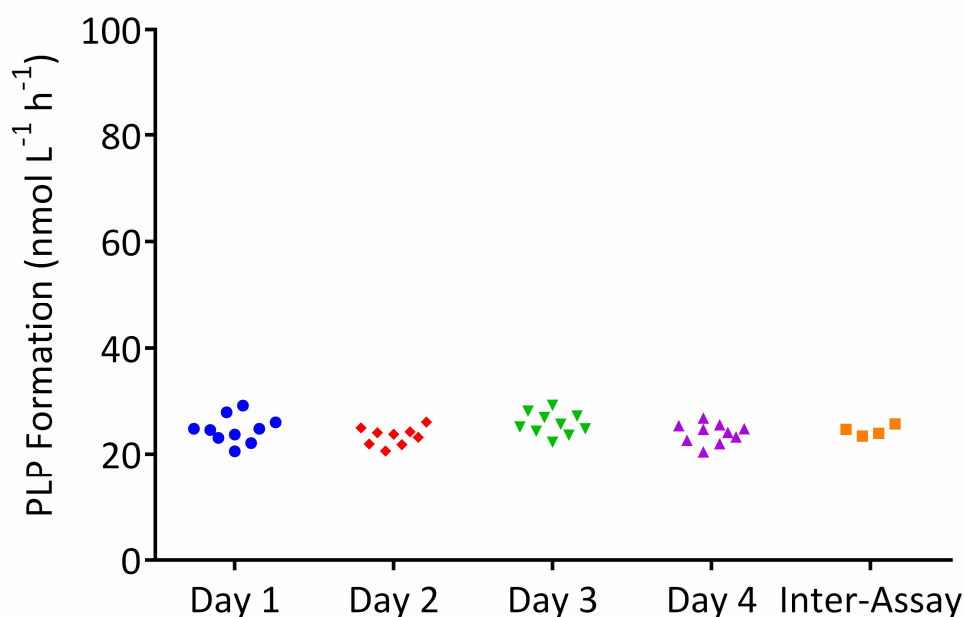


Figure 4.11: Repeatability of PLP formation after a 2 hour incubation with a 3 mm DBS from a healthy adult. Incubation conditions: 20 mmol/L potassium phosphate buffer pH 7.6; 1.5 μ mol/L FMN; 0.3 mmol/L ATP; 3mmol/L MgCl₂; 400 nmol/L PN; 37 °C; 300 rpm agitation; 10 x 3 mm DBS on each day; 2 h incubation. Mean intra-assay %CV = 8.44%. Inter-assay %CV = 4.09%.

The short-term stability of PNPO (and by extension PK) was determined by drying blood spots from a healthy adult control overnight on Whatman 903 DBS collection cards before storage at room temperature and at 37°C for 1, 3, 5, 7 and 14 days prior to analysis. A duplicate set of DBS were also stored inside foil bags with silica desiccant at room temperature, in order to determine the effect of ambient humidity

upon PNPO stability. DBS stored under conditions of ambient humidity at RT and at 37°C showed a reduction in activity of ~55% after 14 days (**Figure 4.12 (a)**). DBS protected from ambient humidity better retained PNPO activity however, with a reduction in activity of only 21% after 14 days storage.

The effect of DBS storage at 4°C, -20°C and -80°C on PNPO activity was determined over a 24 week period (**Figure 4.12 (b)**). Under these conditions, PNPO was found to be more stable than when stored at room temperature. After 24 weeks at 4°C, PNPO activity was approximately 70% of initial levels, at -20°C, 85% of initial levels and at -80°C unaffected by storage. Some variation can be seen in **Figure 4.12 (b)** resulting in a seeming increase in PNPO activity at some time points. This is due to inter-assay variation. For all subsequent experiments, DBS were stored at -80°C prior to analysis.

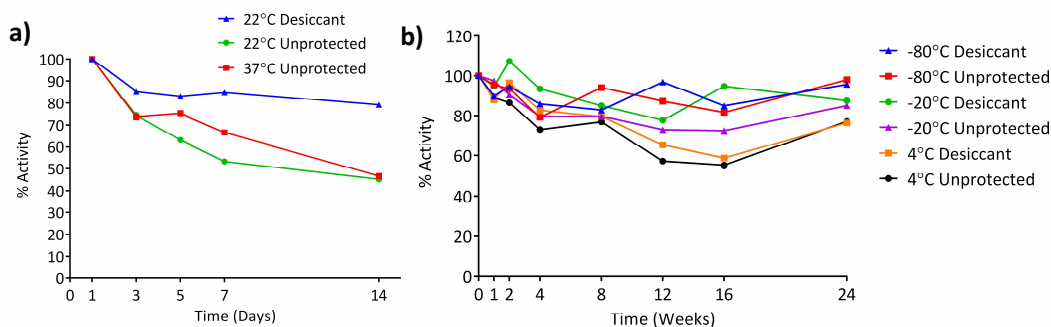


Figure 4.12: Effect of (a) short and (b) long-term storage on PNPO activity measured in a 3 mm DBS from a healthy adult. Incubation conditions: 20 mmol/L potassium phosphate buffer pH 7.6; 1.5 µmol/L FMN; 0.3 mmol/L ATP; 3mmol/L MgCl₂; 400 nmol/L PN; 37 °C; 300 rpm agitation; 1 x 3 mm DBS; 2 h incubation. DBS stored for up to 14 days at 22°C or 37°C with or without desiccant.

During this phase of method development, a potential source of error was identified in the quantification of the B₆ vitamers by LC-MS/MS. Considerable crosstalk was identified between the MRM channels for d₂-PLP (IS used to quantify PLP) and PNP (substrate of PNPO), which had become available commercially subsequent to the start of this project. Whilst both compounds have the same molecular mass some differentiation of the two was possible due to the different MRM transitions used i.e. loss of phosphate (-98) for d₂-PLP quantification and loss of phosphate and water (-116) for PNP quantification. However, because PNP also contains phosphate crosstalk of approximately 10% of the signal of PNP was present. As the compounds co-elute, this could lead to inaccuracy in the measurement of compounds quantified using d₂-PLP as an internal standard. Another internal standard was sought and d₃-

PLP identified as a potential replacement. On investigation, it was confirmed that the PNP to d₃-PLP crosstalk was greatly reduced. Although still approximately 1% of the PNP signal was evident in the d₃-PLP channel due to the proportion of the ¹³C isotope present in PNP, this was deemed a considerable improvement. Hence, all further experimentation was carried out with d₃-PLP used as the IS for PLP quantification.

4.1.1.4 Effects of high dose PLP supplementation on the accuracy of analysis of dried blood spot PNPO activity.

Preliminary results for the optimisation of the coupled PK and PNPO assay system described above were promising. The stability of PK and PNPO on storage in DBS was acceptable and the repeatability of the method was suitable for clinical use. All optimisation had been performed using DBS from healthy volunteers that were not receiving B₆ supplementation. However, problems were identified during further assay optimisation when using DBS from PNPO deficient patients that could potentially lead to false positive or negative results.

The levels of **(a) PN**, **(b) PNP**, **(c) PLP** and **(d) PL** were measured upon incubation of a control DBS and a DBS from a PNPO-deficient subject over a 4 hour incubation period (**Figure 4.13**). PLP formation in the healthy adult control was linear over the 4 hour incubation period and, as expected, higher than that identified in the PNPO deficient subject. However, higher initial concentrations of PLP, PNP and PL were seen in the DBS from the PNPO deficient child at 0 h relative to the control sample. This is indicative of the high endogenous concentrations of B₆ vitamers in the blood of subjects receiving high dose vitamin B₆ supplementation.

An unexpected increase in PLP concentration was seen in the PNPO deficient individual over the 4 h time course studied. A concurrent decrease in PL **(d)** provides an explanation for this increasing PLP concentration. It is likely that PK was able to catalyse the phosphorylation of PL to PLP, hence accurate quantification of PNPO activity by measuring PLP formation using the coupled assay was not possible in this patient.

In a healthy control not receiving supraphysiological B₆ doses, PL concentrations are below the lower limit of quantification (i.e. < 1.25 nmol/L). These concentrations would not affect quantification of PNPO activity. However, in a patient receiving high dose

vitamin B₆ supplementation, concentrations of B₆ vitamers are high enough to obfuscate PNPO activity when measured as the second step in a coupled PN > PNP > PLP enzyme assay.

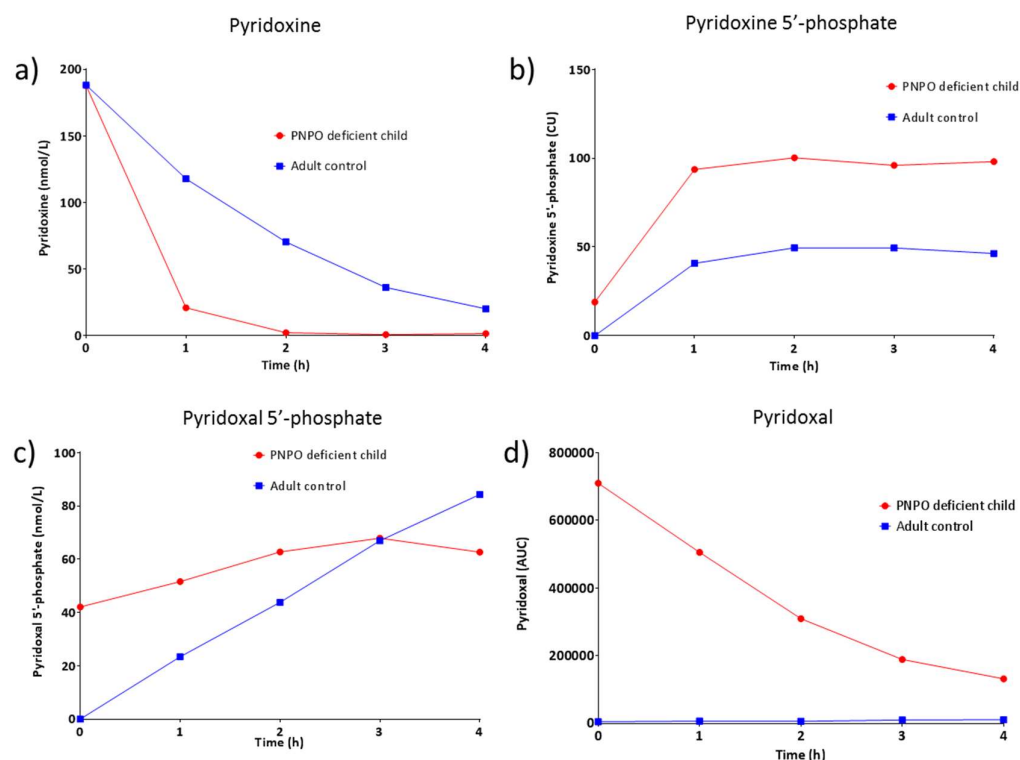


Figure 4.13: Comparison of the B₆ vitamer concentrations upon incubation of a 3 mm DBS from a healthy adult control and a PNPO deficient subject. Incubation conditions as follows: 20 mmol/L potassium phosphate buffer pH 7.6; 400nmol/L PN; 0.3 mmol/L ATP; 3 mmol/L MgCl₂; 37 °C; 300 rpm agitation; 0 – 4 h incubation; 1 x 3 mm DBS. (n=1 at each data point). AUC = area under curve. CU = concentration units.)

In order to further characterise the effect of high PL and PLP concentrations on the analysis of PNPO activity, the assay was repeated using a DBS from a control and with the addition of 100 nmol/L PLP or PL to the reaction buffer. This concentration is similar to the concentrations found in patients receiving supraphysiological vitamin B₆ doses for seizure treatment. **Figure 4.14** shows a) PLP, b) PNP and c) PN concentrations over a four hour incubation period of a control DBS with a reaction buffer containing additional exogenous PLP and PL.

The presence of 100 nmol/L PLP in the reaction buffer resulted in a reduction in the activity of PNPO by approximately 55%. The increase in PLP concentration after 4 hours of incubation when no exogenous PLP is added was 82.5 nmol/L, versus only 37.8 nmol/L with 100 nmol/L PLP added to the reaction buffer. This reduction was

likely due to the effect of product inhibition by PLP on PNPO.^{36, 60} Equally, when 100 nmol/L PL was included in the reaction buffer, 17.5% more PLP was formed after 4 hours of incubation (97.0 vs 82.5 nmol/L). It is likely that this is due to the action of pyridoxal kinase, which is able to phosphorylate both pyridoxal and pyridoxine into their respective 5'-phosphates.

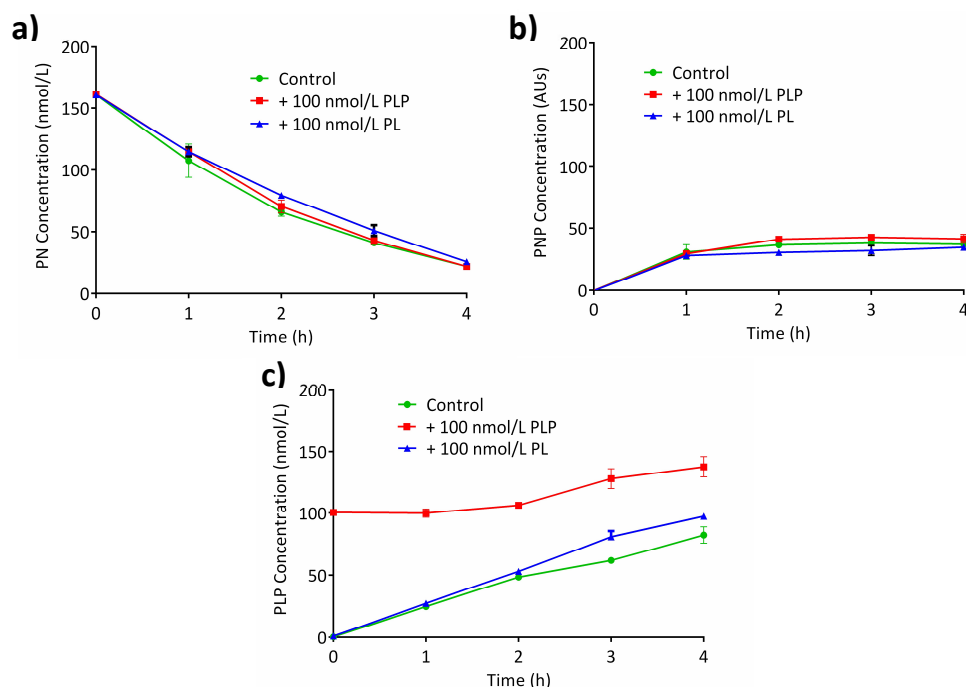


Figure 4.14: Comparison of the B₆ vitamers concentrations upon incubation of a 3 mm DBS from a healthy adult with exogenous B₆ vitamers. Incubation conditions as follows: 20 mmol/L potassium phosphate buffer pH 7.6; 400nmol/L PN + 100 nmol/L PL or PLP; 0.3 mmol/L ATP; 3 mmol/L MgCl₂; 37 °C; 300 rpm agitation; 0 – 4 h incubation; 1 x 3 mm DBS. PNP concentrations expressed in arbitrary units assuming that the ratios are identical to those found in calibration curve created for PLP/d₃-PLP. (n=2 at each data point).

This experiment was repeated with the following modification: i) DBS from a control were incubated with a range of PLP concentrations from 0 – 100 nmol/L added to the reaction buffer ii) The incubation time of all DBS was kept to 2 h; this was to allow an easy comparison between conditions. In the control DBS in **Figure 4.14**, PLP formation and PN consumption were linear to 2 hours in all cases.

The effect of PLP on PNPO activity as measured by the change in PLP concentration is shown in **Figure 4.15**. There was a dramatic reduction in PLP formation as added PLP concentrations were increased. In patients receiving vitamin B₆ supplementation, DBS PLP concentrations of up to 17,000 nmol/L can be found (**Section 3.2**). Given that ~3.2 µL of blood is found in a 3 mm DBS punch and that this will be diluted in a final solution totalling 240 µL, if whole blood concentrations were 17,000 nmol/L you

would expect PLP concentrations of approximately 226 nmol/L. Indeed, the PLP concentration in the T0 3 mm DBS from the PNPO deficient patient in **Figure 4.14** was 42 nmol/L. A reduction in activity of approximately 57% would be expected with this concentration of endogenous PLP (calculated from **Figure 4.15**). The effect of endogenous PLP on PLP synthesis may be due to product inhibition on PNPO. This effect would make the assay unsuitable for the analysis of samples from patients receiving supraphysiological doses of vitamin B₆.

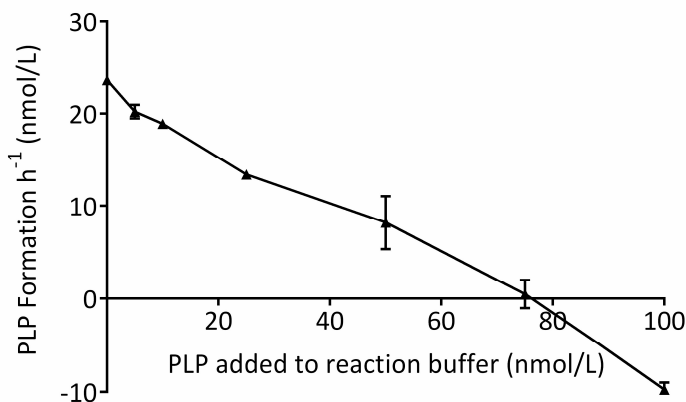


Figure 4.15: PLP formation after the 2 hour incubation of a 3 mm DBS with exogenous B₆ vitamers. Incubation conditions as follows: 20 mmol/L potassium phosphate buffer pH 7.6; 400nmol/L PN (substrate) + 0, 5, 10, 25, 50, 75 or 100 nmol/L PLP; 0.3 mmol/L ATP; 3 mmol/L MgCl₂; 37 °C; 300 rpm agitation; 1 x 3 mm DBS. (n=2 at each data point).

It was postulated that this problem could be addressed by the addition of Tris to the reaction buffer. Tris is known to bind PLP and PL in solution, forming a Schiff base.¹⁸⁰ It is possible that with high (mmol/L) concentrations of Tris in the reaction buffer, free PLP/PL would be bound, reducing the availability of PL for phosphorylation to PLP as well as preventing feedback inhibition by PLP on the PNPO enzyme. However, when optimising the coupled PK and PNPO enzyme assay from DBS using Tris-HCl as the buffer, low PNPO activity was identified. It is likely that this was due to the lack of K⁺, required for PK activity (**Section 4.1.1.3**). In order to address this, incubations were performed with the addition of varying KCl concentrations (0, 20 and 40 mmol/L) alongside 20 mmol/L Tris (pH 7.6) to the reaction buffer, each adjusted to pH 7.6 after KCl addition to ensure this did not affect the final buffer pH. Also included was the assay in its prior form; incubation with 20 mmol/L potassium phosphate buffer, pH 7.6. Published studies suggest that at a tris concentration of 20 mmol/L, approximately 85% of free PLP/PL should be bound.¹⁸⁰

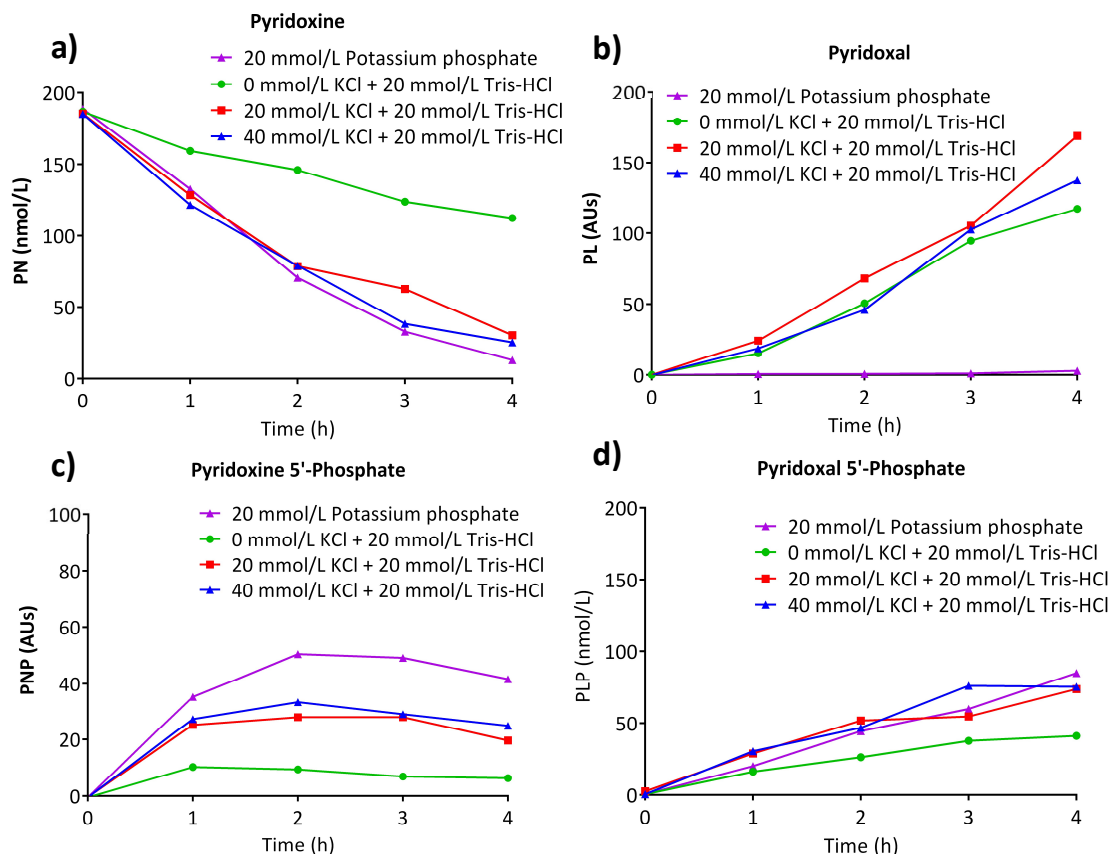


Figure 4.16: Concentrations of B₆ vitamers after incubation of a 3 mm DBS with varying buffer compositions. Incubation conditions as follows: 20 mmol/L potassium phosphate buffer or 0/20/40 mmol/L KCl with 20 mmol/L Tris pH 7.6; 400nmol/L PN; 0.3 mmol/L ATP; 3 mmol/L MgCl₂; 37 °C; 300 rpm agitation; 0 – 4 h incubation; 1 x 3 mm DBS. No stable isotope standards were used for PL and PNP therefore concentrations are expressed in arbitrary units assuming that the ratios of these vitamers to d₂PN and d₃PLP are identical to those found in calibration curves created for PN:d₂-PN and PLP:d₃-PLP, respectively (n=1 at each data point).

Figure 4.16 shows the concentrations of PL, PN, PLP and PNP over a four hour incubation period under these conditions. As previously (**Section 4.1.1.3**), when KCl was not added to the reaction buffer, PN conversion to PNP was reduced (**Figure 4.16 (a) and (c)**). This ultimately resulted in lower PLP formation (**Figure 4.16 (d)**); 41 nmol/L after 4 hours; 48% that achieved when using the potassium phosphate buffer system.

The amount of PLP formed was similar when 20mmol/L Tris-HCl, pH 7.6 containing 20 mmol/L KCl or 40 mmol/L KCl and 20 mmol/L potassium phosphate (74, 75 and 85 nmol/L, respectively) were used as the incubation buffer. This confirmed previous reports that pyridoxal kinase activity requires the presence of a monovalent cation, in this case K⁺.¹⁷⁶ Interestingly, PL formation was observed in all assays in which

potassium phosphate was not present (**Figure 4.16 (b)**). Inorganic (free) phosphate inhibits the various phosphatases present in the blood.¹⁸¹ In the reaction buffers not containing free phosphate it was therefore hypothesised that phosphatases present within the DBS were dephosphorylating PLP to PL. This would introduce variability in measured PNPO activities between DBS from individuals with differing blood phosphatase activities.

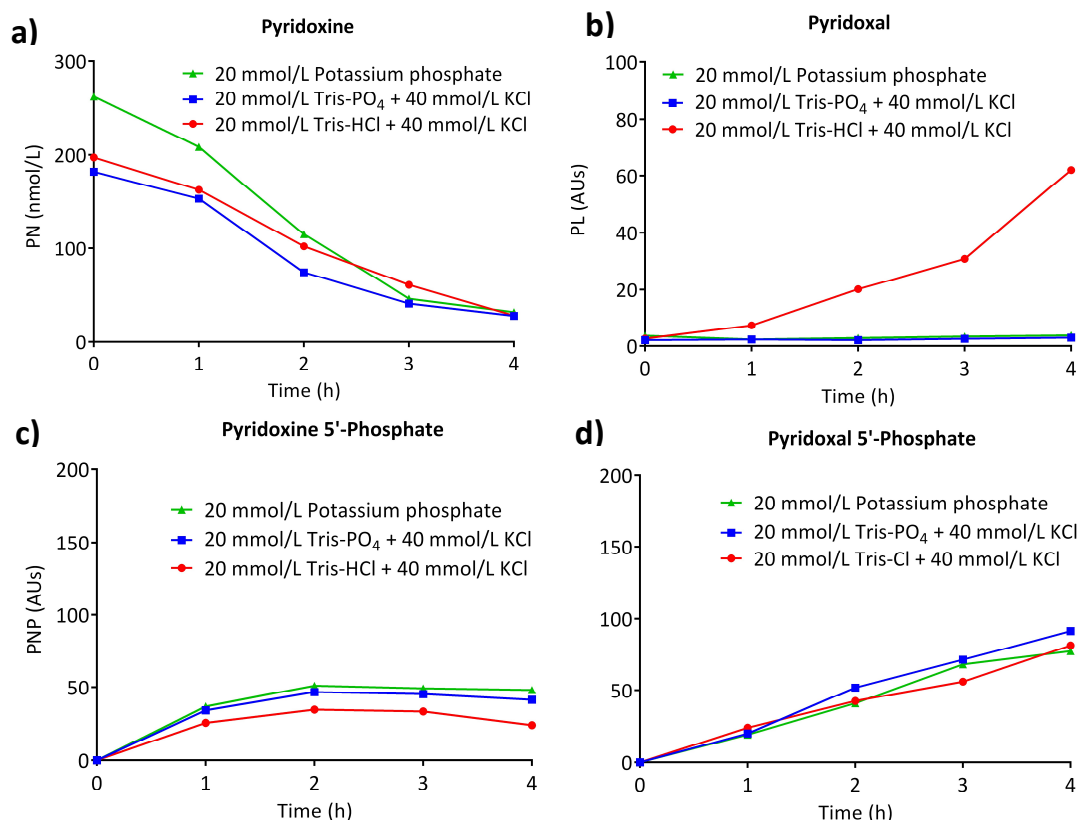


Figure 4.17: Concentrations of B₆ vitamers during incubation of a 3 mm DBS with varying buffer compositions. Incubation conditions as follows: 20 mmol/L potassium phosphate buffer or 40 mmol/L KCl with 20 mmol/L Tris-HCl or Tris PO₄ pH 7.6; 400nmol/L PN; 0.3 mmol/L ATP; 3 mmol/L MgCl₂; 37 °C; 300 rpm agitation; 0 – 4 h incubation; 1 x 3 mm DBS. PL and PNP concentrations expressed in arbitrary units assuming that the ratios are identical to those found in calibration curves created for PN/d₂-PN and PLP/d₂-PLP, respectively (n=1 at each data point).

Hence, it was postulated that a custom Tris-phosphate buffer containing KCl may enable PNPO activity to be measured more accurately. This would provide i) mmol/L concentrations of Tris to complex with free PL/PLP; ii) free phosphate, required to inhibit endogenous phosphatases and iii) K⁺ required for PK activity.

Figure 4.17 shows PN, PLP (nmol/L), PNP and PL (AU) concentrations upon incubation with KCl/Tris-HCl, KCl/Tris-phosphate and potassium phosphate reaction

buffers, all adjusted to pH 7.6. Although PLP formation was similar (78 – 91 nmol/L after 4 hours incubation) in all three forms of the assay, a distinct difference is seen in both the rate of PNP formation and PL formation in the KCl/Tris-HCl buffered assay. The assays using Tris-phosphate/KCl and potassium phosphate showed almost identical results, indicating that a Tris-phosphate/KCl buffer is viable for use for the coupled enzyme assay of PNPO. The inclusion of Tris in the buffer means any potential feedback inhibition of PNPO by PLP would be reduced as described above.

Experiments similar to those performed above to study the effect of high initial PL and PLP concentrations were repeated in this new Tris-phosphate/KCl (pH 7.6) buffer.

Figure 4.18 (a) shows PLP formation upon the incubation of a 3 mm DBS from a healthy adult control in the presence of exogenous PLP at concentrations of 0, 25, 50, 100, 150 and 200 nmol/L. In comparison with the data in **Figure 4.15**, where a potassium phosphate buffer was used to study the effect of exogenous PLP on PNPO activity, PLP formation after 2 hours incubation was increased. However, product inhibition seen in the presence of exogenous PLP caused a reduction in PLP formation of 3%, 20%, 18% and 41%, respectively (after 2 h), as compared to incubations where no PLP had been added.

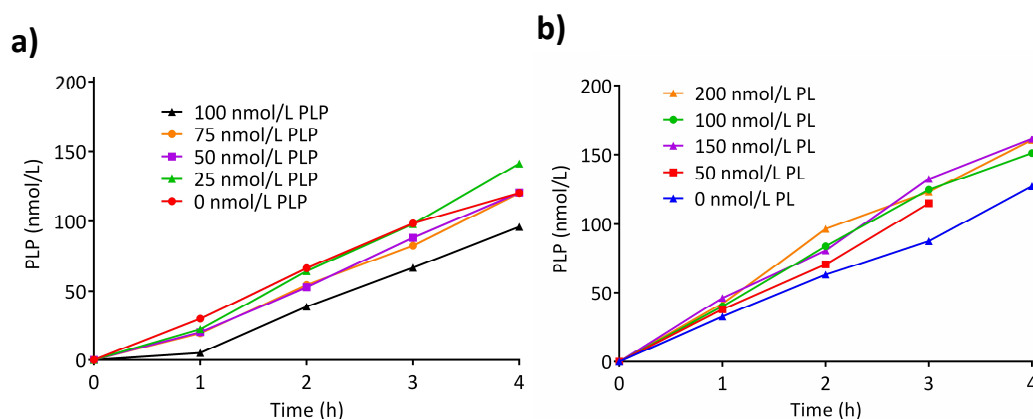


Figure 4.18: Formation of pyridoxal 5'-phosphate after incubation of a 3 mm DBS with varying PL and PLP concentrations. Conditions as follows: 20 mmol/L Tris + 40 mmol/L KCl, adjusted to pH 7.6 with phosphoric acid; 400nmol/L PN + 0 – 200 nmol/L PL/PLP; 0.3 mmol/L ATP; 3 mmol/L MgCl₂; 37 °C; 300 rpm agitation; 0 – 4 h incubation; 1 x 3 mm DBS. (n=1 at each data point). In **Figure 18 (a)**, exogenous PLP at T0 has been subtracted at each time point for clarity. 4 h time point with 50 nmol/L added PL was anomalous (~0 nmol/L PLP) and hence removed.

Figure 4.18 (b) shows PLP formation in the presence of PL (0 - 200 nmol/L). Relative to DBS incubated without exogenous PL an increase in PLP concentration of 18 - 26% was seen.

It was concluded that there were several limitations that made the use of a coupled PK and PNPO assay unsuitable for clinical diagnostic use. Firstly, although the addition of Tris to the reaction buffer limits the effect of high endogenous PL and PLP on PNPO activity, there was still potential for an unacceptable influence upon results for patients with high levels of B₆ vitamers in the blood due to supplementation for seizure treatment. This was due to product inhibition in the case of PLP and due to PL conversion to PLP in the case of PL.

Therefore, under these assay conditions, PNPO activity analysis could only be undertaken prior to B₆ supplementation, when B₆ vitamer concentrations in these individuals were not elevated. However, this would limit the clinical utility of a test that would usually only be requested after a response to vitamin B₆ supplementation had been identified in a patient with epilepsy.

Another inherent problem with using a coupled assay for the quantification of PNPO activity was potential variation in PK activity between subjects. As can be seen in **Figure 4.13 (a)**, phosphorylation of PN (substrate of PK) to PNP was faster in a DBS from the PNPO deficient patient, compared to a healthy adult control. PK activity is also known to vary in the general population; activity in the erythrocytes of African Americans is approximately 50% lower than that of White Americans^{38, 182}. If PK activity was the limiting factor in a coupled assay of PK and PNPO, this could produce PLP formation indicative of variation in PK activity rather than PNPO.

Fortuitously, at this time, PNP became available from a commercial supplier, raising the potential for a single-step PNP > PLP enzyme assay. A PNPO assay using PNP could solve the problems identified when using the coupled assay. **Section 4.1.2** details the investigation and development of a single step PNP > PLP enzyme assay for the quantification of PNPO activity.

4.1.2 Investigation and optimisation of a single-step PNPO enzyme assay from DBS

The commercial availability of two compounds enabled the transition towards a single-step PNPO enzyme assay; i) PNP and ii) d₃-PLP. PNP availability meant a substrate of PNPO was available that provided adequate throughput for accurate and rapid quantification (as opposed to the use of PMP as substrate, which was far slower). The availability of d₃-PLP meant that this PNP could be accurately quantified. Studies in **Section 4.1** showed that d₂-PLP showed a large amount of crosstalk from the PNP MRM channel and was thus unsuitable for use in a PNPO assay, as described in **Section 4.1.1.3**. This section details the development of a single-step LC-MS/MS-based enzyme assay for the measurement of PNPO activity from DBS by quantifying PNP conversion to PLP (**Figure 4.19**).

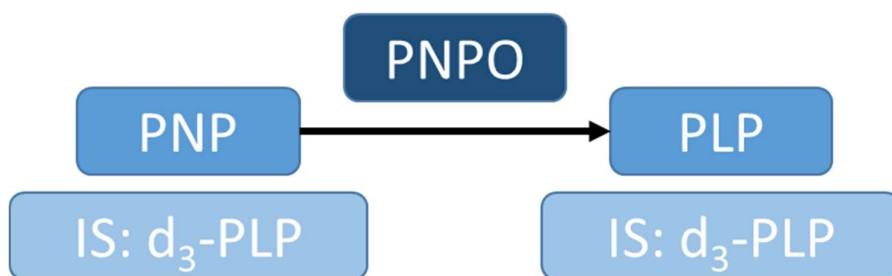


Figure 4.19: Single-step PNPO assay using PNP as substrate. IS = internal standard used for quantification of each analyte; PNP = pyridoxine 5'-phosphate; PLP = pyridoxal 5'-phosphate; PNPO = Pyridox(am)ine 5'-phosphate oxidase.

4.1.2.1 Development of PNPO assay using pyridoxine 5'-phosphate as substrate

Initially, a direct comparison was made between the previously optimised coupled (PN > PNP > PLP) PNPO assay and a single-step (PNP > PLP) assay. **Figure 4.20** shows vitamer concentrations on incubation for 0, 1, 2, 3 and 4 hours with a 3 mm control DBS. Reaction mixtures were varied with regards to substrate, cofactor and buffer composition; these conditions are found in **Table 4.2**.

Table 4.2: Composition of reaction buffers for the measurement of PNPO activity from DBS.

PNP = pyridoxine 5'-phosphate; PN = pyridoxine; PMP = pyridoxamine 5'-phosphate; PL = pyridoxal;
ATP = adenosine-5'-triphosphate; FMN = flavin mononucleotide.

	Type of assay	B ₆ Vitamers added	Cofactors added	Buffer used
Reaction mixture A	Coupled	400 nmol/L PN	3 mmol MgCl ₂ ; 0.3 mmol/L ATP; 1.5 μmol/L FMN	40 mmol/L KCl + 20 mmol/L Tris- PO ₄ pH 7.6
Reaction mixture B	Coupled	400 nmol/L PN	1.5 μmol/L FMN	20 mmol/L Tris-PO ₄ pH 7.6
Reaction mixture C	Single-step	400 nmol/L PNP	1.5 μmol/L FMN	20 mmol/L Tris- PO ₄ pH 7.6
Reaction mixture D	Single-step	400 nmol/L PNP; 200 nmol/L PL; 200 nmol/L PMP	1.5 μmol/L FMN	20 mmol/L Tris- PO ₄ pH 7.6

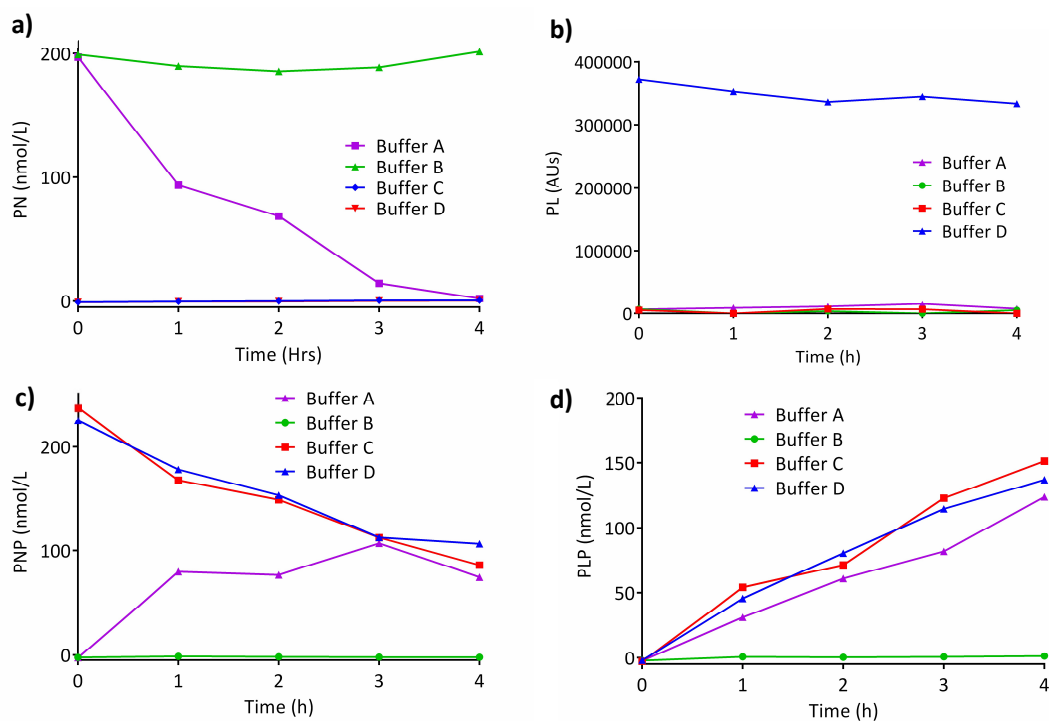


Figure 4.20: Concentrations of B₆ vitamers after incubation of a 3 mm DBS with varying initial B₆ concentrations and different buffers. Compositions of buffers A – D can be found in Table 3.2. Other conditions: 37 °C; 300 rpm agitation; 0 – 4 h incubation; 1 x 3 mm DBS. (n=1 at each data point).

Data showed that: i) As previously (**Section 4.1.1.3**), without the addition of K^+ , Mg^{2+} and ATP to the reaction buffer, pyridoxal kinase activity in the DBS is negligible as measured by $PN > PNP$ conversion in **Reaction Mixture B** and $PL > PLP$ conversion in **Reaction Mixture D** ii) Upon incubation of the DBS with PNP in Tris-phosphate, pH 7.6 with 1.5 $\mu\text{mol/L}$ FMN as cofactor (**Reaction Mixture C**), linear PLP formation was observed, comparable with that formed in the coupled $PN > PNP > PLP$ assay (**Reaction Mixture A**) iii) the addition of exogenous PMP and PL to the reaction buffer at a final concentration of half that of the PNP substrate had no effect upon PNPO activity as measured by PLP formation (**Reaction Mixture D**).

It was concluded that a single-step PNPO enzyme assay using unlabelled PNP as the substrate and monitoring the formation of PLP formed would be a viable method for the measurement of PNPO activity from dried blood spots.

One of the limitations of the coupled PNPO assay was its inability to distinguish between conversion of $PNP > PLP$ by the PNPO enzyme and conversion of $PL > PLP$ by PK in individuals receiving high doses of B_6 supplementation (**Section 4.1.1.4**). In order to confirm that a single-step PNPO assay would not suffer from the same limitations another comparison was made between the coupled and single-step assays. DBS from a control and a PNPO-deficient patient were incubated in **Reaction Mixtures A & C (Table 4.2; Figure 4.21)** for 4 hours and the concentrations of PN, PNP and PLP were determined at time 0, 1, 2, 3 and 4 hours.

In the control DBS, greater PLP formation was seen in the single-step assay than in the coupled PNPO assay. When using the coupled assay, PLP formation was still seen in the DBS from a PNPO deficient patient, hypothesised to consist of PL to PLP conversion through PK. However, when using the single-step PNP to PLP assay minimal PLP formation was apparent across the 4 hour incubation period in a PNPO DBS from a PNPO-deficient patient (**Figure 4.21 (c)**). **Figure 4.21 (b)** confirms that PNP was not converted to PLP in DBS from the PNPO deficient child, but was depleted linearly across the 4 hour period in DBS from an adult control.

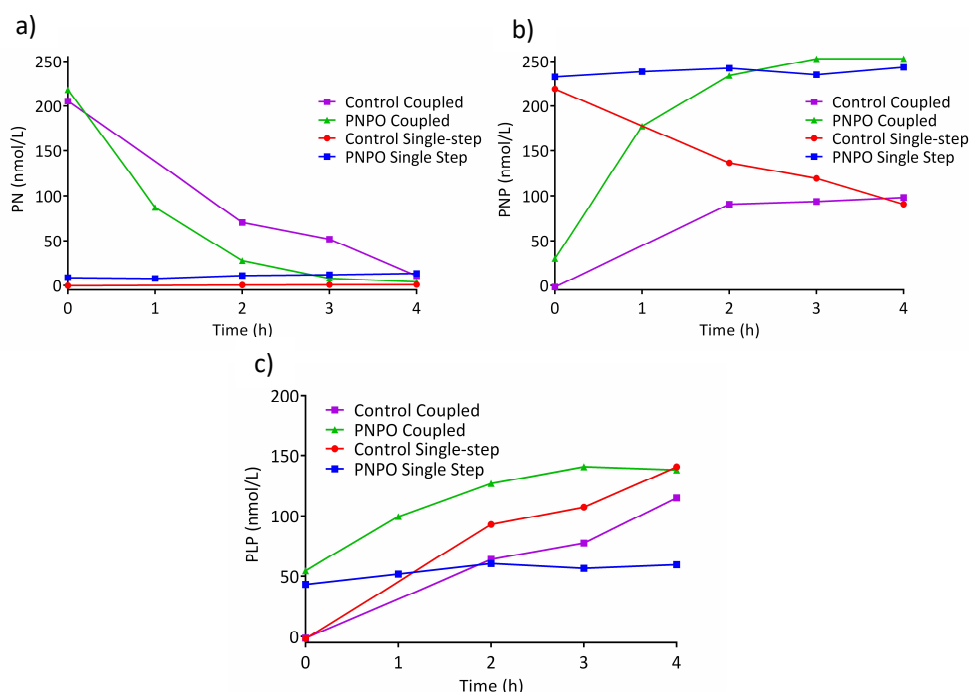


Figure 4.21: Comparison of coupled and single-step PNPO enzyme assay in DBS from a PNPO deficient patient and an adult control. Buffers for the coupled and single-step assays were made according to **Table 4.2** Other conditions: 37 °C; 300 rpm agitation; 0 – 4 h incubation; 1 x 3 mm DBS. (n = 1 at each data point). Control coupled or single-step = control DBS/coupled PK and PNPO assay or single-step PNPO assay; PNPO coupled or single-step = PNPO-deficient individual/coupled PK and PNPO assay.

It was hypothesised that the high endogenous PLP found in patients receiving supplementation could still have an effect upon accuracy of the assay. Because PNPO activity is quantified by measurement of PLP formation, it is important in cases of high endogenous PLP that baseline concentrations are calculated accurately. In **Figure 4.21**, a small increase in PLP concentration occurs in DBS from the PNPO deficient patient, particularly between 0 – 2 hours, before plateauing. When measured between 0 – 2 hours, this equates to 26% of that seen in a DBS from an adult control.

It was thought that, rather than this PLP formation being indicative of residual PNPO activity, it was due to some PLP being retained in the 3 mm DBS during the early stages of incubation before release after a longer incubation at 37°C with agitation at 300 rpm.

In order to test this hypothesis, two samples were run in parallel; one with a 40 second sonication step prior to the addition of reaction buffer, and one without. Sonication had been used for extraction of the B₆ vitamers and pyridoxic acid in **Section 3**. PLP concentrations were compared after 0, 15, 30 and 60 minutes incubation of a control DBS and the same PNPO deficient child analysed previously. In case of sonication, the DBS was first placed in 60 µL 40 mmol/L Tris-phosphate buffer, pH 7.6. After sonication, an additional 60 µL of reaction buffer containing 3 µmol/L FMN and 800 nmol/L PNP was added before incubation at 37°C. It was proposed that the sonication of DBS prior to incubation would ensure that the release of PLP from the T0 DBS was complete and independent of incubation at 37°C and/or agitation. This would mean that the release of PLP would be the same from the T0 and T30 DBS.

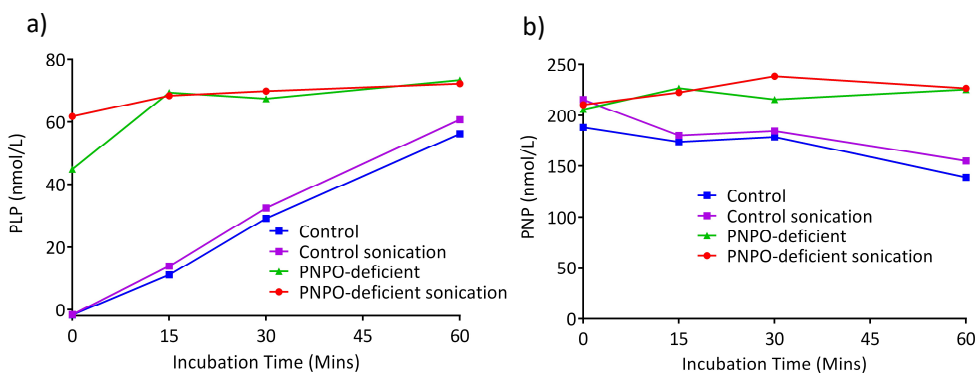


Figure 4.22: Effect of sonication on PNP and PLP concentrations measured prior to incubation with a 3 mm DBS from a PNPO deficient child or adult control. Incubation conditions: 20 mmol/L TrisPO₄ pH 7.6; 1.5 µmol/L FMN; 400 nmol/L PNP; 37 °C; 300 rpm agitation; 1 x 3 mm DBS. (n=1 at each data

Figure 4.22 shows the effect of this 40 second sonication step upon measured PLP concentrations after 0, 15, 30 and 60 minutes. Two important conclusions can be drawn from this data: i) A 40 second sonication step increased the PLP measured in the T0 DBS of a PNPO deficient individual with high endogenous PLP concentrations (receiving high dose PLP supplementation), in this case from 42 nmol/L to 61 nmol/L. ii) PLP formation and hence PNPO activity in a DBS from an adult control was

unaffected by this sonication step, indicating that sonication did not lead to degradation of the PNPO protein.

Anecdotally, it was noted that a red colour pertaining to haem release from the DBS was more prevalent in the buffer containing a T0 DBS that had undergone sonication. It is possible that without sonication some proteins remain bound to the filter paper. In the blood, most PLP is covalently bound to lysine residues of proteins such as haemoglobin and albumin.¹⁸³ Although the TCA precipitation step breaks the Schiff Base forming this covalent bond, sonication solubilises these proteins, facilitating PLP release into solution and measurement by LC-MS/MS. This allows more complete PLP recovery from the T0 bloodspot and therefore more accurate quantification of PNPO activity in individuals with high blood PLP concentrations.

In order to better characterise the effect of sonication on the assay, the sonication step prior to addition of the reaction buffer was varied (0, 30, 60, 120 and 300 seconds). **Figure 4.23** shows the PLP formation from a control DBS after each of these sonication periods. Sonication did not affect PNPO activity. All further experimentation was carried out using a 120 second sonication step prior to incubation.

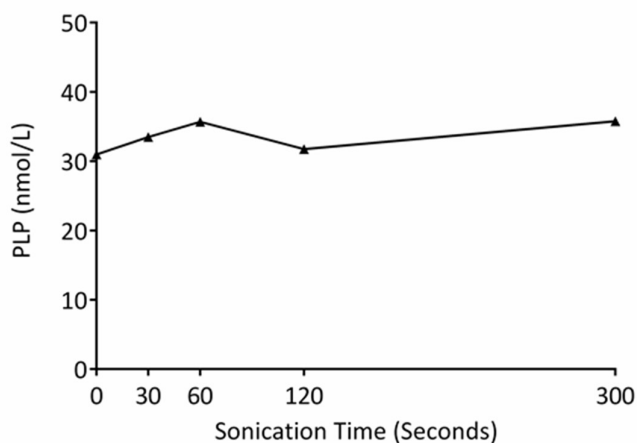


Figure 4.23: Effect of sonication on DBS PNPO activity. A 3 mm DBS from an adult control was sonicated for variable time periods prior to incubation for 30 minutes. Incubation conditions: 20 mmol/L TrisPO₄ pH 7.6; 1.5 µmol/L FMN; 400 nmol/L PNP; 37 °C; 300 rpm agitation; 1 x 3 mm DBS. (n=1 at each data point).

It was also hypothesised that greater PLP recovery from the DBS may be achieved by an additional sonication step after incubation with the TCA reaction stop mixture. TCA addition causes denaturation and precipitation of proteins in solution, the Schiff base binding PLP to these proteins is also broken; PLP is therefore free in solution.

Prior to the implementation of this additional step it was however necessary to ensure that sonication did not cause degradation of PLP when in solution. PLP concentration was measured in a 0.15 N TCA solution spiked with 25 nmol/L d₃-PLP and 100 nmol/L PLP after sonication for 0, 60, 120, 300 and 600 seconds. The recovery of PLP was unaffected by the length of sonication period (data not shown). A sonication period of 300 seconds after the addition of the TCA stop mixture was therefore chosen for all future experimentation.

Subsequent experiments were performed to ensure that the modified protocol including sonication steps released all PLP into solution from the T0 punch, as intended. DBS from a control and PNPO deficient individual were incubated for 0, 5, 10, 15 and 30 minutes. **Figure 4.24** shows the linear formation of PLP from PNP in the control DBS and the PLP concentrations measured over the same time period in a PNPO deficiency DBS. The DBS of a PNPO deficient child did not show an increase in PLP over 30 minutes. However, some fluctuation of PLP concentration is seen, this likely pertains to the variability of either the PLP extraction (optimised as fully as possible with sonication) or the LC-MS/MS method of PLP quantification itself. Further investigation of this is discussed alongside validation of assay precision in **Section 4.1.2.2**. The effects of high endogenous PLP levels on this single-step assay from DBS are discussed further in **Section 4.1.2.3**.

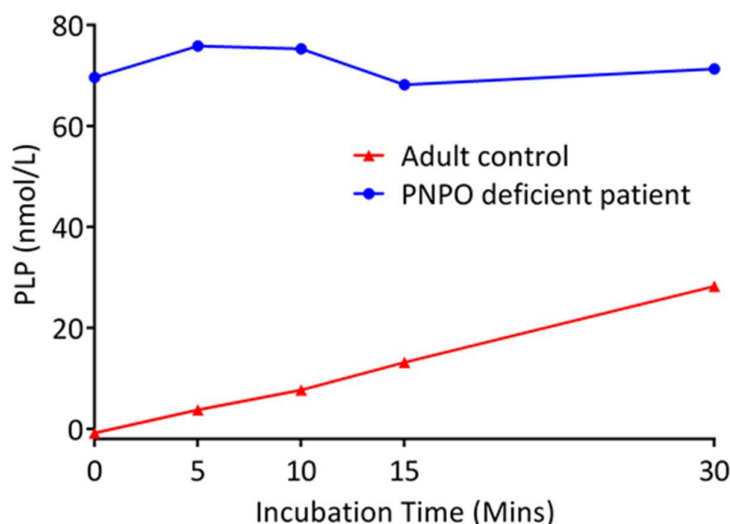


Figure 4.24: Conversion of PNP to PLP by control and PNPO deficient DBS when using optimised sonication protocol. Incubation conditions: 20 mmol/L TrisPO₄ pH 7.6; 1.5 µmol/L FMN; 400 nmol/L PNP; 37 °C; 300 rpm agitation; 1 x 3 mm DBS. (n=1 at each data point).

4.1.2.2 Further optimisation of single-step assay conditions

This section details several steps that were taken in order to ensure the accuracy and clinical utility of a single-step PNPO assay when using PNP as a substrate.

Incubation time and linearity of PLP formation

Experiments were performed to investigate whether PNPO activity was linear as a function of the amount of enzyme by incubating substrate with increasing DBS weight, this was achieved by cutting a 6 mm DBS into sections. It was shown in earlier experimentation (**Sections 4.1.1 & 4.1.2**) that PNPO activity could be quantified from a 3 mm DBS (26 mg). When PLP production was measured with 0 – 80 mg of DBS from a healthy adult volunteer an approximately linear correlation was observed to 30 mg. When a blank punch containing no blood was incubated with PNP, no PLP formation was seen (**Figure 4.25**).

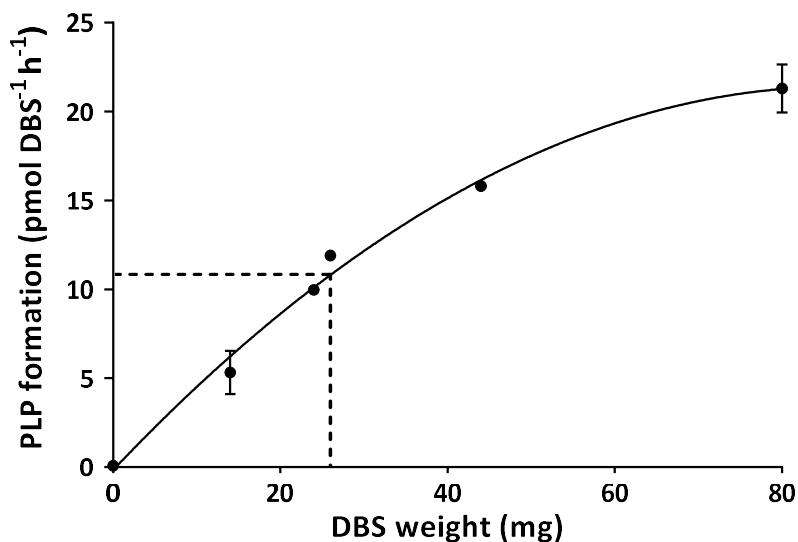


Figure 4.25: PNPO activity as a function of DBS weight. Data point at 0 mg corresponds to a 3mm punch containing no blood. Unbroken line is a second order polynomial best-fit of the data shown. Dashed line corresponds to the approximate weight of a 3mm punch filled with blood (26 mg). Incubation conditions: 20 mmol/L TrisPO₄ pH 7.6; 1.5 μ mol/L FMN; 400 nmol/L PNP; 37 °C; 300 rpm agitation; 30 min incubation. Error bars = SEM (n=2).

In order to optimise the duration of incubation time, PLP formation was monitored over 120 min using DBS from two adult controls and one child control (age 7 months). Formation was linear to 60 min in all subjects (**Figure 4.26**). Subsequently, an incubation time of 30 min was used for all future sample analysis; this was to ensure adequate PLP production for accurate quantification, while simultaneously ensuring assay linearity in subjects with high PNPO activity. This also enabled us to keep incubation time as short as possible to increase throughput and thereby render the assay suitable for clinical diagnostic use.

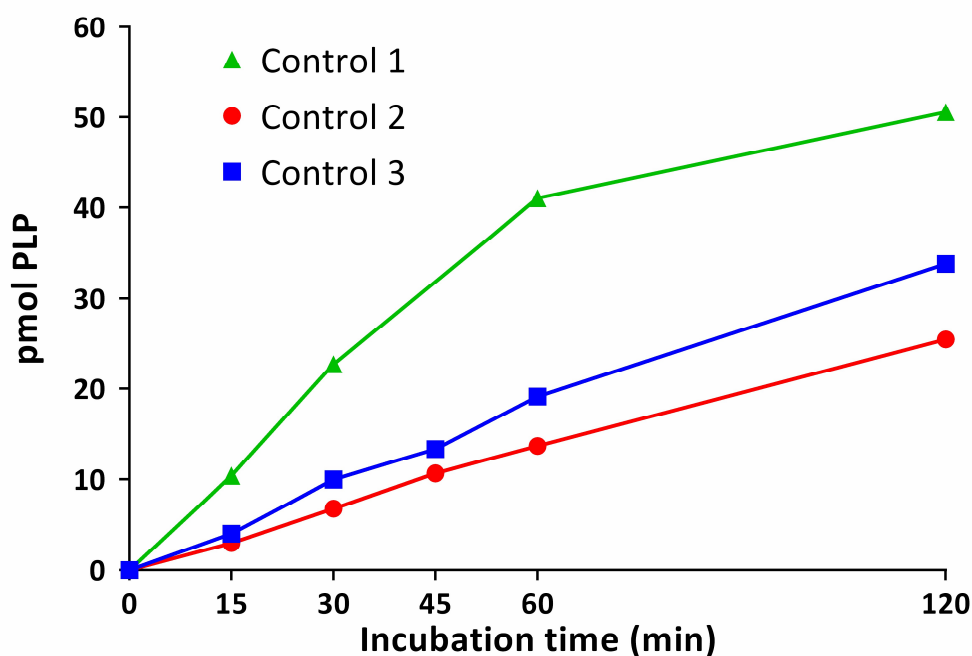


Figure 4.26: PNPO activity as a function of PLP formation from 0-120 min. Control 1; Child hospital control (7 months old); Control 2; Healthy male adult control (33 years old); Control 3; Healthy female adult control (45 years old). Incubation conditions: 20 mmol/L TrisPO₄ pH 7.6; 1.5 µmol/L FMN; 400 nmol/L PNP; 37 °C; 300 rpm agitation; 1 x 3 mm DBS. Each data point represents n=1.

Selection of substrate

The single-step assay had until now been developed using PNP as substrate. It is also possible that PMP would be a viable substrate. Indeed, PMP was considered as a potential substrate early in method development and discarded in favour of the coupled assay (**Section 4.1.1.1**). When a control DBS was incubated in the newly optimised single-step conditions for 30 minutes with 400 nmol/L PMP as substrate, PLP formation was only 14.1% of that seen when of 400 nmol/L PNP was used (**Figure 4.27**). This confirms earlier findings shown in **Figure 4.3**.

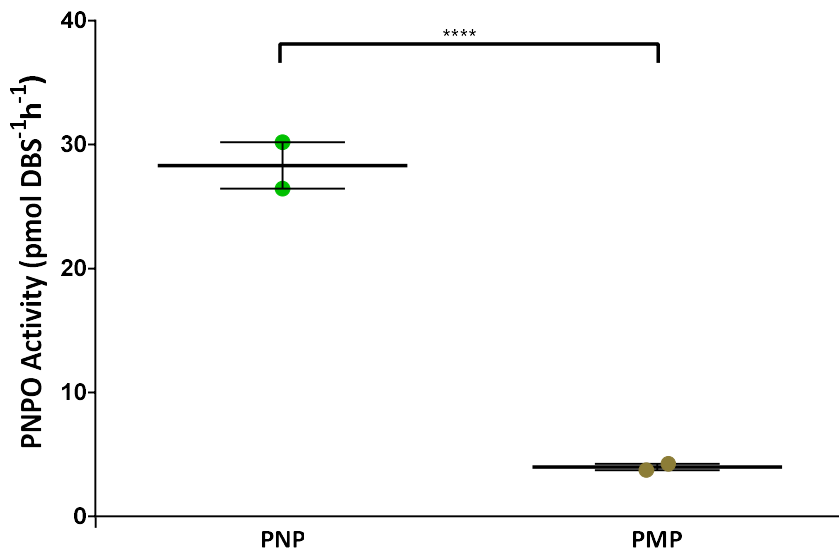


Figure 4.27: Effect of substrate on PNPO activity. Incubation conditions as follows: 20 mmol/L TrisPO₄ pH 7.6; 400nmol/L PNP/PMP; 37 °C; 300 rpm agitation; 30 min incubation; 1 x 3 mm DBS. Error bars = SEM. Statistical analysis was performed using an unpaired t-test: **** = $P < 0.0001$. (n=2).

Michaelis-Menten kinetics were determined for each of these substrates. **Figure 4.28** displays a Lineweaver-Burk plot showing the effect of PNP and PMP substrate concentration on PLP formation. The V_{max} of PNP conversion to PLP on the incubation of a 3 mm adult control DBS was found to be approximately twice that of PMP to PLP (39.5 vs 19.8 pmol DBS⁻¹ h⁻¹). The K_m for PNP was 0.32 μ mol/L as compared to 0.53 μ mol/L for PMP. These K_m values were close to those previously reported (1-2 μ mol/L for both PNP and PMP).^{60, 170} In contrast to the results reported here, human PNPO has been reported to prefer PMP as substrate. However, this prior work was carried out in different buffers and with either recombinant protein or whole blood.^{60, 170} In addition PMP > PLP conversion by *E. Coli* PNPO is extremely pH dependent, with a rapid increase between pH 7 - 8 whereas PNP > PLP conversion is less sensitive to pH.¹⁸⁴ This comparison has not been fully characterised for human PNPO but could explain the relatively sluggish PMP > PLP conversion using this assay system.

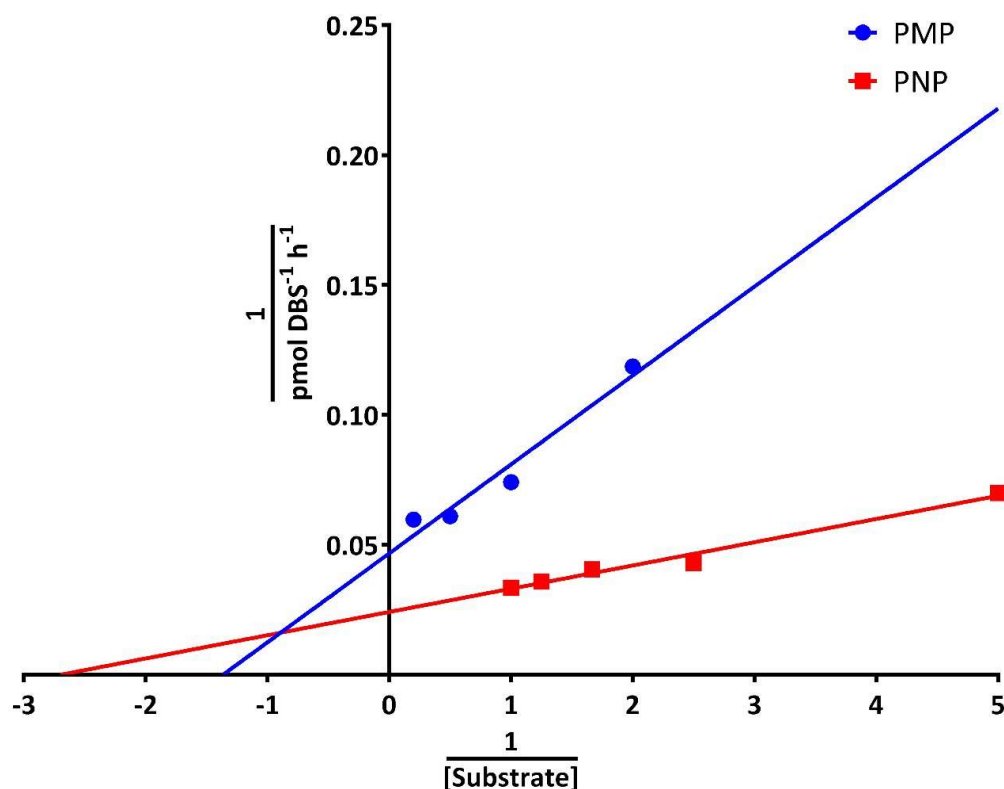


Figure 4.28: Lineweaver-Burk plot showing the effect of substrate concentration on PLP formation.
Incubation conditions: 20 mmol/L TrisPO₄ pH 7.6; 1.5 μ mol/L FMN; 0 - 1 μ mol/L PNP or 0 - 5 μ mol/L PMP; 37 °C; 300 rpm agitation; 1 x 3 mm DBS from a healthy adult control. Calculated V_{\max} : PNP 39.55 \pm 3.55 pmol/DBS/h; PMP 19.76 \pm 1.42 pmol/DBS/h. Calculated K_m : PNP 0.319 \pm 0.081 μ mol/L; PMP 0.530 \pm 0.143 μ mol/L. Michaelis-Menten kinetics calculated using GraphPad Prism 6.05.

Finally, a concentration of 400 nmol/L PNP was used for the assay for several reasons: i) this concentration of PNP permitted analysis of the resulting supernatant by LC-MS/MS without further dilution steps. ii) As previously noted (**Section 4.1.1.4**), there was a small amount of cross talk between the MRM channels for PNP and d₃-PLP (<1%). Although at a concentration of 0.4 μ mol/L (as in the assay in its current form) the effect was negligible, at higher PNP concentrations interference increased proportionally; this could potentially affect results through incorrect PLP quantification. iii) Saturation of the enzyme with substrate would not facilitate detection of PNPO deficiency in patients with mutations that cause an alteration in the K_m of PNPO where the enzyme has residual activity and the V_{\max} and K_{cat} are relatively unaffected. By mildly limiting the substrate concentration but still achieving easily measurable conversion in controls, it is likely that the diagnosis of PNPO deficiency in patients with ‘milder’ mutations is enabled.

Optimisation of FMN Concentration

Since PNPO is an FMN-dependent enzyme, there was concern that the vitamin B₂ status of subjects could affect results. When an adult control DBS was incubated in the presence of endogenous FMN only, 61% of the activity seen upon the addition of 1.5 $\mu\text{mol/L}$ FMN was measured (**Figure 4.29**). To ensure that the concentration of FMN was not limiting PNPO activity, an adult control DBS was incubated with varying concentrations (0.75 – 3.0 $\mu\text{mol/L}$) of FMN. As previously seen for the coupled assay (**Section 4.1.1.2**), no significant difference was observed in PNPO activity hence 1.5 $\mu\text{mol/L}$ was used for all subsequent experimentation.

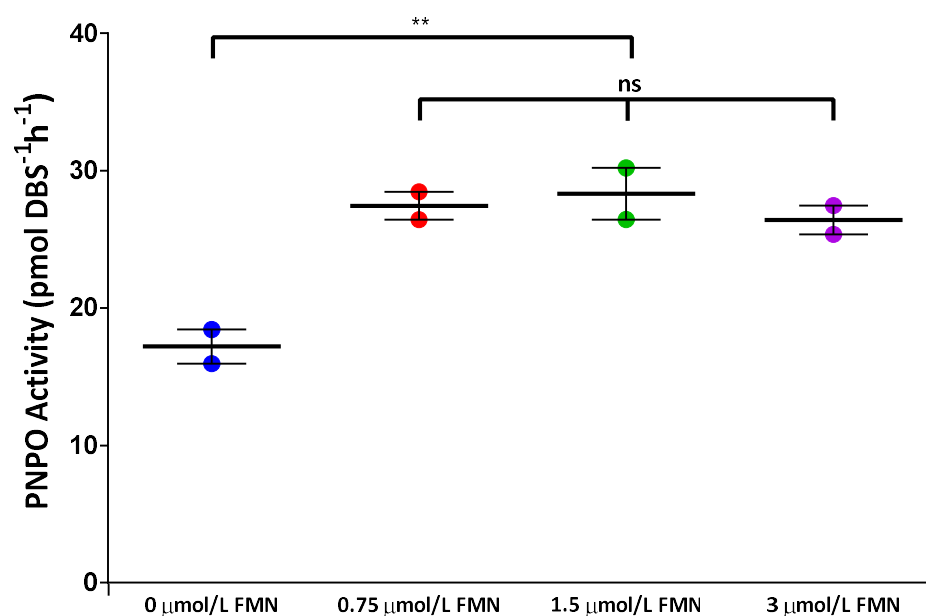


Figure 4.29: Effect of FMN concentration on PLP formation. Incubation conditions: 20 mmol/L TrisPO₄ pH 7.6; 400nmol/L PNP; 37 °C; 300 rpm agitation; 30 min incubation; 1 x 3 mm DBS. Error bars = SEM. Statistical analysis was performed using one-way ANOVA followed by Tukey's multiple comparisons test: ns = no significance; ** = P<0.01. (n=2).

Optimisation of Buffer pH

As described in **Section 4.1.1.2**, the optimal pH for PNPO enzyme activity in erythrocytes is pH 8.0. The pH dependence of PNPO was determined between pH 7.0 – 8.0 and little difference in activity was identified (**Table 4.3**). As previously seen, (**Section 4.1.1.1**) peak splitting was evident at a pH > 7.8. Therefore, pH 7.6 was used for all further experimentation.

Table 4.3: Effect of pH on PNPO Activity using a single step assay. PNPO activity measured in a healthy adult control DBS at pH 7 - 8. Incubation conditions: 20 mmol/L TrisPO₄ (pH adjusted appropriately); 1.5 µmol/L FMN; 400 nmol/L PNP; 37 °C; 300 rpm agitation; 1 x 3 mm DBS; 30 min incubation; n = 3. Error = SEM.

pH	PNPO Activity (pmol/DBS/h)
7.0	16.72 ±0.80
7.2	20.37 ±0.36
7.4	18.43 ±0.98
7.6	19.88 ±1.06
7.8	24.90 ±1.32
8.0	22.72 ±1.78

4.1.2.3 Effect of supraphysiological B₆ vitamer concentrations found in patients on supplementation

Previously, in **Section 4.1.1.4**, the effect of supraphysiological vitamer concentrations on the coupled PK and PNPO assay were characterised. A single-step assay meant that high PL concentrations in patient blood did not interfere with assay results. In order to ensure that the use of a Tris-based buffer in the single-step assay ameliorated the potential feedback inhibition that may occur in the presence of high levels of endogenous PLP, a DBS from a healthy adult control not receiving B₆ supplementation was incubated with varying concentrations (0 – 200 nmol/L) of PLP (**Table 4.4**). These concentrations were chosen as representative of those measured in the DBS of patients receiving high dose B₆ supplementation (**Section 3**).

Table 4.4: Effect of exogenous PLP on PNPO activity. PNPO activity measured in a healthy adult control with varying amounts of PLP added to the reaction buffer, simulating high endogenous levels seen in individuals on B₆ supplementation. 100 % = Activity with no exogenous PLP. Incubation conditions: 20 mmol/L TrisPO₄ pH 7.6; 1.5 µmol/L FMN; 400 nmol/L PNP; 37 °C; 300 rpm agitation; 1 x 3 mm DBS; 30 min incubation. (n=1 in each condition).

PLP added to reaction buffer (nmol/L)	% activity*
0	100.0
25	101.5
50	95.8
100	76.5
150	79.1
200	58.7

Concentrations of PLP were measured in the T0 DBS from 21 PNPO deficient individuals and 27 children with other epilepsies (i.e. other patients) receiving B₆ supplementation. Concentrations of PLP ranged from 0 - 199 nmol/L. The majority of patients receiving B₆ supplementation (16/21 PNPO; 24/27 others) had PLP concentrations lower than 100 nmol/L; 3/21 PNPO and 3/27 other patients on B₆ had PLP concentrations between 100 - 150 nmol/L; 2/21 PNPO deficient patients had concentrations between 150 – 200 nmol/L. No product inhibition of PNPO activity was observed in the presence of concentrations ≤ 50 nmol/L PLP (final concentration after TCA precipitation). However, in the presence of 100 – 150 nmol/L PLP and 200 nmol/L, a decrease in PNPO activity of 15 - 20% and 41% was observed, respectively (**Table 4.4**).

Concentrations of PMP and PNP were measured in DBS from the same cohorts. These vitamers have been reported to be present in the blood of PNPO deficient patients receiving high doses of B₆.²² In patients that were not PNPO deficient, concentrations of PNP and PMP were below the LLOQ (< 1.25 nmol/L). In PNPO deficient patients PNP and PMP concentrations were 0 – 137 nmol/L and 0 – 121 nmol/L, respectively.

Therefore the total substrate concentration (i.e. endogenous PNP or PMP and exogenous PNP) in some PNPO deficient patients will be higher than that found in control samples. In order to determine what effect this may have on the assay a comparison was made between DBS incubated in the presence of high

concentrations of PMP (400 nmol/L) in addition to the normal PNP added as substrate (400 nmol/L) and those incubated under the standard assay conditions (i.e. only 400 nmol/L PNP (**Figure 4.30**). Whilst previous studies using the rabbit liver enzyme have shown that PMP does not inhibit PNPO at any concentration,¹⁸⁵ a 22% decrease in PLP formation was observed. Although this difference was not significant with only two repeats, it is possible that this decrease is indicative of competition between the two substrates, given the lower rate of PMP to PLP conversion using these assay conditions (see **Figure 3.27**). It would be useful to perform the assay with one of the two substrates isotopically labelled, however these were unavailable.

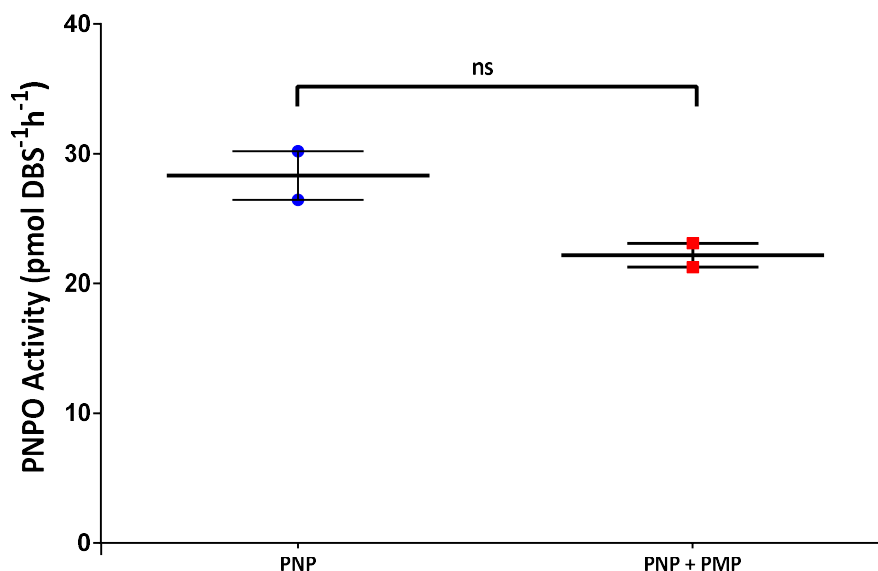


Figure 4.30: Effect of exogenous PMP on PNPO activity measured as PLP formation.

Incubation conditions as follows: 20 mmol/L TrisPO₄ pH 7.6; 400 nmol/L PNP or 400 nmol/L PNP + 400 nmol/L PMP; 1.5 µmol/L FMN; 37 °C; 300 rpm agitation; 30 min incubation; 1 x 3 mm DBS. Error bars = SEM. Statistical analysis was performed using an unpaired t-test: ns = no significance (P = 0.0944); (n=2).

4.1.2.4 Validation of single-step assay

The intra and inter-assay precisions of the assay were determined by measuring PNPO activity from ten different 3 mm DBS punches from an individual on one day. This was repeated, in total, five times over a four week period. %CVs for intra and inter-assay precision were 7.93 and 10.31%, respectively (**Figure 4.31**).

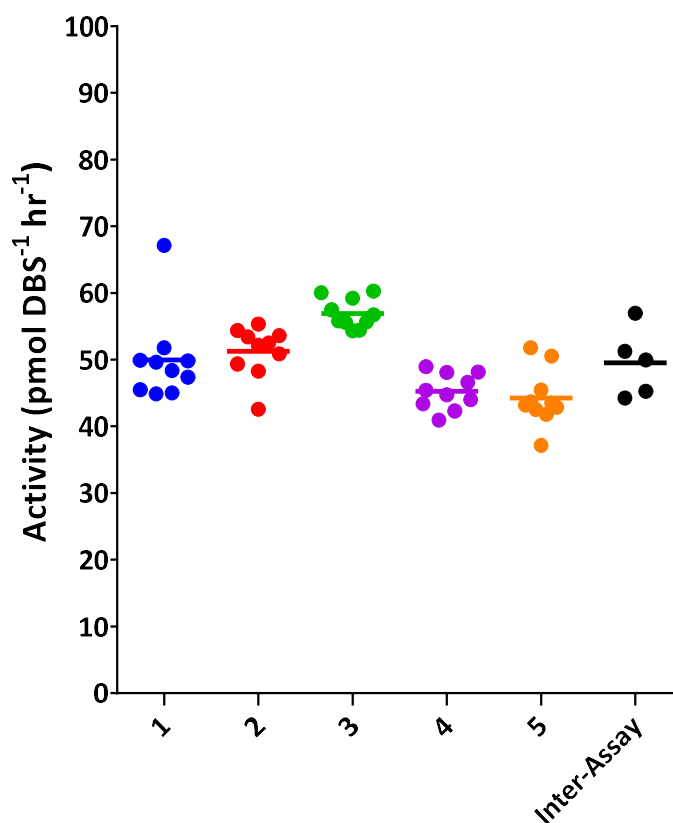


Figure 4.31: Intra and inter-assay validation of a single-step DBS PNPO assay.

Dried blood spots from 5 different cards simultaneously collected from one adult control were run on 5 separate days within a 2 week period, 10 times on each day. Intra and inter-assay %CVs were 7.93 and 10.31%, respectively.

The accuracy of PLP measurement using the LC-MS/MS method described in **Section 2.4** and **Section 3** was characterised with the changes described in this chapter. The LLOQ and ULOQ for both PLP and PNP were set at the upper and lower bounds of the calibration curve created at 1.25 nmol/L and 200 nmol/L, respectively. The Signal/Noise (S/N) ratio at the LLOQ was greater than 10 and therefore the limit of detection (S/N greater than 3) was lower than 1.25 nmol/L. The back-calculated values at LLOQ and ULOQ were monitored to ensure they did not deviate from their

nominal values by more than 20 and 15%, respectively, as suggested by the European Medicines Agency (https://www.ema.europa.eu/documents/scientific-guideline/guideline-bioanalytical-method-validation_en.pdf). QC standards were analysed alongside each run to ensure precision, the %CVs of PLP measurement on five repeated injections of QC standards at 5, 10, 100 and 175 nmol/L were 2.28, 0.90, 2.30 and 3.45%, respectively.

Accuracy of PLP quantification after extraction from a DBS collected from a PNPO deficient patient receiving a dose of 42 mg/kg/d PLP was evaluated. PNPO deficient patients on PLP typically receive 30 – 50 mg/kg/d for the control of their seizures and doses can range between 10 - 72 mg/kg/d⁸⁷ hence 42 mg/kg/d was deemed representative of this cohort. The intra and inter-assay %CVs were acceptable at 5.92 and 7.76%.

4.1.2.5 Stability of dried blood spot PNPO activity

In order to characterise the stability of PNPO activity when stored in a DBS format, cards were stored at different temperatures. Since ambient humidity is known to affect the stability of enzymes when stored in DBS¹⁸⁶, duplicate cards were stored; one with desiccant in a sealed foiled bag, the other under ambient conditions. All cards were first dried for 16 – 24 h at room temperature without desiccant prior to storage. PNPO activity measured after this storage period was compared to baseline values measured after 16 - 24 h drying at room temperature.

Short-term stability studies were carried out by storing cards in the dark for 1, 3, 5, 7, 14 and 28 days at 22°C with and without desiccant (**Figure 4.32**). Cards were subsequently stored at -80°C until day 28 when they were analysed. The day 28 replicates were frozen and thawed once on the day of analysis to ensure an identical number of freeze-thaw cycles for every sample. When stored without desiccant at 22 °C a 17% reduction in activity was seen after 3 days, which increased to a 48% reduction after 28 days. This compares to 8 and 26% reductions in the DBS stored with desiccant in sealed foil bags, indicating a protective advantage of storage under these conditions.

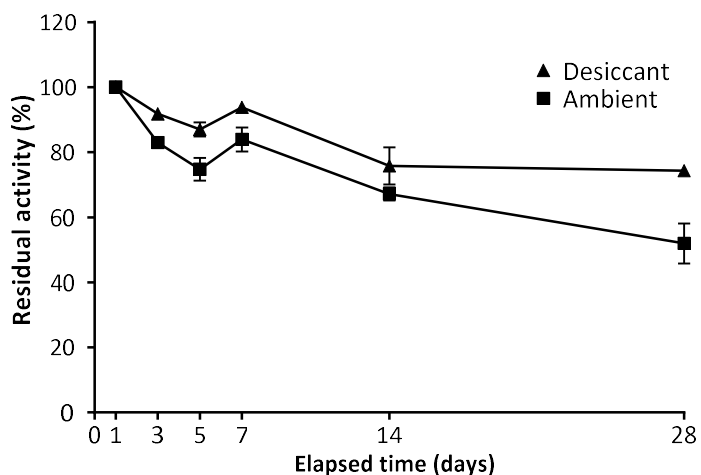


Figure 4.32: Effect of humidity on the short-term stability of the PNPO enzyme in dried blood spots. DBS were stored in sealed foil bags with desiccant (▲) or under ambient conditions (■) at room temperature (22 °C). Error bars indicate SEM. Data points represent the mean percentage of activity compared to that found after 1 day (n=2).

Long-term PNPO enzyme stability was studied by storage of DBS for 1, 4, 8 and 12 weeks at 4 °C, -20°C and -80°C after the same initial 16-24 h drying period at 22 °C as described above (**Figure 4.33**). 73% PNPO activity was retained after storage for 12 weeks at 4°C. DBS stored at -20°C and -80°C retained 93 and 87% activity, respectively. Under these conditions no difference in PNPO activity was identified between DBS cards stored with or without desiccant.

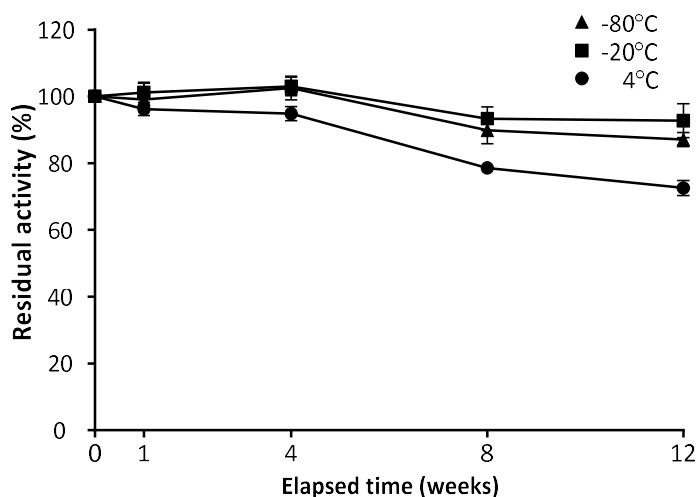


Figure 4.33: Effect of storage temperature on the long-term stability of the PNPO enzyme in dried blood spots. Data points represent the mean percentage of PNPO activity relative to measurement at time zero. Error bars indicate SEM. (n=4). No significant difference was seen between activities of samples with/without desiccant. (4°C = ●; -20°C = ■ and -80°C = ▲)

After stability studies were performed, it was decided that for future analysis: i) DBS should be dried at room temperature (22°C for 16 - 24 h). ii) After this initial period, samples should be placed in sealed zip-lock bags with desiccant and stored at room temperature for no more than 7 days after the sample was taken iii) Thereafter, DBS should be stored at -20°C or below prior to analysis.

4.1.2.6 Investigation of blood haemoglobin measurement from dried blood spots

PNPO enzyme activity in dried blood spots is reliant on the amount of blood contained within the punch taken from the filter paper used for blood collection. Several estimates have been made as to the quantity of blood within a 3 mm DBS punch (such as used in this study), with a consensus of approximately 3.2 µL whole blood,¹⁵⁵ although estimates can be as low as 1.6 µL¹⁸⁷ and as high as 5 µL.¹⁸⁸ The precise amount of whole blood contained within a DBS punch of a given diameter is particularly dependent on the haematocrit of the patient providing the sample and hence the viscosity of blood and its spreading across the filter paper.^{158, 189} Ideally, the results reported utilising an assay from dried blood spots would include a correction factor to compensate for this effect as the amount of PNPO enzyme in the DBS punch will depend on the haematocrit of the sample.

One potential solution to this problem would be the simultaneous analysis of another enzyme within the blood, with a consistent activity according to the haematocrit of the sample. However, this option was discarded due to concerns that the variability of another enzyme in the blood would be too high and not provide a good estimate of haematocrit. PNPO itself is almost ubiquitously expressed and can itself be regarded as a housekeeping enzyme.³⁵ Despite this, PNPO activity can vary widely in the general population^{39, 170} and other enzymes can see this same variation.¹⁹⁰ Correlation of erythrocyte enzyme activities with a variety of factors such as gender, age, circadian rhythm and ethnicity have been identified. These include enzymes involved in antioxidative activity¹⁹¹ and purine metabolism¹⁹².

An alternative approach would be to quantify haemoglobin from the same dried blood spots used for PNPO assay, thus enabling the estimation of haematocrit. A safe and fast method widely used for the determination of the haemoglobin concentration (gHb/dL) in whole blood is the Haemoglobin Reagent Cyanide Free Method

(Instruchemie, NL).¹⁹³ This method uses a buffer that reacts with haemoglobin in the blood, forming alkaline haematin D-575. This compound can be quantified using absorption spectroscopy.

This method was adapted for use on the DBS samples used for PNPO enzyme activity measurement. Parameters to consider if the accurate quantification of gHb/dL from DBS was to be successful were: i) Ensuring that the method had sufficient sensitivity to achieve accurate measurement from the small volumes of blood present in a DBS ii) Ensuring that the elution of haemoglobin from the DBS was consistent between samples, and that the DBS matrix did not interfere with measurement.

A calibration curve was constructed using a haemoglobin standard mixture at the concentrations expected upon elution of whole blood from a 3 mm punch taken from a DBS. This calibration curve showed good linearity ($R^2 > 0.99$) (**Figure 4.34**). The method is designed for monitoring at 575 nm, with the absorption spectrum of alkaline haematin D-575 plateauing between 575 and 605 nm.¹⁹³ Absorption was measured at 595 nm as a 575 nm filter was unavailable for the spectrophotometer used. Measurement was linear across the range evaluated therefore quantification would not be affected.

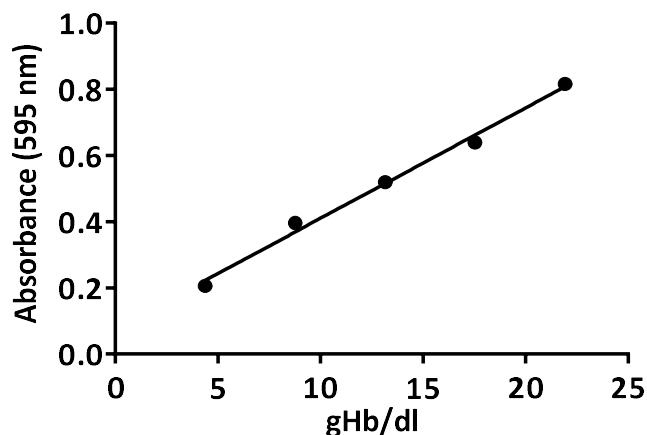


Figure 4.34: Haemoglobin calibration curve. Concentrations shown are those after a correction factor has been applied to compensate for the dilution of a 3 mm DBS in a resuspension solution. $R^2 > 0.99$.

Measurement of haemoglobin (gHb/dL) was carried out from seven healthy adult controls. This was performed by the addition of the alkaline D-575 reagent to a 3 mm DBS and incubation for 30 minutes at room temperature, with agitation at 1000 RPM.

After incubation and centrifugation at 13,000 g for 10 minutes, the absorbance of the supernatant was measured at 595 nm alongside a calibration curve spiked with a haemoglobin standard of known concentration. 3 x 3 mm punches were analysed for each individual. Mean gHb/L values ranged from 12.2 – 15.1 gHb/dL. In healthy adults, the haemoglobin concentration in whole blood typically ranges from 12 – 17 gHb/dL. However, the accuracy and repeatability of measurement was extremely variable between repeated measurements from 3 mm punches taken from the same DBS card (**Figure 4.35**).

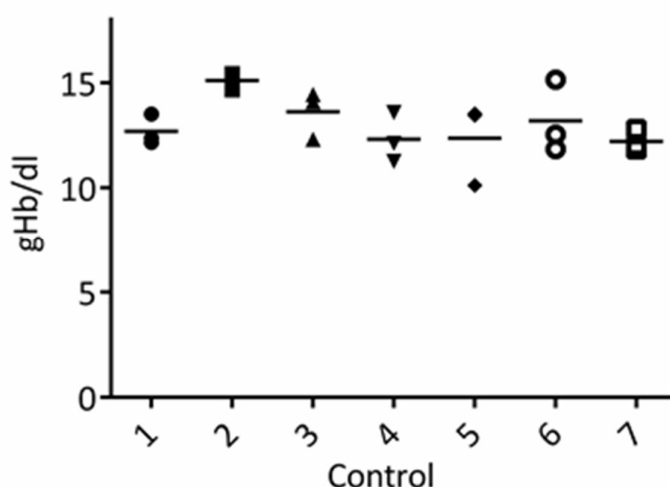


Figure 4.35: Haemoglobin concentration (gHb/dL) measured in 3 mm DBS.

Concentrations shown are those after a correction factor has been applied to compensate for the dilution of a 3 mm DBS in a resuspension solution. Each point is an individual measurement from a single 3 mm DBS punch. Line shown is the mean for

In order to verify that the calculated gHb/dL values were similar to those measured from whole blood, the gHb/dL value was measured from the same whole blood samples from which the DBS were originally spotted onto newborn screening cards. This was performed in the accredited diagnostic laboratory at Great Ormond Street Hospital, also using the Haemoglobin Reagent Cyanide Free Method. A correlation between the values measured from DBS and those from whole blood was poor with an R^2 value of 0.375 (**Figure 4.36**). The slope of linear regression was 1.49, indicating a 49% positive bias when measuring from DBS.

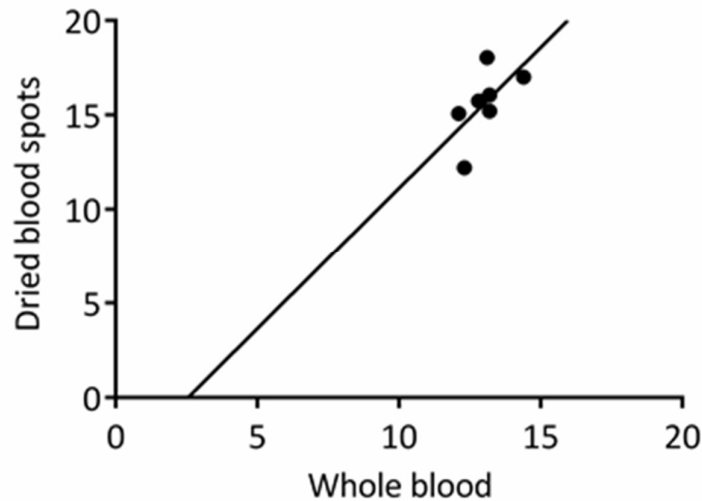


Figure 4.36: Correlation of haemoglobin concentration (gHb/dL) measured from whole blood and DBS. Concentrations shown from DBS are those after a correction factor has been applied to compensate for the dilution of a 3 mm DBS in a resuspension solution. $n = 3$ at each point. Line indicates linear regression.

It was hypothesised that this variation was due to incomplete liberation of blood from the 3 mm punches as, anecdotally, a small amount of Hb could be seen to remain in the punches after incubation. In order to ensure all Hb was removed from the protein saver cards punches were sonicated for 10 minutes after addition of the alkaline D-575 reagent mixture (**Figure 4.37**).

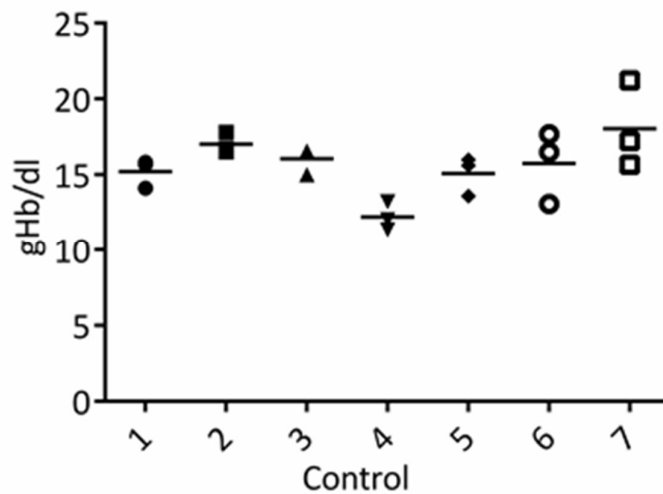


Figure 4.37: Haemoglobin concentration (gHb/dL) measured from 3 mm DBS after a 10 minute sonication step. Concentrations shown are those after a correction factor has been applied to compensate for the dilution of a 3 mm DBS in a resuspension solution. Each point is an individual measurement from a single 3 mm DBS punch. Line shown is the mean for each control.

Unfortunately sonication of the DBS resulted in disintegration of the cellulose matrix of the DBS punch. Despite centrifugation some of the cellulose matrix would remain in suspension. This interfered with subsequent spectroscopic measurements, increasing the absorbance of the solution thereby providing aberrantly high gHb/dL values. This can be seen in, for example, some samples from subjects 6 and 7 (**Figure 4.37**).

The measurement of haemoglobin from DBS was therefore not pursued further due to the inaccuracies inherent in the current protocol. In subsequent experiments PNPO activity was expressed as: pmol PLP (3 mm DBS)⁻¹ hour⁻¹, denoted as pmol/DBS/h. In the future protocols enabling normalisation of PNPO activity to haematocrit could be investigated further. Upon the assessment of individuals in a clinical setting, the haematocrit would usually be measured as part of their care.

4.1.2.7 Analysis of patient samples

Samples were collected from 21 patients with mutations in *PNPO* (age range; 1 day – 25 years), 27 patients with other epilepsies receiving B₆ supplementation (age range; 1 month – 16 years), 38 child hospital controls (age range; 5 days – 15 years) and 7 healthy adult controls. None of the child hospital controls had presented with seizures. In the cohort of patients with other epilepsies receiving B₆ supplementation, PNPO deficiency had been excluded by genetic analysis or another cause of epilepsy had been identified. Identified causes included two individuals with mutations in *ALDH7A1*, one with PROSC deficiency and one with hyperprolinaemia type II. More details of the PNPO deficient cohort can be found in **Table 4.5**.

Upon measurement of PNPO enzyme activity, hospital controls were found to have activities ranging from 10.0 – 95.0 pmol/DBS/h with a mean of 42.0 pmol/DBS/h. This was significantly ($P < 0.0001$) higher than the activity seen in patients with mutations in *PNPO*, who had a mean activity of 1.1 pmol/DBS/h (range: 0.0 – 4.6 pmol/DBS/h). Other epilepsy patients receiving vitamin B₆ supplementation had activities ranging from 23.0 – 85.9 pmol/DBS/h (mean: 55.3 pmol/DBS/h), also significantly higher than activities identified in the PNPO cohort ($P < 0.0001$). Activities from healthy adult controls showed a similar significant difference ($P < 0.01$) (range: 13.8 – 44.0 pmol/DBS/h; mean: 28.3 pmol/DBS/h) (**Figure 4.38**).

Table 4.5: Summary of subjects with mutations identified in PNPO. Control ranges; Children receiving B6 supplementation: 23.0 – 83.9 pmol/DBS/h (n=16); Children not receiving B6 supplementation: 10.0 – 95.0 pmol/DBS/h (n=37); Healthy adults: 13.8 - 44.0 pmol/DBS/h (n=7). n/a = not available; d = day; m = month; y = year; w = week; M = maternal, P = paternal. Subject numbers also correspond to those in **Table 3.4**. * Mother recipient of multivitamin containing pyridoxine during pregnancy **No second mutation found. ***Two seizures in childhood due to delayed doses of PLP

Subject	Age at sampling	Seizure Onset	Mutation/sequence variant	Presumed effect	PNPO Activity (pmol/DBS/h)	References
1	2y	n/a	c.[98A>T] (M) + c.[576C>A] (P)	p.D33V (M) + Y157X (P)	0.0	-
2	1d	None	c.[364-1G>C] + [364-1G>C]	Splice errors	0.7	-
3	9y	5m	c.[347G>A] + c.[347G>A]	p.R116Q + p.R116Q	0.0	Mills <i>et al.</i> 2014
4	5y	No Seizures*	c.[347G>A] + c.[347G>A]	p.R116Q + p.R116Q	0.1	-
5	25y	3h	c.264-21_264-1delinsC (M) + c.[98A>T] (P)	Splice errors (M) + p.D33V (P)	2.0	Mills <i>et al.</i> 2014
6	7y	5h	c.[641dupA] + ? **	p.Q214fs + ? **	0.0	Mills <i>et al.</i> 2014; Raimondi et al 2015
7	6y	30 min	c.[284G>A] (M) + c.[148G>A]; c.[364-1G>A] (P)	p.R95H (M) + p.E50K; Splice errors (P)	0.5	Mills <i>et al.</i> 2014
8	16y	n/a	c.[363+5G>A] + c.[363+5G>A]	Splice errors + Splice errors	1.8	-
9	17y	n/a	c.[363+5G>A] + c.[363+5G>A]	Splice errors + Splice errors	1.8	-
10	12y	10h	c.[347G>A];c.[674G>A] + c.[347G>A];c.[674G>A]	p.R116Q;p.R225H + p.R116Q;p.R225H	0.0	Mills <i>et al.</i> 2014

11	13y	<12h	c.[148G> A]; c.[364-1G>A] + c.[148G> A]; c.[364-1G>A]	p.E50K;Splice errors + p.E50K;Splice errors	3.1	Mills <i>et al.</i> 2005
12	5m	n/a	c.[673C>T] + c.[673C>T]	p.R225C + p.R225C	0.0	-
13	3y	n/a	c.[347G>A] + c.[347G>A]	p.R116Q + p.R116Q	0.0	-
14	5y	90 min	c.[637C>T] + c.[637C>T]	p.P213S + p.P213S	2.3	Mills <i>et al.</i> 2014; Hatch <i>et al.</i> 2015
15	3y	No neonatal seizures ***	c.[637C>T] + c.[637C>T]	p.P213S + p.P213S	4.7	Mills <i>et al.</i> 2014; Hatch <i>et al.</i> 2015
16	11m	3w	c.[194G>T] + c.[194G>T]	p.W65L + p.W65L	0.0	-
17	6y	6h	c.[98A>T] + c.[98A>T]	p.D33V + p.D33V	0.0	Mills <i>et al.</i> 2014
18	4y	unknown	c.[263+2T>C] + c.[263+2T>C]	Splice errors + Splice Errors	3.6	-
19	8y	unknown	c.[686G>A] + c.[407T>C]	p.R229Q + p.L136P	0.0	-
20	9y	3w	c.[98A>T] + c.[98A>T]	p.D33V + p.D33V	2.9	Mills <i>et al.</i> 2014
21	1y	10 months	c.[98A>T] + c.[421C>T]	p.D33V + p.R151C	0.5	-

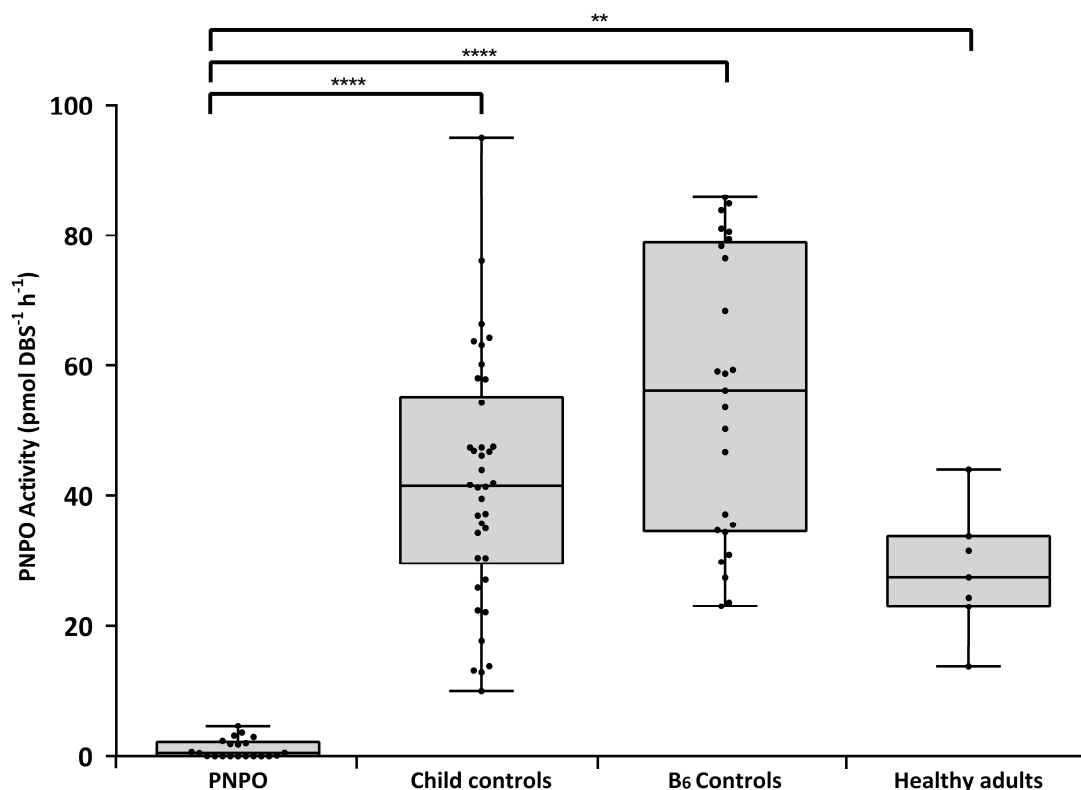


Figure 4.38: DBS PNPO activities of patients with PNPO deficiency relative to control individuals.

Box plots indicate range, interquartile range and median. Statistical analysis was performed using one-way ANOVA followed by Tukey's multiple comparisons test; ** = $P < 0.01$; **** = $P < 0.0001$.

Patients from the PNPO cohort could be clearly delineated from all control cohorts and no false-positives or negatives were identified. In agreement with previous studies¹⁷⁰ there was large variation in the PNPO enzyme activity measured for controls.

It has been shown previously that foetal expression of PNPO is low relative to that in adults.³⁵ It was therefore investigated whether it was possible to differentiate 'control' neonates from PNPO deficient individuals particularly given that PNPO deficiency is a neonatal-onset seizure disorder. Five control neonates (less than one month of age) were included in the 37 child hospital controls analysed. The mean PNPO enzyme activity measured in these neonates was 52.7 pmol/DBS/h (range: 41.3 – 66.3 pmol/DBS/h). This was not significantly different to the activity measured in the overall child hospital control cohort. The youngest neonate (5 days of age) had an activity of

64.3 pmol/DBS/h. No overall correlation of age with PNPO activity was identified when all controls (not receiving B₆ supplementation) were analysed.

Whilst the DBS PNPO enzyme assay is able to accurately identify patients with low PNPO activity and provide a diagnosis of PNPO deficiency, due to the limitations in accurately measuring small amounts of PLP formed, it is difficult to accurately determine the amount of residual activity in PNPO deficient patients, if any is present. It is possible that small differences in the residual PNPO activity of these individuals could be measured if longer incubation periods or very high concentrations of substrate were used. In the future two tiers of PNPO assay could be performed, the first a rapid screen using the assay in its current form to reliably detect PNPO deficient individuals and the second a more lengthy assay to precisely determine whether there is some residual PNP > PLP conversion.

This will provide valuable extra information with regards to the genotype-phenotype correlation in PNPO deficiency. It is presumably more likely that a PNPO deficient individual with residual activity will respond to treatment with PN. This is clinically important as PN is shown to be a safer form of vitamin B₆ supplementation than PLP and should be used preferentially where it provides adequate seizure control. The potential toxicity of high PLP doses is discussed in **Section 6**.

4.2 The effect of the p.R116Q variant on PNPO activity and expression

The PNPO deficient cohort analysed for DBS PNPO activity in **Section 4.1.2.7** included 21 subjects with 17 different genotypes. These included three individuals homozygous for p.R116Q (**Subjects 3, 4 and 13; Table 4.5**). The p.R116Q (c.347G>A) variant is reported in gnomAD with an allele frequency of 0.0547 (512 homozygotes in 138,592 individuals). It has previously been hypothesised that the p.R116Q variant is a susceptibility factor for epilepsy. This variant is predicted to affect FMN binding and/or formation of active PNPO dimers but residual activity of this variant was found to be high (83% of wild-type) *in vitro* when assayed using 2.5 $\mu\text{mol/L}$ PMP as substrate in a potassium phosphate buffer. Indeed, it is known that not all individuals homozygous for p.R116Q present with the seizures typical of PNPO deficiency.⁸⁷ This is also the case in our cohort; two of the patients receive B₆ for the management of seizures but one (**Subject 4**, sister of **Subject 3**) has never presented with seizures and does not require B₆ supplementation. **Subject 3** had been investigated previously using an epilepsy gene panel containing approximately 140 genes and no variants predicted pathogenic were identified.

The PNPO activity in DBS of these individuals (including the asymptomatic sister) was extremely low (< 0.2 pmol/DBS/h). The ability of this method to identify patients homozygous for the p.R116Q variant is particularly important diagnostically since patients with this genotype do not seem to have a raised plasma PM/PA ratio, previously identified as the most consistent biomarker for PNPO deficiency.⁸⁸ The presence of a raised PNP/PLP ratio was also shown in **Section 3** to be inconsistent in these patients. The parents of **Subjects 3 and 4**, both of whom are heterozygous for the p.R116Q mutation, had intermediate PNPO activities of 7.1 and 10.8 pmol/DBS/h.

It is possible that the p.R116Q substitution causes a dramatic reduction in activity under the conditions used in the dried blood spot assay, but still retains some residual activity *in vivo*. This would correlate with the lack of seizures in **Subject 4**. The reason that **Subject 4** has not presented with seizures yet their sibling requires high-dose vitamin B₆ treatment for their epilepsy is unknown. One potential explanation could be that although p.R116Q induces susceptibility to seizures, a 'second hit' is required for clinically apparent epilepsy. This could be either genetic (e.g. variant at another

epilepsy susceptibility locus) or environmental. This second environmental hypothesis is particularly interesting as it could involve differential dietary intake of the B₆ vitamers. For example, since breast milk contains almost entirely PLP and PL, whereas baby formula generally contains PN, if a PNPO deficient child receives breast milk exclusively, this could convey some protection as PNPO activity would not be required for conversion of dietary B₆ to PLP. In addition, as flavin mononucleotide (FMN; a vitamin B₂ derivative) is the cofactor of PNPO, the B₂ status of patients could also affect presentation.

In order to study the effect of p.R116Q on PNPO enzyme activity further we were provided with bacterially expressed recombinant human wild-type and p.R116Q PNPO enzyme by collaborators from the University of Oxford.

4.2.1 Preliminary development of a method to measure activity from bacterially-prepared recombinant PNPO enzyme

Experiments were carried out as described in **Section 2.6** and the activities of wild-type and mutant p.R116Q PNPO enzymes were compared to one another. Incubation conditions (buffer, pH, temperature, substrate/cofactor concentrations) were identical to those used in the DBS assay, no significant difference in PLP formation could be identified between wild-type and mutant forms of protein (**Figure 4.39**). A negative control without the addition of PNPO protein was also analysed; no activity was observed. Product formation (PLP) was linear to 45 minutes and then plateaued.

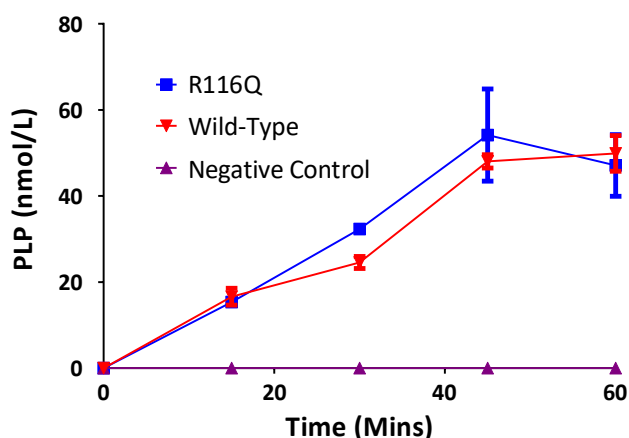


Figure 4.39: Effect of the p.R116Q variant on the activity of recombinant PNPO.

Incubation conditions: 20 mmol/L TrisPO₄ pH 7.6; 1.5 μ mol/L FMN; 400 nmol/L PNP; 37 °C; 300 rpm agitation; 100ng PNPO enzyme; 0 – 60 min incubation. (n = 2). Error bars = SEM.

The enzyme was stored in 1% glycerol at -80°C. After one freeze thaw cycle, PNPO activity was reduced by ~50% (data not shown). For this reason all subsequent experiments comparing wild-type and mutant p.R116Q PNPO were carried out using protein that had undergone an identical number of freeze/thaw cycles.

4.2.2 Effect of flavin mononucleotide concentration on the kinetics of recombinant wild-type and p.R116Q PNPO activity

PNPO is an FMN-dependent enzyme⁵⁹ and p.R116Q has been predicted to have an effect upon FMN binding as it is close to the FMN binding pocket.⁸⁷ PNPO activity

was therefore measured in both the wild-type and p.R116Q proteins in the presence of varying (0, 0.75, 1.5 and 3.0 $\mu\text{mol/L}$) concentrations of FMN (**Figure 4.40**). When no exogenous FMN was added (**Figure 4.40 (a)**) wild-type PNPO activity was significantly higher ($P < 0.0001$) than that of the p.R116Q variant protein. When exogenous FMN was added (0.75, 1.5 and 3 $\mu\text{mol/L}$), no significant difference in activity was identified between wild-type and p.R116Q recombinant PNPO.

When comparing activity of the enzyme when incubated with 1.5 $\mu\text{mol/L}$ FMN to that seen in preliminary experimentation (**Figure 4.39**) under the same conditions (1.5 $\mu\text{mol/L}$ FMN) a considerable reduction in activity was seen suggesting some denaturation of the enzyme had occurred when stored at $-80\text{ }^{\circ}\text{C}$ as well as after freeze/thaw cycles as mentioned above.

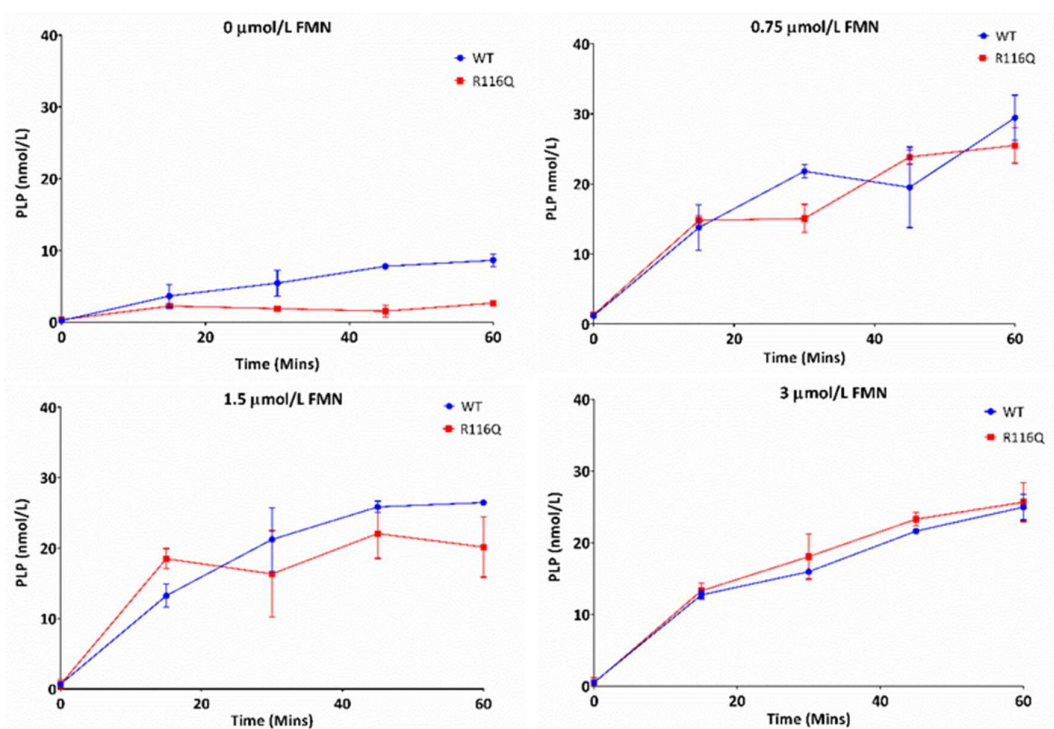


Figure 4.40: Effect of FMN concentration on activity of recombinant wild-type and p.R116Q PNPO enzymes. Incubation conditions: 20 mmol/L TrisPO₄ pH 7.6; 0.0 – 3.0 $\mu\text{mol/L}$ FMN; 400 nmol/L PNP; 37 $^{\circ}\text{C}$; 300 rpm agitation; 100ng PNPO enzyme. ANCOVA analysis was performed on the slopes at each respective FMN concentration. No significant difference was identified when 0.75, 1.5 or 3.0 $\mu\text{mol/L}$ FMN was added. A significant difference was identified in the absence of exogenous FMN ($P = <0.0001$) Error = SEM. ($n = 2$ for each data point).

There was concern that the significant difference between wild-type and p.R116Q PNPO activity without the addition of exogenous FMN could be due to the concentration of residual FMN bound to the recombinant PNPO protein after purification. Although our collaborators attempted the removal of this FMN using hydrophobic interaction chromatography, residual PNPO activity indicates that some FMN remained either in solution or bound to the PNPO protein. A method was developed for the measurement of FMN (**Section 2.6.1**). When FMN was quantified in the T0 time point solutions of wild-type and p.R116Q proteins, similar FMN concentrations of 1.6 and 1.8 nmol/L were detected, respectively (**Figure 4.41**) suggesting that differing FMN concentrations were not responsible for the difference in enzyme activity identified between p.R116Q and wild-type PNPO when incubated without the addition of exogenous FMN.

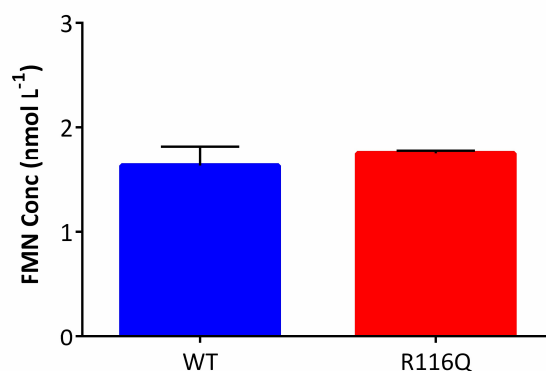


Figure 4.41: FMN concentration in T0 time points of the recombinant PNPO enzyme assay. Error bars indicate SEM. (n = 2).

This experiment was repeated in order to verify the finding. A difference in activity was again apparent with no exogenous FMN but no firm conclusions could be drawn because activity of the PNPO enzyme was reduced yet further (another ~50%) due to the longer period of storage (**data not shown**). Subsequent experiments were performed on a newly synthesised batch of recombinant protein. This protein was immediately divided into many single-use aliquots to ensure additional freeze-thaw cycles were unnecessary.

Kinetics of WT and p.R116Q protein when using PNP and PMP as substrate were studied (**Figure 4.42 (a) and (b)**). 100 ng protein was incubated for 10 minutes with varying substrate concentrations (0 – 10 $\mu\text{mol/L}$ PNP or PMP) and a fixed FMN concentration of 1.5 $\mu\text{mol/L}$ in order to ensure that cofactor availability was not affecting catalytic efficiency. At higher concentrations of PNP some crosstalk with $\text{d}_3\text{-PLP}$, which is used for quantification of PLP, was evident. Hence accurate PLP quantification in samples with higher PNP concentrations was not possible. PLP levels were therefore expressed as the area under the peak. This still allowed measurement and comparison of K_m for each PNPO protein type.

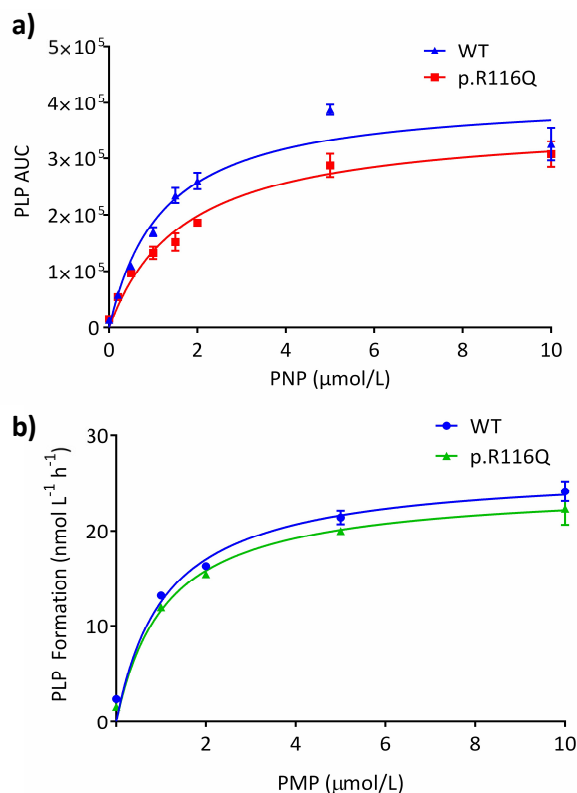


Figure 4.42: Kinetics of PNPO protein when varying concentrations of substrates PNP and PMP.

K_m towards PNP: WT = 1.2 $\mu\text{mol/L}$; p.R116Q = 1.7 $\mu\text{mol/L}$. K_m towards PMP: WT = 1.1 $\mu\text{mol/L}$; p.R116Q = 1.1 $\mu\text{mol/L}$. Error bars indicate SEM. (n = 3 at each point).

A similar issue was detected upon the addition of high PMP concentrations to the reaction mixture. As mentioned previously (**Section 4.1.1.1**), the commercially sourced PMP was found to contain a small, but significant (1.3%) amount of PLP. When adding large PMP concentrations and measuring relatively small quantities of

PLP formation, this interfered with the calculation of PNPO kinetics. However, as the proportion of PLP in the PMP standard was known, the PLP inadvertently added to each sample could be calculated and subtracted from total PLP to calculate PLP formed. As these concentrations were small in relation to those of PMP, it is unlikely they would have influenced results through product inhibition of PNPO; the K_i for PLP has been reported as $3.2 \mu\text{mol/L}$ ⁶⁰ and the maximal PLP concentration as a proportion of the PMP standard was 130 nmol/L (1.3% of $10 \mu\text{mol/L}$ PMP).

The K_m values for wild-type and p.R116Q protein when using PNP as substrate were 1.2 and $1.7 \mu\text{mol/L}$, respectively. The K_m values for PMP were calculated as $1.1 \mu\text{mol/L}$ for both forms of PNPO. These values are almost identical to those calculated by Musayev et al. from recombinant PNPO⁶⁰ (Wild-type K_m : PNP = $1.8 \mu\text{mol/L}$; PMP = $1.0 \mu\text{mol/L}$). It was not possible to measure the V_{max} due to the problems with accurately quantifying PLP formation alongside high PNP concentrations. Since 100 ng of PNPO protein was added per sample, the reaction velocity measured as nmol/L/h can be expressed pmol/mg protein/h using a conversion factor of $\times 2.4$ (e.g. $1 \text{ nmol/L/h} = 2.4 \text{ pmol/mg/h}$).

The FMN-dependency of WT and p.R116Q PNPO protein was characterised by varying FMN concentration upon incubation with $1 \mu\text{mol/L}$ PNP (**Figure 4.43**). This experimentation was a repetition of the earlier kinetic studies using FMN (**Figure 4.40**) but with a new batch of recombinant PNPO protein and lower FMN concentrations. Maximal PNPO activity was evident in the presence of a relatively low FMN concentration of 25 nmol/L indicating saturation of the enzyme with cofactor. No difference in V_{max} was identified between wild-type and p.R116Q protein. The FMN K_m values for wild-type and p.R116Q proteins were 0.5 and 3.3 nmol/L , respectively. This indicated that there is a small difference in catalytic efficiency between the two forms of protein, although the uncertainty of this measurement was large with an R^2 value of 0.33 for both.

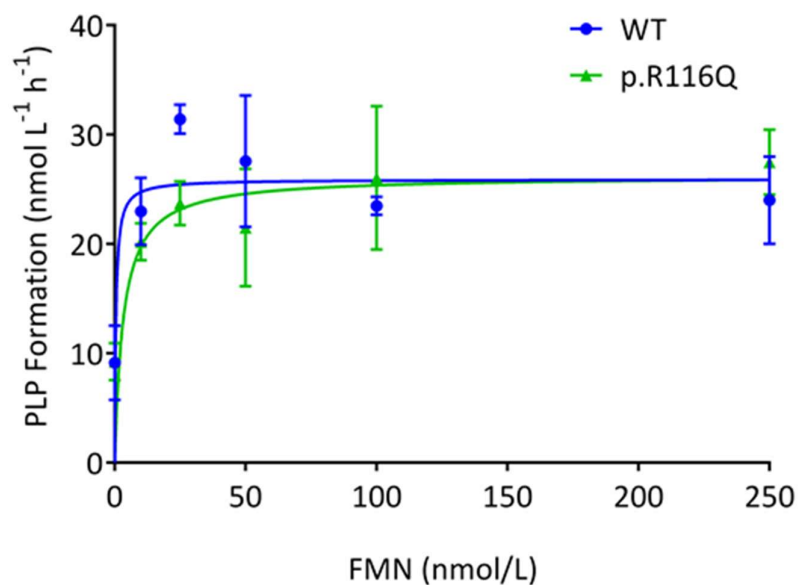


Figure 4.43: Kinetics of the PNPO protein when varying concentrations of FMN. Wild-type: $V_{\max} = 25.9 \text{ nmol/L/h}$; $K_m = 0.46$. p.R116Q: $V_{\max} = 26.2 \text{ nmol/L/h}$; $K_m = 3.3$. Error bars indicate SEM. (n = 3 at each point).

Earlier measurements of FMN (**Figure 4.41**) had been performed without the addition of a stable-isotope-labelled internal standard. In order to accurately quantify measurements of FMN associated with this new batch of recombinant PNPO enzyme a stable isotope of riboflavin was obtained ($^{13}\text{C}_4^{15}\text{N}_2$ -Riboflavin; labelled FMN was not commercially available).

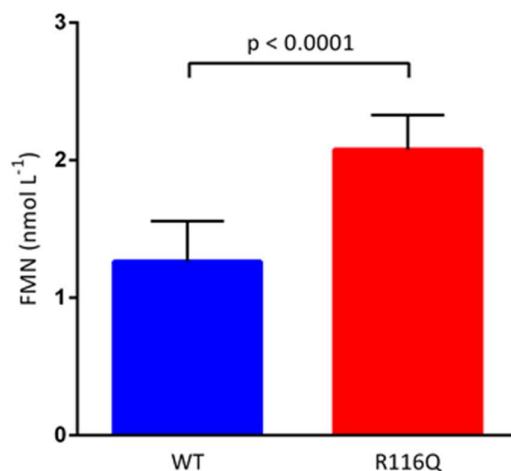


Figure 4.44: Measurement of FMN bound to recombinant PNPO protein using α $^{13}\text{C}_4^{15}\text{N}_2$ -riboflavin internal standard. Means \pm SEM: WT = 1.26 ± 0.08 ; p.R116Q = 2.08 ± 0.07 . Error bars indicate SEM. (n = 15 repeats).

Results showed (**Figure 4.44**) that significantly more FMN was found in p.R116Q than wild-type PNPO (2.1 vs 1.1 nmol/L) ($P < 0.0001$). This suggests that the difference in activity between WT and p.R116Q PNPO protein without the addition of exogenous FMN was not due to protein-bound FMN or FMN contained within the protein lysate.

This section has shown that under the conditions used, little difference in PNPO activity could be identified between p.R116Q and wild-type recombinant PNPO protein. The only effect of this amino acid substitution appears to be a small reduction in enzymatic activity when exogenous FMN is not added to the reaction mixture. This correlates with the location of R116 close to the FMN binding site of PNPO (**Figure 4.45**) but does not necessarily explain the large difference seen *in vivo* between the DBS of subjects homozygous for p.R116Q and wild-type controls, or the seizures experienced by some of these individuals.

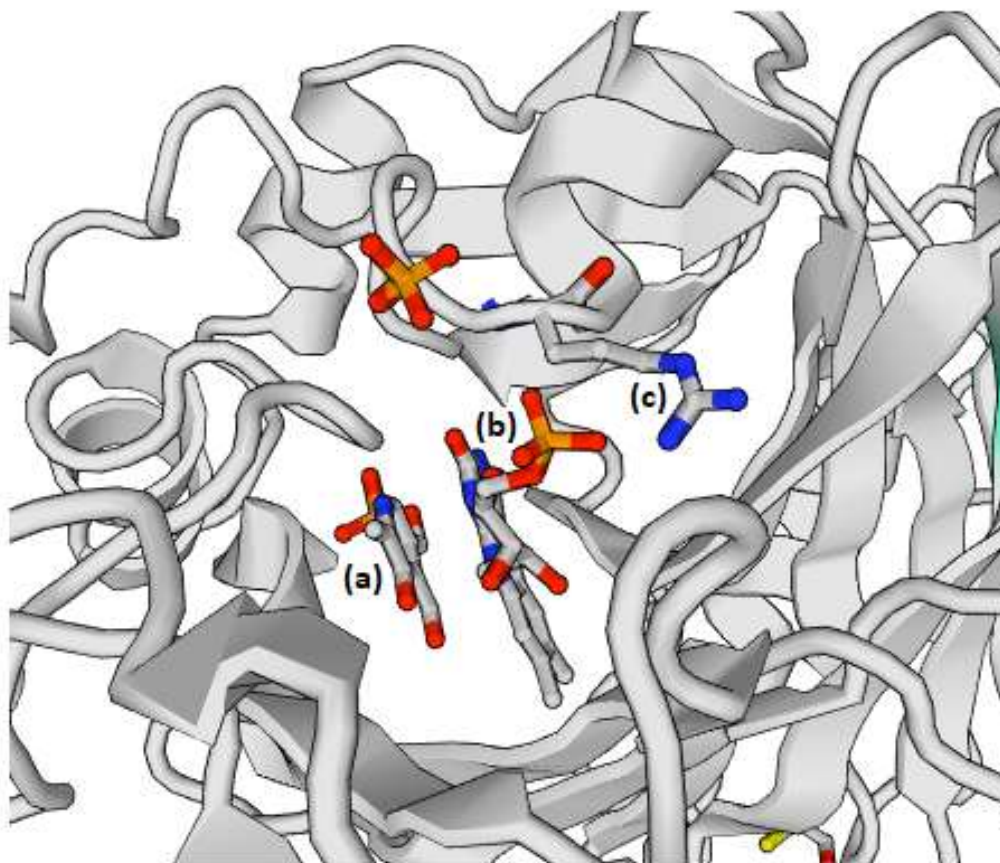


Figure 4.45: Predicted structure of the PNPO active site. The positions of bound (a) pyridoxal 5'-phosphate and (b) Flavin mononucleotide are shown as well as the (c) R116 residue. Adapted from the crystal structure of PNPO determined by Musayev et al. 2003 and stored in the [swissmodel.expasy.org](http://www.expasy.org/swissmodel) repository.

A recently published manuscript has shown that the thermal stability of PNPO is reduced in the presence of p.R116Q – FMN binding is a critical modulator of this effect.⁷⁴ This suggests that the formation of the PNPO-FMN holoenzyme is critical for protein stability. The same study showed that the presence of p.R116Q can disrupt FMN binding ($K_{d(FMN)}$ WT: 13.1 nmol/L; $K_{d(FMN)}$ p.R116Q: 251 nmol/L) and therefore protein expression/function. In addition, the calculated K_m values reported for PNP were 2.0 μ mol/L and 3.1 μ mol/L. Although these were higher than those in this study calculated from **Figure 4.42 (a)**, the ratio of p.R116Q to wild-type K_m was similar (1.55 di Salvo *et al.*, 1.42 in our study). The differences in K_m can be explained by the different buffers used.

In summary, the p.R116Q variant does not significantly impair the enzymatic function of PNPO unless its cofactor, FMN, is restricted. This is likely due to the proximity of R116 to the FMN binding site. However, di Salvo *et al.* have reported that p.R116Q reduces the stability of PNPO, particularly when concentrations of FMN are limited. The effect of the variant on thermal stability of the protein may be relevant to the pathophysiology of some patients homozygous for p.R116Q as these have, in at least one case, been preceded by a febrile illness. Perhaps a higher body temperature during fever precipitates these seizures through the thermal degradation of PNPO protein and subsequent lowering of available PLP.

4.2.3 Development of an LC-MS/MS method for the quantification of PNPO protein in DBS

The findings discussed in **Section 4.2.2** indicate that the thermal stability of p.R116Q PNPO is reduced compared to that of the wild-type protein. In addition, in-silico analysis using the Human Splicing Finder¹⁹⁴ tool shows that the DNA base substitution present in these individuals (c.347G>A) is predicted to interfere with a splicing enhancer in exon 3 of the *PNPO* gene (**Figures 4.46 and 4.47**). Loss of this splice enhancer could lead to aberrant splicing and therefore nonsense-mediated decay, resulting in lower expression of PNPO. It is feasible that this effect could vary according to tissue type as splicing can be tissue specific.¹⁹⁵ In order to further investigate whether decreased expression of p.R116Q PNPO protein might explain low DBS PNPO activity in individuals carrying the p.R116Q variant, an LC-MS/MS

method was developed for measurement of PNPO protein in the same DBS analysed for PNPO activity in **Section 4.1.2.7**.

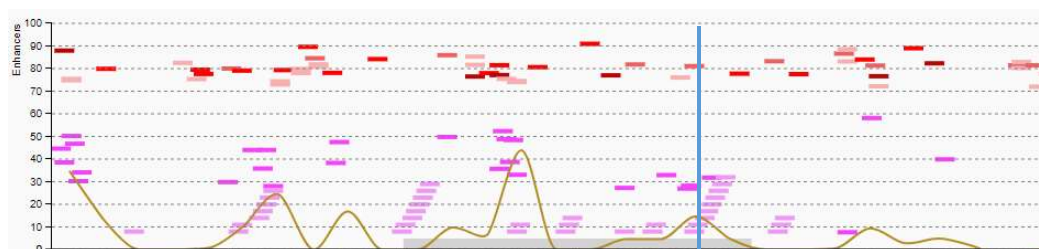


Figure 4.46: Predicted exonic splicing enhancers in exon 3 of the *PNPO* gene. Predicted binding motifs for the splicing factors SF2/ASF, SRp40, SC35 and SRp55 are shown in red. Predicted exonic splicing enhancer hexamers/octamers are shown in pink. The location of c.347G (p.R116) is indicated by the blue vertical line. The variable yellow line indicates the relative strength of exonic splicing enhancer octamers across exon 3 of *PNPO*. Analysis performed using the Human Splicing Finder online tool.¹⁹⁴

Predicted signal	Prediction algorithm	cDNA Position	Interpretation
ESE Site Broken	1 - ESE-Finder - SF2/ASF		Alteration of an exonic ESE site. Potential alteration of splicing.
	2 - HSF Matrices - 9G8		
	3 - PESE Octamers from Zhang & Chasin		
	4 - ESE-Finder - SRp40		
	5 - RESCUE ESE Hexamers		

Figure 4.47: Predicted disruption of exonic splicing enhancer sites by the c.347G>A (p.R116Q) variant in *PNPO*. Analysis performed using the Human Splicing Finder¹⁹⁴ online tool, results indicate possible disruption of an exonic splicing enhancer.

4.2.3.1 Selection of *PNPO*-derived tryptic peptides and LC-MS/MS method development

A targeted MRM-based LC-MS/MS method was developed for the quantification of peptides produced upon the tryptic digestion of intact PNPO protein in dried blood spots. Other sample types such as fibroblasts and whole blood were unavailable. Trypsin digestion enzymatically breaks the dipeptide bond on the C-terminus sides of lysines and arginines in a protein/peptide. The peptides formed upon digestion can be accurately predicted and analysed quantitatively using LC-MS/MS.

Peptides were identified using the Skyline software package (MacCoss Lab Software)¹⁹⁶ and were submitted to BLAST to ensure they were specific to human PNPO. Suitable peptides were custom-synthesised (**Figure 4.48**) and MRM transitions for these were optimised using the Intellistart software package (Waters,

MA, US). The optimised ionisation and fragmentation conditions for each of these peptides are as detailed in **Table 4.6**.

Table 4.6: Peptides selected for LC-MS/MS detection of trypsin digested PNPO protein. Optimised MRM transitions, cone voltages and collision energies obtained using Waters Intellistart software.

Peptide	AA position in protein	Monoisotopic mass (daltons)	MRM Transition	Cone voltage (V)	Collision Energy (V)
1: DGKPSAR	89 - 95	729.37	365.94 > 430.42	2	10
2: FFTNFESR	109 - 116	1046.47	524.31 > 753.65	32	16
3: FFTNFESQK	109 - 117	1146.52	574.43 > 267.27	52	18
4: SSQIGAVVS HQSSVIPDR	164 - 181	1865.95	623.22 > 726.81	2	18

MTCWLRGVTATFGRPAEWPGYLSHLCGRSAAMD LGPMRKSYRGDREAFEETHLTSLDPVKQFAAWF
EEAVQCPDIGEANAMCLATCTR/**DGKPSAR**/MLLLKGFGKDGFR/**FFTNFESR(Q)**/**K**/*GKELDSNPFA
SLVFYWEPLNRQVRVEGPKKLPEEEAECYFHSRPK/**SSQIGAVVSHQSSVIPDREYLR**/KKNEELEQLY
QDQEVPPKPSWGGYVLYPQVMEFWQGQTNRLLHDRVFRRLPTGDSPLGPMTHRGEEDWLYERLAP

Figure 4.48: Amino acid sequence of the PNPO protein. Predicted peptides produced upon tryptic digest and chosen for analysis shown in red. / = relevant tryptic digest sites. * =altered tryptic digest site in the presence of the p.R116Q variant.

Peptides both up and downstream of p.R116Q were chosen to allow the detection of an aberrant protein produced if the c.347 G>A substitution did affect splicing between exons 3 and 4 of PNPO (**Figure 4.48**). If this were the case and a truncated PNPO protein was created but not degraded, peptide 1 would be present but peptide 4 absent. Equally, two peptides (peptides 3 & 4) were chosen that lie at the site of the p.R116Q missense change. Since the amino acid to the C-terminal side of R116 is a lysine, in the presence of the p.R116Q variant, R116 is replaced by Q116 + K117 upon tryptic digestion. Theoretically, this would allow calculation of relative abundancies of wild-type and p.R116Q PNPO protein monomers (for example, in heterozygote carriers).

The liquid chromatography gradients and mobile phase compositions used within this section are described in **Section 2.7.2**. Where adjustments were made to these conditions, these are detailed below. Initially, a 10 minute reversed-phase liquid chromatography gradient using H₂O/acetonitrile with 0.1% formic acid as mobile

phases was used for analysis of the peptides. The column chosen was a Waters CORTECS UPLC C18+ column (1.6µm, 2.1 x 50 mm). Peptides 2, 3 and 4 were retained well on this column, eluting between 2.75 and 2.95 minutes. However, peptide 1 was not retained at all and eluted just <0.25 minutes after injection (**Figure 4.49 (a)**). This is not unexpected as the amino acid residues present in peptide 1 are more polar than those found in those of peptides 2, 3 and 4. Equally, peptide 1 has a particularly basic isoelectric point (pI) of 9.37 as predicted by the online Peptide Calculator tool (<http://www.pep-calc.com>).¹⁹⁷

Several steps were then taken to attempt to improve the retention of peptide 1. Firstly, the column was changed to the Waters Acquity UPLC HSS T3 column (1.8 µm, 2.1 x 50 mm). This column is specifically designed for the retention of polar compounds. The chromatography of each of the later eluting peptides was improved, leading to sharper peaks with improved signal intensity. However, effective retention of peptide 1 was not enabled (**Figure 4.49 (b)**). With compounds of an approximately neutral pI (such as peptides 2, 3 and 4 with pI's of 6.21, 6.20 and 7.12, respectively) further acidification of the mobile phase is a viable strategy to enable efficient retention. However, as a peptide with a basic pKa, this would act only to further charge peptide 1; no retention was seen upon an increased formic acid concentration of 0.2% (**Figure 4.49 (c)**).

Addition of 0.01% HFBA to the mobile phase however did enable retention of peptide 1 (**Figure 4.49 (d)**). As a strong acid, HFBA anions in solution interact with the positively charged peptides, neutralising them. This decreases their hydrophilicity and enables interaction with the hydrophobic C18 stationary phase. This technique is known as ion-pairing.

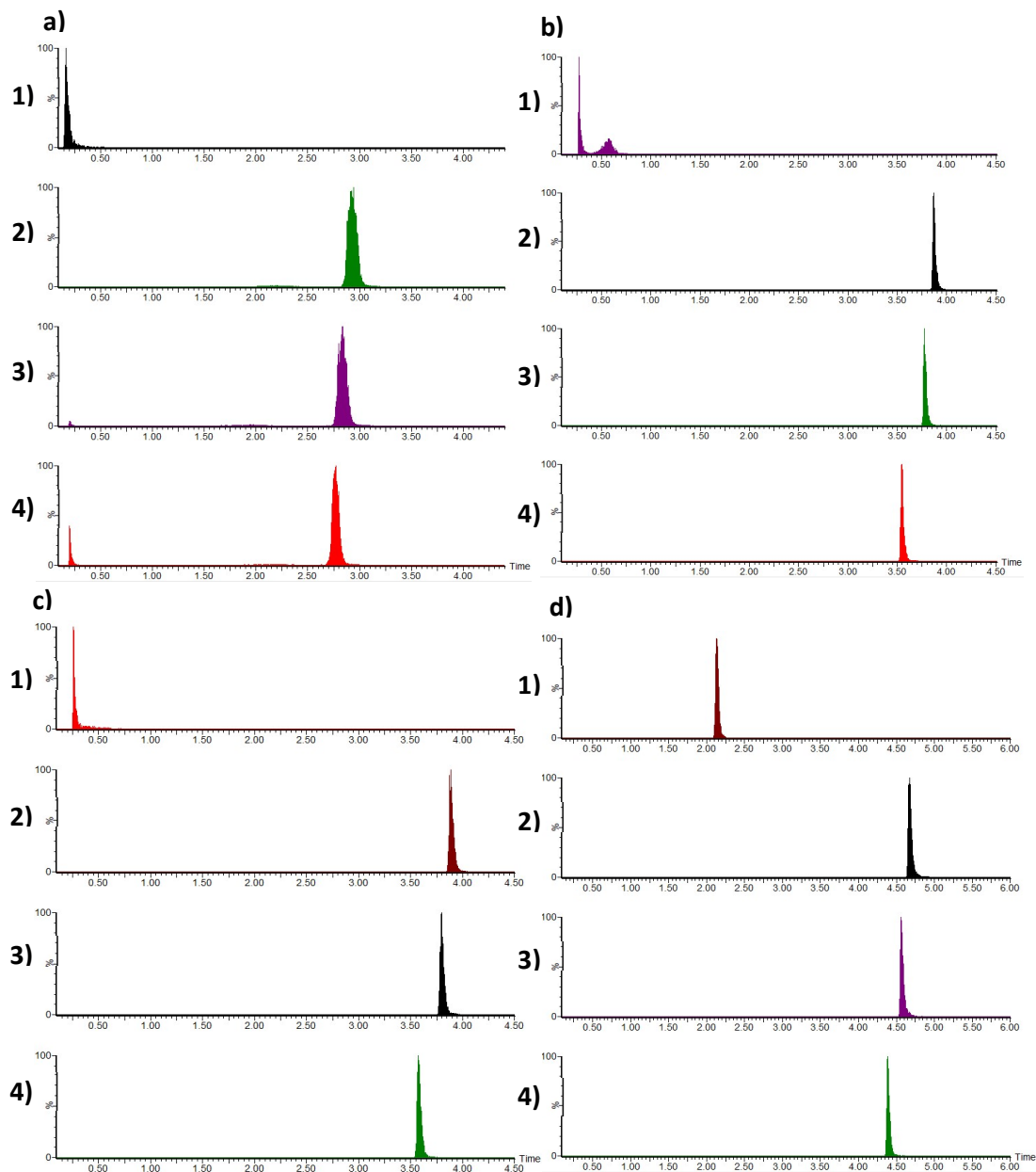


Figure 4.49: Chromatographic separation of peptides selected for UPLC-MS/MS detection from trypsin digested PNPO protein. Numbers 1-4 correspond to the peptides in **Table 4.6**. Conditions: **a)** Cortecs C18+ column, MPA: 0.1% FA in H₂O MPB: 0.1% FA in acetonitrile. **b)** HSS T3 column, MPA: 0.1% FA in H₂O MPB: 0.1% FA in acetonitrile. **c)** HSS T3 column, MPA: 0.2% FA in H₂O MPB: 0.2% FA in acetonitrile. **d)** HSS T3 column, MPA: 0.2% FA + 0.01% HFBA in H₂O MPB: 0.2% FA in acetonitrile. Liquid chromatography gradient used can be found in **Table 2.6**. FA = formic acid; HFBA = heptafluorobutyric acid.

4.2.3.2 Analysis of PNPO peptides in dried blood spots

The linearity of LC-MS/MS detection of the peptides was measured from 0.1 pmol/L – 150 pmol/L). With an injection volume of 10 μ L, the response was linear over this range ($R^2 > 0.99$).

The elution and tryptic digestion of peptides 1, 2, 3 and 4 derived from control DBS was performed using a previously optimised protocol (**Section 2.7.3**). A transition for the detection of a peptide pertaining to human serum albumin was also monitored (AVMDDFAAFVEK; MRM: 671.99 > 587.02) in addition to the optimised MRM transitions for peptides 1, 2, 3 and 4. Serum albumin is the most abundant plasma protein¹⁹⁸ and therefore should be easily identified, indicating successful digestion. The area of the peak identified upon LC-MS/MS analysis was used for quantification.

Peaks pertaining to peptides 1, 2, 3 or 4 could not be identified even though it had already been shown that PNPO protein was present in the DBS as PNPO activity had already been measured successfully (**Section 4.1.2**). Whilst it was possible to identify albumin, indicating that digestion was successful, sensitivity was poor; the signal from such an abundant protein should have been higher. Albumin had an area under peak value of 408 in the 2 punch digest and 1597 in the 4 punch digest. It was hypothesised that this was caused by ion suppression due to the sample matrix. To address this, desalting and removal of small compounds was performed by binding the peptides to a C18 solid-phase extraction column. By adjusting the organic/aqueous composition, salts and polar compounds are first eluted as a separate fraction, the compounds of interest are then analysed after elution in a fraction of interest.

After this procedure (see **Section 2.7.3**) analysis was repeated. Unfortunately, detection of PNPO specific peptides was still unsuccessful. When peptides 1, 2, 3 and 4 were spiked into the digest eluent from 2 DBS punches at 100 pmol/L, peaks were identified at the expected retention times, indicating that the inability to detect the peptides of interest was not due to dramatic changes in chromatography (e.g. retention time shift).

However, the areas under peaks from peptides 2, 3 and 4 when spiked at 100 pmol/L into the digest eluent of 2 DBS punches were only 7.6, 30.2 and 15.9% that of a pure 100 pmol/L standard with a sample matrix of 97% H₂O 3% ACN. This is an example of the effect of sample matrix on detection by LC-MS/MS. Conversely, the signal from peptide 1 was 43.4% higher than that in the H₂O:ACN standard. This could be an

example of ion enhancement but, since peptide 1 was also not detected in DBS, it did suggest that a factor other than ion suppression was the reason for non-detection of the PNPO-derived peptides.

A TCA acetone precipitation step was added prior to digestion. This was used to remove contaminants and highly abundant proteins such as albumin, theoretically aiding the detection of peptides derived from lower-abundancy proteins. In addition, 500 ng of recombinant p.R116Q and wild-type PNPO proteins (described in **Section 4.2.2**) were digested alongside DBS samples and 500 ng of the protein yeast enolase was added to all samples. Tryptic digestion of yeast enolase produces a well characterised peptide (SIVPSGASTGVHEALEMR; MRM: 614.6 > 547.9) and would act as a positive digestion control.

Table 4.7: Peptides detected from tryptic digests of DBS and spiked standards. Exp. = expected due to spiked protein or endogenous presence in DBS; Ident. = detection of the peptide at the correct retention time. YE = yeast enolase.

Composition	Human Serum Albumin		Yeast Enolase (YE)		PNPO Peptide 1		PNPO Peptide 2		PNPO Peptide 3		PNPO Peptide 4	
	Exp.	Ident	Exp.	Ident	Exp.	Ident	Exp.	Ident	Exp.	Ident	Exp.	Ident
0.5 µg YE + recombinant WT PNPO	×	×	✓	✓	✓	✓	✓	✓	×	×	✓	✓
0.5 µg YE + recombinant p.R116Q PNPO	×	×	✓	✓	✓	✓	×	×	✓	✓	✓	✓
4 x 3 mm DBS punches + 0.5 µg YE	✓	✓	✓	✓	✓	×	✓	×	×	×	✓	×
4 x 3 mm DBS punches + 0.5 µg YE + 0.5 µg recombinant WT PNPO	✓	✓	✓	✓	✓	✓	✓	✓	×	×	✓	✓
4 x 3 mm DBS punches + 0.5 µg YE + 0.5 µg recombinant p.R116Q PNPO	✓	✓	✓	✓	✓	✓	×	×	✓	✓	✓	✓

Several digestions were performed with varying combinations of recombinant protein, yeast enolase and 3 mm punches from dried blood spots (as shown in **Table 4.7**). Target peptides from yeast enolase and albumin were successfully detected in all samples, indicating that tryptic digestion was successful. In samples containing recombinant wild-type and p.R116Q PNPO protein, the expected peptides were identified (Peptide 1, 2 and 4 in wild-type; Peptide 1, 3 and 4 in p.R116Q PNPO).

However, it is important to note that the LC-MS/MS signal and therefore abundance of these peptides was very low (**Figure 4.50**). Poorly resolved and uneven peaks suggest a signal close to the lower detection limit of the LC-MS/MS instrumentation.

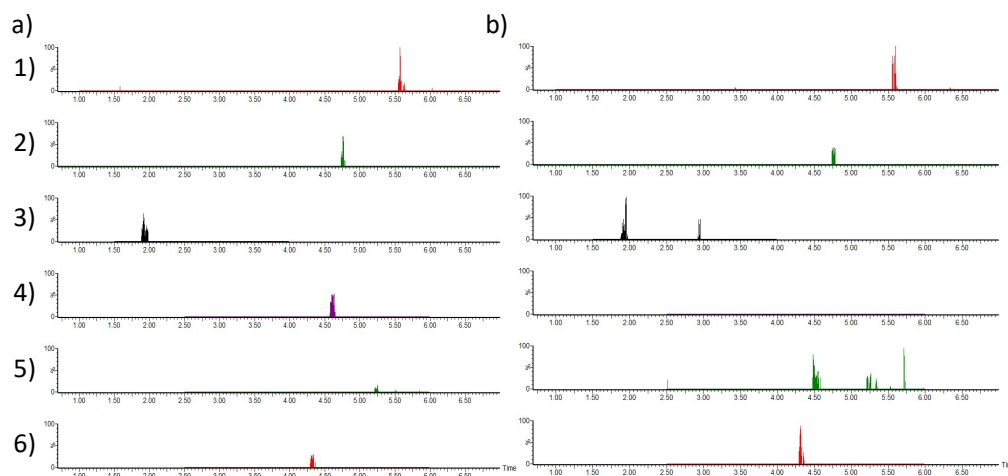


Figure 4.50: Examples of chromatograms obtained upon LC-MS/MS analysis of DBS digests spiked with a) wild-type and b) p.R116Q recombinant PNPO protein. Chromatograms: **1)** Albumin - AVMDDFAAAFVEK; MRM: 671.99 > 587.02; RT 5.2 min **2)** Yeast enolase - SIVPSGASTGVHEALEMR; MRM: 614.6 > 547.9; RT 4.75 min **3)** PNPO Peptide 1 – DGKPSAR; MRM: 365.94 > 430.42; RT 1.9 min **4)** PNPO Peptide 2 – FFTNFESR; MRM: 524.31 > 753.65; RT 4.6 min **5)** PNPO Peptide 3 – FFTNFESQK; MRM: 574.43 > 267.27; RT 4.5 min **6)** PNPO Peptide 4 – SSQIGAVVSHQSSVIPDR; MRM: 623.22 > 726.81; RT 4.4 min.

Despite the addition of a TCA acetone precipitation step, peptides 1-4 were not detected in 4 x 3 mm DBS punches from a healthy adult control. This was not improved by an increase in injection volume from 10 to 20 μ L (**data not shown**). Two additional steps were taken in order to improve the LC-MS/MS signal: i) HFBA was removed from the mobile phase. ii) The liquid chromatography gradient was extended to a 45 minute method from the 10 minute method used previously. The removal of HFBA from the mobile phase meant that peptide 1 would no longer be quantifiable but, since HFBA can cause ion suppression¹⁹⁹, it was possible that detection of peptides 2, 3 and 4 would be enabled. The extension of a reversed-phase LC-MS/MS method can improve sensitivity as fewer compounds will co-elute with analytes of interest, reducing ion suppression.

These steps were successful in increasing the signal derived for the peptides of interest. For example, the area under curve (AUC) of peptide 2 detected from the digest containing 4 x 3 mm DBS punches with 500 ng yeast enolase and recombinant

wild-type PNPO increased from 263 > 881 > 4525 with the removal of HFBA and the 45 minute method extension, respectively.

Despite these further optimisations, no signal specific for the endogenous peptides of interest was detected in DBS that had not been spiked with recombinant PNPO. It is possible that with larger volumes of concentrated blood this would be a viable assay. However, these were not available from the patients of interest.

4.3 Discussion & future work

The formulation of a PNPO assay using dried blood spots, as described here, exemplifies the importance of careful consideration of a multitude of factors such as substrate type, reaction buffer composition and incubation time when developing a diagnostic enzyme assay. A complicating factor in this case was the effect of supraphysiological vitamin B₆ concentrations in patients receiving B₆ for seizure treatment. Despite this, success was achieved and the development of an enzyme assay for the detection of PNPO deficiency from dried blood spots will prove a valuable tool for the rapid diagnosis of this disorder in infants and young children.

This assay is the first specific and reliable biochemical test for PNPO deficiency viable for use in the modern clinical environment and has since been published in *Analytical Chemistry*.⁸⁹ It is likely that the test can be used in conjunction with the measurement of B₆ vitamers from DBS (**Section 3**) for the biochemical diagnosis of PNPO deficiency. For example, vitamer concentrations (specifically PNP/PLP ratio) could be useful in cases in which borderline PNPO activity is measured using the DBS enzyme assay. This analysis may be particularly valuable as both tests can be carried out from the same DBS sample.

It is becoming increasingly apparent that even in the genomic era the pathogenicity of genetic variants identified must be assessed in order to provide a definitive diagnosis. Within the field of metabolic disorders the most effective and conclusive technique with which to do this is biochemical testing. Despite this, complications and paradoxes may be identified – this is apparent in the case of the p.R116Q variant in PNPO.

Although it was found that the enzymatic characteristics of recombinant p.R116Q protein appear to differ little from those of the wild-type protein, it is known that some individuals present with the B₆-dependent seizures characteristic of PNPO deficiency. Equally, no PNPO activity was detected in dried blood spots from these patients. The identification of differences in activity when the FMN cofactor was limited suggested that conformational changes upon cofactor binding or the cofactor binding itself could be pathological in these patients. Since this work was performed, other groups have also identified substantial differences in the thermal stability of wild-type and p.R116Q protein. If the levels of p.R116Q PNPO protein are held in a delicate balance in these patients they could be particularly susceptible to deficiencies of vitamins B₆ or B₂.

PNPO activity could also vary on a tissue-specific basis. Indeed, this would provide an explanation for the undetectable activity identified in the dried blood spots of asymptomatic p.R116Q homozygous individuals.

Although the activity of recombinant p.R116Q protein towards different substrates (i.e. PNP and PMP) was characterised, a direct comparison was not made using DBS from p.R116Q homozygotes. Ideally in the future this should be investigated as it is possible that activity towards PMP is retained in DBS despite no measurable conversion of PNP to PLP.

Unfortunately, it was not possible to detect PNPO protein in dried blood spots by LC-MS/MS analysis of peptides derived from this tryptic digestion. The detection of peptides derived from trypsin digestion of proteins is affected by factors such as digestion efficiency²⁰⁰ and matrix effects specific to each protein/peptide.²⁰¹ Future studies would prioritise the use of larger sample volumes to facilitate the detection of PNPO-derived peptides. In addition, a wider range of peptides could be chosen for analysis as it is possible that those chosen were not present in high enough concentrations to allow detection due to, for example, poor digestion efficiency. It is possible that additional work such as further sample clean-up steps or other techniques such as high resolution mass spectrometry would allow quantification of PNPO expression in blood, or other tissues. A technique such as 2D-gel electrophoresis prior to digestion could provide a 'clean fraction' of PNPO protein for LC-MS/MS analysis, but this would require a sample type with more volume than DBS.²⁰² It would be important as part of future work to better characterise the tissue-specific expression of PNPO protein and whether the presence of the p.R116Q is a modifier in this process.

As a relatively common variant with an allele frequency of 0.0547, it is possible that p.R116Q is an important modifier of epilepsy. If PLP or PN, relatively inexpensive and safe medications, could be used as an adjunct to the treatment of seizures it would be an important development in epileptology. Furthermore, if PLP or PN were known to be more effective in individuals hetero/homozygous for p.R116Q, this would be an example of a potential use of NGS data for the specific and personalised treatment of individuals on a case-by-case basis. In the near future, with the continuing decrease in price and widespread adoption of NGS, this will become increasingly feasible – the difficulty comes with interpreting the data collected.

5. BIOCHEMICAL CHARACTERISATION OF A NOVEL NEUROPATHY CAUSED BY DEFICIENCY OF PYRIDOXAL KINASE

Inherited peripheral neuropathies (Charcot-Marie-Tooth [CMT] disease) are relatively common neuromuscular disorders, affecting 0.04% of the population.²⁰³ However, treatment is currently symptomatic²⁰⁴⁻²⁰⁵ and the genetic basis of CMT is identified in only a quarter of cases.²⁰⁶ The mechanisms behind CMT are unclear but defects are often found in genes encoding proteins involved in axonal transport and the cytoskeleton.²⁰⁷ Peripheral neuropathy may also occur with other pathologies in inborn errors of metabolism presenting in childhood.

In collaboration with the UCL Institute of Neurology, we have recently identified three siblings with early-onset sensorimotor, axonal, peripheral neuropathy as well as adult-onset optic atrophy (**Subjects PK1, 2 and 3**). All three siblings reported disabling peripheral neuropathy from early childhood followed by optic atrophy later in life. **Subject PK1** (79 years old) was wheelchair bound and **Subject PK2** (74 years old) also had limited mobility, requiring assistance in order to walk. **Subject PK3** was deceased at the time of this study.

Historically, considerable genetic and biochemical investigations were carried out on these individuals but failed to identify any known specific cause for their disorder, this is described by Chalmers *et al.*²⁰⁸

More recently, collaborators performed whole genome sequencing on these patients. When filtered according to variants that segregated with the disease, a homozygous p.A228T variant in the *PDXK* gene, encoding pyridoxal kinase (PK), was identified. PK is the enzyme responsible for phosphorylation of the B₆ vitamers pyridoxine, pyridoxamine and pyridoxal, making it integral for maintaining an adequate supply of pyridoxal 5'-phosphate (PLP), the active cofactor form of vitamin B₆.²⁰⁹

Typically, disorders of vitamin B₆ metabolism lead to early-onset epileptic encephalopathy responsive to high doses of vitamin B₆.^{2, 4} The individuals identified with the p.A228T variant in PK had not reported seizures as a feature of their disorder, an unexpected finding. It was deemed important to characterise the effect of p.A228T on the function of PK biochemically.

Although other inborn errors of vitamin B₆ metabolism haven't been linked to peripheral neuropathies, there are known situations in which perturbation of normal B₆ homeostasis can lead to this disorder. For example, extremely high doses of pyridoxine are known to cause neuropathy.¹¹⁰ In addition, the tuberculosis medication isoniazid^{109, 210}, 4'-O-methyl pyridoxine (ginkgotoxin)²¹¹ and respiratory medication

theophylline¹⁰⁸ are each known to cause peripheral neuropathy. The proposed mechanism for this effect is thought to be PLP deficiency through either inactivation of PLP or inhibition of PK.²¹²⁻²¹⁴

Studies by collaborators showed that the levels of PK protein in fibroblasts homozygous for the p.A228T variant were similar to those in wild-type fibroblasts. This indicated that any conformational change induced by the p.A228T variant did not cause instability or degradation of the protein; alteration of PK enzymatic activity was therefore the more likely pathogenic mechanism, if it was indeed pathogenic.

This chapter describes the development and utilisation of an LC-MS/MS-based enzyme assay from bacterially-prepared recombinant PK protein to assess the effect of p.A228T on the enzymatic activity of PK. In addition, the development of an assay for measurement of PK activity in dried blood spots is described. These DBS were collected from individuals homozygous for A228T-PK in order to assess the *in vivo* effect of the variant identified.

5.1 Investigation of the *in vitro* effect of p.A228T on the enzyme kinetics of recombinant pyridoxal kinase

In the diagnosis of inborn errors of metabolism there is an ever-present need to assess the pathogenicity of genetic variants identified, particularly as novel variants are identified by next generation sequencing (NGS). *In-silico* assessment of p.A228T indicated that the variant was not expected to be pathogenic; it was predicted tolerated/benign by SIFT/Polyphen, respectively. Although alanine (A) and threonine (T) belong to different amino acid classes (A = aliphatic; T = polar neutral), their structures are relatively similar. **(Figure 5.1 (a)).**

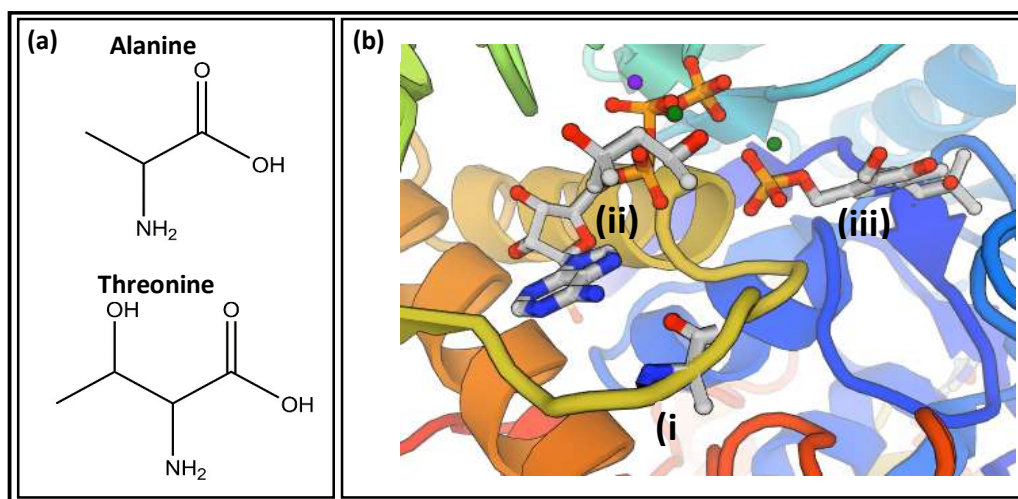


Figure 5.1: (a) Structures of the amino acids alanine and threonine (b) Predicted structure of the PK active site. Positions of the (i) A228 residue (ii) ATP binding site and (iii) PL/PLP binding site are indicated (PLP & ATP shown bound). Positions of divalent cations (Mg^{2+}) shown as green circles. Monovalent cation (K^+) shown as a purple circle. Adapted from the crystal structure determined by Gandhi *et al.* 2012 and stored in the swissmodel.expasy.org repository.

Despite this *in silico* prediction, evidence such as an autosomal recessive inheritance pattern and the aforementioned link between disrupted vitamin B₆ metabolism and peripheral neuropathy meant that biochemical characterisation of p.A228T was warranted. In addition, the structure of pyridoxal kinase, as predicted by X-ray crystallography²¹⁴, shows the A228 residue is present at the active site, close to the ATP binding pocket but not interacting directly with ATP itself **(Figure 5.1 (b))**. One could, therefore, hypothesise that p.A228T may effect ATP binding and the catalytic

activity of PK. Furthermore, plasma PLP concentrations below the normal range were identified in the two siblings studied (7.5 and 9 nmol/L; normal range: 15 - 73 nmol/L)

Similar methodology to that used in **Section 3.2** was used to study the kinetics of pyridoxal kinase and specifically the effect of the p.A228T substitution. This experimentation was carried out using bacterially-expressed human recombinant protein, prepared by collaborators.

5.1.1 The effect of pyridoxal concentration on enzyme activity

Experiments were performed by incubating 100 ng recombinant wild-type and p.A228T PK protein for 10 minutes in a 20 mmol/L potassium phosphate buffer, pH 6.1 containing 300 $\mu\text{mol/L}$ MgCl_2 , 300 $\mu\text{mol/L}$ ATP. These conditions had been previously used by di Salvo *et al.* for the assay of recombinant pyridoxal kinase.²¹⁵ As discussed in **Section 3.1**, PK requires both a monovalent and divalent cation for optimal activity (in this case K^+ and Mg^{2+}) and has an optimal pH from 6 – 7.¹⁷⁶ Di Salvo *et al.* suggested that pH 6.1 was the optimal pH and the K_m of pyridoxal approximately 30 $\mu\text{mol/L}$.²¹⁵ The pyridoxal concentration was therefore varied between 0 – 100 $\mu\text{mol/L}$.

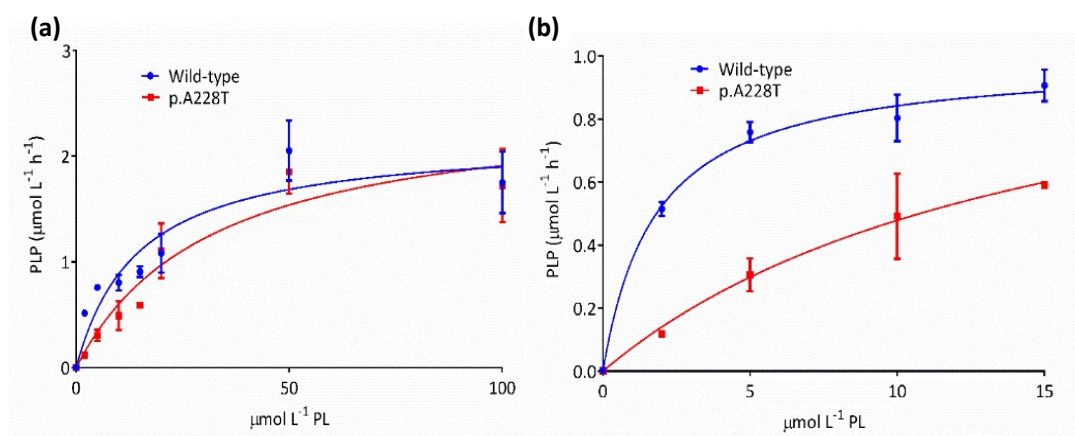


Figure 5.2: Effect of pyridoxal concentration on pyridoxal kinase activity. K_m for PL: WT = 14.5 $\mu\text{mol/L}$; p.A228T = 31.9 $\mu\text{mol/L}$ as calculated from the nonlinear fit of PLP formation. Conditions: 20 mmol/L potassium phosphate pH 6.1; 0 - 100 $\mu\text{mol/L}$ PL; 300 $\mu\text{mol/L}$ MgCl_2 ; 300 $\mu\text{mol/L}$ ATP; 37°C; 10 minute incubation. Error bars indicate SEM. (n = 3 at each point). (a) is a nonlinear fit of PLP formation between 0 – 100 $\mu\text{mol/L}$ PL; (b) is a nonlinear fit of PLP formation between 0 – 15 $\mu\text{mol/L}$ PL.

Figure 5.2 (a) shows the dependence of PK activity on pyridoxal concentration as measured by pyridoxal phosphate formation after a 10 minute incubation period, represented by plotting reaction velocity ($\mu\text{mol/L/h}$) against the substrate concentration. As 100 ng PK protein was added to each solution, the reaction velocity can also be expressed as nmol/mg protein/h using a conversion factor of $\times 2.4$ (e.g. $1 \mu\text{mol/L/h} = 2.4 \text{ nmol/mg/h}$). K_m values were calculated as the substrate concentration at half the maximum velocity of reaction (i.e. at saturating substrate concentrations). A K_m of $14.5 \mu\text{mol/L}$ was determined for wild-type protein and a K_m of $31.9 \mu\text{mol/L}$ for the p.A228T PK protein. This indicates a two-fold lower catalytic efficiency in the presence of p.A228T. At low pyridoxal concentrations ($0 - 15 \mu\text{mol/L}$) the difference in PLP formation was particularly pronounced (**Figure 5.2 (b)**). This is important as physiological concentrations of free pyridoxal are likely to be in the nanomolar range.¹⁵⁹

5.1.2 Effect of adenosine 5'-triphosphate on enzyme activity

Given the proximity of the A228 amino acid residue to the ATP binding site of PK, it was hypothesised that p.A228T would have a greater impact on ATP kinetics than pyridoxal kinetics. Recombinant PK was incubated with ATP ($0 - 500 \mu\text{mol/L}$) and $10 \mu\text{mol/L}$ pyridoxal in initial experiments. Unless mentioned, other conditions were the same as those described in **Section 5.1.1**.

Figure 5.3 (a) shows the dependence of PK activity on ATP concentration. The K_m of wild-type PK was approximately ten times lower than that of p.A228T protein ($4.4 \mu\text{mol/L}$ vs $41.5 \mu\text{mol/L}$). The p.A228T variant therefore has a greater effect on ATP binding than on PL binding, where only a two-fold difference in K_m could be identified. Similarly to experiments investigating PL, the effect at low ATP concentrations was particularly pronounced (**Figure 5.3 (b)**).

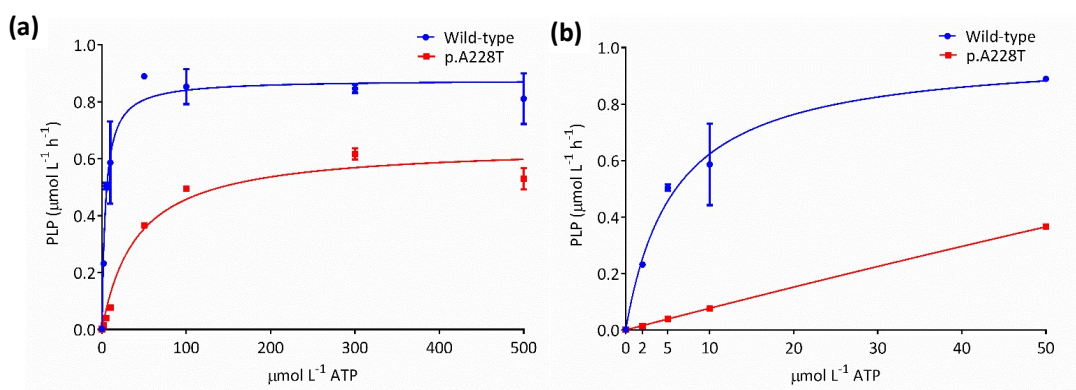


Figure 5.3: Kinetics of recombinant PK protein when varying ATP concentration. K_m of ATP: WT = 4.4 μmol/L; p.A228T = 41.5 μmol/L as calculated from the nonlinear fit of PLP formation. Conditions: 20 mmol/L potassium phosphate pH 6.1; 10 μmol/L PL; 300 μmol/L MgCl₂; 0 – 500 μmol/L ATP; 37°C; 10 minute incubation. Figure 5.3 (a) is a nonlinear fit of PLP formation between 0 – 500 μmol/L ATP; Figure 5.3 (b) is a nonlinear fit of PLP formation between 0 – 50 μmol/L ATP. Error bars indicate SEM. (n = 3 at each point).

In order to expand upon the data shown in **Figure 5.3**, two alterations were made in subsequent experimentation. Firstly, the pyridoxal concentration was increased to 50 μmol/L as 10 μmol/L was lower than the K_m identified. This concentration of PL saturates the protein whilst concentrations higher than this introduced inhibition (approximately 15% lower activity at 100 μmol/L compared to 50 μmol/L PL). The second modification was to increase the MgCl₂ concentration to 3 mmol/L in order to ensure that all ATP was in its Mg-bound form. The phosphotransfer from ATP to substrate is dependent upon ATP binding to Mg; this neutralises negative charges on the polyphosphate chain.^{214, 216} Indeed, ATP affinity for Mg is extremely high and *in vivo* there is usually very little free ATP present in the cell.²¹⁷ Previous studies have shown that physiologically, MgATP is the most important cation-ATP complex utilised by the PK enzyme.¹⁷⁶

Figure 5.4 shows the effect of ATP concentration on pyridoxal kinase activity measured by PLP formation in the presence of 50 $\mu\text{mol/L}$ pyridoxal and 3 mmol/L MgCl_2 . Intriguingly, the V_{max} of p.A228T PK protein was higher than that of wild-type protein (p.A228T = 2.1 $\mu\text{mol/L/h}$; WT = 1.0 $\mu\text{mol/L/h}$).

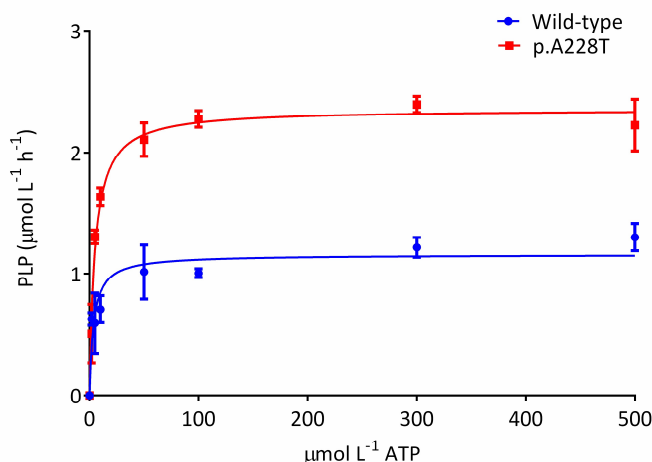


Figure 5.4: Kinetics of recombinant PK protein when varying ATP concentration in the presence of an excess of MgCl_2 and PL. V_{max} : WT = 1.16 $\mu\text{mol/L/h}$; p.A228T = 2.36 $\mu\text{mol/L/h}$. K_m : WT = 3.7 $\mu\text{mol/L}$; p.A228T = 4.8 $\mu\text{mol/L}$ as calculated from the nonlinear fit of PLP formation. Conditions: 20 mmol/L potassium phosphate pH 6.1; 50 $\mu\text{mol/L}$ PL; 3 mmol/L MgCl_2 ; 0 – 500 $\mu\text{mol/L}$ ATP; 37°C; 10 minute incubation. Error bars indicate SEM. (n = 3 at each point).

In human¹⁷⁶, *T. Bruce*²¹⁸ and *E. Coli*²¹⁹ PK, different divalent cations (Mg^{2+} , Zn^{2+} and Mn^{2+}) have been shown to affect PK activity in different ways. It is possible that the structural alteration of human PK caused by p.A228T could raise the K_m of Mg^{2+} , hence increasing activity in the conditions used in **Figure 5.4**. Additional work is required to confirm this hypothesis. The K_m of p.A228T protein with PL as substrate was still higher at 4.8 $\mu\text{mol/L}$ compared to 3.7 μmol for wild-type protein.

Studies on the enzyme kinetics of pyridoxal kinase have been carried out by varying Mg^{2+} and ATP concentrations independently²¹⁸ or by varying MgATP concentration.²¹⁵ In the work shown in **Figures 5.3 and 5.4**, Mg^{2+} concentrations were kept constant at either 0.3 or 3 mmol/L , respectively. However, this was added in the form of MgCl_2 and was not adjusted alongside the variation in ATP concentration.

Next, MgATP was varied from 0 – 500 $\mu\text{mol/L}$, while keeping other parameters identical (**Figure 5.5**); sigmoidal enzymes kinetics were clearly identified. This was unexpected, upon the variation of only one substrate (of the two used, pyridoxal and ATP) standard Michaelis-Menten kinetics were predicted. Indeed, studies by other groups using MgATP had shown Michaelis-Menten kinetics. However, due to the increased sensitivity of this LC-MS/MS-based method, we were able to detect activity at far lower MgATP concentrations than the 50 - 800 $\mu\text{mol/L}$ previously used when studying MgATP kinetics. It is possible that other groups were unable to detect the sigmoidal relationship observed in our data.

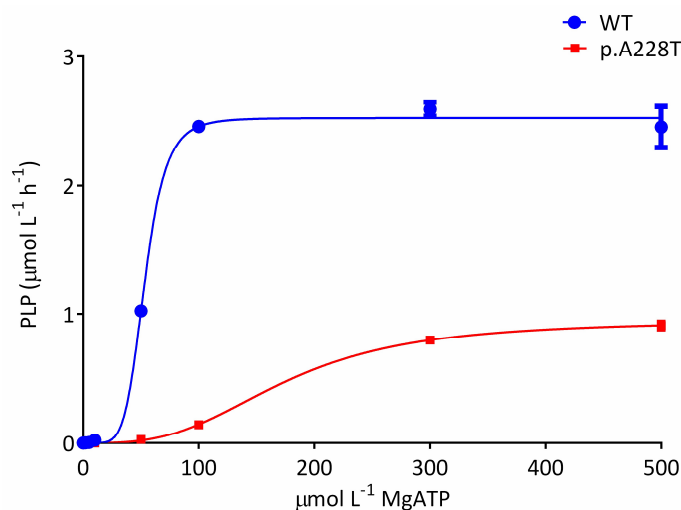


Figure 5.5: Sigmoidal kinetics of recombinant PK protein using MgATP as substrate. V_{max} : WT = 2.52 $\mu\text{mol/L/h}$; p.A228T = 0.95 $\mu\text{mol/L/h}$. K_{half} : WT = 53.4 $\mu\text{mol/L}$; p.A228T = 174.4 $\mu\text{mol/L}$ as calculated from the sigmoidal fit of PLP formation, shown in this graph when plotting velocity ($\mu\text{mol/L/h}$) against substrate concentration ($\mu\text{mol/L}$). Conditions: 20 mmol/L potassium phosphate pH 6.1; 50 $\mu\text{mol/L}$ PL; 0 - 500 $\mu\text{mol/L}$ MgATP; 37°C; 10 minute incubation. Error bars indicate SEM. (n = 3 at each point). K_{half} = the concentration of substrate that produces half the maximum enzyme velocity.

In addition, an assumption was made that the concentrations of Mg^{2+} and ATP in the purchased MgATP compound were equimolar. It is possible that, if excess Mg^{2+} was present in the MgATP complex, the variation in Mg^{2+} and ATP concentration was not equal across the range tested. If Mg^{2+} and ATP were equimolar, Mg^{2+} should be 4.8% of the total weight of the MgATP sourced from Sigma-Aldrich (Product number A9187). However, the product specification showed that Mg^{2+} ions constituted anywhere from 2.5 – 13.5% of the total weight of the product (measured by ICP-MS) meaning assumptions could not be made according to the exact proportion of Mg^{2+} contained therein.

This is also complicated by the fact that, as previously mentioned, two Mg^{2+} ions are shown bound at the active site of PK, one stabilising the β and γ phosphates of ATP and another at the 5'-phosphate of PLP.²¹⁴ It could be hypothesised that Mg^{2+} is important in releasing PLP from the active site after the completion of a catalytic cycle. It is certainly critical for the neutralisation of negative charges during phosphotransfer. Alterations in the molarity of Mg^{2+} ions in solution could affect the observed enzyme kinetics by altering these processes.

The K_{half} and V_{max} for MgATP both indicate reduced activity of the p.A228T enzyme, in accordance with previous results in **Figures 5.3 and 5.4** (Wild-type: $K_{half} = 53.4 \mu\text{mol/L}$; $V_{max} = 2.5 \mu\text{mol/L/h}$, p.A228T: $K_{half} = 174.4 \mu\text{mol/L}$; $V_{max} = 0.9 \mu\text{mol/L/h}$. However, *in vivo*, intracellular free ATP concentrations are usually in the low mmol/L range²²⁰, saturating concentrations for the pyridoxal kinase enzyme. This would make the more dramatic reduction in activity seen at low ATP concentrations unimportant *in vivo*.

In conclusion, PK protein carrying the p.A228T variant, although still capable of the enzymatic conversion of PL to PLP, showed alterations in enzyme kinetics consistent with reduced catalytic activity.

5.2 The effect of p.A228T on the activity of pyridoxal kinase in red blood cells

In order to confirm the potential pathogenicity of the p.A228T variant, PK activity was measured *in vivo* using dried blood spot (DBS) samples taken from control individuals and the patients in whom the variant was identified.

Previous assays have been used to measure PK activity from erythrocytes.^{38, 178, 221-222} However, these assays used washed red blood cells separated from plasma in a relatively complex procedure and/or radioactive substrates. The simplicity of sample collection and volume in DBS is an advantage, as discussed in **Section 4**.

It was already shown in **Section 4** that pyridoxal kinase activity was measurable from a 3 mm dried blood spot (DBS) as the first step of a coupled PN>PNP>PLP enzyme assay. When designing this new PK assay, the choice of substrate was considered. It was postulated that the best method for the sole measurement of PK activity from DBS would be the quantification of pyridoxal 5'-phosphate (PLP) formation on incubation with pyridoxal (PL). If either of the other two physiological substrates (PN or pyridoxamine (PM)) were used, an added complication would be conversion of their phosphorylated products (PNP or pyridoxamine 5'-phosphate (PMP), respectively), to PLP by the PNPO enzyme. Quantification of PLP formation was carried out using the same LC-MS/MS method described elsewhere (**Section 2.4**).

5.2.1 Method development

The protocol developed for measuring PK activity measurement was an adaptation of the previously developed coupled PNPO enzyme assay described in **Section 4**. Alterations were made to the buffer type as well as the substrate, as described below. Two 3 mm DBS punches were placed in 60 µL 40 mmol/L potassium phosphate buffer pH 6.1 and sonicated for 2 minutes before the addition of 60 µL reaction buffer containing 300 µmol/L ATP & MgCl₂ or 300 µmol/L MgATP and 10 µmol/L pyridoxal. 120 µL of a 0.3 N TCA reaction stop mix was then added immediately to the T0 tube and to the other reaction tubes after their allotted incubation time. Samples were then left on ice for 45 minutes prior to sonication for 5 minutes and then centrifuged at 14,000 *g* for 10 minutes. The supernatant was taken for analysis.

The buffer used was similar to that optimised for the study of recombinant PK protein, and that using the coupled PK/PNPO assay; 300 $\mu\text{mol/L}$ MgCl_2 and 300 $\mu\text{mol/L}$ ATP (or 300 $\mu\text{mol/L}$ MgATP) had previously been shown to saturate the PK enzyme in **Section 5.1**. 10 $\mu\text{mol/L}$ pyridoxal was chosen as the substrate concentration based on the K_m of wild-type recombinant PK protein for pyridoxal. This pyridoxal concentration had also been used by Kark *et al.* for the assay of PK activity from haemolysates.²²² Previous experiments (**Section 5.1**) utilising recombinant PK protein showed that the activities of WT and p.A228T PK enzyme were readily distinguishable at this concentration. Saturating PL concentrations would be less representative of physiological conditions as PL concentrations are in the nanomolar range *in vivo*.

In order to optimise the incubation time, a 3 mm DBS punch from an adult control was incubated over a 30 minute period. PLP formation was linear ($R^2 = 0.99$) over this time period (**Figure 5.6**). A 10 minute incubation period was therefore used for all subsequent experiments. PLP formation was measured by subtracting the PLP from the T0 punch from that in the T10 punch and expressed as pmol PLP/DBS/h.

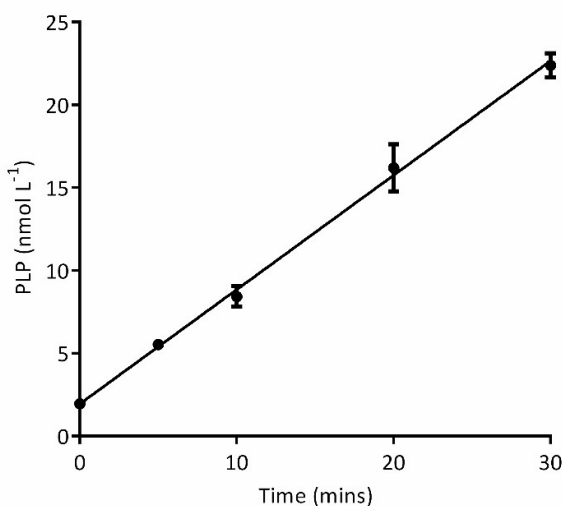


Figure 5.6: Pyridoxal kinase activity in a 3 mm DBS. Conditions: 20 mmol/L potassium phosphate pH 6.1; 10 $\mu\text{mol/L}$ PL; 300 $\mu\text{mol/L}$ MgATP ; 37°C. $R^2 = 0.99$. Error bars indicate SEM. (n = 3 at each point).

5.2.2 Analysis of patient samples

An initial experiment was carried out using 3 mm DBS punches from the two p.A228T homozygote siblings (**Subjects PK1 and PK2**) and the p.A228T heterozygote daughter (**Subject PKHET1**) of **Subject PK1**. Also analysed were DBS from the 78-year-old spouse of **Subject PK1** and three healthy adult controls (**Figure 5.7**). Reduced PK activity was evident in **Subjects PK1 and PK2**; 1.3 and 2.7 pmol/DBS/h, respectively. The PK activity of the spouse of **Subject PK1** and 3 healthy controls ranged from 12.4 to 20.7 with a mean of 15.4 pmol/DBS/h. The heterozygote daughter of **Subject PK1** had an intermediate activity of 6.6 pmol/DBS/h. Importantly, a small amount of residual activity was detected for the individuals homozygous for p.A228T, which correlated with *in vitro* experimentation showing that p.A228T protein retains some ability to catalyse PLP formation from pyridoxal.

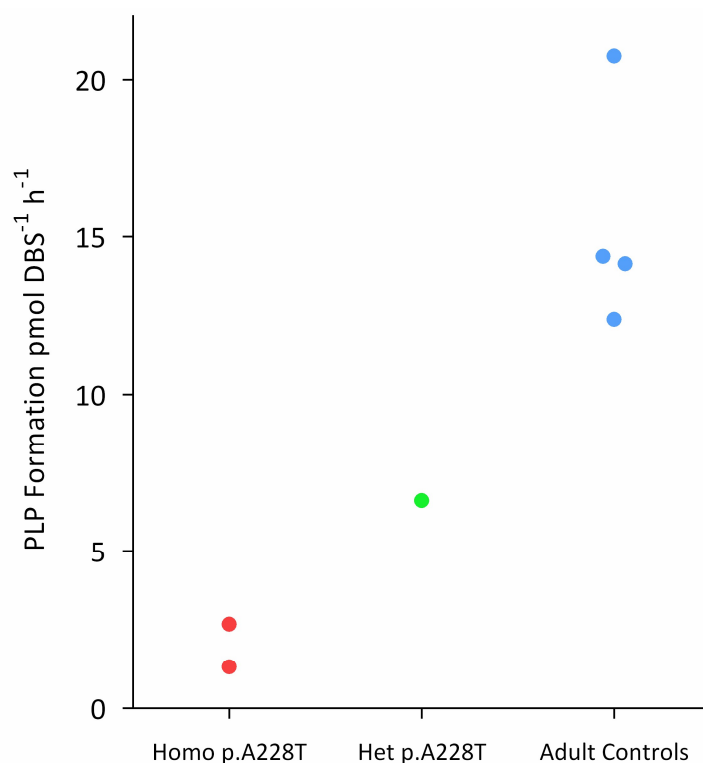


Figure 5.7: Preliminary pyridoxal kinase assay from DBS indicated reduced PK activity in p.A228T individuals. Conditions: 20 mmol/L potassium phosphate pH 6.1; 10 $\mu\text{mol/L}$ PL; 300 $\mu\text{mol/L}$ MgCl_2 300 $\mu\text{mol/L}$ ATP; 37°C. PK activities: Subjects PK1 and PK2 = 1.3 and 2.7 pmol/DBS/h; heterozygous p.A228T = 6.6 pmol/DBS/h; mean of 4 adult controls = 15.5 pmol/DBS/h. (n = 3 at each point).

In order to confirm the low blood PK activity of **Subjects PK1 and PK2**, DBS were collected from 22 adults whose ages ranged from 15 – 92 years (**Table 5.1**). These were individuals attending an outpatient's clinic of the National Hospital for Neurology and Neurosurgery, London, UK. Samples were retrieved from individuals with varying ethnicities as published work has shown lower PK activity in blood samples from African Americans compared to White Americans.²²¹

Table 5.1: Summary of control and affected subjects collected for DBS pyridoxal kinase activity analysis. PKC21 is the wife of subject PK1. Subjects PK1 and PK2 are siblings. Subject PKHET1 is the daughter of subject PK1 and Subject PKC21.

Subject	Age	Gender	Ethnicity	PK activity in DBS (pmol/DBS/h)
PKC1	25	Female	African	4.4
PKC2	50	Female	Caucasian	9.1
PKC3	71	Female	Indian	4.2
PKC4	50	Female	Caucasian	4.2
PKC5	49	Female	Caucasian	7.8
PKC6	48	Male	Caucasian	8.7
PKC7	30	Male	Caucasian	6.0
PKC8	70	Female	Caucasian	9.0
PKC9	35	Female	East Asian	5.4
PKC10	27	Male	Caucasian	12.3
PKC11	52	Female	African	2.6
PKC12	71	Female	Caucasian	10.1
PKC13	92	Male	Caucasian	9.8
PKC14	55	Male	South Asian	7.7
PKC15	15	Male	Caucasian	7.7
PKC16	64	Female	Caucasian	7.6
PKC17	56	Male	Caucasian	5.9
PKC18	38	Female	Caucasian	11.7
PKC19	31	Male	Arabic	14.7
PKC20	34	Male	Caucasian	10.1
PKC21	78	Female	Cypriot	9.0
PK p.Ala228Thr homozygous				
PK1	79	Male	Cypriot	1.1
PK2	74	Female	Cypriot	0.9
PK p.Ala228Thr/WT				
PKHET1	52	Female	Cypriot	4.9

PK activity for each of these individuals was measured (**Figure 5.8**). Controls (n = 22) had activities ranging from 2.6 – 14.7 pmol/DBS/h (mean = 8.2 pmol/DBS/h). This wide variety in activity has been identified previously.²²¹ The two individuals of African descent in our control cohort had relatively low activities of 2.6 and 4.5 pmol/DBS/h.

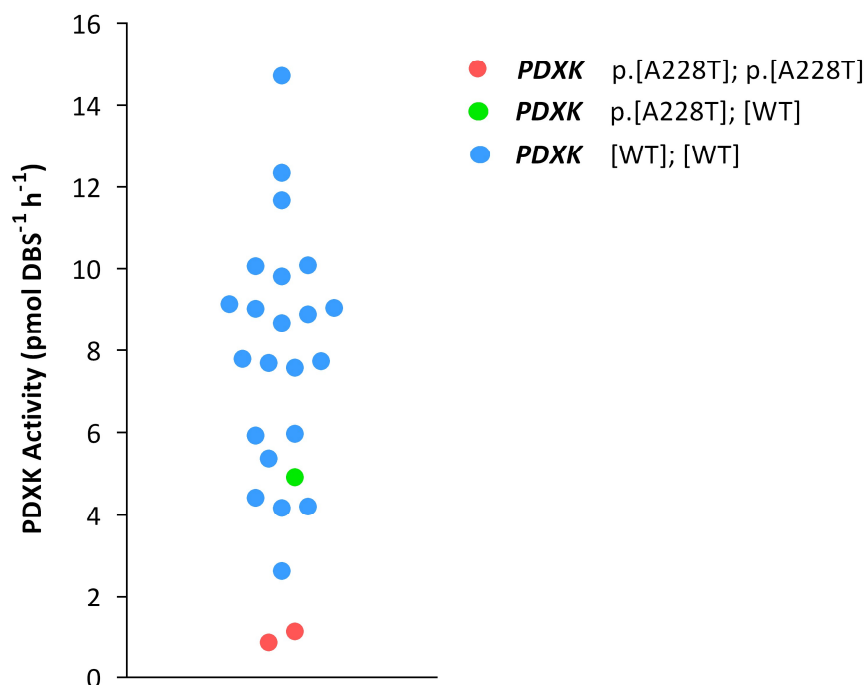


Figure 5.8: Pyridoxal kinase activities in controls and subjects PKHET1, PK1 and PK2. A non-parametric Mann-Whitney test was carried out to compare the two p.A228T individuals to controls and a significant difference was identified ($p = 0.0072$). Each point is the mean of the analysis of 2 separate DBS.

Published work measuring PK activity in haemolysates using both pyridoxal²²² and [³H]pyridoxine^{38, 40, 221} as substrates has reported activities of 30 - 120 nmol PLP/gHb/h. If each DBS is assumed to contain 3.2 μ L of whole blood at 14 gHb/dL (individual patient haematocrits were unavailable), results in pmol/DBS/h can be converted to nmol/gHb/h using a conversion factor of x2.2; resulting in activities of 5.7 – 31.7 nmol/gHb/h in our control cohort. This is lower than those reported previously. Differences in methodology that could account for this discrepancy include the use of DBS rather than a haemolysate and the pH of buffers used.

The PK activities measured for **Table 5.1** and **Figure 5.8** are lower than those determined for **Figure 5.7**. For example, the mean activity measured from control DBS was 47% lower, at 8.2 pmol/DBS/h instead of 15.4 pmol/DBS/h. The later data

was collected using 300 $\mu\text{mol/L}$ MgATP as substrate, earlier experiments used 300 $\mu\text{mol/L}$ MgCl₂ & 300 $\mu\text{mol/L}$ ATP, providing an explanation for this difference. The effect of different types of ATP substrate on PK activity is discussed in **Section 5.1.2**.

As before (**Figure 5.7**), PK activities in **Subjects PK1 and PK2** were lower than all controls analysed at 1.1 and 0.9 pmol/DBS/h, respectively. The heterozygous subject HET1 had activity of 4.9 pmol/DBS/h, within the normal range. A significant difference was identified between subjects PK1 and PK2 vs the 22 controls ($p = 0.007$) using a Mann-Whitney test. These results indicated that **Subjects PK1 and PK2** were indeed PK deficient in the blood.

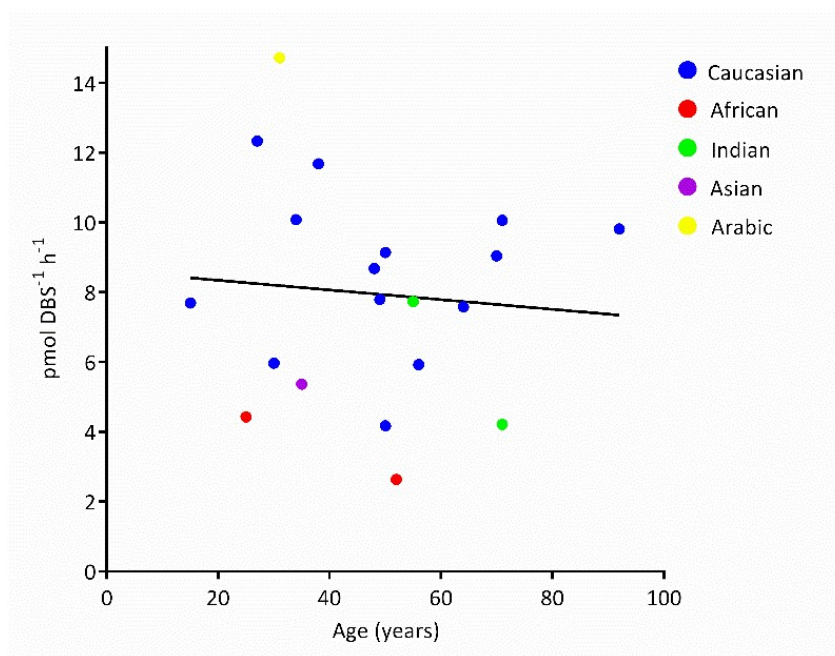


Figure 5.9: Age does not affect erythrocyte pyridoxal kinase activity. The line displayed is that generated on linear regression of the data sets; there was no relationship between PK activity and age ($R^2 = 0.007$). Spearman correlation r value was -0.12 with a two-tailed P value of 0.63. Each point is the mean of the analysis of 2 separate DBS.

Given the age of **Subjects PK1 and PK2** (79 and 74 years old, respectively) it was important to identify any correlation of blood PK activity with age (**Figure 5.9**). No correlation was observed; the nonparametric Spearman correlation r value was -0.12 with a two-tailed P value of 0.63. This data indicated that the low PK activities of **Subjects PK1 and PK2** were not due to their age. It should be noted that DBS from children have not been analysed (apart from one 15-year-old adolescent). In the human foetus, PK activity increases throughout gestation.²²³ It is possible that an age-

related correlation does exist in childhood, particularly the neonatal period, to our knowledge this has not been studied.

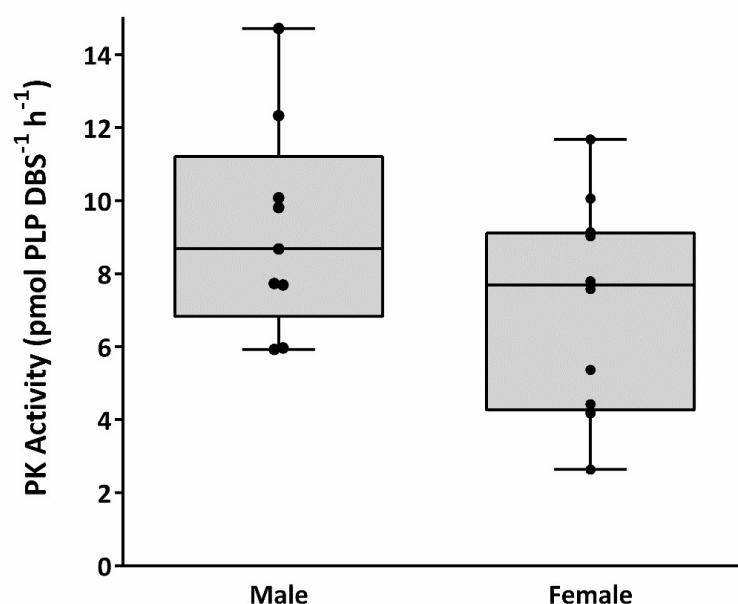


Figure 5.10: Effect of gender on pyridoxal kinase activity. Unpaired T test P value = 0.11; each point is the mean of the analysis of 2 separate DBS.

Whilst there was no correlation of PK activity with age, there was a difference approaching significance ($p = 0.11$) between the measured PK activities in males and females (Means = 9.2 and 7.1 pmol/DBS/h, respectively; **Figure 5.10**). This has not been reported previously. On average, females have a lower haematocrit compared to males (~12% lower)²²⁴, which could account for at least part of the reduction in PK activity seen (29%). A lower haematocrit of the blood spotted onto a DBS can lead to a reduced blood volume within the 3 mm punch taken for analysis (discussed in detail in **Section 4.1.2.6**). Equally, as PK is a red cell enzyme, a lower red cell count per mL would lead to lower measured PK activity. Unfortunately, it was not possible to investigate this further in our cohort as the haematocrits or haemoglobin levels of the samples analysed had not been measured. In the future, it would be valuable to obtain a larger cohort of samples in order to confirm this finding.

5.3 Effect of the c.(-306_-305insGCGCGGCG) insertion in the PK promoter region on enzymatic activity of pyridoxal kinase in red blood cells.

Reports suggest that there is a wide range of erythrocytic PNPO^{89, 170} and PK²²¹ activities within the human population. With regards to PK, it has been speculated that this variation is due to the presence or absence of the c.(-306_-305insGCGCGGCG) variant, thought to introduce an erythroid-specific core promoter binding protein (CPBP) binding site in the 5' region of the *PDXK* gene. The absence of this variant has been suggested to be the cause of reduced PK activity in the erythrocytes of Black Americans.⁴⁰ It is possible that the reduced dried blood spot PK activity identified in the two p.A228T homozygous individuals and/or the lowest values amongst the control samples was caused by the absence of this insertion. The *PDXK* promoter region was therefore sequenced for each of the samples.

5.3.1 Optimisation of the amplification of the *PDXK* promoter region.

Primers used for the amplification of genomic DNA by PCR must be designed with several parameters in mind.²²⁵ A summary of ideal primer design parameters for the amplification and sequencing of genomic DNA, as well as the set of primers designed for amplification of the *PDXK* promoter region, is shown in **Table 5.2**. Standard PCR conditions used can be found in **Section 2.12.3.1; Table 2.10**. These conditions formed a basis from which the parameters were altered to facilitate amplification of the *PDXK* promoter region. The 5' promoter regions of genes are often difficult to amplify given their high %GC content, causing higher T_m 's and the formation of secondary structures such as hairpins; the 5' region of *PDXK* is GC-rich with a GC content of approximately 75%. Techniques and protocols have been developed to facilitate the amplification of these regions; some are discussed below.

Table 5.2: Optimal parameters for PCR primer design and primer sequences for amplification of the *PDXK* 5' promoter region. Parameters adapted from Baumforth *et al.*²²⁵ T_m = melting temperature; GC% = percentage of bases that are either C or G in the sequence chosen.

Parameter	Range			
Primer length	18-24 bases			
T _m	55 – 65°C; T _m of primers should not differ by more than 2°C			
Primer GC content	40 - 60%			
Amplicon size	100 – 1000 bp typical but variable according to application			
Annealing temperature	Typically 2°C below the primer T _m			
3' End stability	Less than 3 Gs or Cs in the last 5 bases			
Primer dimers	Self-complementarity should be avoided			
Runs of bases	No more than 3-4 of the same base in a run			
Secondary structures	Primers predicted to form secondary structures such as hairpin loops should be avoided.			
Specificity	Each primer should differ by more than 3 bases from other genomic DNA regions			
Primers selected for amplification of the 5' promoter region of <i>PDXK</i>				
Primer name	Sequence	T _m (°C)	GC%	Predicted Amplicon size
Primer Prom_F	5'-GCGGTTCCCTTGGGTATC-3'	57.5	61.1	470 bp
Primer Prom_R	5'-ACGCCTCCTTCTGACCTC-3'	58.3	61.1	

Two primers (Primers Prom_F & R) were designed for the amplification of the PK 5' promoter region using the parameters shown in **Table 5.2**. Amplification of 50 ng control DNA was attempted under standard conditions (See **Section 2.12.3.1**) using annealing temperatures ranging from 54 – 64 °C. Some nonspecific signal was identified at lower temperatures but none of the products corresponded to an amplicon of the predicted length (470 bp) (**Figure 5.11**).

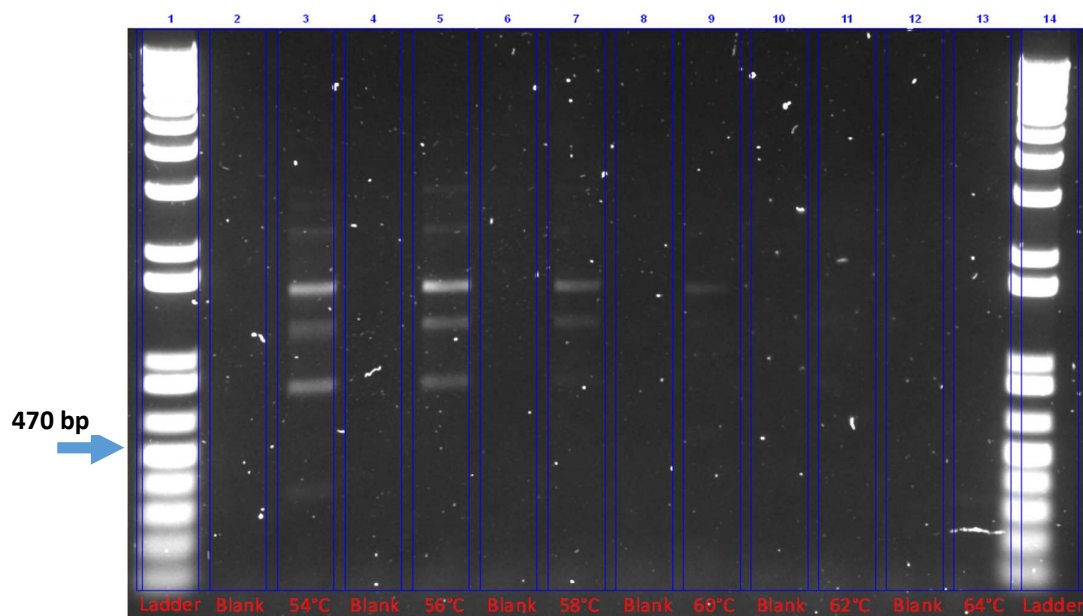


Figure 5.11: Annealing temperature optimisation of primers Prom F & Prom R. Invitrogen 1 Kb Plus DNA ladder used for DNA sizing. No bands specific for the desired amplicon of 470 bp were identified at any annealing temperature. Non-specific bands can be visualised at 50 – 54°C. Blank = 1 µL H₂O in place of 1 µL 50 ng/L control genomic DNA. PCR conditions as specified in **Section 2.12.3.1**; **Table 2.10** unless stated.

Subsequent experiments involved reducing the MgCl₂ concentration from 1.5 mmol/L to 1 mmol/L in order to discourage non-specific amplification and increasing the number of amplification cycles from 35 to 38, to increase the quantity of PCR product amplified. Unfortunately, under these conditions no bands were detected irrespective of the annealing temperature used (54 – 64°C) (**data not shown**). One technique often used to enhance PCR amplification of GC-rich areas of the genome, such as the PK 5' promoter region, is the addition of organic compounds such as betaine and dimethyl sulphoxide (DMSO) to the reaction mixture.²²⁶⁻²²⁷ These compounds promote amplification by destabilising secondary and tertiary DNA structures such as the DNA double helix.²²⁸ This facilitates the melting of DNA and coupling of primers to their target sequences, hence facilitating DNA amplification by Taq polymerase.

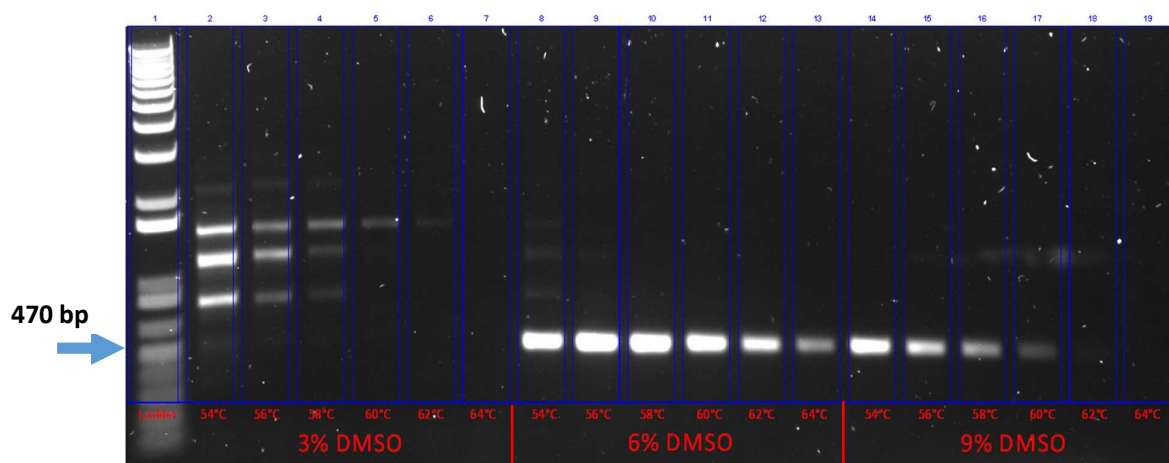


Figure 5.12: Effect of DMSO on the amplification of the *PDXK* 5'-promoter region. Invitrogen 1 Kb Plus DNA ladder utilised for DNA sizing. PCR conditions as specified in **Section 2.12.3.1**; **Table 2.10** unless specified.

Several concentrations of DMSO (3, 6 and 9%) were trialled with annealing temperatures of between 54 – 64°C (**Figure 5.12**). Under some conditions, gel electrophoretic analysis showed a strong and specific signal at the expected molecular weight of the target amplicon (470 bp). Non-specific products were evident at lower temperatures and in the presence of 3% DMSO. The strongest and most specific signal was seen when the reaction was carried out using an annealing temperature of 58°C and 6% DMSO. All subsequent experimentation was therefore carried out using these conditions.

DNA was extracted from the same dried blood spots that had been used to determine PK enzyme activity using a QIAamp DNA micro kit (QIAGEN, Venlo, Netherlands). The concentration of genomic dsDNA in the final elution solution was low for each of these DBS extracts, close to or below the 2 ng/μL LLOQ of the DNA quantification technique used (NanoDrop ND-1000 UV-VIS Spectrophotometer).

No PCR product was evident for many of the samples when 1 μL (50 ng) of DNA and 35 PCR cycles were used for amplification (**Figure 5.13 (a)**). However, when the DNA quantity was doubled to 2 μL (100 ng) and the number of PCR cycles was increased to 38 it led to successful amplification of the target DNA sequence (**Figure 5.13 (b)**). Although the signal from some individuals was low or showed some non-specific bands, resulting products were sequenced successfully.

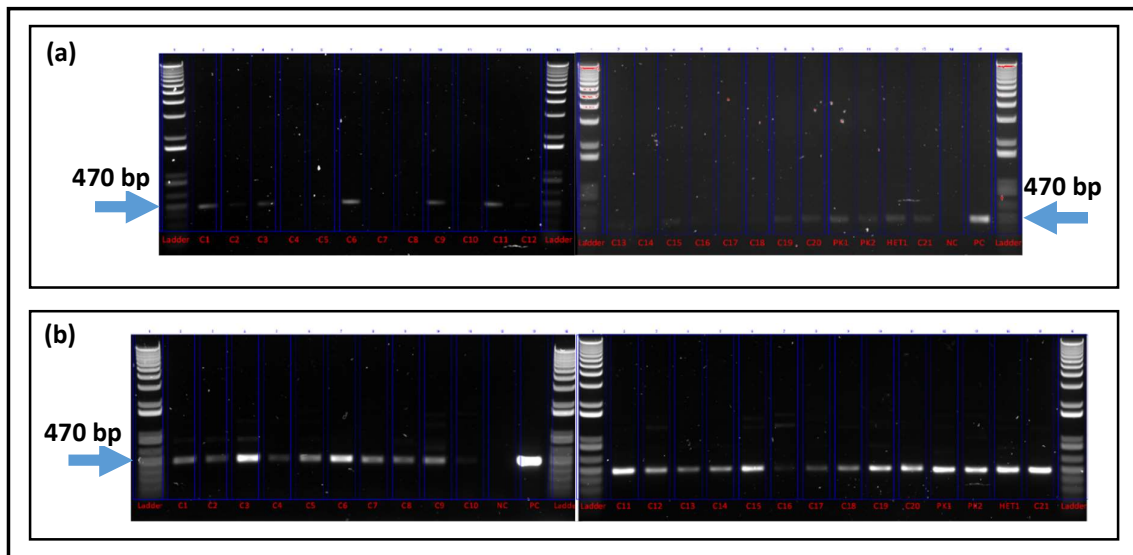


Figure 5.13: Amplification of the *PDXK* 5'-promoter region using genomic DNA extracted from DBS taken from PK-deficient individuals and controls. Invitrogen 1 Kb Plus DNA ladder used for DNA sizing. PCR conditions as specified in Section 2.12.3.1; Table 2.10 unless adjusted as described in the main text. PC = positive control (genomic DNA extracted from whole blood of a control) NC = negative control (H₂O in place of genomic DNA).

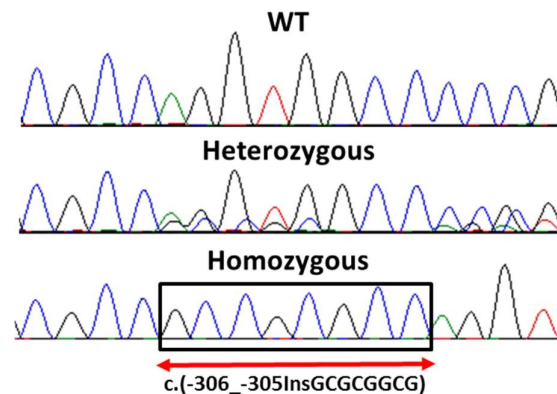


Figure 5.14: Representative electropherograms of the wild-type, heterozygous and homozygous c.(-306_-305InsGCGCGGCG) alleles from DBS extracts.

Examples of electropherograms from individuals homozygous for the c.(-306_-305InsGCGCGGCG) and wild-type alleles, as well as a heterozygous individual, are shown in **Figure 5.14**. Four controls were homozygous for the wild-type allele, two were heterozygous and fifteen were homozygous for the c.(-306_-305InsGCGCGGCG) insertion. Subjects PK1 and PK2 were both homozygous for the wild-type allele (**Table 5.3**).

Table 5.3: Presence of the *PDXK* variant c.(-306_-305InsGCGGGCG) in subjects collected for DBS pyridoxal kinase activity analysis. For the genotype of promoter region: Ins/WT indicates the presence or absence of c.(-306_-305InsGCGGGCG), respectively.

Subject	Age	Gender	Ethnicity	Genotype of promoter region (Ins = insertion present; WT = insertion absent)	PK activity in DBS (pmol/DBS/h)
PKC1	25	Female	African	Ins ; Ins	4.4
PKC2	50	Female	Caucasian	Ins ; Ins	9.1
PKC3	71	Female	Indian	Ins ; WT	4.2
PKC4	50	Female	Caucasian	Ins ; Ins	4.2
PKC5	49	Female	Caucasian	Ins ; Ins	7.8
PKC6	48	Male	Caucasian	Ins ; Ins	8.7
PKC7	30	Male	Caucasian	WT ; WT	6.0
PKC8	70	Female	Caucasian	Ins ; Ins	9.0
PKC9	35	Female	East Asian	Ins ; Ins	5.4
PKC10	27	Male	Caucasian	Ins ; Ins	12.3
PKC11	52	Female	African	Ins ; WT	2.6
PKC12	71	Female	Caucasian	WT ; WT	10.1
PKC13	92	Male	Caucasian	Ins ; Ins	9.8
PKC14	55	Male	South Asian	Ins ; Ins	7.7
PKC15	15	Male	Caucasian	Ins ; Ins	7.7
PKC16	64	Female	Caucasian	WT ; WT	7.6
PKC17	56	Male	Caucasian	WT ; WT	5.9
PKC18	38	Female	Caucasian	Ins ; Ins	11.7
PKC19	31	Male	Arabic	Ins ; Ins	14.7
PKC20	34	Male	Caucasian	Ins ; Ins	10.1
PKC21	78	Female	Cypriot	Ins ; Ins	9.0
PK p.Ala228Thr homozygous					
PK1	79	Male	Cypriot	WT ; WT	1.1
PK2	74	Female	Cypriot	WT ; WT	0.8
PK p.Ala228Thr/WT					
PKHET1	52	Female	Cypriot	Ins ; WT	4.9

5.3.2 Dried blood spot pyridoxal kinase activity does not correlate with the presence of the c.(-306_-305InsGCGCGGCG) insertion in the promoter region of *PDXK*

A comparison of the DBS PK activity from individuals homozygous for the c.(-306_-305InsGCGCGGCG) insertion and wild-type alleles showed that the presence of this insertion did not significantly alter PK kinase activity (**Figure 5.15**). The mean PK activity in controls homozygous for the 'wild-type' allele was 7.4 pmol/DBS/h (range 5.9 – 10.1 pmol/DBS/h; n = 4). In DBS from controls homozygous for the insertion, mean activity was 8.8 pmol/DBS/h (range 4.2 – 14.7 pmol/DBS/h; n=15). Hence, the reduction in activity seen in the patients is not due to the presence or absence of this insertion. Intriguingly, the two control individuals heterozygous for the insertion had among the lowest activities (2.6 and 4.2 pmol/DBS/h). However, the numbers in this study were too small to determine whether this was a real biochemical effect or simply an anomaly based on insufficient data.

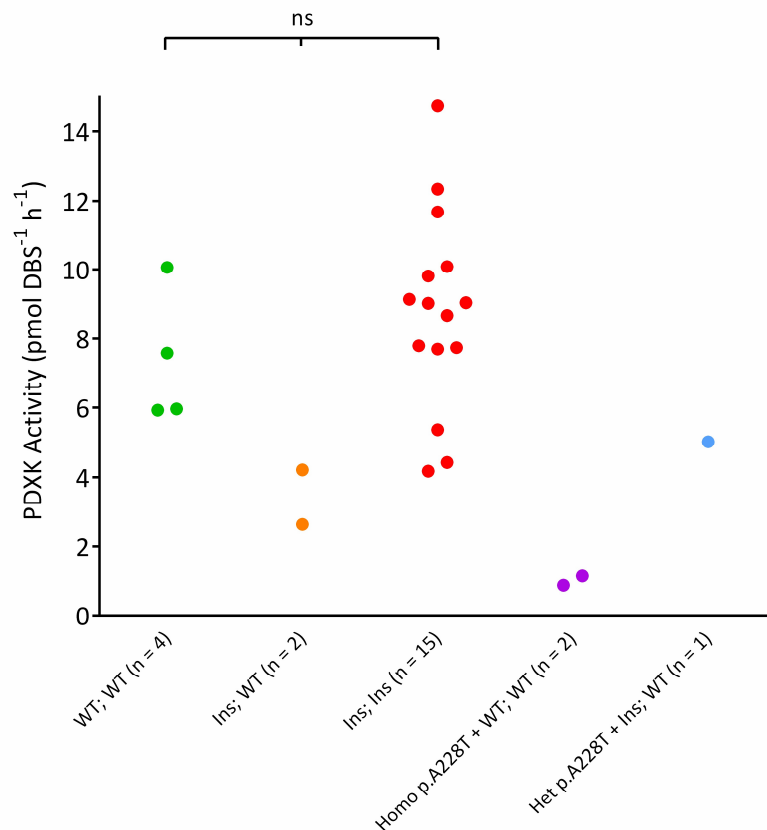


Figure 5.15: Comparison of pyridoxal kinase activity with genotype data for c.(-306_-305InsGCGCGGCG). ns = not significant. WT = Wild-type; Ins = c.(-306_-305InsGCGCGGCG) insertion present.

It is worth noting that although this variant was initially described as an 'insertion' event, more recent data has shown that the prevalence of the insertion allele is >50% in the general population. The overall allele frequency from the Genome Aggregation Database (gnomAD) is 0.56 from 28,218 alleles. The only ethnicity for which the allele frequency is less than 0.5 is African (0.44). In our cohort (including patients with the p.A228T variant) the allele frequency of c.(-306_-305InsGCGCGGCG) was 0.69.

5.4 Discussion & future work

5.4.1 Implications of the association between vitamin B₆ metabolism and peripheral neuropathy

Subsequent to the genetic and biochemical diagnosis of pyridoxal kinase deficiency for **Subjects PK1 and PK2**, a treatment regime was initiated that consisted of moderate (50 mg/day) PLP supplementation. PLP was chosen as high doses of pyridoxine have been shown to cause peripheral neuropathy.¹¹⁰ The aetiology of pyridoxine-induced neuropathy is unclear but it was important to avoid exacerbating the disorder in these patients.

As discussed elsewhere (**Section 1.1.1**), on ingestion, the phosphorylated B₆ vitamers are hydrolysed by intestinal phosphatases and absorbed as the non-phosphorylated forms. Despite **Subjects PK1 and PK2** having plasma PLP concentrations (7.5 & 9 nmol/L, respectively) below the normal range (15 – 73 nmol/L) before supplementation, within four weeks plasma PLP concentrations had increased to 492 and 407 nmol/L, above the normal range of individuals not receiving B₆ supplementation. This suggested that the patients had some residual PK activity, supporting our biochemical findings. PLP levels have remained higher than the reference range after 12 months of continuous supplementation at 50 mg/day.

In addition, **Subjects PK1 and PK2** improved clinically. Prior to supplementation, both individuals had impaired mobility; **Subject PK1** was confined to a wheelchair. On follow-up after 12 months, both patients were able to walk unaided. In addition, neuropathy had been causing considerable chronic pain which, on treatment, subsided completely; withdrawal of pain medication was enabled.

It has been reported that a mouse model lacking the circadian PAR bZip transcription factors DBP, HLF and TEF develops seizures attributed to lowered expression of the *pdxk* gene encoding pyridoxal kinase; brain levels of dopamine and serotonin were reduced.⁴¹ A model of *Drosophila melanogaster* with suppressed expression of its *PDXK* homologue developed what was thought to be a Parkinsonian phenotype.²²⁹ A link between pyridoxal kinase and Parkinson's disease has also been established in a human dopaminergic cell line.²³⁰ These findings suggest that PK deficiency in the brain would lead to PLP deficiency causing either seizures or a Parkinson's disease-like movement disorder. However, this was not seen in our patients. On the other

hand, as mentioned in the introduction to this section, peripheral PLP deficiency is known to lead to neuropathy. This is apparent in the case of drugs that form a complex with PLP (e.g. isoniazid) and those that inhibit pyridoxal kinase (e.g. theophylline¹⁰⁸ and ginkgotxin²¹¹). These compounds also lead to seizures at higher doses.

It has been shown that the regulation of PK activity is tissue-specific in PLP-deficient rats. Activity is preserved in the brain but reduced in the peripheries.²³¹ Interestingly, the same preservation of brain activity is not seen for other B₆ metabolic enzymes. It is possible that the neurological system is protected through the modulation of PK transcription in conditions of B₆ deficiency. The mechanism by which this adaptation is carried out is currently unknown although PK expression is known to vary according to the action of transcription factors linked to the circadian rhythm in mice⁴¹ and MocR-like transcription factors in *Salmonella*.⁴²

One hypothesis for the attenuated PLP deficiency in these patients is that the residual enzymatic activity of p.A228T PK protein is able to provide adequate PLP within the central nervous system (as well as in other organs such as the liver) but not in the peripheral nerves. Given that the effect of p.A228T on enzyme activity is more pronounced at low substrate concentrations, the diseased state caused by PLP deficiency could be present only in tissues where these substrates are in limited supply. The axonal transport or import mechanism into the axons of peripheral neurones could be insufficient to provide the substrate concentrations required to compensate for the deleterious effect of the p.A228T variant in PK.

Individuals with other B₆ metabolic disorders such as PDE and PNPO deficiency have not reported peripheral neuropathy as part of their disorder, only that linked to high doses of pyridoxine. However, it is possible that individuals with other B₆ metabolic disorders who present with seizures receive treatment in the form of B₆ supplementation before peripheral neuropathy becomes a feature of their disorder. These patients start treatment with B₆ supplements on (or before) diagnosis. In addition, very few patients have been reported to present with these disorders past infancy. Typically, the oldest cases present in early childhood (4-5 years of age; one case of ALDH7A1 deficiency has presented at age 19).²³² **Subject PK1** reported first experiencing his symptoms at age 8.

More broadly, it could be hypothesised that a (perhaps small) proportion of genetic peripheral neuropathies are caused by deficiency of the PK enzyme. Screening

patients using the newly developed DBS enzyme assay described would be a useful process. Potentially, if some genetic neuropathies could be treated with PLP, an inexpensive and relatively safe drug, this would be of huge benefit for management of these disorders. For clinicians, the measurement of plasma PLP in individuals with peripheral neuropathy could be a simple and useful test that could indicate whether PLP supplementation may be a beneficial treatment.

The identification of this novel disorder of B₆ metabolism further underlines the intricate link between vitamin B₆ and the function of both the central and peripheral nervous systems. As discussed previously (**Section 1.2**), seizures caused by PLP deficiency are thought to be caused by deranged neurotransmitter metabolism in the brain.²⁰⁹ However, this has never been conclusively proven to be the sole cause of these seizures and is probably a simplistic explanation. The optic atrophy and axonal peripheral neuropathy in the PK deficient patients described are similar to features of inherited disorders leading to mitochondrial dysfunction. Indeed, the patients described were initially suspected to have a mitochondrial disorder and were investigated as such prior to NGS technologies becoming available.

Transcriptomic co-expression analysis of the human tibial nerve performed by collaborators (including populations of neurones and Schwann cells) showed that *PDXK* was expressed alongside genes involved in the oxidation-reduction process. Equally, *PDXK* was expressed strongly in nervous tissues when compared to other cell types. This correlates with the importance of B₆ metabolism in central and peripheral nerves but also indicates a link to mitochondrial function.

Recently a mitochondrial B₆ transporter has been identified in yeast (Mtm1p)³⁰ and its homologue in *Drosophila* has been linked to neuronal survival.³¹ To date a human mitochondrial B₆ transporter has not been characterised but two orthologues of the Mtm1p gene exist in the human genome (*SLC25A39/40*); *SLC25A39* lies at a susceptibility locus for epilepsy.²³³ The mitochondrial metabolism of Schwann cells is linked to long-term peripheral nerve survival.²³⁴ Multiple PLP-dependent enzymes are mitochondrial or have mitochondrial isoforms including those involved in haem synthesis (δ -Aminolevulinate synthase), the one-carbon pathway (serine hydroxymethyltransferase), the glycine decarboxylase complex and branched-chain amino acid aminotransferase.

Overall, our knowledge of human metabolism and the important role than PLP plays as a cofactor is insufficient to come to a firm conclusion as to the biochemical mechanisms behind the neuronal dysfunction present in both the central and peripheral nervous systems during the PLP-deficient state. It is likely that the answer is a complex multifactorial one including multiple metabolic pathways with multiple simultaneous pathological mechanisms.

5.4.2 Further biochemical characterisation of pyridoxal kinase and activity variation in the general population

In order to fully characterise the p.A228T PK protein, additional studies exploring factors such as the thermal stability, pH dependency and substrate specificity (e.g. towards PN and PM) of this mutant PK protein will need to be performed in the future. The method presented for the assessment of PK enzyme kinetics is more sensitive and accurate than those reported previously, this is of value to the field of B₆ metabolism. In particular, it would be important to confirm sigmoidal kinetics of MgATP saturation as this had not previously been identified. A full characterisation of PK kinetics is important as it could have implications for the treatment of patients receiving high doses of B₆ vitamers, for example, if high concentrations were liable to inhibit the enzyme.

The conclusion that p.A228T diminished PK activity but resulted in an intact and catalytically active protein was supported by collaborator's work showing that expression of p.A228T PK in fibroblasts was normal as measured using a western blot. This indicated a stable protein conformation. However, structural changes were apparent by far and near-UV circular dichroism. In particular, the α -helix and β -sheet proportion was altered and conformational changes were identified in aromatic side chains at the catalytic site. In addition, collaborators showed through isothermal titration calorimetry that ATP binding was impaired in p.A228T PK. This supported modelling data showing that p.A228 is close to the ATP binding site, and our data indicating that the kinetics alterations caused by p.A228T are particularly ATP-dependent.

The development of an assay which uses dried blood spots for the measurement of PK activity could be useful for the assessment of PK function in larger cohorts and

thereby identifying potential population differences. This could have two major implications. Firstly, if low PK activity is detected in certain individuals, they could be more susceptible to peripheral neuropathy (or seizures, though this could be unlikely given the phenotypes of patients in our study) and, if so, receptive to PLP supplementation. Secondly, it has long been postulated that low activity of the B₆ metabolic enzymes could be a protective mechanism against malaria due to the inability of *Plasmodium falciparum* to produce its own PLP.^{182, 235} Although Flanagan and Beutler suggested they had identified the mechanism behind low erythrocyte PK activity in black Americans (the c.-306_-305InsGCGCGGCG variant)⁴⁰, our data conflicted with theirs. A study looking at PK (and PNPO) activities in dried blood spots taken from large cohorts could lead to an improved understanding of the possible role of PK in malaria and provide new avenues for treatment.

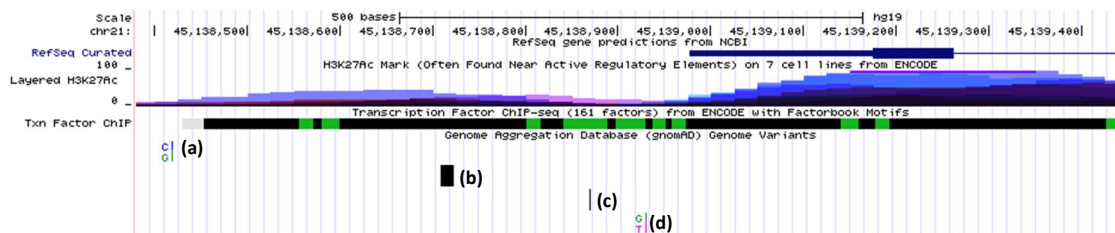


Figure 5.16: The *PDXK* 5'-promoter region showing common variants with a minor allele frequency (MAF) greater than 0.1 in GnomAD. Variants: (a) rs9981249; c.-756C>G; MAF = 0.57 (b) rs72004735; c.-466_-460delGCGGGGC; MAF = 0.70 (c) rs146826482; c.-306_-305InsGCGCGGCG; MAF = 0.57 (d) rs62229179; c.-246G>T; MAF = 0.57. H3K27ac is the acetylation of the 27th lysine of the H3 histone protein. This indicates a transcription activation site at this location; variants at this site are more likely to affect expression of the gene. The 'RefSeq Curated' track shows exon 1 and the 5' UTR region as well as part of intron 1-2 of the *PDXK* gene. Data collected using the UCSC Human Genome Browser (<http://genome.ucsc.edu/>) and utilising the GRCh37/hg19 genome assembly.

Since the report of Flanagan and Beutler in 2006, considerable additional data has been collected on natural variation of the *PDXK* gene. For example, in-silico analysis using the UCSC Human Genome Browser²³⁶ shows that just four variants with a minor allele frequency of greater than 0.1 are found in the *PDXK* 5'-promoter region. These could potentially alter PK protein expression and/or provide a tissue-specific expression profile (**Figure 5.16**).

The area of the *PDXK* 5'-promoter region sequenced to provide the data in **Figure 5.15** also included the variant (b): c.-466_-460delGCGGGGC. This allowed analysis of the inheritance of this variant as well as correlation with PK activity. Overall 3/24

individuals were homozygous for the 'wild-type' allele, with 21/24 homozygous for the c.-466_-460delGCGGGGC allele. The allele frequency of this 'minor' allele in our cohort (0.875) was higher than that of the c.-306_-305InsGCGCGGCG 'minor' allele (0.69). Inheritance of these variants was also not concurrent in specific individuals. This suggests that these variants are not inherited together, at least in our cohort. Again, the presence of variant **(b)** did not significantly affect PK activity measured from DBS (data not shown).

As mentioned above in **Section 5.4.1**, work has been carried out in bacteria to study the mechanisms regulating expression of the B₆ salvage pathway enzymes. MocR-like transcription factors have been shown to bind pyridoxal 5'-phosphate²³⁷⁻²³⁸ and regulate the expression of a PK orthologue in *Salmonella typhimurium*.⁴² This system has yet to be extended to higher organisms, however. One potential modulator of pyridoxal kinase expression in mammals is the circadian rhythm. In the brain circadian oscillations of clock genes are known to alter expression of the PAR bZip transcription factors TEF, DBP and HLF which in turn control the transcription of many genes including PK. Indeed, in a mouse model, the genetic deletion of these transcription factors leads to epilepsy. This is hypothesised by Gachon *et al.* to be due to PLP deficiency caused by insufficient PK activity.⁴¹ Important additional work would be to use RNA sequencing technology to identify tissue-specific, circadian and feedback modulation of PK expression (as well as other B₆ metabolic enzymes) and assess the implications of this regulatory pathway on B₆ metabolism, particularly with regards to neurological health.

6. STABILITY AND SUITABILITY OF PYRIDOXAL 5'- PHOSPHATE FOR THE TREATMENT OF VITAMIN B₆-RESPONSIVE DISORDERS

The United States National Institutes of Health (NIH) recommended daily allowance (RDA) of pyridoxine intake for adults is 1.3 mg/d and the recommended upper limit is 100 mg/d.²³⁹ Assuming a weight of 80 kg, these translate to 0.016 mg/kg/d and 0.8 mg/kg/d, respectively. No RDA specific to PLP has been established. Patients with seizure disorders responsive to vitamin B₆ typically require oral doses of pyridoxine or PLP from 10 – 50 mg/kg/d in order to control their seizures. Doses as high as 100 mg/kg/d have been used and doses lower than 10 mg/kg/d have also been reported as being effective.^{27, 65, 103, 240-241} These supraphysiological doses are reflected in the blood of a supplemented patient, with concentrations of the B₆ vitamers orders of magnitude higher than those of controls (**Section 3**).

High doses of pyridoxine are known to cause peripheral neuropathy thought to be due to inhibition of PLP-dependent enzymes, as discussed in **Section 5.1** and **Section 5.4**. Peripheral neuropathy has been described in adults after long term (> 1 year) pyridoxine supplementation, even with doses lower than the recommended upper limit (50 mg/d).¹⁰⁷ It can also be a side-effect in ALDH7A1-deficient individuals receiving pyridoxine for treatment of their seizures²³² and has been reported in at least one PNPO-deficient child (Patient 10; Mills *et al.* 2014⁸⁷)

There are reports of raised liver function tests (LFTs) and hepatic cirrhosis in patients with PNPO deficiency receiving high-dose (> 30 mg/kg/d) PLP supplementation.^{99, 103} As of early 2019, in the most severe case, this has necessitated a liver transplant in one PNPO deficient child.^(unpublished data) There is one report of a patient with homocystinuria suffering from ‘hepatitis’ (probably PLP-induced liver damage) on 1,000 mg/d PLP²⁴² and another describing 14/28 patients presenting with transiently raised liver function tests upon treatment with high-dose PLP (30 – 50 mg/kg/d) for the control of infantile spasms.²⁴³

PLP is a photolabile compound; this was investigated initially more than 50 years ago²⁴⁴ and has been studied by others in subsequent decades.¹⁰⁵⁻¹⁰⁶ 4-Pyridoxic Acid 5'-Phosphate (PAP) and PLP dimers were identified as photodegradants but, apart from a brief study of the degradation rates of different B₆ vitamers in CSF²¹ and one looking at the stability of plasma PLP²⁴⁵, little work has been performed on the subject over the last 30 years.

It is currently unknown whether the hepatic dysfunction seen in patients receiving high doses of PLP is due to a secondary effect of PNPO deficiency itself, the presence of

extremely high B₆ vitamer concentrations in the liver, or the ingestion of potentially hepatotoxic photodegradants of PLP. To date, however, no PNPO patients receiving PN (rather than PLP) for the treatment of their seizures have been reported to develop hepatic dysfunction. Indeed, no reports describe PN supplementation as causing deranged liver function tests or liver damage in any disorder. This suggests that PNPO deficiency is not causing the pathology, rather it is a side-effect of supraphysiological PLP doses. However, this could be countered with the hypothesis that pyridoxine-responsive PNPO deficient individuals have a milder form of the disorder with some residual PNPO activity.^{87, 98} This could also be protecting their liver.

Coman *et al.* have hypothesised that the mechanism behind this hepatic dysfunction could be linked to high concentrations of B₆ vitamers modulating purinergic P2 receptors on hepatic stellate cells.²⁴⁶ These cells are known to initiate fibrosis through increased production of collagen upon P2 receptor activation. PLP and its derivatives are known to act upon P2 receptors.²⁴⁷ It is also possible that degradation products of PLP could be acting upon P2 receptors and causing hepatic fibrosis in patients on high-dose PLP supplementation. PLP is photolabile and if prepared in aqueous solution, photodegradation could occur prior to patient administration, leading to the ingestion of any PLP photolysis products.¹⁰⁴

In recent years, advice on the preparation of PLP supplements has been increasingly stringent; advising the protection of aqueous PLP from light and its immediate administration after dissolution. It is generally advised to supplement with the lowest dose that allows seizure control.

In order to investigate the photodegradative products of PLP and identify whether they could be responsible for the hepatic dysfunction in individuals receiving high-dose PLP supplementation, LC-MS/MS was used for the analysis of photodegraded PLP.

Using this technique, the qualitative confirmation of two photoproducts (PAP and a diketone PLP dimer) was performed. PAP formation from PLP was also quantified using LC-MS/MS over a time course under controlled light irradiation. The preliminary identification of other potential photodegradation products was carried out. The potential hepatotoxicity of these products and implications for the treatment of patients is discussed.

Finally, the PLP content and photodegradation rates of several commercially available PLP formulations were assessed in an environment that closely replicated the preparation of these solutions for administration to patients. Currently, patients are treated using over-the-counter nutraceuticals; defined as 'Nutritional products that provide health and medical benefits, including the prevention and treatment of disease'.²⁴⁸ These are not subject to the same regulations that apply to pharmaceutical products. Currently, no pharmaceutically licensed form of pyridoxal 5'-phosphate is available in Europe and the United States. This part of the project was carried out in collaboration with the UCL School of Pharmacy in order to assess the need for a pharmaceutical-grade PLP formulation.

6.1 Characterisation of the pyridoxal 5'-phosphate photodegradation profile

6.1.1 Investigation and identification of pyridoxal 5'-phosphate photodegradants

PLP is known to be unstable in aqueous solution at a neutral pH under light irradiation, undergoing rapid photolysis.^{106, 244} PLP photodegradation products were prepared by, after mixing, leaving an aqueous 1 mmol/L PLP solution in a sealed glass vial on a sunlit shelf for 144 hours (6 days). Samples were taken from this solution after 0, 1, 5, 72 and 144 hours, frozen and kept in the dark at -20°C until analysis, in order to halt photodegradation. Previous work has shown that the photodegradation products of PLP differ according to the presence or absence of oxygen.²⁴⁴ In this study all solutions were oxygenated by mixing prior to incubation. All samples underwent an identical number of freeze-thaw cycles. After defrosting, solutions were analysed by Flow Injection Analysis-Mass Spectrometry. This consists of the direct infusion of the photodegraded PLP solutions, with no liquid chromatography separation step. This was carried out in order to identify potential photodegradants according to their *m/z* ratios.

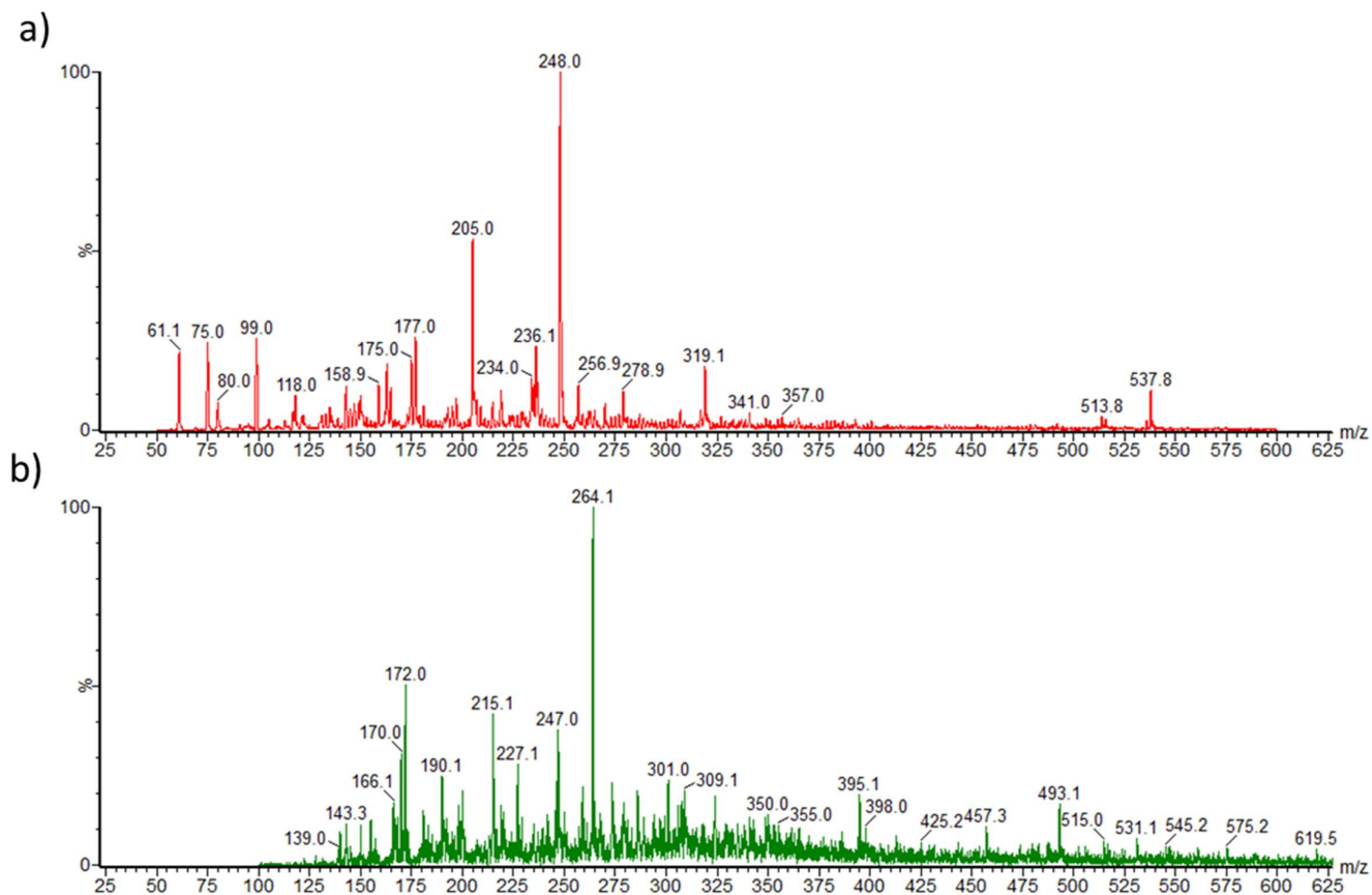


Figure 6.1: MS1 Scan acquisitions after (a) 0 and (b) 72 h light irradiation of a 1 mmol/L PLP solution. 1 minute acquisition time. PLP = m/z 248.0. Spectra collected using flow injection analysis-mass spectrometry (combined flow with 97.5% H₂O w/ 3.7% Acetic acid + 0.01% HFBA, 2.5% Methanol) in positive ion mode using a cone voltage of 27 V.

Initial analyses were performed using a full scan with the MS1 quadrupole. At $T = 0$ h, the most intense peak was detected at m/z 248.0, corresponding to the $[M+H]^+$ ion of PLP (**Figure 6.1a**). However, at later time points mass spectra were difficult to interpret given the appearance of many potential PLP photodegradants over a wide range of m/z ratios (**Figure 6.1b**). All spectra also contained many unidentified peaks, likely related to contaminants or from the mobile phase used. For example, in **Figure 6.1a** there is a peak known to correspond to an acetic acid-Fe-O complex ($[(C_2H_4O_2)_6-6H+3Fe+O]$) at m/z 537.8.

Further investigation was therefore carried out using neutral loss scans pertaining to a loss of H_3PO_4 upon fragmentation (-98) (**Figure 6.2**). This allowed the identification of all compounds containing a phosphate moiety and resulted in a more easily interpretable mass spectrum, with the caveat that non-phosphorylated PLP photodegradants would not be detected.

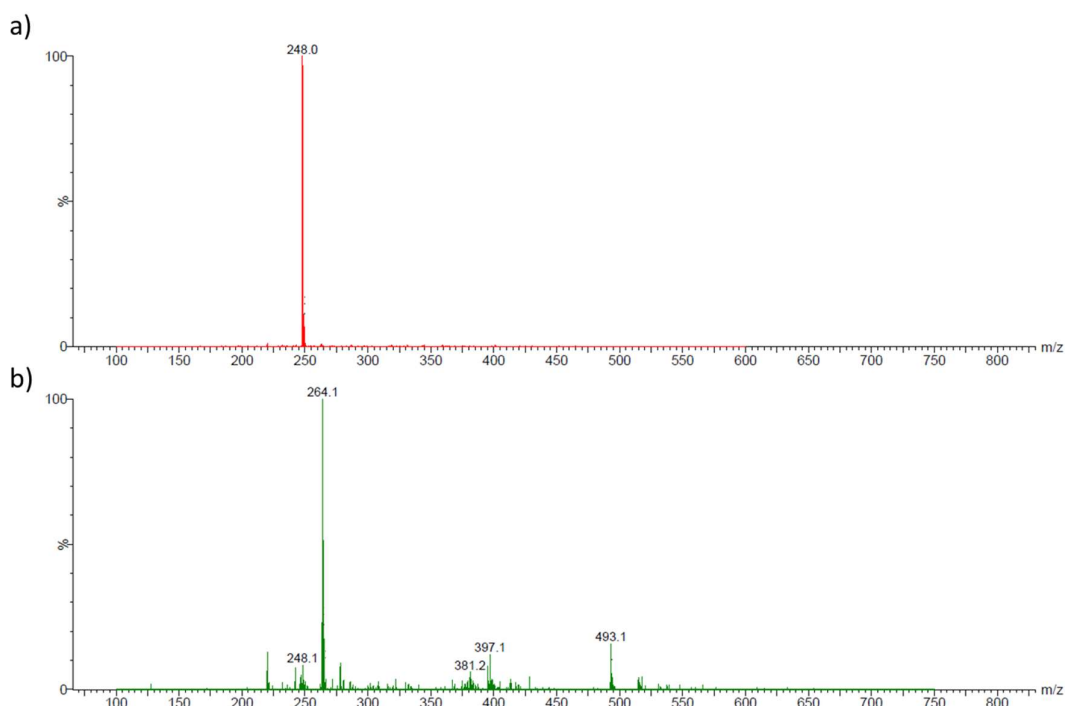


Figure 6.2: Neutral loss (- 98) acquisitions after (a) 0 and (b) 72 h light irradiation of a 1 mmol/L PLP solution. 1 minute acquisition time. Parent ions of m/z ratios -98 are shown. PLP = m/z 248.0. Spectra collected using flow injection analysis-mass spectrometry (combined flow with 97.5% H_2O w/ 3.7% Acetic acid + 0.01% HFBA, 2.5% Methanol) in positive ion mode and a cone voltage of 27 V. The collision energy was 16 V.

Several potential photodegradants were identified with an m/z of 264, 381, 397 and 493 (**Figure 6.2**). The compounds at m/z 264 and 493 were postulated to correspond to 4-pyridoxic acid 5'-phosphate and a PLP dimer¹⁰⁵ (**Figure 6.3**).

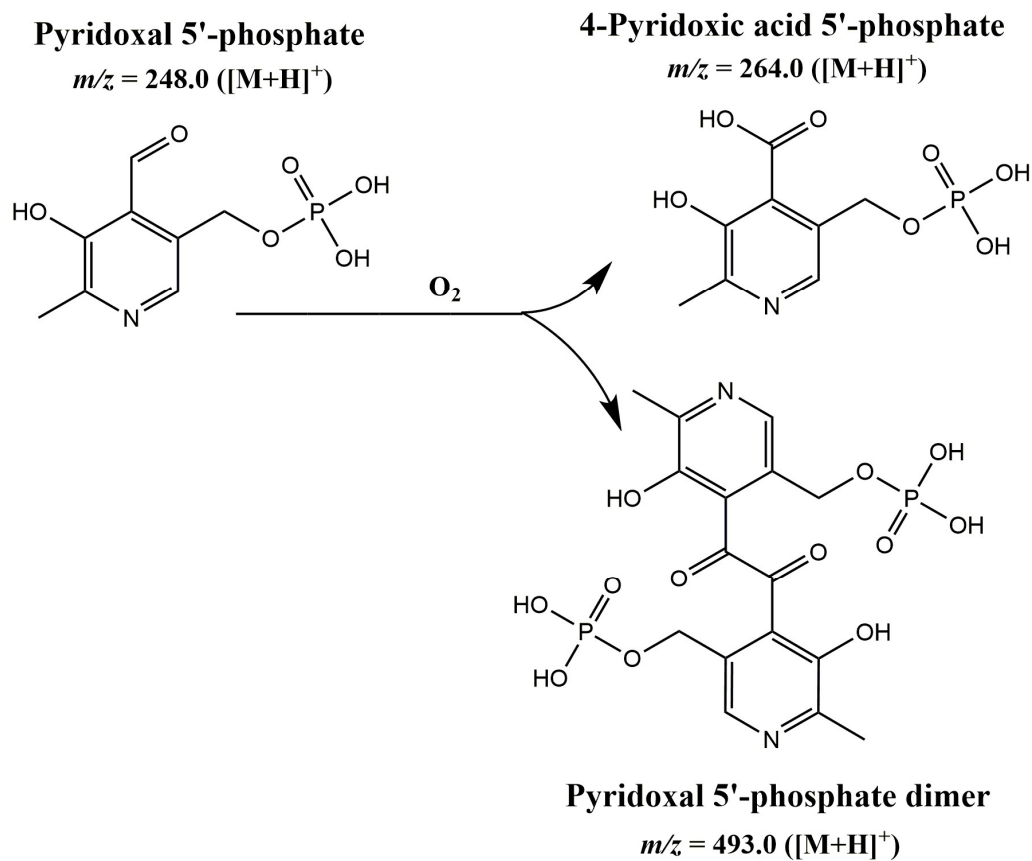


Figure 6.3: Postulated PLP photodegradation products

Table 6.1: Parameters used for the MRM-based identification of PLP, PL, PA and photodegradants of PLP. Transitions arranged according to retention time on LC-MS/MS analysis. d₃-pyridoxal 5'-phosphate was used as an internal standard during later experimentation for quantification of pyridoxal 5'-phosphate and 4-pyridoxic acid 5'-phosphate. Compounds other than PLP, PL, PA and d₃-PLP were identified using neutral loss scans of -98 as shown in **Figure 6.2**.

Proposed analyte	Retention time (min)	Precursor ion (m/z)	Product ion (m/z)	Cone voltage (V)	Collision energy (V)	Loss upon Fragmentation
?PLP Dimer	0.49	493.10	395.00	27	16	H ₃ PO ₄
4-Pyridoxic acid 5'-phosphate	0.82	264.07	166.07	27	16	H ₃ PO ₄
d ₃ -pyridoxal 5'-phosphate	0.96	251.16	152.18	30	18	H ₃ PO ₄
Pyridoxal 5'- phosphate	0.96	248.00	150.01	30	18	H ₃ PO ₄
Pyridoxic Acid	1.02	184.06	147.99	18	18	2H ₂ O
Pyridoxal	1.08	168.10	150.05	21	12	H ₂ O
Compound m/z 381 peak 1	2.12	381.04	283.04	27	16	H ₃ PO ₄
Compound m/z 397	2.20	397.00	299.00	27	16	H ₃ PO ₄
Compound m/z 381 peak 2	2.39	381.04	283.04	27	16	H ₃ PO ₄

In order to confirm that several potential photodegradation products of PLP were formed upon exposure to light these products were quantified over the 144 h time period. MRM transitions were created using the precursor and product ions of the compounds identified, these are shown in **Table 6.1**. All photodegraded solutions were diluted to a nominal value of 100 nmol/L PLP (assuming no degradation) and analysed using the same LC-MS/MS method used for B₆ vitamer analysis (**Section 2.4** and **Section 3**). Peaks derived from MRM transitions corresponding to the identified products were quantified by calculating the AUC for each compound at

respective time points (**Figure 6.4**). Two peaks were identified for the compound with a parent m/z of 381; these were quantified separately.

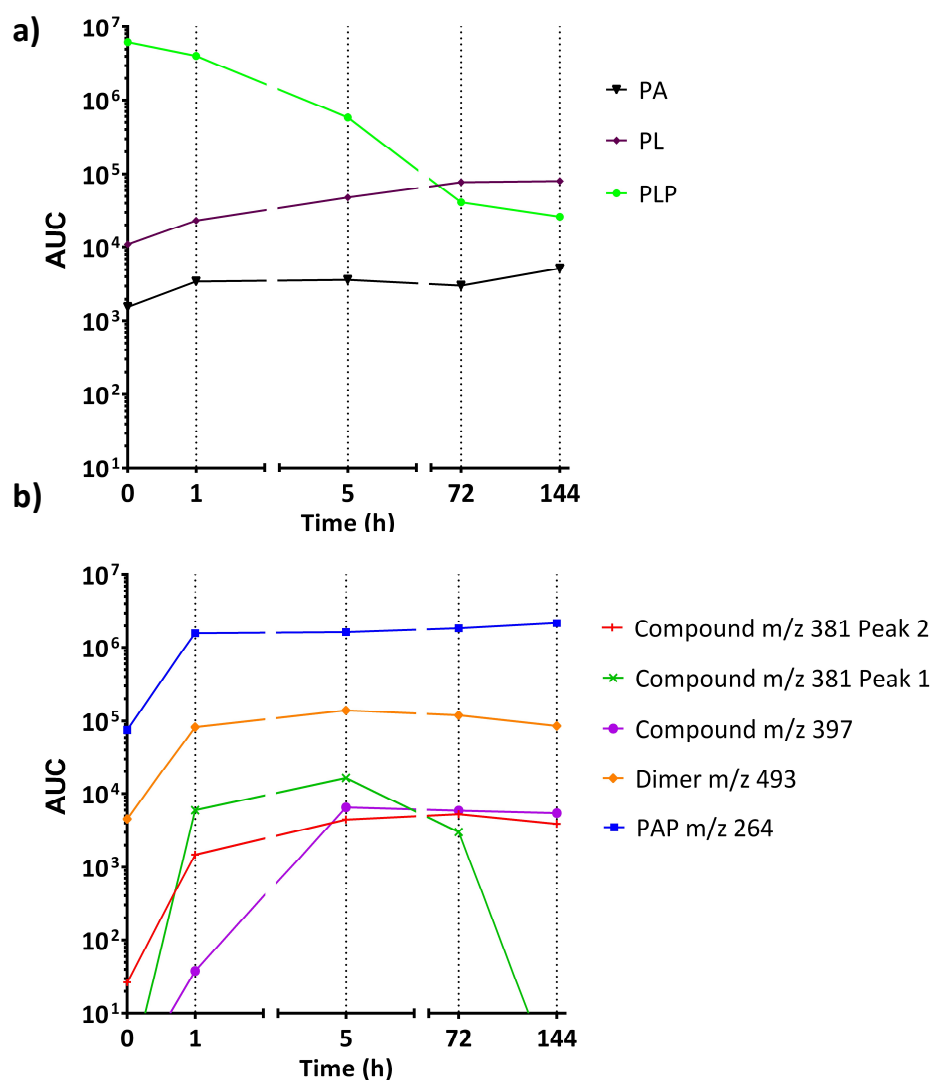


Figure 6.4: Formation of PLP photodegradation products. At each data point $n=1$. AUC = area under curve. a) = known compounds; b) = postulated photodegradation products. Points below Y-axis graph limit were undetectable at this time point.

Depletion of PLP was seen over the 144 h incubation period, this is consistent with work of others.^{21, 106} A corresponding increase in several other compounds was seen; the two compounds with the largest signals were those with parent ions with m/z ratios of 264 and 493. These correspond to the predicted masses of PAP and the diketone dimer of PLP, respectively. The signal from the transition thought to correspond to

PAP increased rapidly from 0 - 1 h to an AUC of approximately 1,582,000 before slowing to an eventual 2,197,000 after 144 h. The signal from the compound with m/z of 493 increased more slowly to 139,000 after 5 h, before declining again to 86,000 after 144 h (**Figure 6.4**). This could be indicative of either reversible formation of the diketone dimer or formation by a first step followed by subsequent degradation via a second step.

A small signal derived from PL, PA, PAP and the dimer can be seen at $T=0$. Although samples were chilled and protected from light before deliberate light irradiation, the presence of these compounds was thought to be due to some degradation occurring during sample preparation. In the case of PL, this could also be due to a small amount of PL as an impurity in the PLP standard (Applichem; > 98% purity by HPLC).

The levels of pyridoxal (PL) and 4-pyridoxic acid (PA) also increased across the time course. It is possible that this is due to hydrolysis of PLP to PL and PAP to PA. It has been reported that PLP hydrolysis to PL is the most prevalent degradative mechanism in the absence of light irradiation at a low PLP concentration (1 $\mu\text{mol/L}$), particularly at a low pH.¹⁰⁶ However, initial PLP concentrations of 1 mmol/L were used in the experiment shown in **Figure 6.4**, 1000 times higher than the concentration in the previously published work. PL formation in our experiment was insignificant compared to that of PAP and the PLP dimer, with concentrations below the limit of quantification (<0.5% of initial PLP at $T=0$).

In order to provide additional evidence that the compound identified at m/z 264 pertained to PAP, a flow injection analysis-mass spectrometry daughter scan of the 1 mmol/L $T=72$ h photodegraded PLP solution was performed for m/z 264 and significant fragment ions at 246 and 166 were identified. These are hypothesised to correspond to $[\text{M}+\text{H}-\text{H}_2\text{O}]^+$ and $[\text{M}+\text{H}-\text{H}_2\text{O}-\text{H}_3\text{PO}_4]^+$, respectively (**Figure 6.5**). This fragmentation pattern would be expected from a pyridine derivative containing a carboxyl group, such as PAP.²⁴⁹⁻²⁵⁰

***m/z* 264 (precursor ion; PAP)**

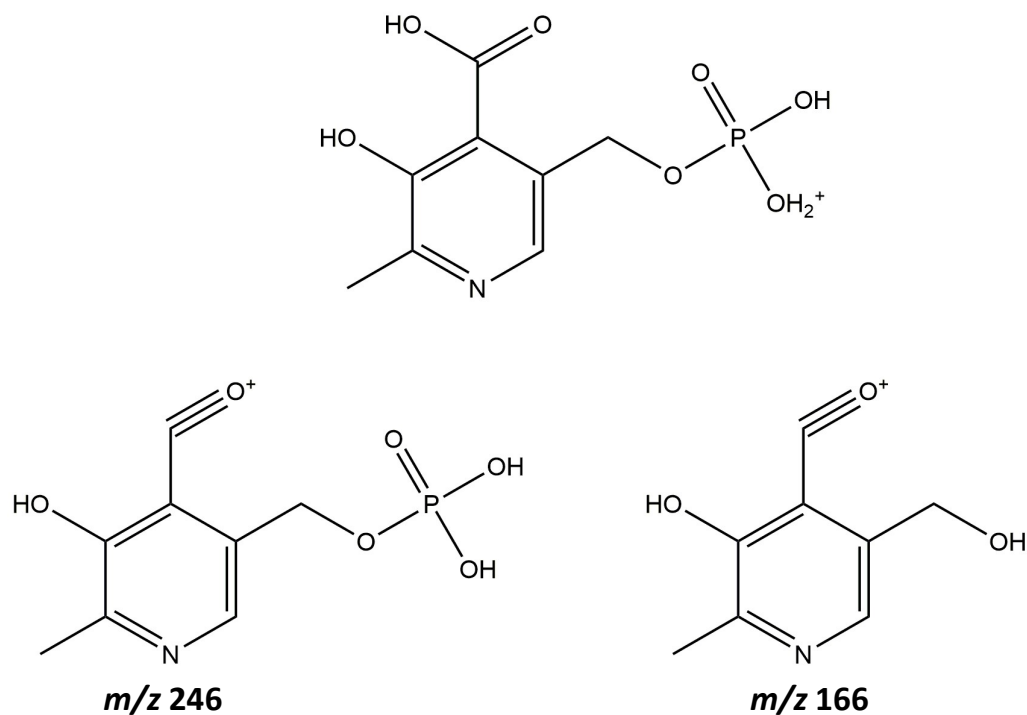


Figure 6.5: Postulated structures of MS fragments derived from *m/z* 264, identified as pyridoxic acid 5'-phosphate. At each data point $n=1$. AUC = area under curve. a) = known compounds; b) = postulated photodegradation products. Points below Y-axis graph limit were undetectable at this time point.

In order to confirm the identity of this compound, a custom synthesised PAP standard was purchased. Fragmentation of this was compared to of the compound of *m/z* 264; the patterns were found to be identical. Furthermore, the PAP standard eluted at the same retention time (0.82 min) as the previously identified compound of *m/z* 264 on LC-MS/MS analysis.

6.1.2 The effect of light irradiation on the rate of pyridoxal 5'-phosphate degradation and 4-pyridoxic acid 5'-phosphate formation

In order to accurately quantify the PAP formation from 1 mmol/L PLP over time, under conditions of light irradiation, samples were sealed and placed in a light box over a 24 hour period. PAP and PLP were quantified using d_3 -PLP as an internal standard; similar to the methodology used in **Section 3** for the quantification of B₆ vitamers and pyridoxic acid. The 1 mmol/L PLP solutions, after light irradiation for 0, 1, 4 and 24 h were frozen at -20°C until LC-MS/MS analysis at which time they were diluted to a nominal concentration of 100 nmol/L.

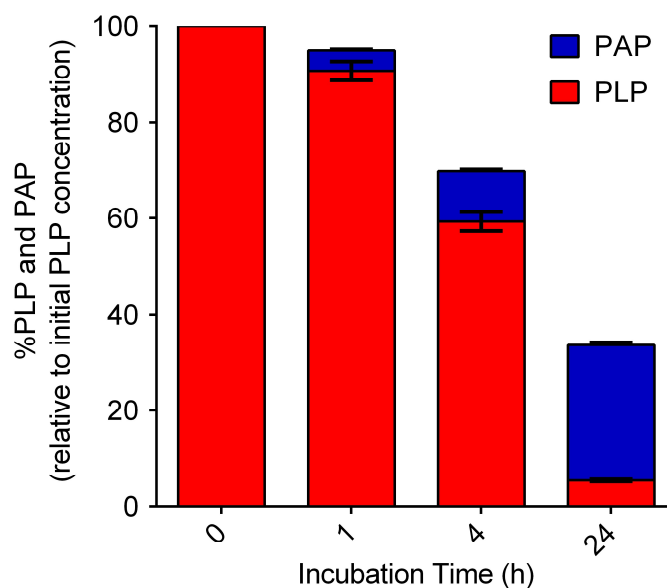


Figure 6.6: Percentage PLP and PAP levels after light irradiation. Error bars correspond to SEM. (n=3)

Quantification of PLP lost and PAP formed after 0, 1, 4 and 24 h of light irradiation is shown in **(Figure 6.6)**. Percentage loss or formation was calculated as a proportion of the original 100 nmol/L PLP concentration with 94.7% of the total PLP lost after 24 h of light irradiation. PAP formed over 24 h constituted only 22.7% (± 4.6), 20.2% (± 1.8) and 27.5% (± 4.6) of the 'missing fraction' of PLP after 1, 4 and 24 hours, respectively. This confirms work by Reiber (1972) showing that photolysis of PLP produces mostly compounds other than PAP, such as the diketone dimer with m/z 493.

6.2 Confirmation of a diketone pyridoxal 5'-phosphate dimer as a pyridoxal 5'-phosphate photodegradation product

As discussed in the introduction to this chapter, this project was part of a collaboration with the UCL School of Pharmacy. During their investigation of photodegraded PLP using HPLC-UV/VIS, these collaborators identified a major degradation product eluting before PLP. This compound had a different retention time to that of the pure PAP standard. The major PLP photodegradants identified by Reiber were described as the '288 nm absorbing species' due to their peak absorbance at this wavelength; the wavelength monitored during HPLC-UV/VIS analysis was 285 nm so an intense signal would be expected from these compounds. Collection of the HPLC eluent and spectrophotometric measurement between 200 – 500 nm showed that there was a compound that absorbed maximally at 296 nm (**Figure 6.7**), close to Reiber's '288 nm absorbing species'. PLP has an absorbance maximum of 388 nm and PAP 313 nm, hence the peak is unlikely to correspond to either of these compounds.¹⁰⁵

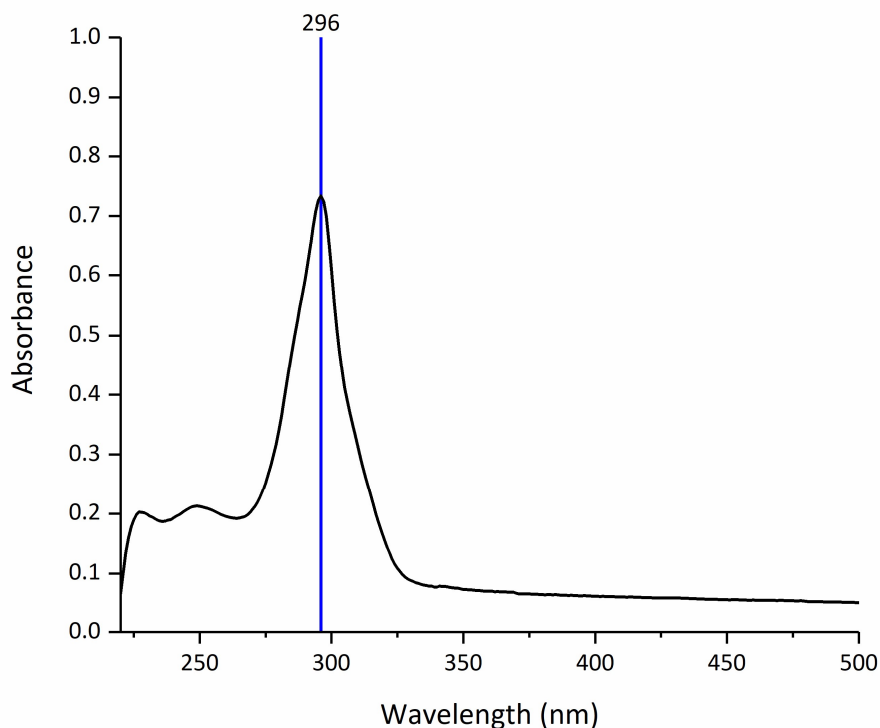


Figure 6.7: Absorbance spectrum of the HPLC eluent thought to be a PLP diketone dimer.

It was hypothesised that this peak with a maximal absorption of 296 nm corresponded to the postulated PLP dimer that had an m/z of 493 and eluted at 0.49 mins using the LC-MS/MS method shown in **Section 6.1**. A fraction derived from the HPLC-UV/VIS peak was analysed using an MS1 scan and flow injection analysis-mass spectrometry. As predicted, the most abundant ion identified had an m/z ratio of 493, with additional peaks at m/z of 395, 297, 515 and 247 (**Figure 6.8**). These were predicted to correspond to $[M+H-H_3PO_4]^+$, $[M+H-2(H_3PO_4)]^+$, $[M+Na]^+$ and $[M+2H]^{2+}$ of the diketone dimer shown in **Figure 6.3**.

This evidence provides yet further evidence that the peak at m/z 493 does indeed correspond to a PLP diketone dimer. However, the compound could not be accurately quantified as its predicted instability did not facilitate custom synthesis as for PAP. It is therefore unknown how much of the uncharacterised proportion of PLP photolysis products this dimer constitutes. This would be important future work.

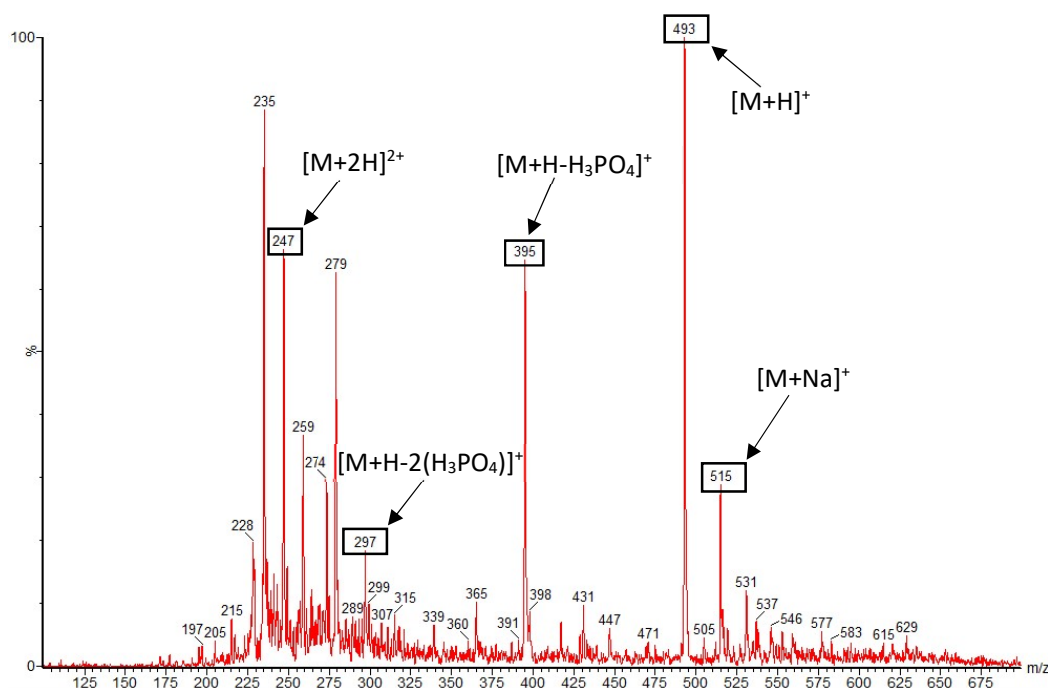


Figure 6.8: Mass spectrum of the eluent fraction thought to correspond to a PLP diketone dimer. Data collected using a MS1 scan 0 – 1000 Da; Cone voltage ramped between 0 – 27 V; Capillary Voltage = 2.5 kV; Source temp. = 150°C; Desolvation temp. = 150°C. m/z ratios of interest highlighted as appropriate.

6.3 Assessment of commercially available pyridoxal 5'-phosphate dietary supplements

Patients treated with PLP for seizure control in Europe and the United States currently have to rely on over-the-counter nutraceutical products. These are subject to less stringent regulation than pharmaceutically licensed compounds and are not recommended for clinical use. Indeed companies selling these products typically include disclaimers on their products such as 'This product is not intended to diagnose, treat, cure, or prevent any disease' (Thorne, New York, US). The dose that patients receive is titrated to that which allows seizure control and is often far higher than the dose that would be taken as a vitamin supplement by a healthy individual. Variation of PLP content between products could lead to inaccurate dosage and poor seizure control upon change of formulation.

We assessed the PLP content and photodegradation rate of several widely available nutraceutical PLP capsules/tablets from: Country Life, New York, US; Solgar, Aldbury, UK; Thorne, New York, US and Vitacost, Florida, US. Each brand of PLP was sold in capsules or tablets of 50 mg. A > 98% pure PLP standard (Applichem, Darmstadt, Germany) was also analysed.

Experimentation mimicked, as closely as possible, the procedure used to prepare PLP supplementation of patients with PLP-dependent epilepsy. When in tablet form, they were ground using a mortar and pestle before dissolution in Milli-Q H₂O at a concentration of 5 mg/mL (20.24 mmol/L PLP) and agitation for one hour in the dark to ensure all PLP was dissolved. Capsules were prepared by emptying the contents into MQH₂O, before preparation as above. After dilution to a nominal 100 nmol/L, PLP content was assessed using the LC-MS/MS-based method for B₆ vitamers quantification detailed elsewhere (**Section 2.4**).

Table 6.2: Quantification of PLP contained in 50 mg nutraceutical formulations.

Error = SD; n = 3 tablets/capsules analysed.

Formulation	Form	PLP (mg) measured from a 50 mg (nominal) capsule
Pure PLP (Applichem)	Powder	50.9 ±1.5
Countrylife	Tablet	3.0 ±2.0
Solgar	Tablet	43.0 ±15.7
Thorne	Capsule	60.0 ±10.0
Vitacost	Tablet	44.7 ±12.7

The recovery of pure PLP was accurate, with 50.9 ±1.5 mg measured from a nominal 50 mg (**Table 6.2**). However, other formulations had variable PLP content. The Countrylife formulation contained only 3.0 ±2.0 mg within a tablet purported to contain 50 mg. Tablets/capsules from Solgar, Thorne and Vitacost had PLP contents of 43.0 ±15.7, 60.0 ±10.0 and 44.7 ±12.7 mg, respectively. However, the variability of PLP measurement was large for these products and 50 mg was within the error of measurement for each of them (< 1 SD). This variability was not due to poor precision of the LC-MS/MS assay for PLP measurement: The coefficient of variation for PLP quantitation using this method was determined previously as < 5% at all concentrations tested (**Section 4.1.2.4**). It is unlikely that PLP was still bound to excipients in the formulations as TCA was used in the method, this cleaves PLP bound to proteins or other molecules, bringing PLP into solution.

Preparations were also analysed for the presence of other B₆ vitamers to ensure that PLP was indeed the main B₆ vitamer within them. No other B₆ vitamers were detected above the lower limit of quantification (< 0.25 mg per tablet/capsule).

It was shown in **Figure 6.5** that 94.7% of a 1 mmol/L solution of PLP was photodegraded after 24 hours of light irradiation. This experiment was repeated with a higher concentration of 5 mg/mL (20.24 mmol/L) to mimic clinical preparation, alongside the same nutraceutical products investigated previously (**Table 6.3**). Light irradiation was carried out at room temperature after mixing for 60 minutes in the dark to solubilise PLP. It was hypothesised that if PLP was bound to excipients found in the tablets/capsules sold as nutraceuticals, this could convey some protection from photodegradation. This would be analogous to the binding of PLP to albumin in the blood.

Table 6.3: Proportion of PLP lost and PAP formed on light irradiation of 5 mg/mL PLP formulations.

Error = SD; N = 3. *For the Countrylife tablet, PLP lost was expressed as > 91.7% as remaining PLP after 24 hours light irradiation was below 0.25 mg, meaning more than 91.7% of the original 3.0 mg had been photodegradation. Light irradiation was for 24 hours.

Formulation	Form	PLP lost (% of initial PLP)	PAP Formed (% of PLP lost)
Pure PLP (Applichem)	Powder	83.5 ±2.7	27.5 ±0.7
Countrylife	Tablet	> 91.7*	22.9 ±10.2
Solgar	Tablet	81.2 ±3.7	23.1 ±5.3
Thorne	Capsule	78.4 ±9.3	26.6 ±11.5
Vitacost	Tablet	84.0 ±11.1	18.7 ±10.6

No significant difference ($p < 0.05$) was identified when comparing the rate of PLP photodegradation or PAP formation between any of the formulations studied. A pure PLP solution at 20.24 mmol/L revealed a slightly lower photodegradation rate at 83.5% after 24 hours compared to 94.7% from a 1 mmol/L solution. This correlates with previous reports that PLP photolysis occurs at a slower rate at higher concentrations.²⁴⁴ The proportion of PAP formed as a percentage of PLP lost was identical in the 20.24 and 1 mmol/L solutions, at 27.5%.

One limitation of the work detailed in this section is the wide variability between repeated analyses of each product. Vials were divided into separate 2.5 ml vials for light irradiation. Insoluble excipients were present in all of the formulations, these were homogenised before division. It is possible, if PLP was bound to excipients in the formulations, that an uneven amount of PLP was divided between these vials due to incomplete homogenisation, accounting for the variability identified. This is supported by accurate recovery of the pure PLP solutions; these were fully dissolved and contained no excipients.

Further investigation into the composition of commercially available PLP nutraceutical products was carried out by the aforementioned collaborators at the UCL School of Pharmacy and is detailed in our recently published manuscript.¹⁰⁴

6.4 Discussion & future work

The confirmation of PAP and a diketone PLP dimer as photodegradants of PLP was a useful step towards determining the pathogenic mechanism behind liver damage in PNPO deficient individuals receiving PLP for seizure treatment. It appeared that a large proportion of degraded PLP was unaccounted for by PAP formation and that other uncharacterised and potentially hepatotoxic photodegradants are produced.

Morrison and Long²⁴⁴ observed the formation of a dihydroxy PLP dimer in place of a diketone dimer upon the light irradiation of PLP in the absence of oxygen. No evidence of this dihydroxy dimer was identified in our work. Indeed, prior to the incubation of PLP, each mixture was stirred for 30 – 60 minutes to ensure that all PLP was in solution. This likely oxygenated the solution and made dihydroxy dimer formation undetectable. Morrison and Long created an oxygen-free solution by purging with nitrogen gas.

PAP is known to inhibit transaminases and could potentially be hepatotoxic.^{33, 251-252} However, it is unlikely to cross the gut barrier before hydrolysis to PA, the natural excretory product of vitamin B₆ in humans. PAP is therefore unlikely to cause the hepatic cirrhosis seen in patients on high doses of PLP. As PAP accounts for only 20-30% of the PLP photodegradants, it does not rule out the implication of another compound.

A study at the Department of Pharmaceutical and Pharmacological Sciences in Leuven, Belgium, has recently been published regarding the identity of the additional degradation products.²⁵³ That study closely mirrored our work and further confirmed the formation of PAP and a diketone dimer upon the photodegradation of PLP. They also identified 4-pyridoxolactone (m/z 166) as a degradation product and proposed several others, including one that may explain the identity of the ion of m/z 381 in our study. However, they did not quantify these compounds or determine their potential hepatotoxicity.

In the future, determining whether the PLP photodegradants identified are present in the blood of patients receiving high-dose PLP supplementation would be a priority. This would help determine whether they could be hepatotoxic and indeed whether they are even absorbed after oral ingestion.

The most severe example of hepatotoxicity in a PNPO deficient patient is that of a 13-year-old who, after chronic liver dysfunction, developed hepatocellular carcinoma on PLP supplementation of > 50 mg/kg/d (unpublished communication). Otherwise this individual was healthy and developmentally normal. The patient received a liver transplant; it was hoped a healthy liver with intact PNPO activity would reduce PLP dependency and facilitate a move towards PN supplementation. However, the patient remained PLP dependent at a similar dose (both intravenous and oral; withdrawal or weaning produced seizures) and did not respond to PN supplementation. This indicates the importance of organ-specific rather than systemic B₆ metabolism in providing adequate PLP to the brain.

The fate of the donor liver given to this individual will be interesting. If damaged over time, high B₆ vitamer concentrations or PLP photodegradants would be implicated in the liver pathology. If not, it would indicate that the PNPO deficiency itself is causative. A combination of these factors is perhaps likely. For example, it is known that high PNP and PMP levels are present in the blood of PNPO deficient patients. If these were causing liver damage, in a liver with intact PNPO activity these could be metabolised to PLP and eventually excreted as PA, sparing the liver. It is known that high concentrations of PN can inhibit PLP-dependent enzymes, this is thought to be the mechanism behind pyridoxine-induced peripheral neuropathy.¹¹⁰ It remains to be seen whether any PNPO-deficient patients receiving PN for seizure treatment develop liver dysfunction, to our knowledge however this has not yet been seen.

Part of the difficulty identifying the pathology behind hepatic dysfunction in these PNPO deficient patients is that most known individuals are still in childhood due to the relatively recent discovery of PNPO deficiency as an inborn error of metabolism. Indeed, this work is given greater urgency by the worry that, as these patients age, hepatic dysfunction could become a more common presentation. In addition, it appears that at least some PNPO deficient patients can have a good quality of life with no developmental delay if treated appropriately.^{65, 87} Making this treatment safe would be a major step towards the long-term wellbeing of these individuals.

A priority would be the development of a reliable pharmaceutically licensed formulation of PLP, to ensure accurate dosage. For example, the low amounts of PLP solubilised in the product sold by Countrylife is particularly dangerous, given that non-response to these supplements can be taken to be diagnostically indicative of a seizure disorder that does not respond to PLP.

7. THE IDENTIFICATION OF NOVEL GENETIC CAUSES OF VITAMIN B₆-RESPONSIVE EPILEPSY

Since the identification of vitamin B₆-dependent epilepsy by Hunt *et al.* over 60 years ago²⁴⁰, considerable effort has been spent identifying the underlying genetic causes of these inherited disorders. In the last 15 years, mutations in the *ALDH7A1*, *PNPO* and *PLPBP* genes have been identified as being causative of B₆-dependent epilepsies. However, it has become clear that variants in these genes cannot explain all the seizure disorders that are treatable by vitamin B₆ supplementation. Wang *et al.* showed that 11/94 patients with idiopathic intractable epilepsy showed a dramatic and sustained response to PLP supplementation.¹¹³ Ohtahara *et al.* reported that a similar proportion of individuals with West Syndrome responded to vitamin B₆ supplementation (13.9% of 216 individuals) and that treatment was effective in patients both with and without identifiable brain pathologies.¹¹⁴ In Japan vitamin B₆ supplementation is used more widely than in Europe or the US with 67.4% of institutions using vitamin B₆ as the first choice drug for the treatment of West Syndrome.²⁵⁴

It is currently uncertain whether the anti-epileptic effect of pharmaceutical doses of vitamin B₆ is because higher PLP levels allow the brain to better control concentrations of excitatory and inhibitory neurotransmitters at the synapse (see **Section 1.1**), or whether other mechanisms are responsible. For example, it is possible that the neuroinflammation caused by ATP-mediated activation of P2X7 receptors is antagonised by high PLP concentrations thus halting the feedback loop of neuronal inflammation caused by ATP release that can lead to the kindling of further seizures.⁴⁸⁻⁵⁰

Understanding the mechanism behind the anticonvulsant effect of vitamin B₆ could help us to understand which genetic epilepsies are likely to benefit from vitamin B₆ supplementation as their mechanisms can vary wildly. For example, if B₆ was effective as a sodium channel agonist/antagonist this treatment could be useful in channelopathies such as *SCN1A*-related epilepsy (MIM: [182389]) but less so in mTORopathies causing structural changes (e.g. focal cortical dysplasia) such as focal epilepsy due to *DEPDC5* mutations (MIM: [614191]).

7.1 Investigation of individuals with B₆-responsive epilepsy using next generation sequencing technology

Genetic causes are thought to be responsible for 70 – 80% of epilepsy cases.²⁵⁵ Currently, the first stage of genetic testing is often targeted sequencing of specific candidate genes or a gene panel containing a number of potential candidate genes.²⁵⁶ If this is unsuccessful in achieving a diagnosis, it is possible to use either whole exome or whole genome sequencing (WES or WGS) to identify a genetic basis for the patient's seizures. This is important for the identification of novel genetic disorders and valuable in providing a diagnosis for the patients and their families.²⁵⁷ In addition, NGS technologies can identify mutations that are not found using more targeted techniques (e.g. intronic variants).²⁵⁸ For these reasons, as well as continually diminishing prices as the technology matures, the use of WES and WGS as a first-line diagnostic tool for epilepsy is increasing.²⁵⁹

This chapter describes the investigation of five individuals with vitamin B₆-responsive epilepsy using whole exome/genome sequencing. These patients had thus far escaped diagnosis by more targeted approaches. It was hoped that novel disorders conveying B₆-responsive epilepsy would be identified through the investigation of potentially pathogenic variants in these individuals; thereby providing a diagnosis for these patients.

After filtering according to parameters detailed in **Section 7.1.1**, the variants predicted as potentially pathogenic in these individuals were manually assessed. Specific attention was paid to variants in genes encoding proteins associated with vitamin B₆ metabolism, known/predicted epileptic loci and PLP-dependent enzymes.

7.1.1 Assessment of variants identified using NGS technology that could lead to B₆-dependent epilepsy

DNA was extracted from whole blood. In four cases (**Subjects NGS1, NGS2, NGS4 and NGS5**), the DNA was sequenced by the Universitair Medisch Centrum Groningen (UMCG). In one case (**Subject NGS3**), data was sent to BGI Genomics (Hong Kong) for sequencing, in collaboration with GOSgene (UCL GOS Institute of Child Health). In all cases, the raw data was processed and aligned by GOSgene (UCL GOS Institute of Child Health). All patients included in this study presented with a previously intractable seizure disorder that responded to vitamin B₆ supplementation. In all cases, known causes of B₆-dependent epilepsy were already excluded either genetically or biochemically (e.g. ALDH7A1, PLPHP, PNPO deficiencies, hypophosphatasia).

The QIAgen Ingenuity Variant Analysis (IVA) pipeline was used in order to assess the pathogenicity of each variant identified. This utilises a cascade of filters in order to exclude variants that are unlikely to be pathogenic, leading to the identification of a relatively small number of variants that can then be manually assessed. Typically, for WGS, this results in the reduction of variants identified from >5,000,000 to <10, depending on the exact parameters used for filtering. **Figure 7.1** gives a summary of these filters and the default parameters used for analysis can be found in **Section 2.11**.

Whereas the first three layers in the filtering cascade (i.e. 'call confidence', 'common variants' and 'predicted deleterious') were kept consistent, the filters for inheritance and for biological context were adjusted for each patient. Where available, parental DNA was compared to that of the patients in order to identify the mode of inheritance. The genes interrogated with regard to biological context included, unless specified: i) a list of 112 genes known to use vitamin B₆ as a cofactor or implicated in vitamin B₆ metabolism ii) 73 genes on the early infantile epileptic encephalopathy (EIEE) panel used by GOSH iii) 237 genes known to code for ion channels in the human genome. A complete list of these genes can be found in the appendix (**Section 9.2**). Visualisation of identified variants was carried out using the Integrated Genomics Viewer (IGV) software package in order to exclude sequencing artefacts that were not automatically excluded by IVA.

The following **Sections 7.1.1.1 – 7.1.1.4** describe the five patients with B₆-responsive epilepsy investigated using NGS technologies. A brief case report of each individual is included before a summary of the potentially pathogenic variants identified and a discussion of these variants within the context of their disorders.

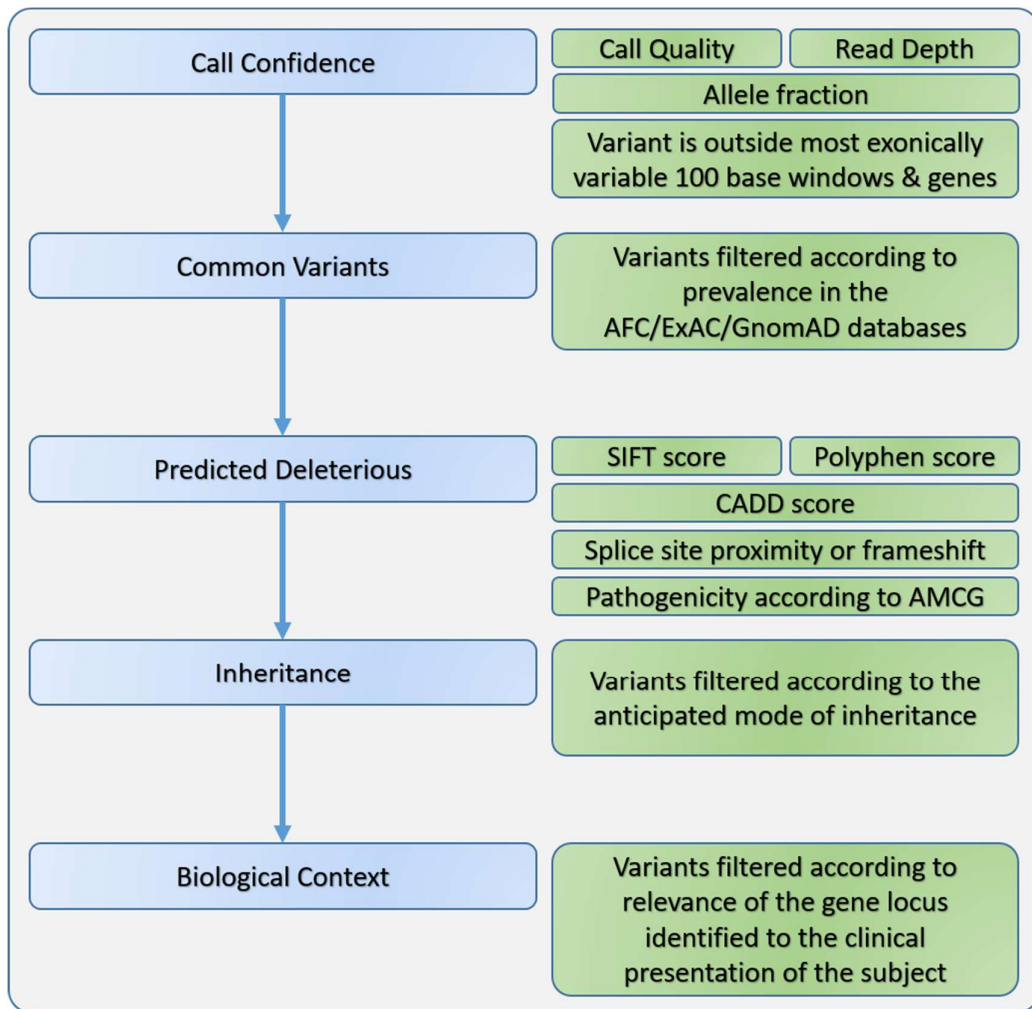


Figure 7.1: Summary of the filter cascade used for variant analysis. Blue boxes = level of the filter cascade; filtering is carried out sequentially from top to bottom. Green boxes = description of the parameters used at each level of filtering. More detailed parameters for each filter can be found in **Section 2.11**. Analysis performed using the QIAgen Ingenuity Variant Analysis software tool. AFC = Allele Frequency Community; ExAC = Exome Aggregation Consortium; GnomAD = Genome Aggregation Database; CADD = Combined Annotation Dependent Depletion; SIFT = Sorting Intolerant from Tolerant; AMCG = American College of Medical Genetics.

7.1.1.1 Subject NGS1

The following clinical and biochemical data was provided by the treating clinician at the Universitair Medisch Centrum Groningen (UMCG), The Netherlands. WGS data was provided to us by the UMCG in order to assist in the diagnosis of this patient. No parental WGS data was supplied so filtering according to inheritance was not possible. However, parental DNA was available so where appropriate segregation could be checked using Sanger sequencing.

Subject NGS1 was a male born at 35 weeks whose seizures began hours after birth. Brain MRI was normal. Seizures did not resolve with midazolam. At day 4 IV pyridoxine was introduced (dose unknown). At day 6 EEG showed less intensive multifocal epileptic features than an earlier EEG. At day 8 he was switched from pyridoxine to oral pyridoxal 5'-phosphate (30 mg/kg/day). Over the next several days he improved clinically with fewer seizures. At day 10 levetiracetam was introduced. Thereafter, seizures have been well controlled with breakthrough seizures treated by increases of levetiracetam dosage.

Biochemical studies in the neonatal period at the UMCG showed normal plasma alkaline phosphatase and urinary α -AASA (0.3 $\mu\text{mol}/\text{mmol}$ creatinine), excluding hypophosphatasia and pyridoxine-dependent epilepsy due to mutations in *ALDH7A1*, respectively. PNPO and PLPHP deficiencies were also excluded by sequencing the *PNPO* and *PLPBP* genes. At day 6, when the patient was receiving pyridoxine supplementation, CSF analysis showed low tyrosine (1 $\mu\text{mol}/\text{L}$; ref 11-53 $\mu\text{mol}/\text{L}$) and slightly low homovanillic acid (HVA) (419 nmol/L; ref 543 – 1102 nmol/L). 5-hydroxyindoleacetic acid (5-HIAA) was normal. Concentrations of other neurotransmitters and amino acids were normal. Low HVA could indicate PLP deficiency through a secondary AADC deficiency but low tyrosine and normal 5-HIAA dispute this conclusion.

Table 7.1: CSF B₆ Vitamers and pyridoxic acid concentrations in Subject 1. ND = not detected. Subject 1 was receiving pyridoxine supplementation.

B ₆ vitamer	Concentration nmol/L (ref. range)
Pyridoxal 5'-phosphate	16.5 (7-23)
Pyridoxamine 5'-phosphate	ND (0-0)
Pyridoxal	6110 (12-48)
Pyridoxine	2700 (0-0)
Pyridoxamine	84 (0-0.1)
Pyridoxic acid	629 (0.4-15.5)

CSF B₆ vitamers were also measured at this stage at the UMCG (**Table 7.1**). As the patient was receiving pyridoxine supplementation of an unknown dose, it was difficult to draw definitive conclusions from B₆ vitamer concentrations. However, it was intriguing that the concentrations of pyridoxal, pyridoxine, pyridoxamine and pyridoxic acid were raised well above reference ranges but PLP was within the normal range. Although not as high as other vitamers, CSF PLP is usually raised in patients receiving pyridoxine supplementation.²⁶⁰ A very high pyridoxal/pyridoxal 5'-phosphate ratio could indicate pyridoxal kinase deficiency; this was investigated during NGS analysis but no abnormalities were found in the *PDXK* gene or in the PAR bZip transcription factors (*DBP*, *HLF* and *TEF*), known to modulate the expression of *PDXK*.

Data was analysed using the IVA pipeline (**Section 2.11**) and nine variants considered most likely to cause this patient's B₆-responsive seizures were identified (**Table 7.2**).

One variant identified was the heterozygous change c.6471C>A in *CACNA1A*. The *CACNA1A* gene encodes a protein subunit of the P/Q-type calcium channel. Autosomal dominant mutations in *CACNA1A* are known to cause several disorders including familial migraines [MIM: 141500], episodic ataxia [MIM: 108500] and early

infantile epileptic encephalopathy [MIM: 617106]. Furthermore, there is one report of a patient with a *de novo* variant in *CACNA1A* with absence seizures treatable by pyridoxine supplementation.²⁶¹ This evidence alongside the fact that this variant had not previously been seen in GnomAD led to the further investigation of the possible pathogenicity of this variant. However, the missense change caused by c.6471C>A is relatively mild (aspartic acid > glutamate), introducing just one additional CH₂ in the amino acid side-chain. Accordingly, this variant was predicted tolerated/benign by the SIFT/Polyphen variant pathogenicity analysis tools, respectively. Sanger sequencing of parental DNA revealed that the heterozygous c.6471C>A variant was inherited maternally and was not a *de novo* variant. The optimised primers and conditions used for this analysis can be found in the appendix (**Section 9.1**). Episodic ataxia caused by mutations in *CACNA1A* is known to have incomplete penetrance.²⁶² However, in this case with the relatively severe clinical presentation, it was considered unlikely that this *CACNA1A* variant was causing the severe neonatal epileptic phenotype of **Subject NGS1**.

Table 7.2: Candidate variants that may be causative for the B₆-responsive seizures of Subject NGS1. Variants identified using whole genome sequencing. Data filtered according to the parameters defined in **Sections 2.11 & 9.1**. Ppi = inorganic pyrophosphate; ECM = extracellular matrix; PIP = phosphatidylinositol phosphate

Gene	Mutation; Amino acid change	Zygosity	Prevalence; gnomAD (no. of homozygotes)	Protein function [UniProtKB – ref]	SIFT/Polyphen prediction	Most relevant disease association & observations
CACNA1A	c.6471C>A; p.D2157E	Heterozygous	Novel	Voltage-dependent P/Q-type calcium channel subunit [UniProtKB - O00555]	SIFT: Tolerated Polyphen: Benign	Autosomal dominant epileptic encephalopathy. Also linked to migraines and episodic ataxia (MIM: [601011]).
SLC15A5	c.1403T>C; p.M468T	Homozygous	0.002% (0 homozygotes)	Protein oligopeptide cotransporter (proton symporter) [UniProtKB - A6NIM6]	SIFT: Damaging Polyphen: Probably damaging	Unknown - mostly uncharacterised protein. 50% homology to other SLC15 proteins. Poor expression in almost all tissues studied. ²⁶³ Gene only present in vertebrates. Met468 not conserved in zebrafish.
ZIC1	c.761C>T; p.T254M	Heterozygous	Novel	Acts as a transcriptional activator. Involved in neurogenesis. [UniProtKB – Q15915]	SIFT: Damaging Polyphen: Probably damaging	Autosomal dominant craniosynostosis and intellectual disability – but not linked to seizures (MIM: [616602]).
GRIK3	c.2599C>T; p.R867C	Heterozygous	0.002% (0 homozygotes)	Glutamate receptor ionotropic, kainate 3 [UniProtKB – Q13003]	SIFT: Tolerated Polyphen: Possibly damaging	Autosomal recessive GRIK2 mutations cause developmental delay. In addition, het deletion of GRIK3 is linked to developmental delay. ²⁶⁴

<i>PI4KB</i>	c.110T>G; p.V37G	Heterozygous	Novel	Phosphatidylinositol 4-kinase beta – first committed step in PIP synthesis [UniProtKB – Q9UBF8]	SIFT: Damaging Polyphen: Benign – often V>L or A	Not linked to disease but a well-conserved gene – Loss of function and missense variants are rare.
<i>RUBCN</i>	c.3050T>G; p.L1017R	Heterozygous	0.033% (0 homozygotes)	Negatively regulates PI3K complex II (PI3KC3-C2) function in autophagy – late endosome maturation [UniProtKB – Q92622]	SIFT: Damaging Polyphen: Probably damaging	Spinocerebellar ataxia, autosomal recessive. (MIM: [613516]). Also causes developmental delay and epilepsy but heterozygotes unaffected.
<i>TRIM9</i>	c.265A>C; p.T89P	Heterozygous	Novel	E3 ubiquitin-protein ligase; may play a role in regulation of neuronal functions [UniProtKB – Q9C026]	SIFT: Tolerated Polyphen: Benign	Not linked to disease but a well-conserved gene – loss of function and missense variants are rare.
<i>ANKH</i>	c.959C>T; p.T320M	Heterozygous	0.001% (0 homozygotes)	Regulates intra- and extracellular levels of inorganic pyrophosphate (PPi), probably functioning as PPi transporter. [UniProtKB – Q9HCJ1]	SIFT: Damaging Polyphen: Possibly damaging	Extrudes intracellular PPi to the ECM. Mutations cause craniometaphyseal dysplasia and chondrocalcinosis (autosomal dominant). (MIM: [605145])
<i>NOTCH1</i>	c.508A>G; p.K170E	Heterozygous	Novel	Signalling and cell fate during development. [UniProtKB – P46531]	SIFT: Damaging Polyphen: Possibly damaging	Autosomal dominant Adams-Oliver syndrome (aplasia cutis congenita + terminal limb defects) (MIM: [190198]) - specific phenotype with no epilepsy.

The segregation of c.1403T>C (p.M468T) in *SLC15A5* was analysed using Sanger sequencing. Primers were designed and optimised for analysis; conditions can be found in the appendix (**Section 9.1**). Both parents were heterozygous for this variant and **Subject NGS1** was confirmed homozygous, fitting a classical autosomal recessive inheritance pattern. No homozygotes have been reported in GnomAD (0.002% allele frequency) and the variant is predicted to be damaging by both SIFT and Polyphen. To our knowledge, no pathogenic variants in *SLC15A5* have been previously identified that lead to B₆-responsive seizures or indeed any other disorder.

The protein encoded by *SLC15A5* has been assigned, by sequence similarity, to a family of 5 promiscuous di/tripeptide transporters and likely has a similar function, though this has not been characterised. Orthologues of the gene are present in all vertebrates but *SLC15A5* is poorly expressed in all human tissues studied.²⁶³

Functional studies are therefore needed to elucidate the function of the *SLC15A5* transporter and whether it has a role in the metabolism of vitamin B₆. However, the closely related *SLC15A3* & 4 transporters are known to transport histidine as well as di/tripeptides.²⁶⁵ *SLC15A4* transports carnosine, a histidyl dipeptide and effective carbonyl scavenger.²⁶⁶ Carbonyl scavengers are depleted in PLPHP deficiency, presumable due to their reaction with 'unprotected' PLP. If *SLC15A5* also transports histidyl dipeptides such as carnosine these could be accumulating and producing a localised PLP deficiency by reacting with free PLP.

In addition, PLP is the cofactor for histidine decarboxylase (HDC), the enzyme responsible for histidine conversion to histamine (**Table 1.1**). Autosomal dominant mutations in HDC are linked to Tourette syndrome.²⁶⁷ It is feasible that a tissue-specific histidine or histamine deficiency caused by impaired histidine transport (due to impaired *SLC15A5* function) could manifest as a neurological disorder treatable by vitamin B₆ supplementation, though this remains purely speculative.

7.1.1.2 Subject NGS2

Less clinical and biochemical information is available for this patient. They presented with intractable seizures within hours of birth up to the age of 1.5 years, culminating in up to 30 seizures per day. The patient was severely developmentally delayed, with no psychomotor development. The only treatment thought to have any effect on seizure frequency was PLP supplementation. This was eventually stopped due to excessive vomiting, a documented side-effect of oral PLP administration.¹⁰⁴

Parental DNA was not available for analysis via the WGS pipeline. It was therefore not possible to filter variants according to inheritance for this individual. Otherwise, standard filters were used for analysis through the IVA pipeline. The seven best candidate variants are detailed in **Table 7.3**.

The variant considered most likely to be pathogenic in this patient was identified in the *GABRD* gene. This was a heterozygous missense change, c.1156A>T (p.N386Y). This variant has been reported only once previously, in heterozygote form, in gnomAD (238,052 alleles). It is predicted to be damaging by SIFT but benign by Polyphen. Heterozygous *GABRD* variants have previously been linked to epilepsy susceptibility; *GABRD* encodes the δ -subunit of the GABAA receptor.²⁶⁸ Given the important function PLP has as a cofactor for the biosynthesis and degradation of GABA, it is feasible that epilepsy caused by GABA receptor dysfunction would respond to vitamin B₆ supplementation. Parental DNA was not available to confirm whether the variant was *de novo* and hence more likely to be considered pathogenic; this has been previously suggested as the mode of inheritance for *GABRD*-related epilepsy. This analysis emphasises the importance of parental DNA for the diagnosis of genetic epilepsies, particularly as many of these disorders are caused by *de novo* heterozygous mutations.

Table 7.3: Candidate variants for the B₆-responsive seizures of Subject NGS2. Variants identified using whole genome sequencing. Data filtered according to the parameters defined in Sections 2.11 & 9.1. GEFS+ = Generalized epilepsy with febrile seizures plus; kb = 1,000 base pairs. CoA = Coenzyme A; ADP = adenosine diphosphate; A3,5BP = adenosine 3',5'-bisphosphate.

Gene	Mutation; Amino acid change	Zygosity	Prevalence; gnomAD (no. of homozygotes)	Protein function [UniProtKB – ref]	SIFT/Polyphen prediction	Most relevant disease association & observations
GABRD	c.1156A>T; p.N386Y	Heterozygous	0.001% (0 homozygotes)	GABA(A) receptor subunit delta [UniProtKB – O14764]	SIFT = Damaging PolyPhen = Benign	Dibbens <i>et al.</i> ²⁶⁸ found heterozygous mutations in GABRD (E177A + R220H) in two families with GEFS+ and identified them as susceptibility factors for generalised epilepsy (MIM: [137163]).
CPZ	c.817C>T; p.R273C,	Homozygous	0.092% (1 homozygote)	Cleaves substrates with C- terminal arginine residues [UniProtKB – Q66K79]	SIFT = Probably damaging PolyPhen = Possibly damaging	Low CPZ activity interrupts the effect of thyroid hormone on alkaline phosphatase and Col10a1 expression. ²⁶⁹
TRIM17	c.525+2T>G; predicted to affect splicing + c.525+6T>G; predicted to affect splicing	Compound heterozygous	0.081%; 0.008% (0 homozygotes; 0 homozygotes)	E3 ubiquitin-protein ligase [UniProtKB – Q9Y577]	+2, +6 splice site mutations so not analysed using SIFT/Polyphen +2 predicted damaging, +6 not damaging when using the human splicing finder tool. ¹⁹⁴	Thought to control neuronal apoptosis + autophagy.

TRIM21	c.1055A>G; p.E352G	Heterozygous	0.013% (0 homozygotes)	E3 ubiquitin-protein ligase [UniProtKB – P19474]	SIFT = Damaging PolyPhen = Possibly Damaging	TRIM21 is thought to ubiquitinate proteins, leading to protein degradation. ²⁷⁰
SLC25A42	c.499T>G; p.Y167D	Heterozygous	0.021% (0 homozygotes)	Mitochondrial CoA/ADP or A3,5BP cotransporter (CoA import) [UniProtKB – Q86VD7]	SIFT = Damaging PolyPhen = Possibly Damaging	Deficiency causes a newly identified mitochondrial myopathy ²⁷¹ (MIM: [610823])
ANK2	c.6884C>T; p.T2295I	Heterozygous	Novel	Required for proper localisation of several ion channels in the heart and in rod photoreceptors [UniProtKB – Q01484]	SIFT = Tolerated PolyPhen = Benign	Linked to cardiac dysfunction + long QT syndrome but no direct epilepsy link (MIM: [106410]).
SLC6A3 (DAT1)	c.1676>T; p.A559V	Heterozygous	0.042% (0 homozygotes)	Dopamine transporter. Terminates the action of dopamine by its high affinity sodium-dependent reuptake into presynaptic terminals [UniProtKB – Q01959]	SIFT = Tolerated PolyPhen = Benign	Homozygous mutations lead to neonatal dystonia/hypotonia, in one case misdiagnosed as EE. ²⁷² Leads to high HVA and high HVA/5-HIAA ratio. Inheritance is autosomal recessive although in one patient was as a result of an 8.1kb deletion (MIM: [126455]).

7.1.1.3 Subject NGS3

Subject NGS3 was a patient treated at Great Ormond Street Hospital (GOSH). She was hypotonic from birth with stereotypic movements, microcephaly and infantile spasms with a spike-wave pattern rather than the more common hypsarrhythmia on EEG analysis. The patient was also developmentally delayed. Seizures were resistant to standard antiepileptic drugs but well controlled by PLP supplementation. The use of PLP appeared to improve developmental progress but delay was still apparent. Known genetic causes of vitamin B₆-dependent epilepsy (mutations in *PNPO*, *ALDH7A1*, *PLPBP*) were excluded through genetic testing and the GOSH early infantile epileptic encephalopathy (EIEE) gene panel did not reveal any causative mutations.

WGS analysis was performed as described previously. Maternal DNA was also analysed and filtering was therefore adjusted according to predicted inheritance patterns. Paternal DNA was unavailable for both initial WGS and Sanger sequencing to study the segregation of identified variants. The seven candidate variants identified are summarised in **Table 7.4**. The variants thought most likely to lead to the phenotype are discussed in more detail below. None of these variants are in genes known to be directly linked to vitamin B₆ metabolism.

Two potentially deleterious heterozygous variants were identified in the *SLC4A3* gene. This encodes a widely expressed Cl⁻/HCO₃⁻ anion exchange protein, known to be particularly important for regulating the intracellular pH of neurones. A known variant in *SLC4A3* is linked to epilepsy in humans²⁷³ and in mice disruption of this gene leads to a reduced seizure threshold.²⁷⁴ Although poorly understood, dysregulation of intracellular pH is thought to lead to the promotion of neuronal hyperexcitability.²⁷⁵ The *SLC4A3* variants identified were c.815A>G (p.H272R) and c.-318_-306delCCGCGCGTGGGGG, both variants were heterozygous. c.815A>G is a novel missense variant, not reported in GnomAD and predicted to be damaging by both Polyphen and SIFT. c.-318_-306delCCGCGCGTGGGGG is also not reported in GnomAD and lies in a gene regulatory area, according to the USCS genome browser.

It is possible that these variants together could be pathogenic as the result of a compound heterozygous inheritance pattern (one variant from each parent). However, maternal DNA showed that neither of these variants were present in heterozygous form, excluding this mode of inheritance. It remains possible that one

of these variants was inherited from the father of **Subject NGS3** while the other was *de novo*. However, paternal DNA was not available to confirm or exclude this possibility.

Table 7.4: Candidate variants for the B₆-responsive seizures of Subject NGS3. Variants identified using whole genome sequencing data filtered according to the parameters defined in Sections 2.11 & 9.1. TFAP2A = Transcription factor AP-2 alpha.

Gene	Mutation; Amino acid change	Zygosity	Prevalence; gnomAD (no. of homozygotes)	Protein function [UniProtKB – ref]	SIFT/Polyphen prediction	Most relevant disease association & observations
SLC4A3 (AE3)	c.815A>G;p. H272R + c.- 318_- 306delCCGC GCGTGGGG G	Compound heterozygous	c.815A>G;p.H272R = novel c.-318_- 306delCCGCGCGTGG GGG = 0.014% (0 homozygotes)	Mediates neuronal pH via Cl ⁻ /HCO ₃ ⁻ exchange. [UniProtKB – P48751]	(c.815A>G;p.H272R) : SIFT = Damaging; PolyPhen = Probably damaging. (c.-318_- 306delCCGCGCGTGGGGG) lies at a TFAP2A binding site.	Linked to epilepsy through the regulation of intracellular pH of neurones but no patients identified with pathogenic SLC4A3 variants. ²⁷³⁻ 275
ALG13	c.2338T>G; p.L780V	Homozygous	0.012% (0 homozygotes; 20 hemizygotes)	Glycosylation and possibly deubiquitination. [UniProtKB – Q9NP73]	SIFT = Tolerated PolyPhen = Likely Benign	Congenital disorder of glycosylation (MIM: [300776]) – X-linked dominant mutations can lead to early infantile epileptic encephalopathy.
GRK2	c.859G>A, p.G287R	Heterozygous (not found in mother - ? <i>de novo</i> if not inherited from father)	Novel	Responsible for short- term desensitization of the potassium channels GIRK1 (KCNJ3; MIM: [601534]) and GIRK4 (KCNJ5; MIM: [600734]). [UniProtKB – P25098]	SIFT = Damaging Polyphen = Probably Damaging	Low levels induce glutamate-mediated neuronal death in a cell model. ²⁷⁶ However, in mouse models only linked to cardiac dysfunction. ²⁷⁷

<i>RAB5A</i>	c.313C>T; p.Q105*	Heterozygous	Novel	Required for the fusion of plasma membranes and early endosomes. GTP regulated. RAB5B very similar. [UniProtKB – P20339]	Stop gain	Not currently implicated in any disorder. Important in endosome formation/phagocytosis (MIM: [179512]).
<i>COL14A1</i>	c.2444G>A; p.G815D	Homozygous (mother heterozygous)	0.002% (0 homozygotes)	Large structural glycoprotein (1,000kD) of the interstitial ECM. [UniProtKB – Q05707]	SIFT = Damaging Polyphen = Probably Damaging	None known (MIM: [120324]).
<i>SMYD2</i>	c.875G>A; p.R292Q	Homozygous (mother heterozygous)	0.021% (0 homozygotes)	Protein-N-Lysine methyltransferase that methylates both histone and non-histone proteins. [UniProtKB – Q9NRG4]	SIFT = Tolerated Polyphen = Benign	None – possible oncogene (MIM: [610663]).
<i>CHRNE</i>	c.313G>A; p.V105M	Heterozygous (?de novo) Mother = wild-type allele	0.002% (0 homozygotes)	Subunit of acetylcholine receptor. [UniProtKB – Q04844]	SIFT = Damaging Polyphen = Possibly Damaging	Mutations can cause myasthenia. Usually autosomal recessive but can be autosomal dominant. No epilepsy link (MIM: [100725]).

Another candidate variant identified was a homozygous c.2338T>G (p.L780V) change in the *ALG13* gene. This gene is on the X chromosome. The protein encoded by *ALG13* is involved in glycosylation and X-linked dominant variants are known to lead to early infantile epileptic encephalopathy (MIM: 300884). The mother of this individual however was heterozygous for the variant suggesting that it is unlikely to be cause of **Subject NGS3**'s disorder as inheritance of two alleles would require the father to be hemizygous. However, upon further investigation by our collaborators from GOSgene, a large run of homozygosity (ROH) of approximately 50 Mb was identified in the same area as *ALG13*. This ROH spanned from bases 79,675,080-129,174,142 on chromosome X in the Homo sapiens (human) genome assembly GRCh37 (hg19).

Usually, a ROH of this size would indicate a large deletion, leading to hemizygosity of this region of the chromosome. However, analysis by GOSgene showed that there was no drop in the read depth of this region in the patient compared to the mother. This indicated segmental isodisomic uniparental disomy (UPD) of the region rather than a large deletion. Segmental isodisomic UPD is a phenomenon whereby a section of a chromosome is inherited from a single chromosome derived from one parent; both alleles can be inherited from that single parent. This conveys an increased chance of inheriting autosomal recessive genetic diseases (or, in this case, perhaps an X-linked dominant disease in a female).²⁷⁸ However, a more common pathogenic mechanism of UPD is that imprinted genes are inherited uniparentally. Imprinted genes are those that can be silenced, meaning expression of a gene on one chromosome is halted, with only the second copy expressed.²⁷⁹ The inheritance of two identical gene copies from a single parent can lead to the silencing of both copies of a gene (or neither). Disorders that can be caused by this include Prader-Willi (MIM: [176270]) and Silver-Russell (MIM: [180860]) syndromes.

Complicating matters, in this case, is the presence of the UPD region on the X chromosome. In human females, one copy of the X chromosome is silenced in each cell (X-inactivation); this means that all genes on the X chromosome are, in effect, subject to imprinting. The exact mechanism by which X-inactivation occurs is not fully understood, but the X-inactivation centre (XIC) is known to be important.²⁸⁰ This is present approximately 6 mb from the beginning of the 50 mb homozygous region in this patient and is therefore unlikely to be affected. However, not all genes on the

inactivated X chromosome are silenced, with some (including *ALG13*) partially escaping this process.²⁸¹⁻²⁸²

Due to the presence of the UPD region on the X chromosome, it was hypothesised that genes in this region could be affected by aberrant silencing (linked to X-inactivation) leading to altered expression of the gene products. A list of all genes within the homozygous region was retrieved using the UCSC genome browser. This consisted of 380 known genes.

These 380 genes were then searched for predicted pathogenic homozygous variants using the IVA tool, none were identified. In addition, no genes encoding PLP-dependent enzymes or linked to vitamin B₆ metabolism were found. However, several genes implicated in genetic epilepsy and/or developmental delay were identified. These are listed in **Table 7.5**.

Table 7.5: Genes linked to early infantile epileptic encephalopathy and developmental delay in the isodisomic region of chromosome X in Subject 3. Variants identified using whole genome sequencing. Data filtered according to the parameters defined in the appendix (**Section 9.1**). Information obtained from <https://www.omim.org>. EIEE = early infantile epileptic encephalopathy

Gene	Protein function	Implicated disorder
<i>ALG13</i>	Constitutes the UDP-GlcNAc transferase	EIEE36; MIM: [300884]
<i>UBE2A</i>	A ubiquitin-conjugating enzyme important for protein degradation	Developmental delay, Nascimento-type; MIM: [300860]
<i>PCDH19</i>	A cell-cell adhesion protein	EIEE9; MIM: [300088]
<i>PLP1</i>	Component of central nervous system myelin	Pelizaeus-Merzbacher disease; MIM: [312080]

The *PCDH19* gene is found in this isodisomic area. The EIEE caused by *PCDH19* dysfunction is usually female-restricted dominant by inheritance. It is thought that a homogenous cell population of either mutant or wild-type cells does not lead to disease. Instead, a mixed population leads to aberrant cell-cell communication in the brain and hence the phenotype observed. Males with only one allele (either wild-type or mutant) do not present with EIEE. However, affected females are mosaics due to

X-inactivation occurring on different alleles, they therefore develop a mixed population of cells.²⁸³⁻²⁸⁴ In this patient, it is possible that *PCDH19* is being silenced on neither or both X chromosome/s, due to the isodisomic nature of the region. This would lead to a mixed population of cells (with regards to *PCDH19* expression) and hence the phenotype of neurological disease observed.

It is possible that aberrant silencing or overexpression of any one or more of the genes listed in **Table 7.4** is leading to the phenotype of **Subject NGS3**. Further work would be needed to define the precise mechanism involved, this could include transcriptomic analysis in order to characterise the expression of genes within the UPD region.

7.1.2 Subjects NGS4 & NGS5

Subject NGS4 presented with a refractory epilepsy at three days of age. The concentration of PLP in the CSF was low prior to treatment. PLP was found to control seizures where pyridoxine was ineffective. At five years of age seizures worsened and PLP was no longer fully effective. At this time nocturnal epilepsy also became a feature of the disorder. Development was normal. IVA was used to search for pathogenic variants related to vitamin B₆ metabolism or other epilepsy disorders. However, no plausible candidates were identified. Subsequently it was found (using a SNP array by collaborators in UMCG) that a 107 kb deletion was present on the long arm of chromosome 20; an area that included the *KCNQ2* gene at 20q13.33. This was considered likely to be pathogenic; duplications and deletions of the *KCNQ2* gene have previously been linked to epilepsy disorders.²⁸⁵

Subject NGS5 presented with drug-resistant epilepsy at three months of age. They became seizure free on the introduction of PLP to their treatment regime (dose unknown). PLP was later withdrawn at seven months of age before seizure recurrence one month later. Since then seizures have been well controlled with pyridoxine supplementation. The patient is now six years old. Sequencing of the *PNPO*, *ALDH7A1* and *PLPBP* genes did not reveal any pathogenic variants. A heterozygous splice site variant was identified in the *KCNQ2* gene (c.297-1G>C). Sanger sequencing was performed on the parents of **Subject NGS5** and c.297-1G>C was absent in both, confirming it as a *de novo* variant. This, in addition to its location on an exon boundary, meant that the variant was considered pathogenic.

7.2 Investigation of the effect of B₆ vitamers on the M-current facilitated by KCNQ2 channels

To our knowledge, at least six patients (including **Subjects NGS4 and NGS5** above) with *de novo* mutations or copy number variations in *KCNQ2* have recently been shown to respond to treatment with B₆.^{116-117, 286} (& unpublished observations) Better understanding of the mechanism by which seizures are controlled by B₆ in patients with mutations in *KCNQ2* would help us to understand which genetic epilepsies could benefit from treatment with pharmacological doses of vitamin B₆.

Two of these patients had low CSF PLP prior to treatment which could be significant with regards to the B₆ response seen specifically with mutations in *KCNQ2*. In other patients CSF PLP was either normal or had not been measured. Low CSF PLP has also (inconsistently) been found in larger childhood epilepsy cohorts. Overall, these patients with *KCNQ2* mutations also seemed to show a better response to PLP than PN, a finding reported in a wider cohort of children with genetic epilepsy by Wang *et al.*¹¹³

Potassium voltage-gated channel subfamily Q member 2 (KCNQ2)-related epilepsy is an autosomal dominant disorder that can lead to a phenotype ranging from relatively mild benign familial neonatal seizures (BFNE) to severe neonatal epileptic encephalopathy (NEE).²⁸⁵ The KCNQ2 protein is an integral part of the KCNQ or 'M'-channels, responsible for carrying the M-current, important for modulating the resting potential of neurones and hence regulating neuronal excitability.¹¹⁸ Retigabine is a recently developed anti-epileptic drug that functions by opening KCNQ channels.¹¹⁹ Valproate is also thought to maintain the M-current as part of its anti-epileptic action.¹²⁰

Why seizures caused by mutations in *KCNQ2* would respond to vitamin B₆ supplementation has not been investigated previously. There are several potential hypotheses that may explain the mechanism behind this response:

- i. Vitamin B₆ attenuates the potentially neurotoxic effects of reactive oxygen species (ROS) production which can occur due to unregulated neuronal firing; the B₆ vitamers have known antioxidant properties.⁵¹
- ii. PLP is a ligand of KCNQ2 channels and directly modulates the M-current.

- iii. The M-current is modulated by P2X7 receptors, at which PLP is a known antagonist.
- iv. PLP, through its activity as a cofactor, restores the balance of neurotransmitters, particularly glutamate/GABA, thereby countering excessive neuronal excitability.

This section details experiments carried out in order to elucidate the mechanism behind the B₆ response of the epilepsy in patients with mutations in *KCNQ2* by using the electrophysiological technique patch clamping to measure the M-current amplitude from single cells.¹¹⁸

7.2.1 The effect of PL and PLP on the M-current in CHO cells overexpressing KCNQ2/3

M channels are formed by a tetramer comprised of two KCNQ2 and two KCNQ3 protein subunits.¹¹⁸ Chinese hamster ovary (CHO) cells transfected with the genes encoding these proteins have previously been shown to express a measurable M-current susceptible to pharmacological manipulation.²⁸⁷ This cell model was prepared by collaborators at the UCL department of Neuroscience, Physiology & Pharmacology. We were able to use this model to study the M-current of single cells and their response to PLP and PL.

Initial experiments were performed in order to confirm the expression of KCNQ2/3 channels in CHO cells. This was carried out by detecting the M-current through perforated patching (**Figure 7.2a**). A perforated patch is achieved by manoeuvring a borosilicate glass pipette with an aperture of approximately 1 μm into contact with the membrane of a suitable cell and applying negative pressure to the pipette. This forms a 'gigaseal' on the cell membrane (a seal with an electrical resistance $> 1 \text{ G}\Omega$). The patch is then permeabilised using amphotericin. Amphotericin treatment makes the cell permeable to monovalent ions such as K^+ , Na^+ and Cl^- while remaining impermeable to larger molecules and proteins. It is then possible to measure the M-current by monitoring the current, in nanoamperes (nA), which occurs when the potential difference across the cell membrane is changed from -60 mV (inside

negative) to 0 mV using electrodes; one within the patching pipette and another in the bath solution.

A choice was made to use perforated patching in place of whole-cell patching because this method is less disruptive to the integrity of the cell membrane and therefore allows measurement of electrophysiological characteristics for a longer period before cell death.

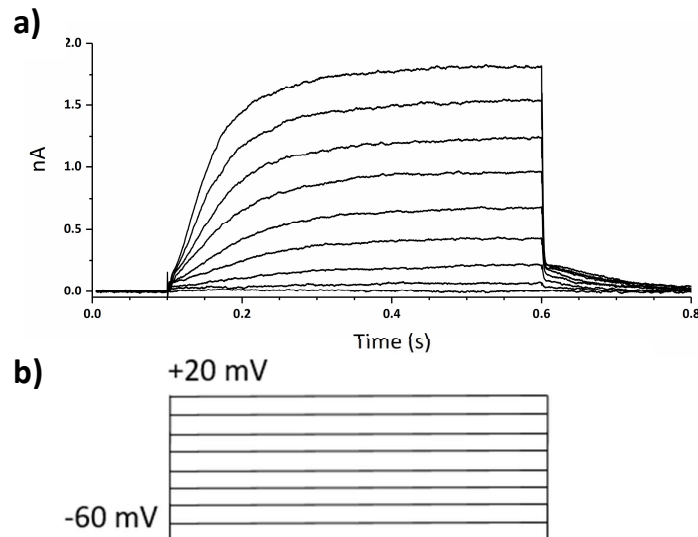


Figure 7.2: M-Current measured in CHO cells overexpressing KCNQ2/3 channels. Recording (a) shows the M-current measured with a perforated patch electrode using the step protocol shown in (b). The step protocol depolarised the cell in 10 mV steps from -60 mV to +20 mV.

In CHO cells transfected with KCNQ2/3 channels the amplitude of the M-current measured is proportional to the number of M-channels open. The protocol used involved holding the membrane potential at -60 mV, before applying pulses at -60 to +20 mV, in ascending 10 mV steps for 500 ms. After each step the potential would be returned to the -60 mV resting potential for 5 seconds before proceeding to the next step of the protocol (**Figure 7.2b**). The peak current measured at 0 mV was used to quantify the M-current in each cell. An amplitude of approximately 0.5 – 1.5 nA would be expected at this voltage.²⁸⁷

The effect of compounds on the M-current can be tested by applying them to the bath solution in which the cells are contained. This solution is continuously replenished and can be exchanged rapidly. In order to test whether this bath solution exchange was effective, the step protocol shown in **Figure 7.2b** was carried out at one-minute

intervals before and after exchange of a standard bath solution (composition in **Section 2.14.1**) with one containing 10 $\mu\text{mol/L}$ linopirdine (PubChem CID: 3932). This compound blocks the M-current with an IC_{50} of 2.4 $\mu\text{mol/L}$.²⁸⁸ A reduction of the M-current amplitude of 31.8% (mean reduction of 3 cells) was observed after application of linopirdine to the bath solution, compared to the amplitude measured from the same cell prior to its addition.

Using the same protocol, the effect of 10 $\mu\text{mol/L}$ PLP on the measured M-current was tested by its addition to the bath solution. A concentration of 10 $\mu\text{mol/L}$ was chosen as this is expected to be at least ten times higher than free concentrations *in vivo*, but within the range potentially expected in patients receiving supplementation, based on circulating blood concentrations (**Section 3**). No difference in the measured M-current of each individual cell could be identified after exchanging the standard bath solution for that containing 10 $\mu\text{mol/L}$ PLP. The mean amplitude of both conditions was almost identical and any difference was not statistically significant (Control bath solution = 0.346 ± 0.144 nA; PLP bath solution = 0.353 ± 0.133 nA ($n = 12$ cells) (**Figure 7.3a**).

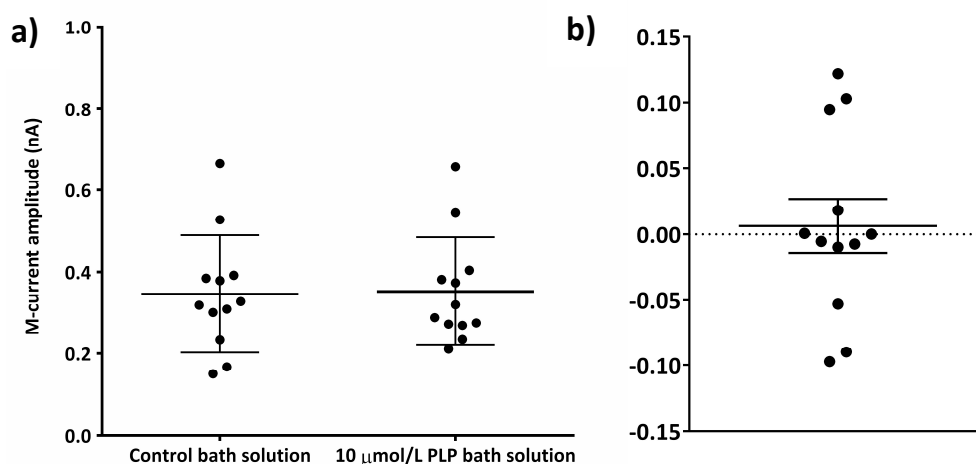


Figure 7.3: The effect of 10 $\mu\text{mol/L}$ PLP on the M-current in CHO cells over-expressing KCNQ2/3 channels. a) The M-current amplitude measured at 0 mV before and after the addition of 10 $\mu\text{mol/L}$ PLP to the bath solution ($n=12$). b) The change in M-current amplitude from each individual cell measured before and after 10 $\mu\text{mol/L}$ PLP ($n=12$). Error bar = SD; central line = mean.

The effect of PLP on the M-current can also be quantified as the change in amplitude before and after the exchange of the standard bath solution for that containing PLP. This was found not to deviate significantly from zero (Mean change = $0.006 \text{ nA} \pm 0.07$;

n = 12 cells), providing further evidence that a bath solution containing PLP had no effect on the M-current (**Figure 7.3b**).

It is not fully understood how the B₆ vitamers cross the cell membrane but it is thought that the non-phosphorylated vitamers are able to move across more easily than the phosphorylated forms.¹⁶ It was hypothesised that, although 10 µmol/L PLP had not altered the M-current, the same concentration of PL may do so. If the effect of vitamin B₆ upon KCNQ2/3 channels was dependent upon intracellular concentrations, it is possible that PL would affect the M-current by entering the cell, whereas PLP would remain in the extracellular bath solution. However, this was found not to be the case, with 10 µmol/L PL not significantly diminishing or enhancing the measured M-current (Control bath solution = 0.563 nA ±0.272; PL bath solution = 0.535 nA ±0.267; n = 3 cells).

7.2.2 The effect of growth in B₆-depleted medium upon the M-current in CHO cells overexpressing KCNQ2/3

The experiments described above (**Section 7.2.1**) were performed with CHO cells that had been established and maintained in replete media that contains pyridoxine. Cells therefore contained what could be considered normal vitamin B₆ concentrations prior to the acute application of PLP/PL. Further experiments were performed to investigate whether chronic vitamin B₆ depletion could affect the M-current strength. This effect on the M-current could occur, for example, if B₆ vitamer concentrations affected the localisation of the KCNQ2/3 tetramers to the cell membrane. This occurs through a PIP₂ regulated pathway and is inhibited by G_q receptor innervation.²⁸⁹ CHO cells have previously been used as a model to characterise the link between this pathway and KCNQ2/3 channels.²⁹⁰

CHO cells were cultured in both the cell culture medium previously used (Ham's F-12 with normal fetal bovine serum (FBS)) and in a B₆-depleted Ham's F-12 medium. The standard Ham's F-12 medium contains 62 µg/L (367 nmol/L) pyridoxine. The B₆-depleted medium was identical in all aspects except for the removal of pyridoxine. The B₆-depleted cell culture media was supplemented with FBS that had been dialysed to ensure that this was not a source of B₆ vitamers. Oppici *et al.* have used a similar protocol of B₆ depletion.²⁹¹ Cells were transitioned over a 6 week period from

normal medium into the B₆-depleted medium. B₆-depleted cell lines were viable although they grew slower than those in replete media.

The concentrations of B₆ vitamers in: i) B₆-depleted Ham's F-12 medium; ii) normal Ham's F-12 medium; iii) dialysed FBS; iv) normal FBS were measured and are shown in **Figure 7.4**. In addition, B₆ vitamers were measured from the cell culture mixtures of: v) 10% dialysed FBS in B₆-depleted Ham's F-12 medium 1; vi) 0% normal FBS in Normal Ham's F-12 medium. This was carried out using the LC-MS/MS-based method detailed in **Section 2.4.1**.

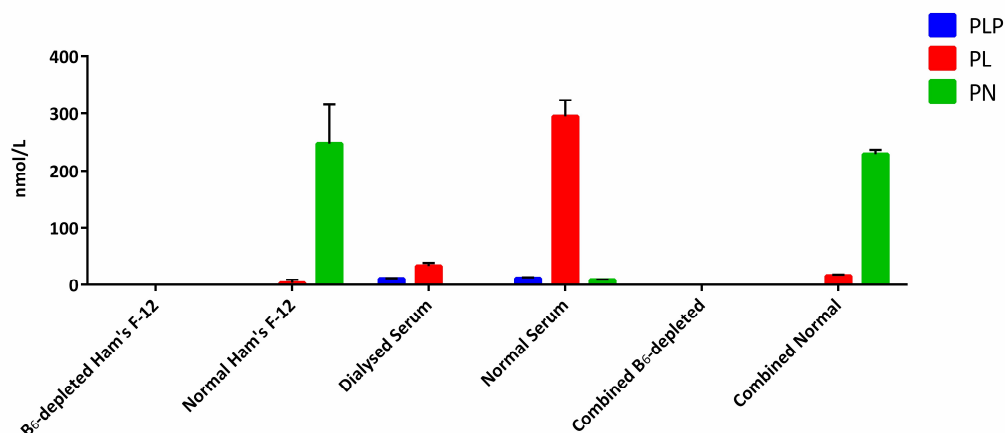


Figure 7.4: The B₆ vitamers concentrations in media used for the culture of normal and B₆-depleted CHO cells. n=3; Error bars = SD.

Only PLP, PL and PN were measurable in the media mixtures, with other vitamers below the limit of detection (6 nmol/L for this experiment; see **Section 2.4.3.2**). Normal Ham's F-12, as expected, contained mostly PN, at a concentration of 247 nmol/L. Also present was a small amount of PL (7 nmol/L). Normal serum contained a high concentration of PL (295 nmol/L) and lower concentrations of PLP (12 nmol/L) and PN (9 nmol/L). This high PL/PLP ratio could be due to either phosphatases still active during the preparation of FBS or differences in foetal B₆ metabolism. For example, preterm infants are reported to have a higher PL/PLP ratio than term infants in both serum and CSF.²⁹² Dialysed FBS contained lower concentrations of PL (33 nmol/L) and PLP (11 nmol/L) but no PN. The B₆-depleted Ham's F-12 and the mixture of this with 10% dialysed FBS contained no measurable B₆ vitamers. Dialysed FBS contains low amounts of PLP and PL, therefore it can be assumed that the B₆-depleted cell culture medium supplemented with dialysed serum also contains

vitamers but at a concentration below 6 nmol/L (i.e. the LLOQ). Residual low B₆ concentrations are likely required for cell viability.

B₆ vitamer concentrations were measured in cell lysates from the B₆-depleted cell line and compared to the normal cell line. Lysates were prepared by freeze thawing the cells, as described by Oppici *et al.*²⁹¹ (**Section 2.13.1**). Results were normalised to the protein concentration of the lysate, measured using the bicinchoninic acid (BCA) assay (**Section 2.13.2**) and expressed as pmol/mg protein (**Figure 7.5**).

PLP (Normal medium: 3.27 pmol/mg protein; B₆-depleted medium: 1.02 pmol/mg protein) and PMP (Normal medium: 2.82 pmol/mg protein; B₆-depleted medium: 0.93 pmol/mg protein) were detectable in both the depleted and replete cell lines. Levels of both vitamers were lower in the B₆-depleted lysates, with an approximately 3-fold drop in both, confirming B₆ depletion. A concentration of pyridoxine similar to those of PLP and PMP was detected in the B₆ depleted cell line. This was unexpected as no PN was present in the media of these cells, as shown in **Figure 7.4**. No other B₆ vitamers were detectable in lysates from either cell line.

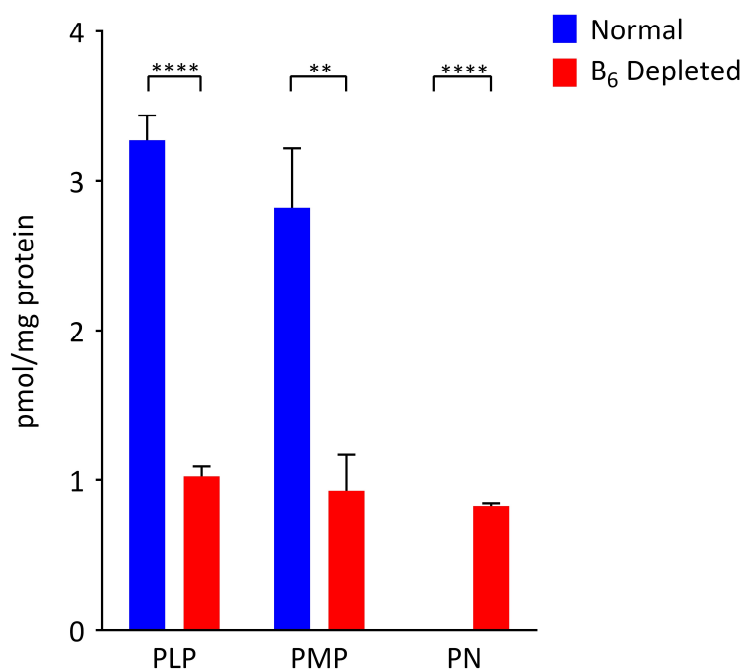


Figure 7.5: The concentration of the B₆ vitamers in normal and B₆-depleted CHO cells. n=3; Error bars = SD; ** = p < 0.01; **** p < 0.0001. Normal = CHO cells cultured in standard Ham's F-12 medium with the addition of standard serum; B₆ depleted = CHO cells cultured in B₆-depleted Ham's F-12 with the addition of dialysed serum.

Subsequent to B₆ depletion the M-current was measured in both populations (i.e. B₆ depleted and replete CHO cells) as described in **Section 7.2.1**. The mean M-current measured was found to be slightly higher in the B₆-depleted cell line (Normal = 0.569 ±0.307 nA (n = 15) B₆-depleted = 0.721 ±0.258 nA (n = 14) (**Figure 7.6**). However, this difference was not significant ($p = 0.161$).

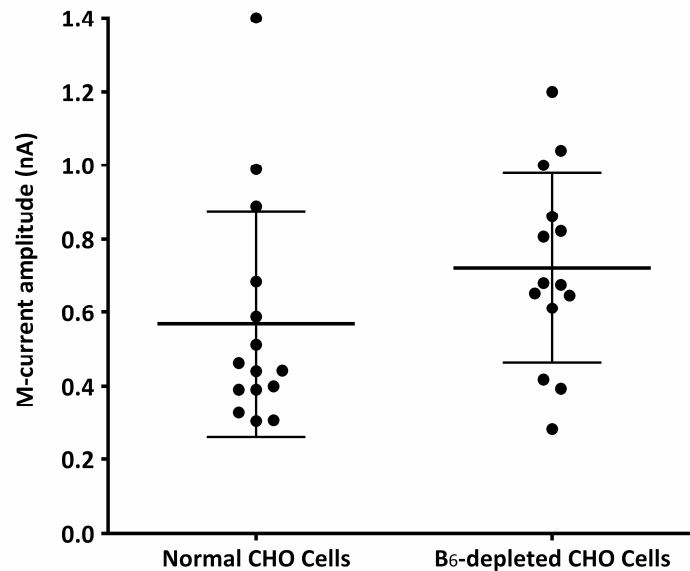


Figure 7.6: The M-current amplitude of normal and B₆-depleted CHO cells.

Normal cells n=14; B₆-depleted cells n=15. Error bar = SD; central line = mean.

In summary, no effect on the M-current could be measured during the acute application of PLP or PL to the bath solution. In addition, there was no significant effect of culturing the CHO cells in a custom B₆-depleted medium. This B₆ depletion was confirmed by measuring the B₆ status of the CHO cells used for M-current measurement. Additional work could be performed in order to further investigate the mechanism by which patients with *KCNQ2* variants respond to vitamin B₆ supplementation. This is discussed below.

7.3 Discussion & future work

7.3.1 Investigation of patients with vitamin B₆-dependent epilepsy using NGS data

In the cohort of five individuals investigated, two conclusive diagnoses were achieved in **Subjects NGS4 and NGS5**. Both were found to have mutations in the *KCNQ2* gene. This provides additional evidence for a link between KCNQ2-related epilepsy and vitamin B₆.

In **Subjects NGS1, NGS2 and NGS3**, no mutations were found in genes known to cause vitamin B₆ dependent epilepsy or linked to the metabolism of vitamin B₆. In all three of the patients however either novel candidates or variants of unknown significance were discovered but their pathogenicity was not confirmed. Although *in silico* tools such as SIFT and PolyPhen were used to determine the evolutionary conservation and structural effect of variants identified, these results are often inconclusive, particularly where novel gene loci or large abnormalities such as **Subject 3's** area of UPD are implicated. Hence, it is also important to assess the predicted biochemical effect of a variant functionally; this can often be challenging as many pathways are still poorly characterised.

The processing of data and assessment of millions of potentially benign or pathogenic variants is a problem in an ever-growing genetic landscape. This will become easier as our understanding of human genomics and biochemistry expands but is also a perfect arena for machine learning and artificial intelligence due to the required integration, understanding and analysis of huge datasets and pathways. Considerable work is currently being performed towards this end²⁹³, the culmination of which would be the integration of several 'omics' technologies (such as genomics, epigenomics, proteomics, metabolomics and transcriptomics) to provide a complete biological snapshot of each individual patient (or cell type within that patient), leading to a rapid and accurate diagnosis.²⁹⁴ Hopefully this will also lead to a new era of the personalised treatment for individual patients.

7.3.2 The mechanism of response to vitamin B₆ supplementation in patients with mutations in *KCNQ2*

Under the conditions tested, there was no direct effect of PLP or PL on the M-current facilitated by KCNQ2/3 channels expressed in CHO cells. There is wide scope for further investigation of the response of patients with mutations in KCNQ2 to vitamin B₆. This includes testing whether higher concentrations of PL/PLP than the 10 µmol/L used would modulate the M-current. There was a concern that these extremely high concentrations of PL or PLP could damage cells through aldehyde stress. However, recent work has shown that PN is in fact more toxic to cells in culture than PL and PLP, with the latter two vitamers proving non-toxic even at concentrations of 100 µmol/L.¹¹¹ It is possible that PL and PLP are present at these concentrations physiologically, as shown by the data from DBS in **Section 4**.

It is known that a relatively minor reduction in M-current of 20 – 30% can increase neuronal excitability.²⁹⁵ It is possible that a minor change like this would be important *in vivo* but undetectable by the patch-clamping technique used, at least without increasing the number of replicates by an order of magnitude, something that was beyond the scope of this study.

Concerning the M-current in B₆-depleted cell lines, whilst no significant difference was seen, it is possible that the depletion of cells was inadequate. Although lower B₆ vitamer concentrations were detected and cell growth was notably slower, further B₆ depletion may have been required to see an effect of the B₆ vitamers on the measurable M-current.

During the acute application of B₆ vitamers to CHO cells, it is possible that both PLP and PL were unable to cross the cell membrane and were retained in the bath solution. The transporters that carry B₆ vitamers across the cell membrane are, as yet, uncharacterised (see **Section 1.1.1**). If intracellular concentrations are more important than those extracellularly in modulating the M-current, an effect would not have been seen using the approach used. In future studies, the B₆ vitamer of interest could be included inside the pipette used for patching. This could allow diffusion into the cytosol but would be ineffective with perforated clamping, as used in this study, as amphotericin permeabilisation does not permit the movement of PL or PLP across the cell membrane, only ions such as K⁺ and Cl⁻. It could be used with whole-cell

patch clamping; however, this would result in inferior data as recording would only be permitted for short amounts of time.^{118, 296}

A P2X7 receptor analogue is expressed in CHO cells²⁹⁷, useful future work would be the investigation of the effect of P2X7R activation by ATP on the M-current. As mentioned previously, PLP is a known P2X7R antagonist. If an effect of ATP upon the M-current was identified, it would be important to identify whether this could be antagonised by PLP within a CHO cell model.

Finally, a caveat of these experiments is that they were carried out in CHO cells. This is a good model for the direct pharmacological manipulation of KCNQ2/3 channels. However, if *in vivo* the effects of B₆ depletion on the M-current are facilitated by neuron-specific mechanisms or by effects upon gene expression these would not be identified in a CHO cell model. It would be valuable to repeat this experimentation in a neuronal cell line that innately expresses KCNQ2/3 channels.

8. SUMMARY AND FUTURE WORK

Over the past 20 years it has become increasingly apparent that vitamin B₆ supplementation can be useful in the treatment of a number of genetic seizure disorders. Several of these disorders have been defined as those directly affecting B₆ metabolism. These include PNPO⁶³, PLPHP²⁷ and ALDH7A1⁶⁴ deficiencies. However, supplementation is also useful in other genetic epilepsies and vitamin B₆ appears to have a general anticonvulsant effect.¹¹⁴ This thesis describes the development of novel techniques for the diagnosis of B₆-dependent disorders as well as molecular investigation of the proteins involved in these disorders and the metabolism of vitamin B₆. A particular focus was the use of mass spectrometry techniques for analysis and dried blood spots (DBS) as a sample medium.

Chapter 3 details the assessment of DBS as a sample source for the measurement of B₆ vitamers. DBS were found to be a suitable storage medium and the method was used in order to profile the B₆ vitamers in patients with PNPO deficiency and other B₆-dependent epilepsies receiving B₆ supplementation. A raised pyridoxine 5'-phosphate/pyridoxal 5'-phosphate (PNP/PLP) ratio was found to be diagnostically indicative of PNPO deficiency, though it did not allow complete delineation of PNPO deficient patients from others receiving B₆ supplementation. Unfortunately, only a limited cohort was collected for the other B₆-dependent disorders. In the future it would be important to profile the DBS B₆ vitamers in larger numbers of individuals with other B₆-dependent epilepsy disorders (e.g. PLPHP and ALDH7A1 deficiencies) to identify whether B₆ vitamer profiles could be useful for diagnosis.

An important finding from this work was additional evidence that the phosphorylated B₆ vitamers are compartmentalised within red blood cells. In particular, high concentrations of PNP in the case of PNPO deficient patients were found due to substrate accumulation. More work should be carried out on the effect of high concentrations of other vitamers on B₆-dependent enzymes. It is thought, for example, that high PN concentrations can cause peripheral neuropathy by inhibiting these enzymes.¹¹¹ It is quite possible that this also occurs for PNP. If so, there could be implications for the prognosis of PNPO deficient individuals.

Chapter 4.1 describes the development of a novel diagnostic enzyme assay for the diagnosis of pyridox(am)ine 5'-phosphate oxidase (PNPO) deficiency from DBS using liquid chromatography-tandem mass spectrometry (LC-MS/MS). The method was fully validated for the clinical diagnostic arena and can be performed rapidly with a turnaround time of less than 24 hours. This is of great clinical utility as a good

developmental outcome can be obtained when appropriate treatment of this disorder is initiated promptly.^{65, 87} Assay of the PNPO enzyme from DBS was found to provide a more conclusive diagnosis of PNPO deficiency than DBS B₆ vitamers profiles. However, profiling of the B₆ vitamers from DBS could be used in conjunction with DBS PNPO activity to provide a stronger diagnosis in cases, for example, of borderline enzyme activity.

In **Chapter 5**, biochemical characterisation of the homozygous p.A228T variant in *PDXK*, encoding pyridoxal kinase (PK), is detailed. This variant was identified by collaborators in a Cypriot family presenting with peripheral neuropathy. Pathogenicity of p.A228T was confirmed using LC-MS/MS to assay for the PK enzyme in DBS and in recombinant PK protein. Treatment with 50 mg/d PLP was commenced in two elderly siblings of the family described; this was found to improve their presentation. The identification of this treatable disorder has implications for genetic peripheral neuropathies; the development of a rapid assay from DBS could enable the screening of larger populations for this disorder.

Section 4.2 describes the biochemical characterisation of the PNPO p.R116Q variant. In DBS from p.R116Q homozygotes, enzyme activity was undetectable but studies with the recombinant enzyme activity showed that this variant had comparable activity to that of the wild-type enzyme, except for when its cofactor, flavin mononucleotide (FMN) was limited. Some individuals homozygous for p.R116Q present with seizures characteristic of PNPO deficiency but others are asymptomatic. A recent publication has reported that thermal stability of the p.R116Q PNPO protein is reduced.⁷⁴ It is possible that low blood PNPO activity in the DBS patients is due to this reduced stability but perhaps activity was retained in others tissues such as the brain, protecting from seizures, future work would study this hypothesis.

That the activity of B₆ metabolic enzymes could be tissue-specific in at least some cases is interesting. This is also implicated in the pathogenesis of the *PDXK* p.A228T variant in the patients described in **Section 5** as they were not reported to have developed seizures at any point in their lives. It is possible that mechanisms exist to protect the brain from PLP deficiency but these have not been characterised in humans. A study into the tissue-specific regulation of B₆ vitamers metabolism should be an important part of any future work.

Overall, **Chapters 3, 4 and 5** exemplify how modern advances in LC-MS/MS technology have enabled the use of lower sample volumes found in DBS as a source for analytes monitored for the diagnosis of inborn errors of metabolism (IEMs). This has implications outside the field of B₆-dependent disorders and it is likely that DBS will be increasingly useful, particularly for the measurement of enzyme activity in IEMs. In addition, the assays developed to assess the *in vitro* effect of PK and PNPO variants were performed in 96-well plates using an extremely small amount of recombinant enzyme (100 ng/well). This technique can be adapted for other enzymes and could be important for the characterisation of newly identified variants of unknown significance.

In cohorts of genetic epilepsy patients, PLP appears more effective than pyridoxine for seizure treatment.¹¹³ Many PNPO patients require PLP supplementation for control of their seizures as pyridoxine is not effective. Some PNPO deficient patients receiving long-term PLP supplementation seem to develop hepatic cirrhosis and in one case, hepatocellular carcinoma.^{103, 246} **Chapter 6** describes an assessment of the rate and profile of PLP degradation in solutions prepared similarly to those used in a clinical environment. 4-Pyridoxic acid 5'-phosphate (PAP) and a diketone PLP dimer were identified as PLP degradation products. This work will help to inform the treatment of patients. Identification of the mechanism by which high-dose PLP supplementation causes liver damage is important for the long-term outcome of these patients. Future work should include this as a priority.

Chapter 7.1 describes the investigation of several patients with B₆ responsive epilepsy using next generation sequencing technology. Sequencing data was studied from these patients in order to achieve a diagnosis for these patients or to identify a novel gene implicated in B₆-responsive epilepsy. In three of these individuals, pathogenic variants were not discovered but candidates in a number of genes are detailed. In the remaining two individuals, pathogenic abnormalities in the *KCNQ2* gene were identified. This added to the mounting evidence that *KCNQ2*-related epilepsy is amenable to treatment with vitamin B₆ supplementation.^{116-117, 286}

Finally, **Chapter 7.2** describes the use of electrophysiological techniques to establish the effect of PLP and PL on the *KCNQ2*-facilitated M-current expressed in a cell model. No effect of the acute application of these B₆ vitamers was detected. In addition, culture of these cells in B₆ depleted medium did not affect the M-current amplitude. More advanced models such as a neuronal cell line or *KCNQ2*

haploinsufficient mice would be useful as further work in order to elucidate the mechanism behind a B₆ response in KCNQ2-related epilepsy. This would also have implications with regards to the mechanism behind a response to PLP in wider epilepsy cohorts and could lead to the development of novel treatment protocols.

Indeed, this leads us to the overarching question of what is causing a response to B₆ supplements in patients with variants not thought to directly impact B₆ metabolism itself. There are currently three main hypothesis as to the cause of this effect, only one of which is related to the activity of PLP as a cofactor: i) supplementation is able to restore imbalances of neurotransmitters such as GABA and glutamate. ii) PLP is able to quench reactive oxygen species that are produced as a result of uncontrolled neuronal firing in cases of epilepsy. iii) PLP can inhibit the activation of P2X7 receptors, this could reduce neuroinflammation from excitotoxicity following seizures. In the future, models should be developed in order to identify the specific mechanisms involved.

9. APPENDIX

9.1 Conditions used for PCR amplification of candidate variants identified by next generation sequencing

Table 9.1: Primers and conditions used to amplify the regions containing pathogenic variants of unknown significance identified using NGS analysis. F = primer complementary to the forward strand; R = primer complementary to the reverse strand; bp = base pairs; T_m = annealing temperature used during PCR amplification. Other conditions are as stated in Section 2.12.3.1; Tables 2.10 & 2.11. Sanger sequencing was performed as described in Section 2.12.4.2

Primer	Variant of interest	Sequence 5' → 3'	T _m (°C)	MgCl ₂ (mmol/L)	Predicted product size (bp)
CACNA1A_F	c.6471C>A	AGACCATCTCAGACACCAGC	64	1.5	398
CACNA1A_R		GCCCTAGAGATCCCCTGAAC			
SLC15A5_F	c.1403T>C	TCATTGTAGCTGGGTCAAGGT	56	1.5	455
SLC15A5_R		AAGACTGCACTGACAAAGCC			
KCNQ2_F	c.297A>G	GTAACAGGAAGCGGAAGACAGACG	64	1.5	510
KCNQ2_R		GACGTTGCCAAAGGATGAGGCTG			

9.2 Gene lists used as biological context filters during analysis of next generation sequencing data using Ingenuity Variant Analysis

Table 9.2: Genes encoding PLP-dependent proteins or proteins implicated in the metabolism of vitamin B₆.

AADAT	CIN	KBL	PNPO
AADC	CSAD	KIAA0251	PRED79
AAT1	CSD	KIAA0526	PROSC
AAT2	CTH	KIAA1252	PSA
ABAT	DDC	KIAA1945 ODCP	PSAT1
ADC	ECA39	KYNU	PYGB
AGT2	ECA40	LCB1	PYGL
AGXT	FAS	LCB2	PYGM
AGXT2	FASN	MARC1	SCL
ALAS1	FTCD	MARC2	SCLY
ALAS2	GABAT	MOCOS	SDH
ALAS3	GAD	MOSC1	SDS
ALASE	GAD1	MOSC2	SDSL
ALASH	GAD2	MTHFR	SEPSECS
ALT2	GAD65	NFS1	SEPSECS
ASB	GAD67	NIFS	SGPL1
BCAT1	GCAT	OAT	SHMT1
BCAT2	GOT1	ODC1	SHMT2
BCATM	GOT2	OK/SW-cl.121	SLA/LP
BCT1	GPT	pcap	SPTLC1
BCT2	GPT1	PDXDC1	SPTLC2
C20orf38	GPT2	PDXK	SPTLC2L
C21orf124	hCG_18250	PDXP	SPTLC3
C21orf97	hCG_30593	PHOSPHO2	SRR
CBS	HDC	PKH	TAT
CCBL1	HUSSY-08	PLP	THNSL1
CCBL1	KAT2	PLPP	THNSL2
CCBL2	KAT3	PNK	TRNP48

Table 9.3: Genes on the early infantile epileptic encephalopathy gene panel at Great Ormond Street Hospital.

ADSL	GABRA1	PCDH19	SPTAN1
ALG13	GABRB3	PIGA	STX1B
ARHGEF9	GATAD2B	PIGQ	STXBP1
ARX	GRIN1	PLCB1	SYNGAP1
ATP1A3	GRIN2A	PNKP	TBC1D24
ATRX	GRIN2B	POLG	TCF4
CBL	HCN1	PRRT2	UBE2A
CDKL5	IQSEC2	QARS	UBE3A
CHD2	KCNA2	RYR3	WDR45
CHRNA2	KCNB1	SCN1A	ZEB2
CHRNA4	KCNC1	SCN2A	SPTAN1
CHRNB2	KCNQ2	SCN8A	STX1B
CNTNAP2	KCNT1	SIK1	STXBP1
CSNK1G1	KIF1BP	SLC12A5	SYNGAP1
DNM1	KIAA1279	SLC13A5	TBC1D24
DOCK7	LGI1	SLC16A2	TCF4
DYRK1A	MAGI2	SLC25A22	UBE2A
EHMT1	MBD5	SLC2A1	UBE3A
FASN	MECP2	SLC35A2	WDR45
FOXP1	MEF2C	SLC6A1	ZEB2
GABBR2	NRXN1	SLC9A6	

Table 9.4: Genes in the human genome known to encode ion channels.

Voltage-gated Calcium Channel Genes			
CACNA1A	CACNA1H	CACNB1	CACNG4
CACNA1B	CACNA1I	CACNB2	CACNG5
CACNA1C	CACNA1S	CACNB3	CACNG6
CACNA1D	CACNA2D1	CACNB4	CACNG7
CACNA1E	CACNA2D2	CACNG1	CACNG8
CACNA1F	CACNA2D3	CACNG2	
CACNA1G	CACNA2D4	CACNG3	
Cholinergic Receptor Genes			
CHRNA1	CHRNA4	CHRNA9	CHRNA4
CHRNA10	CHRNA5	CHRNA1	CHRNA1
CHRNA2	CHRNA6	CHRNA2	CHRNA2
CHRNA3	CHRNA7	CHRNA3	CHRNA3
Chloride Channel Genes			
CLCN1	CLCN4	CLCN6	CLCNKA
CLCN2	CLCN5	CLCN7	CLCNKB
CLCN3			
Dopamine Receptor Genes			
DRD1	DRD3	DRD4	DRD5
DRD2			
GABA Receptor Genes			
GABBR1	GABRA4	GABRB3	GABRG3
GABBR2	GABRA5	GABRD	GABRP
GABRA1	GABRA6	GABRE	GABRQ
GABRA2	GABRB1	GABRG1	GABRR1
GABRA3	GABRB2	GABRG2	GABRR2
Glycine Receptor Genes			
Gcom1	GLRA3	GRIA1	GRIA3
GLRA1	GLRB	GRIA2	GRIA4
GLRA2			
Ionotropic Glutamate Receptor Genes			
GRID1	GRIK3	GRIN2A	GRIN3A
GRID2	GRIK4	GRIN2B	GRINA
GRIK1	GRIK5	GRIN2C	
GRIK2	GRIN1	GRIN2D	
Metabotropic Glutamate Receptor Genes			
GRM1	GRM3	GRM5	GRM7
GRM2	GRM4	GRM6	GRM8
Cyclic Nucleotide-gated Channel Genes			
HCN1	HCN2	HCN3	HCN4
Serotonin Receptor Genes			
HTR1A	HTR1F	HTR3B	HTR4
HTR1B	HTR2A	HTR3C	HTR5A
HTR1D	HTR2C	HTR3D	HTR6
HTR1E	HTR3A	HTR3E	HTR7
Voltage-gated Potassium Channel Genes			
KCNA1	KCNC1	KCNG1	KCNQ2

KCNA10	KCNC2	KCNG2	KCNQ3
KCNA2	KCNC3	KCNG3	KCNQ4
KCNA3	KCNC4	KCNG4	KCNQ5
KCNA4	KCND1	KCNH1	KCNRG
KCNA5	KCND2	KCNH2	KCNS1
KCNA6	KCND3	KCNH3	KCNS2
KCNA7	KCNE1	KCNH4	KCNS3
KCNAB1	KCNE1L	KCNH5	KCNT1
KCNAB2	KCNE2	KCNH6	KCNV1
KCNAB3	KCNE3	KCNH7	KCNV2
KCNB1	KCNE4	KCNH8	
KCNB2	KCNF1	KCNQ1	
Potassium Inwardly Rectifying Channel Genes			
KCNJ1	KCNJ14	KCNJ3	KCNJ8
KCNJ10	KCNJ15	KCNJ4	KCNJ9
KCNJ11	KCNJ16	KCNJ5	
KCNJ12	KCNJ2	KCNJ6	
Twin Pore Potassium Channel Genes			
KCNK1	KCNK15	KCNK3	KCNK7
KCNK10	KCNK16	KCNK4	KCNK9
KCNK12	KCNK17	KCNK5	
KCNK13	KCNK2	KCNK6	
Calcium Activated Potassium Channel Genes			
KCNMA1	KCNMB3	KCNN1	KCNN3
KCNMB2	KCNMB4	KCNN2	KCNN4
Ryanodine Receptor Genes			
RYR1	RYR2	RYR3	
Voltage-gated Sodium Channel Genes			
SCN10A	SCN2A2	SCN4A	SCN8A
SCN11A	SCN2B	SCN4B	SCN9A
SCN1A	SCN3A	SCN5A	
SCN1B	SCN3B	SCN7A	

Reference list

1. Sarma, P. S.; Snell, E. E.; Elvehjem, C. A., The vitamin B6 group; biological assay of pyridoxal, pyridoxamine, and pyridoxine. *J Biol Chem* **1946**, *165* (1), 55-63.
2. Clayton, P. T., B6-responsive disorders: a model of vitamin dependency. *J Inherit Metab Dis* **2006**, *29* (2-3), 317-26.
3. Percudani, R.; Peracchi, A., The B6 database: a tool for the description and classification of vitamin B6-dependent enzymatic activities and of the corresponding protein families. *BMC Bioinformatics* **2009**, *10*, 273.
4. Wilson, M. P.; Plecko, B.; Mills, P. B.; Clayton, P. T., Disorders affecting vitamin B6 metabolism. *J Inherit Metab Dis* **2019**.
5. Austin, S. M.; Waddell, T. G., Prebiotic synthesis of vitamin B6-type compounds. *Orig Life Evol Biosph* **1999**, *29* (3), 287-96.
6. Mukherjee, T.; Hanes, J.; Tews, I.; Ealick, S. E.; Begley, T. P., Pyridoxal phosphate: biosynthesis and catabolism. *Biochim Biophys Acta* **2011**, *1814* (11), 1585-96.
7. Magnusdottir, S.; Ravcheev, D.; de Crecy-Lagard, V.; Thiele, I., Systematic genome assessment of B-vitamin biosynthesis suggests co-operation among gut microbes. *Front Genet* **2015**, *6*, 148.
8. Gregory, J. F., 3rd; Trumbo, P. R.; Bailey, L. B.; Toth, J. P.; Baumgartner, T. G.; Cerda, J. J., Bioavailability of pyridoxine-5'-beta-D-glucoside determined in humans by stable-isotopic methods. *J Nutr* **1991**, *121* (2), 177-86.
9. Morrison, L. A.; Driskell, J. A., Quantities of B6 vitamers in human milk by high-performance liquid chromatography. Influence of maternal vitamin B6 status. *J Chromatogr* **1985**, *337* (2), 249-58.
10. Vanderslice, J. T.; Brownlee, S. R.; Cortissoz, M. E., Liquid chromatographic determination of vitamin B-6 in foods. *J Assoc Off Anal Chem* **1984**, *67* (5), 999-1007.
11. Viñas, P.; Balsalobre, N.; López-Eroz, C.; Hernández-Córdoba, M., Determination of Vitamin B6 Compounds in Foods Using Liquid Chromatography with Post-Column Derivatization Fluorescence Detection. *Chromatographia* **2004**, *59* (5), 381-386.
12. Coursin, D. B., Convulsive seizures in infants with pyridoxine-deficient diet. *J Am Med Assoc* **1954**, *154* (5), 406-8.
13. Baird, J. S.; Ravindranath, T. M., Vitamin B deficiencies in a critically ill autistic child with a restricted diet. *Nutr Clin Pract* **2015**, *30* (1), 100-3.
14. Gerlach, A. T.; Thomas, S.; Stawicki, S. P.; Whitmill, M. L.; Steinberg, S. M.; Cook, C. H., Vitamin B6 deficiency: a potential cause of refractory seizures in adults. *JPEN J Parenter Enteral Nutr* **2011**, *35* (2), 272-5.

15. Merrill, A. H., Jr.; Henderson, J. M., Vitamin B6 metabolism by human liver. *Ann N Y Acad Sci* **1990**, *585*, 110-7.
16. Albersen, M.; Bosma, M.; Knoers, N. V.; de Ruiter, B. H.; Diekman, E. F.; de Ruijter, J.; Visser, W. F.; de Koning, T. J.; Verhoeven-Duif, N. M., The intestine plays a substantial role in human vitamin B6 metabolism: a Caco-2 cell model. *PLoS One* **2013**, *8* (1), e54113.
17. Stanulovic, M.; Jeremic, V.; Leskovac, V.; Chaykin, S., New pathway of conversion of pyridoxal to 4-pyridoxic acid. *Enzyme* **1976**, *21* (4), 357-69.
18. Ubbink, J. B.; Serfontein, W. J.; Becker, P. J.; de Villiers, L. S., Effect of different levels of oral pyridoxine supplementation on plasma pyridoxal-5'-phosphate and pyridoxal levels and urinary vitamin B-6 excretion. *The American journal of clinical nutrition* **1987**, *46* (1), 78-85.
19. Bohney, J. P.; Fonda, M. L.; Feldhoff, R. C., Identification of Lys190 as the primary binding site for pyridoxal 5'-phosphate in human serum albumin. *FEBS Lett* **1992**, *298* (2-3), 266-8.
20. Kinoshita, T., Biosynthesis and deficiencies of glycosylphosphatidylinositol. *Proc Jpn Acad Ser B Phys Biol Sci* **2014**, *90* (4), 130-43.
21. van der Ham, M.; Albersen, M.; de Koning, T. J.; Visser, G.; Middendorp, A.; Bosma, M.; Verhoeven-Duif, N. M.; de Sain-van der Velden, M. G., Quantification of vitamin B6 vitamers in human cerebrospinal fluid by ultra performance liquid chromatography-tandem mass spectrometry. *Anal Chim Acta* **2012**, *712*, 108-14.
22. Footitt, E. J.; Clayton, P. T.; Mills, K.; Heales, S. J.; Neergheen, V.; Oppenheim, M.; Mills, P. B., Measurement of plasma B6 vitamers profiles in children with inborn errors of vitamin B6 metabolism using an LC-MS/MS method. *J Inherit Metab Dis* **2013**, *36* (1), 139-45.
23. Said, Z. M.; Subramanian, V. S.; Vaziri, N. D.; Said, H. M., Pyridoxine uptake by colonocytes: a specific and regulated carrier-mediated process. *Am J Physiol Cell Physiol* **2008**, *294* (5), C1192-7.
24. Stolz, J.; Vielreicher, M., Tpn1p, the plasma membrane vitamin B6 transporter of *Saccharomyces cerevisiae*. *J Biol Chem* **2003**, *278* (21), 18990-6.
25. Szydlowski, N.; Burkle, L.; Pourcel, L.; Moulin, M.; Stolz, J.; Fitzpatrick, T. B., Recycling of pyridoxine (vitamin B6) by PUP1 in *Arabidopsis*. *Plant J* **2013**, *75* (1), 40-52.
26. Stolz, J.; Wohrmann, H. J.; Vogl, C., Amiloride uptake and toxicity in fission yeast are caused by the pyridoxine transporter encoded by *bsu1+* (*car1+*). *Eukaryot Cell* **2005**, *4* (2), 319-26.
27. Darin, N.; Reid, E.; Prunetti, L.; Samuelsson, L.; Husain, R. A.; Wilson, M.; El Yacoubi, B.; Footitt, E.; Chong, W. K.; Wilson, L. C.; Prunty, H.; Pope, S.; Heales, S.; Lascelles, K.; Champion, M.; Wassmer, E.; Veggiotti, P.; de Crecy-Lagard, V.; Mills, P. B.; Clayton, P. T.,

Mutations in PROSC Disrupt Cellular Pyridoxal Phosphate Homeostasis and Cause Vitamin-B6-Dependent Epilepsy. *American journal of human genetics* **2016**, 99 (6), 1325-1337.

28. Whittaker, J. W., Intracellular trafficking of the pyridoxal cofactor. Implications for health and metabolic disease. *Archives of biochemistry and biophysics* **2016**, 592, 20-6.

29. Johnstone, D. L.; Al-Shekaili, H. H.; Tarailo-Graovac, M.; Wolf, N. I.; Ivy, A. S.; Demarest, S.; Roussel, Y.; Ciapaite, J.; van Roermund, C. W. T.; Kernohan, K. D.; Kosuta, C.; Ban, K.; Ito, Y.; McBride, S.; Al-Thihli, K.; Abdelrahim, R. A.; Koul, R.; Al Futaisi, A.; Haaxma, C. A.; Olson, H.; Sigurdardottir, L. Y.; Arnold, G. L.; Gerkes, E. H.; Boon, M.; Heiner-Fokkema, M. R.; Noble, S.; Bosma, M.; Jans, J.; Koolen, D. A.; Kamsteeg, E. J.; Drogemoller, B.; Ross, C. J.; Majewski, J.; Cho, M. T.; Begtrup, A.; Wasserman, W. W.; Bui, T.; Brimble, E.; Violante, S.; Houten, S. M.; Wevers, R. A.; van Faassen, M.; Kema, I. P.; Lepage, N.; Care4Rare Canada, C.; Lines, M. A.; Dymont, D. A.; Wanders, R. J. A.; Verhoeven-Duif, N.; Ekker, M.; Boycott, K. M.; Friedman, J. M.; Pena, I. A.; van Karnebeek, C. D. M., PLPHP deficiency: clinical, genetic, biochemical, and mechanistic insights. *Brain* **2019**.

30. Whittaker, M. M.; Penmatsa, A.; Whittaker, J. W., The Mtm1p carrier and pyridoxal 5'-phosphate cofactor trafficking in yeast mitochondria. *Archives of biochemistry and biophysics* **2015**, 568, 64-70.

31. Slabbaert, J. R.; Kuenen, S.; Swerts, J.; Maes, I.; Uytterhoeven, V.; Kasprovicz, J.; Fernandes, A. C.; Blust, R.; Verstreken, P., Shawn, the Drosophila Homolog of SLC25A39/40, Is a Mitochondrial Carrier That Promotes Neuronal Survival. *J Neurosci* **2016**, 36 (6), 1914-29.

32. Nilsson, R.; Schultz, I. J.; Pierce, E. L.; Soltis, K. A.; Naranuntarat, A.; Ward, D. M.; Baughman, J. M.; Paradkar, P. N.; Kingsley, P. D.; Culotta, V. C.; Kaplan, J.; Palis, J.; Paw, B. H.; Mootha, V. K., Discovery of genes essential for heme biosynthesis through large-scale gene expression analysis. *Cell Metab* **2009**, 10 (2), 119-30.

33. Fonda, M. L., Purification and characterization of vitamin B6-phosphate phosphatase from human erythrocytes. *J Biol Chem* **1992**, 267 (22), 15978-83.

34. Jeanclos, E.; Albersen, M.; Ramos, R. J. J.; Raab, A.; Wilhelm, C.; Hommers, L.; Lesch, K. P.; Verhoeven-Duif, N. M.; Gohla, A., Improved cognition, mild anxiety-like behavior and decreased motor performance in pyridoxal phosphatase-deficient mice. *Biochim Biophys Acta Mol Basis Dis* **2018**.

35. Kang, J. H.; Hong, M. L.; Kim, D. W.; Park, J.; Kang, T. C.; Won, M. H.; Baek, N. I.; Moon, B. J.; Choi, S. Y.; Kwon, O. S., Genomic organization, tissue distribution and deletion mutation of human pyridoxine 5'-phosphate oxidase. *Eur J Biochem* **2004**, 271 (12), 2452-61.

36. Choi, S. Y.; Churchich, J. E.; Zaiden, E.; Kwok, F., Brain pyridoxine-5-phosphate oxidase. Modulation of its catalytic activity by reaction with pyridoxal 5-phosphate and analogs. *J Biol Chem* **1987**, 262 (25), 12013-7.

37. Zhang, L.; Zhou, D.; Guan, W.; Ren, W.; Sun, W.; Shi, J.; Lin, Q.; Zhang, J.; Qiao, T.; Ye, Y.; Wu, Y.; Zhang, Y.; Zuo, X.; Connor, K. L.; Xu, G., Pyridoxine 5'-phosphate oxidase is a

novel therapeutic target and regulated by the TGF-beta signalling pathway in epithelial ovarian cancer. *Cell Death Dis* **2017**, *8* (12), 3214.

38. Chern, C. J.; Beutler, E., Biochemical and electrophoretic studies of erythrocyte pyridoxine kinase in white and black Americans. *American journal of human genetics* **1976**, *28* (1), 9-17.
39. Anderson, B. B.; Giuberti, M.; Perry, G. M.; Salsini, G.; Casadio, I.; Vullo, C., Low red blood cell glutathione reductase and pyridoxine phosphate oxidase activities not related to dietary riboflavin: selection by malaria? *The American journal of clinical nutrition* **1993**, *57* (5), 666-72.
40. Flanagan, J. M.; Beutler, E., The genetic basis of human erythrocyte pyridoxal kinase activity variation. *Haematologica* **2006**, *91* (6), 801-4.
41. Gachon, F.; Fonjallaz, P.; Damiola, F.; Gos, P.; Kodama, T.; Zakany, J.; Duboule, D.; Petit, B.; Tafti, M.; Schibler, U., The loss of circadian PAR bZip transcription factors results in epilepsy. *Genes & development* **2004**, *18* (12), 1397-412.
42. Tramonti, A.; Milano, T.; Nardella, C.; di Salvo, M. L.; Pascarella, S.; Contestabile, R., Salmonella typhimurium PtsJ is a novel MocR-like transcriptional repressor involved in regulating the vitamin B6 salvage pathway. *FEBS J* **2017**, *284* (3), 466-484.
43. Tanaka, T.; Scheet, P.; Giusti, B.; Bandinelli, S.; Piras, M. G.; Usala, G.; Lai, S.; Mulas, A.; Corsi, A. M.; Vestri, A.; Sofi, F.; Gori, A. M.; Abbate, R.; Guralnik, J.; Singleton, A.; Abecasis, G. R.; Schlessinger, D.; Uda, M.; Ferrucci, L., Genome-wide association study of vitamin B6, vitamin B12, folate, and homocysteine blood concentrations. *American journal of human genetics* **2009**, *84* (4), 477-82.
44. Cerqueira, N. M.; Fernandes, P. A.; Ramos, M. J., Computational Mechanistic Studies Addressed to the Transamination Reaction Present in All Pyridoxal 5'-Phosphate-Requiring Enzymes. *J Chem Theory Comput* **2011**, *7* (5), 1356-68.
45. Palm, D.; Klein, H. W.; Schinzel, R.; Buehner, M.; Helmreich, E. J., The role of pyridoxal 5'-phosphate in glycogen phosphorylase catalysis. *Biochemistry* **1990**, *29* (5), 1099-107.
46. Tarailo-Graovac, M.; Shyr, C.; Ross, C. J.; Horvath, G. A.; Salvarinova, R.; Ye, X. C.; Zhang, L. H.; Bhavsar, A. P.; Lee, J. J.; Drogemoller, B. I.; Abdelsayed, M.; Alfaradhi, M.; Armstrong, L.; Baumgartner, M. R.; Burda, P.; Connolly, M. B.; Cameron, J.; Demos, M.; Dewan, T.; Dionne, J.; Evans, A. M.; Friedman, J. M.; Garber, I.; Lewis, S.; Ling, J.; Mandal, R.; Mattman, A.; McKinnon, M.; Michoulas, A.; Metzger, D.; Ogunbayo, O. A.; Rakic, B.; Rozmus, J.; Ruben, P.; Sayson, B.; Santra, S.; Schultz, K. R.; Selby, K.; Shekel, P.; Sirrs, S.; Skrypnik, C.; Superti-Furga, A.; Turvey, S. E.; Van Allen, M. I.; Wishart, D.; Wu, J.; Wu, J.; Zafeiriou, D.; Kluijtmans, L.; Wevers, R. A.; Eyedoux, P.; Lehman, A. M.; Vallance, H.; Stockler-Ipsiroglu, S.; Sinclair, G.; Wasserman, W. W.; van Karnebeek, C. D., Exome Sequencing and the Management of Neurometabolic Disorders. *N Engl J Med* **2016**, *374* (23), 2246-55.

47. Ramos, R. J.; Pras-Raves, M. L.; Gerrits, J.; van der Ham, M.; Willemsen, M.; Prinsen, H.; Burgering, B.; Jans, J. J.; Verhoeven-Duif, N. M., Vitamin B6 is essential for serine de novo biosynthesis. *J Inherit Metab Dis* **2017**, *40* (6), 883-891.
48. Theriault, O.; Poulin, H.; Thomas, G. R.; Friesen, A. D.; Al-Shaqha, W. A.; Chahine, M., Pyridoxal-5'-phosphate (MC-1), a vitamin B6 derivative, inhibits expressed P2X receptors. *Can J Physiol Pharmacol* **2014**, *92* (3), 189-96.
49. Beamer, E.; Fischer, W.; Engel, T., The ATP-Gated P2X7 Receptor As a Target for the Treatment of Drug-Resistant Epilepsy. *Front Neurosci* **2017**, *11*, 21.
50. Sebastian-Serrano, A.; Engel, T.; de Diego-Garcia, L.; Olivos-Ore, L. A.; Arribas-Blazquez, M.; Martinez-Frailes, C.; Perez-Diaz, C.; Millan, J. L.; Artalejo, A. R.; Miras-Portugal, M. T.; Henshall, D. C.; Diaz-Hernandez, M., Neurodevelopmental alterations and seizures developed by mouse model of infantile hypophosphatasia are associated with purinergic signalling deregulation. *Hum Mol Genet* **2016**.
51. Bilski, P.; Li, M. Y.; Ehrenshaft, M.; Daub, M. E.; Chignell, C. F., Vitamin B6 (pyridoxine) and its derivatives are efficient singlet oxygen quenchers and potential fungal antioxidants. *Photochem Photobiol* **2000**, *71* (2), 129-34.
52. Tully, D. B.; Allgood, V. E.; Cidlowski, J. A., Modulation of steroid receptor-mediated gene expression by vitamin B6. *FASEB J* **1994**, *8* (3), 343-9.
53. Oka, T., Modulation of gene expression by vitamin B6. *Nutr Res Rev* **2001**, *14* (2), 257-66.
54. Phillips, R. S., Chemistry and diversity of pyridoxal-5'-phosphate dependent enzymes. *Biochim Biophys Acta* **2015**, *1854* (9), 1167-74.
55. Vazquez, M. A.; Munoz, F.; Donoso, J.; Garcia Blanco, F., Stability of Schiff bases of amino acids and pyridoxal-5'-phosphate. *Amino Acids* **1992**, *3* (1), 81-94.
56. Christmann-Franck, S.; Fermandjian, S.; Mirambeau, G.; Der Garabedian, P. A., Molecular modelling studies on the interactions of human DNA topoisomerase IB with pyridoxal-compounds. *Biochimie* **2007**, *89* (4), 468-73.
57. Kajita, R.; Goto, T.; Lee, S. H.; Oe, T., Aldehyde stress-mediated novel modification of proteins: epimerization of the N-terminal amino acid. *Chem Res Toxicol* **2013**, *26* (12), 1926-36.
58. Garaycochea, J. I.; Crossan, G. P.; Langevin, F.; Mulderrig, L.; Louzada, S.; Yang, F.; Guilbaud, G.; Park, N.; Roerink, S.; Nik-Zainal, S.; Stratton, M. R.; Patel, K. J., Alcohol and endogenous aldehydes damage chromosomes and mutate stem cells. *Nature* **2018**, *553* (7687), 171-177.
59. Wada, H.; Snell, E. E., The enzymatic oxidation of pyridoxine and pyridoxamine phosphates. *J Biol Chem* **1961**, *236*, 2089-95.

60. Musayev, F. N.; Di Salvo, M. L.; Ko, T. P.; Schirch, V.; Safo, M. K., Structure and properties of recombinant human pyridoxine 5'-phosphate oxidase. *Protein Sci* **2003**, *12* (7), 1455-63.
61. Benesch, R.; Benesch, R. E.; Kwong, S.; Acharya, A. S.; Manning, J. M., Labeling of hemoglobin with pyridoxal phosphate. *J Biol Chem* **1982**, *257* (3), 1320-4.
62. Tremino, L.; Forcada-Nadal, A.; Rubio, V., Insight into vitamin B6 -dependent epilepsy due to PLPBP (previously PROSC) missense mutations. *Hum Mutat* **2018**, *39* (7), 1002-1013.
63. Mills, P. B.; Surtees, R. A.; Champion, M. P.; Beesley, C. E.; Dalton, N.; Scambler, P. J.; Heales, S. J.; Briddon, A.; Scheimberg, I.; Hoffmann, G. F.; Zschocke, J.; Clayton, P. T., Neonatal epileptic encephalopathy caused by mutations in the PNPO gene encoding pyridox(am)ine 5'-phosphate oxidase. *Hum Mol Genet* **2005**, *14* (8), 1077-86.
64. Mills, P. B.; Struys, E.; Jakobs, C.; Plecko, B.; Baxter, P.; Baumgartner, M.; Willemssen, M. A.; Omran, H.; Tacke, U.; Uhlenberg, B.; Weschke, B.; Clayton, P. T., Mutations in antequitin in individuals with pyridoxine-dependent seizures. *Nat Med* **2006**, *12* (3), 307-9.
65. Hatch, J.; Coman, D.; Clayton, P.; Mills, P.; Calvert, S.; Webster, R. I.; Riney, K., Normal Neurodevelopmental Outcomes in PNPO Deficiency: A Case Series and Literature Review. *JIMD Rep* **2015**.
66. van Karnebeek, C. D.; Tiebout, S. A.; Niermeijer, J.; Poll-The, B. T.; Ghani, A.; Coughlin, C. R., 2nd; Van Hove, J. L.; Richter, J. W.; Christen, H. J.; Gallagher, R.; Hartmann, H.; Stockler-Ipsiroglu, S., Pyridoxine-Dependent Epilepsy: An Expanding Clinical Spectrum. *Pediatric neurology* **2016**, *59*, 6-12.
67. Plecko, B.; Zweier, M.; Begemann, A.; Mathis, D.; Schmitt, B.; Striano, P.; Baethmann, M.; Vari, M. S.; Beccaria, F.; Zara, F.; Crowther, L. M.; Joset, P.; Sticht, H.; Papuc, S. M.; Rauch, A., Confirmation of mutations in PROSC as a novel cause of vitamin B 6 -dependent epilepsy. *J Med Genet* **2017**, *54* (12), 809-814.
68. Shiraku, H.; Nakashima, M.; Takeshita, S.; Khoo, C.-S.; Haniffa, M.; Ch'ng, G.-S.; Takada, K.; Nakajima, K.; Ohta, M.; Okanishi, T.; Kanai, S.; Fujimoto, A.; Saitsu, H.; Matsumoto, N.; Kato, M., PLPBP mutations cause variable phenotypes of developmental and epileptic encephalopathy. *Epilepsia Open* *0* (ja).
69. Farrant, R. D.; Walker, V.; Mills, G. A.; Mellor, J. M.; Langley, G. J., Pyridoxal phosphate de-activation by pyrroline-5-carboxylic acid. Increased risk of vitamin B6 deficiency and seizures in hyperprolinemia type II. *J Biol Chem* **2001**, *276* (18), 15107-16.
70. Baumgartner-Sigl, S.; Haberlandt, E.; Mumm, S.; Scholl-Burgi, S.; Sergi, C.; Ryan, L.; Ericson, K. L.; Whyte, M. P.; Hogler, W., Pyridoxine-responsive seizures as the first symptom of infantile hypophosphatasia caused by two novel missense mutations (c.677T>C, p.M226T; c.1112C>T, p.T371I) of the tissue-nonspecific alkaline phosphatase gene. *Bone* **2007**, *40* (6), 1655-61.

71. Kuki, I.; Takahashi, Y.; Okazaki, S.; Kawawaki, H.; Ehara, E.; Inoue, N.; Kinoshita, T.; Murakami, Y., Vitamin B6-responsive epilepsy due to inherited GPI deficiency. *Neurology* **2013**, *81* (16), 1467-9.
72. Mills, P. B.; Footitt, E. J.; Mills, K. A.; Tuschl, K.; Aylett, S.; Varadkar, S.; Hemingway, C.; Marlow, N.; Rennie, J.; Baxter, P.; Dulac, O.; Nabbout, R.; Craigen, W. J.; Schmitt, B.; Feillet, F.; Christensen, E.; De Lonlay, P.; Pike, M. G.; Hughes, M. I.; Struys, E. A.; Jakobs, C.; Zuberi, S. M.; Clayton, P. T., Genotypic and phenotypic spectrum of pyridoxine-dependent epilepsy (ALDH7A1 deficiency). *Brain* **2010**, *133* (Pt 7), 2148-59.
73. Srinivasaraghavan, R.; Parameswaran, N.; Mathis, D.; Burer, C.; Plecko, B., Antiquitin Deficiency with Adolescent Onset Epilepsy: Molecular Diagnosis in a Mother of Affected Offsprings. *Neuropediatrics* **2018**, *49* (2), 154-157.
74. di Salvo, M. L.; Mastrangelo, M.; Nogues, I.; Tolve, M.; Paiardini, A.; Carducci, C.; Mei, D.; Montomoli, M.; Tramonti, A.; Guerrini, R.; Contestabile, R.; Leuzzi, V., Pyridoxine-5'-phosphate oxidase (Pnpo) deficiency: Clinical and biochemical alterations associated with the C.347g>A (P..Arg116Gln) mutation. *Molecular genetics and metabolism* **2017**, *122* (1-2), 135-142.
75. Flynn, M. P.; Martin, M. C.; Moore, P. T.; Stafford, J. A.; Fleming, G. A.; Phang, J. M., Type II hyperprolinaemia in a pedigree of Irish travellers (nomads). *Arch Dis Child* **1989**, *64* (12), 1699-707.
76. Whyte, M. P.; Zhang, F.; Wenkert, D.; McAlister, W. H.; Mack, K. E.; Benigno, M. C.; Coburn, S. P.; Wagdy, S.; Griffin, D. M.; Ericson, K. L.; Mumm, S., Hypophosphatasia: validation and expansion of the clinical nosology for children from 25 years experience with 173 pediatric patients. *Bone* **2015**, *75*, 229-39.
77. Ng, B. G.; Freeze, H. H., Human genetic disorders involving glycosylphosphatidylinositol (GPI) anchors and glycosphingolipids (GSL). *J Inherit Metab Dis* **2015**, *38* (1), 171-8.
78. Struys, E. A.; Nota, B.; Bakkali, A.; Al Shahwan, S.; Salomons, G. S.; Tabarki, B., Pyridoxine-dependent epilepsy with elevated urinary alpha-amino adipic semialdehyde in molybdenum cofactor deficiency. *Pediatrics* **2012**, *130* (6), e1716-9.
79. Nasr, E.; Mamak, E.; Feigenbaum, A.; Donner, E. J.; Mercimek-Mahmutoglu, S., Long-term treatment outcome of two patients with pyridoxine-dependent epilepsy caused by ALDH7A1 mutations: normal neurocognitive outcome. *J Child Neurol* **2015**, *30* (5), 648-53.
80. Guerin, A.; Aziz, A. S.; Mutch, C.; Lewis, J.; Go, C. Y.; Mercimek-Mahmutoglu, S., Pyridox(am)ine-5-Phosphate Oxidase Deficiency Treatable Cause of Neonatal Epileptic Encephalopathy With Burst Suppression: Case Report and Review of the Literature. *J Child Neurol* **2015**, *30* (9), 1218-25.
81. Pavone, L.; Mollica, F.; Levy, H. L., Asymptomatic type II hyperprolinaemia associated with hyperglycinaemia in three sibs. *Arch Dis Child* **1975**, *50* (8), 637-41.

82. van de Ven, S.; Gardeitchik, T.; Kouwenberg, D.; Kluijtmans, L.; Wevers, R.; Morava, E., Long-term clinical outcome, therapy and mild mitochondrial dysfunction in hyperprolinemia. *J Inherit Metab Dis* **2014**, *37* (3), 383-90.
83. Whyte, M. P., Hypophosphatasia: An overview For 2017. *Bone* **2017**.
84. Mechler, K.; Mountford, W. K.; Hoffmann, G. F.; Ries, M., Ultra-orphan diseases: a quantitative analysis of the natural history of molybdenum cofactor deficiency. *Genet Med* **2015**, *17* (12), 965-70.
85. de Roo, M. G. A.; Abeling, N.; Majoie, C. B.; Bosch, A. M.; Koelman, J.; Cobben, J. M.; Duran, M.; Poll-The, B. T., Infantile hypophosphatasia without bone deformities presenting with severe pyridoxine-resistant seizures. *Molecular genetics and metabolism* **2014**, *111* (3), 404-407.
86. Haidar, Z.; Jalkh, N.; Corbani, S.; Fawaz, A.; Chouery, E.; Megarbane, A., Atypical pyridoxine dependent epilepsy resulting from a new homozygous missense mutation, in ALDH7A1. *Seizure* **2018**, *57*, 32-33.
87. Mills, P. B.; Camuzeaux, S. S.; Footitt, E. J.; Mills, K. A.; Gissen, P.; Fisher, L.; Das, K. B.; Varadkar, S. M.; Zuberi, S.; McWilliam, R.; Stodberg, T.; Plecko, B.; Baumgartner, M. R.; Maier, O.; Calvert, S.; Riney, K.; Wolf, N. I.; Livingston, J. H.; Bala, P.; Morel, C. F.; Feillet, F.; Raimondi, F.; Del Giudice, E.; Chong, W. K.; Pitt, M.; Clayton, P. T., Epilepsy due to PNPO mutations: genotype, environment and treatment affect presentation and outcome. *Brain* **2014**, *137* (Pt 5), 1350-60.
88. Mathis, D.; Abela, L.; Albersen, M.; Burer, C.; Crowther, L.; Beese, K.; Hartmann, H.; Bok, L. A.; Struys, E.; Papuc, S. M.; Rauch, A.; Hersberger, M.; Verhoeven-Duif, N. M.; Plecko, B., The value of plasma vitamin B6 profiles in early onset epileptic encephalopathies. *J Inherit Metab Dis* **2016**.
89. Wilson, M. P.; Footitt, E. J.; Papandreou, A.; Uudelepp, M. L.; Pressler, R.; Stevenson, D. C.; Gabriel, C.; McSweeney, M.; Baggot, M.; Burke, D.; Stodberg, T.; Riney, K.; Schiff, M.; Heales, S. J. R.; Mills, K. A.; Gissen, P.; Clayton, P. T.; Mills, P. B., An LC-MS/MS-Based Method for the Quantification of Pyridox(am)ine 5'-Phosphate Oxidase Activity in Dried Blood Spots from Patients with Epilepsy. *Anal Chem* **2017**, *89* (17), 8892-8900.
90. Walker, V.; Mills, G. A., N-(pyrrole-2-carboxyl) glycine a diagnostic marker of hyperprolinaemia type II: mass spectra of trimethylsilyl derivatives. *Clin Chim Acta* **2009**, *405* (1-2), 153-4.
91. Mills, P. B.; Footitt, E. J.; Ceyhan, S.; Waters, P. J.; Jakobs, C.; Clayton, P. T.; Struys, E. A., Urinary AASA excretion is elevated in patients with molybdenum cofactor deficiency and isolated sulphite oxidase deficiency. *J Inherit Metab Dis* **2012**, *35* (6), 1031-6.
92. Wempe, M. F.; Kumar, A.; Kumar, V.; Choi, Y. J.; Swanson, M. A.; Friederich, M. W.; Hyland, K.; Yue, W. W.; Van Hove, J. L. K.; Coughlin, C. R., 2nd, Identification of a novel biomarker for pyridoxine-dependent epilepsy: Implications for newborn screening. *J Inherit Metab Dis* **2019**.

93. Schmitt, B.; Baumgartner, M.; Mills, P. B.; Clayton, P. T.; Jakobs, C.; Keller, E.; Wohlrab, G., Seizures and paroxysmal events: symptoms pointing to the diagnosis of pyridoxine-dependent epilepsy and pyridoxine phosphate oxidase deficiency. *Dev Med Child Neurol* **2010**, *52* (7), e133-42.
94. Bayoumi, R. A.; Kirwan, J. R.; Smith, W. R., Some effects of dietary vitamin B 6 deficiency and 4-deoxypyridoxine on -aminobutyric acid metabolism in rat brain. *J Neurochem* **1972**, *19* (3), 569-76.
95. Baumeister, F. A.; Gsell, W.; Shin, Y. S.; Egger, J., Glutamate in pyridoxine-dependent epilepsy: neurotoxic glutamate concentration in the cerebrospinal fluid and its normalization by pyridoxine. *Pediatrics* **1994**, *94* (3), 318-21.
96. Goto, T.; Matsuo, N.; Takahashi, T., CSF glutamate/GABA concentrations in pyridoxine-dependent seizures: etiology of pyridoxine-dependent seizures and the mechanisms of pyridoxine action in seizure control. *Brain & development* **2001**, *23* (1), 24-9.
97. Waymire, K. G.; Mahuren, J. D.; Jaje, J. M.; Guilarte, T. R.; Coburn, S. P.; MacGregor, G. R., Mice lacking tissue non-specific alkaline phosphatase die from seizures due to defective metabolism of vitamin B-6. *Nat Genet* **1995**, *11* (1), 45-51.
98. Plecko, B.; Paul, K.; Mills, P.; Clayton, P.; Paschke, E.; Maier, O.; Hasselmann, O.; Schmiedel, G.; Kanz, S.; Connolly, M.; Wolf, N.; Struys, E.; Stockler, S.; Abela, L.; Hofer, D., Pyridoxine responsiveness in novel mutations of the PNPO gene. *Neurology* **2014**, *82* (16), 1425-33.
99. Webster, R. I., Challenges in the management of pyridoxamine 5'-phosphate oxidase (PNPO) deficiency. *Pathology* **2016**, *48 Suppl 1*, S15.
100. Ormazabal, A.; Oppenheim, M.; Serrano, M.; Garcia-Cazorla, A.; Campistol, J.; Ribes, A.; Ruiz, A.; Moreno, J.; Hyland, K.; Clayton, P.; Heales, S.; Artuch, R., Pyridoxal 5'-phosphate values in cerebrospinal fluid: reference values and diagnosis of PNPO deficiency in paediatric patients. *Molecular genetics and metabolism* **2008**, *94* (2), 173-7.
101. Levtova, A.; Camuzeaux, S.; Laberge, A. M.; Allard, P.; Brunel-Guitton, C.; Diadori, P.; Rossignol, E.; Hyland, K.; Clayton, P. T.; Mills, P. B.; Mitchell, G. A., Normal Cerebrospinal Fluid Pyridoxal 5'-Phosphate Level in a PNPO-Deficient Patient with Neonatal-Onset Epileptic Encephalopathy. *JIMD Rep* **2015**, *22*, 67-75.
102. Footitt, E. J.; Heales, S. J.; Mills, P. B.; Allen, G. F.; Oppenheim, M.; Clayton, P. T., Pyridoxal 5'-phosphate in cerebrospinal fluid; factors affecting concentration. *J Inherit Metab Dis* **2011**, *34* (2), 529-38.
103. Sudarsanam, A.; Singh, H.; Wilcken, B.; Stormon, M.; Arbuckle, S.; Schmitt, B.; Clayton, P.; Earl, J.; Webster, R., Cirrhosis associated with pyridoxal 5'-phosphate treatment of pyridoxamine 5'-phosphate oxidase deficiency. *JIMD Rep* **2014**, *17*, 67-70.
104. Mohamed-Ahmed, A. H.; Wilson, M. P.; Albuera, M.; Chen, T.; Mills, P. B.; Footitt, E. J.; Clayton, P. T.; Tuleu, C., Quality and stability of extemporaneous pyridoxal phosphate

preparations used in the treatment of paediatric epilepsy. *J Pharm Pharmacol* **2017**, *69* (4), 480-488.

105. Reiber, H., Photochemical reactions of vitamin B 6 compounds, isolation and properties of products. *Biochim Biophys Acta* **1972**, *279* (2), 310-5.

106. Shephard, G. S.; Labadarios, D., Degradation of vitamin B6 standard solutions. *Clin Chim Acta* **1986**, *160* (3), 307-11.

107. Dalton, K.; Dalton, M. J., Characteristics of pyridoxine overdose neuropathy syndrome. *Acta Neurol Scand* **1987**, *76* (1), 8-11.

108. Ubbink, J. B.; Delport, R.; Becker, P. J.; Bissbort, S., Evidence of a theophylline-induced vitamin B6 deficiency caused by noncompetitive inhibition of pyridoxal kinase. *J Lab Clin Med* **1989**, *113* (1), 15-22.

109. Laine-Cessac, P.; Cailleux, A.; Allain, P., Mechanisms of the inhibition of human erythrocyte pyridoxal kinase by drugs. *Biochem Pharmacol* **1997**, *54* (8), 863-70.

110. Kulkantrakorn, K., Pyridoxine-induced sensory ataxic neuronopathy and neuropathy: revisited. *Neurol Sci* **2014**, *35* (11), 1827-30.

111. Vrolijk, M. F.; Opperhuizen, A.; Jansen, E.; Hageman, G. J.; Bast, A.; Haenen, G., The vitamin B6 paradox: Supplementation with high concentrations of pyridoxine leads to decreased vitamin B6 function. *Toxicol In Vitro* **2017**, *44*, 206-212.

112. Iyer, A.; Appleton, R., Improving Outcomes in Infantile Spasms: Role of Pharmacotherapy. *Paediatr Drugs* **2016**, *18* (5), 357-66.

113. Wang, H. S.; Kuo, M. F.; Chou, M. L.; Hung, P. C.; Lin, K. L.; Hsieh, M. Y.; Chang, M. Y., Pyridoxal phosphate is better than pyridoxine for controlling idiopathic intractable epilepsy. *Arch Dis Child* **2005**, *90* (5), 512-5.

114. Ohtahara, S.; Yamatogi, Y.; Ohtsuka, Y., Vitamin B(6) treatment of intractable seizures. *Brain & development* **2011**, *33* (9), 783-9.

115. Hawkins, N. A.; Kearney, J. A., Hlf is a genetic modifier of epilepsy caused by voltage-gated sodium channel mutations. *Epilepsy Res* **2016**, *119*, 20-3.

116. Reid, E. S.; Williams, H.; Stabej Ple, Q.; James, C.; Ocaka, L.; Bacchelli, C.; Footitt, E. J.; Boyd, S.; Cleary, M. A.; Mills, P. B.; Clayton, P. T., Seizures Due to a KCNQ2 Mutation: Treatment with Vitamin B6. *JIMD Rep* **2016**, *27*, 79-84.

117. Klotz, K. A.; Lemke, J. R.; Korinthenberg, R.; Jacobs, J., Vitamin B6-Responsive Epilepsy due to a Novel KCNQ2 Mutation. *Neuropediatrics* **2017**, *48* (3), 199-204.

118. Brown, D. A.; Passmore, G. M., Neural KCNQ (Kv7) channels. *Br J Pharmacol* **2009**, *156* (8), 1185-95.

119. Raol, Y. H.; Lapidès, D. A.; Keating, J. G.; Brooks-Kayal, A. R.; Cooper, E. C., A KCNQ channel opener for experimental neonatal seizures and status epilepticus. *Ann Neurol* **2009**, *65* (3), 326-36.
120. Kay, H. Y.; Greene, D. L.; Kang, S.; Kosenko, A.; Hoshi, N., M-current preservation contributes to anticonvulsant effects of valproic acid. *J Clin Invest* **2015**, *125* (10), 3904-14.
121. Akiyama, T.; Akiyama, M.; Hayashi, Y.; Shibata, T.; Hanaoka, Y.; Toda, S.; Imai, K.; Hamano, S. I.; Okanishi, T.; Yoshinaga, H.; Kobayashi, K., Measurement of pyridoxal 5'-phosphate, pyridoxal, and 4-pyridoxic acid in the cerebrospinal fluid of children. *Clin Chim Acta* **2016**, *466*, 1-5.
122. Martinc, B.; Grabnar, I.; Vovk, T., The role of reactive species in epileptogenesis and influence of antiepileptic drug therapy on oxidative stress. *Curr Neuropharmacol* **2012**, *10* (4), 328-43.
123. Danielyan, K. E.; Simonyan, A. A., Protective abilities of pyridoxine in experimental oxidative stress settings in vivo and in vitro. *Biomed Pharmacother* **2017**, *86*, 537-540.
124. Goyal, M.; Fequiere, P. R.; McGrath, T. M.; Hyland, K., Seizures with decreased levels of pyridoxal phosphate in cerebrospinal fluid. *Pediatric neurology* **2013**, *48* (3), 227-31.
125. Baxter, P., Pyridoxine or pyridoxal phosphate for intractable seizures? *Arch Dis Child* **2005**, *90* (5), 441-2.
126. Green, A.; Pollitt, R. J., Population newborn screening for inherited metabolic disease: current UK perspectives. *J Inherit Metab Dis* **1999**, *22* (4), 572-9.
127. Recent Advances in the Clinical Application of Mass Spectrometry. *EJIFCC* **2016**, *27* (4), 264-271.
128. Mak, C. M.; Lee, H. C.; Chan, A. Y.; Lam, C. W., Inborn errors of metabolism and expanded newborn screening: review and update. *Crit Rev Clin Lab Sci* **2013**, *50* (6), 142-62.
129. Stone, J. A.; Fitzgerald, R. L., Liquid Chromatography-Mass Spectrometry Education for Clinical Laboratory Scientists. *Clin Lab Med* **2018**, *38* (3), 527-537.
130. Pitt, J. J., Principles and applications of liquid chromatography-mass spectrometry in clinical biochemistry. *Clin Biochem Rev* **2009**, *30* (1), 19-34.
131. Mittal, R. D., Tandem mass spectroscopy in diagnosis and clinical research. *Indian J Clin Biochem* **2015**, *30* (2), 121-3.
132. Swartz, M. E., UPLC™: An Introduction and Review. *Journal of Liquid Chromatography & Related Technologies* **2005**, *28* (7-8), 1253-1263.
133. Novakova, L.; Matysova, L.; Solich, P., Advantages of application of UPLC in pharmaceutical analysis. *Talanta* **2006**, *68* (3), 908-18.

134. De Nicolo, A.; Cantu, M.; D'Avolio, A., Matrix effect management in liquid chromatography mass spectrometry: the internal standard normalized matrix effect. *Bioanalysis* **2017**, *9* (14), 1093-1105.
135. Furey, A.; Moriarty, M.; Bane, V.; Kinsella, B.; Lehane, M., Ion suppression; a critical review on causes, evaluation, prevention and applications. *Talanta* **2013**, *115*, 104-22.
136. Chace, D. H.; Millington, D. S.; Terada, N.; Kahler, S. G.; Roe, C. R.; Hofman, L. F., Rapid diagnosis of phenylketonuria by quantitative analysis for phenylalanine and tyrosine in neonatal blood spots by tandem mass spectrometry. *Clin Chem* **1993**, *39* (1), 66-71.
137. Sowell, J.; Pollard, L.; Wood, T., Quantification of branched-chain amino acids in blood spots and plasma by liquid chromatography tandem mass spectrometry for the diagnosis of maple syrup urine disease. *J Sep Sci* **2011**, *34* (6), 631-9.
138. Venditti, L. N.; Venditti, C. P.; Berry, G. T.; Kaplan, P. B.; Kaye, E. M.; Glick, H.; Stanley, C. A., Newborn screening by tandem mass spectrometry for medium-chain Acyl-CoA dehydrogenase deficiency: a cost-effectiveness analysis. *Pediatrics* **2003**, *112* (5), 1005-15.
139. Ensenuer, R.; Fingerhut, R.; Maier, E. M.; Polanetz, R.; Olgemoller, B.; Roschinger, W.; Muntau, A. C., Newborn screening for isovaleric acidemia using tandem mass spectrometry: data from 1.6 million newborns. *Clin Chem* **2011**, *57* (4), 623-6.
140. Auray-Blais, C.; Lavoie, P.; Tomatsu, S.; Valayannopoulos, V.; Mitchell, J. J.; Raiman, J.; Beaudoin, M.; Maranda, B.; Clarke, J. T., UPLC-MS/MS detection of disaccharides derived from glycosaminoglycans as biomarkers of mucopolysaccharidoses. *Anal Chim Acta* **2016**, *936*, 139-48.
141. Orsini, J. J.; Martin, M. M.; Showers, A. L.; Bodamer, O. A.; Zhang, X. K.; Gelb, M. H.; Caggana, M., Lysosomal storage disorder 4+1 multiplex assay for newborn screening using tandem mass spectrometry: application to a small-scale population study for five lysosomal storage disorders. *Clin Chim Acta* **2012**, *413* (15-16), 1270-3.
142. Legnini, E.; Orsini, J. J.; Muhl, A.; Johnson, B.; Dajnoki, A.; Bodamer, O. A., Analysis of acid sphingomyelinase activity in dried blood spots using tandem mass spectrometry. *Ann Lab Med* **2012**, *32* (5), 319-23.
143. Mazzacuva, F.; Mills, P.; Mills, K.; Camuzeaux, S.; Gissen, P.; Nicoli, E. R.; Wassif, C.; Te Vruchte, D.; Porter, F. D.; Maekawa, M.; Mano, N.; Iida, T.; Platt, F.; Clayton, P. T., Identification of novel bile acids as biomarkers for the early diagnosis of Niemann-Pick C disease. *FEBS Lett* **2016**, *590* (11), 1651-62.
144. Prinsen, H.; Schiebergen-Bronkhorst, B. G. M.; Roeleveld, M. W.; Jans, J. J. M.; de Sain-van der Velden, M. G. M.; Visser, G.; van Hasselt, P. M.; Verhoeven-Duif, N. M., Rapid quantification of underivatized amino acids in plasma by hydrophilic interaction liquid chromatography (HILIC) coupled with tandem mass-spectrometry. *J Inherit Metab Dis* **2016**, *39* (5), 651-660.

145. Wagner, M.; Tonoli, D.; Varesio, E.; Hopfgartner, G., The use of mass spectrometry to analyze dried blood spots. *Mass Spectrom Rev* **2016**, *35* (3), 361-438.
146. Golbahar, J.; Altayab, D. D.; Carreon, E., Short-term stability of amino acids and acylcarnitines in the dried blood spots used to screen newborns for metabolic disorders. *J Med Screen* **2014**, *21* (1), 5-9.
147. Zimmerman, R. K.; Slater, M. E.; Langer, E. K.; Ross, J. A.; Spector, L. G., Long-term stability of folate in dried blood spots stored in several conditions. *J Pediatr* **2013**, *163* (2), 596-597 e1.
148. Cowans, N. J.; Stamatopoulou, A.; Liitti, P.; Suonpaa, M.; Spencer, K., The stability of free-beta human chorionic gonadotrophin and pregnancy-associated plasma protein-A in first trimester dried blood spots. *Prenat Diagn* **2011**, *31* (3), 293-8.
149. Guthrie, R.; Susi, A., A Simple Phenylalanine Method for Detecting Phenylketonuria in Large Populations of Newborn Infants. *Pediatrics* **1963**, *32*, 338-43.
150. Zhang, X. K.; Elbin, C. S.; Chuang, W. L.; Cooper, S. K.; Marashio, C. A.; Beauregard, C.; Keutzer, J. M., Multiplex enzyme assay screening of dried blood spots for lysosomal storage disorders by using tandem mass spectrometry. *Clin Chem* **2008**, *54* (10), 1725-8.
151. Zhang, X. K.; Elbin, C. S.; Turecek, F.; Scott, R.; Chuang, W. L.; Keutzer, J. M.; Gelb, M., Multiplex lysosomal enzyme activity assay on dried blood spots using tandem mass spectrometry. *Methods Mol Biol* **2010**, *603*, 339-50.
152. Reuser, A. J.; Verheijen, F. W.; Bali, D.; van Diggelen, O. P.; Germain, D. P.; Hwu, W. L.; Lukacs, Z.; Muhl, A.; Olivova, P.; Piraud, M.; Wuyts, B.; Zhang, K.; Keutzer, J., The use of dried blood spot samples in the diagnosis of lysosomal storage disorders--current status and perspectives. *Molecular genetics and metabolism* **2011**, *104* (1-2), 144-8.
153. Tortorelli, S.; Turgeon, C. T.; Gavrilov, D. K.; Oglesbee, D.; Raymond, K. M.; Rinaldo, P.; Matern, D., Simultaneous Testing for 6 Lysosomal Storage Disorders and X-Adrenoleukodystrophy in Dried Blood Spots by Tandem Mass Spectrometry. *Clin Chem* **2016**, *62* (9), 1248-54.
154. Verma, J.; Thomas, D. C.; Kasper, D. C.; Sharma, S.; Puri, R. D.; Bijarnia-Mahay, S.; Mistry, P. K.; Verma, I. C., Inherited Metabolic Disorders: Efficacy of Enzyme Assays on Dried Blood Spots for the Diagnosis of Lysosomal Storage Disorders. *JIMD Rep* **2017**, *31*, 15-27.
155. Hall, E. M.; Flores, S. R.; De Jesus, V. R., Influence of Hematocrit and Total-Spot Volume on Performance Characteristics of Dried Blood Spots for Newborn Screening. *Int J Neonatal Screen* **2015**, *1* (2), 69-78.
156. Selyanko, A. A.; Hadley, J. K.; Brown, D. A., Properties of single M-type KCNQ2/KCNQ3 potassium channels expressed in mammalian cells. *J Physiol* **2001**, *534* (Pt 1), 15-24.

157. Bok, L. A.; Maurits, N. M.; Willemsen, M. A.; Jakobs, C.; Teune, L. K.; Poll-The, B. T.; de Coo, I. F.; Toet, M. C.; Hagebeuk, E. E.; Brouwer, O. F.; van der Hoeven, J. H.; Sival, D. A., The EEG response to pyridoxine-IV neither identifies nor excludes pyridoxine-dependent epilepsy. *Epilepsia* **2010**, *51* (12), 2406-11.
158. O'Mara, M.; Hudson-Curtis, B.; Olson, K.; Yueh, Y.; Dunn, J.; Spooner, N., The effect of hematocrit and punch location on assay bias during quantitative bioanalysis of dried blood spot samples. *Bioanalysis* **2011**, *3* (20), 2335-47.
159. Midttun, O.; Hustad, S.; Solheim, E.; Schneede, J.; Ueland, P. M., Multianalyte quantification of vitamin B6 and B2 species in the nanomolar range in human plasma by liquid chromatography-tandem mass spectrometry. *Clin Chem* **2005**, *51* (7), 1206-16.
160. Sakurai, T.; Asakura, T.; Matsuda, M., Transport and metabolism of pyridoxine and pyridoxal in mice. *J Nutr Sci Vitaminol (Tokyo)* **1987**, *33* (1), 11-9.
161. Bode, W.; van den Berg, H., Pyridoxal-5'-phosphate and pyridoxal biokinetics in aging Wistar rats. *Exp Gerontol* **1991**, *26* (6), 589-99.
162. Schenker, S.; Johnson, R. F.; Mahuren, J. D.; Henderson, G. I.; Coburn, S. P., Human placental vitamin B6 (pyridoxal) transport: normal characteristics and effects of ethanol. *Am J Physiol* **1992**, *262* (6 Pt 2), R966-74.
163. Ooylan, L. M.; Hart, S.; Porter, K. B.; Driskell, J. A., Vitamin B-6 content of breast milk and neonatal behavioral functioning. *J Am Diet Assoc* **2002**, *102* (10), 1433-8.
164. Gritz, E. C.; Bhandari, V., The human neonatal gut microbiome: a brief review. *Front Pediatr* **2015**, *3*, 17.
165. Guirard, B. M.; Snell, E. E., Physical and kinetic properties of a pyridoxal reductase purified from bakers' yeast. *Biofactors* **1988**, *1* (2), 187-92.
166. Herrero, S.; Gonzalez, E.; Gillikin, J. W.; Velez, H.; Daub, M. E., Identification and characterization of a pyridoxal reductase involved in the vitamin B6 salvage pathway in Arabidopsis. *Plant Mol Biol* **2011**, *76* (1-2), 157-69.
167. Nakano, M.; Morita, T.; Yamamoto, T.; Sano, H.; Ashiuchi, M.; Masui, R.; Kuramitsu, S.; Yagi, T., Purification, molecular cloning, and catalytic activity of *Schizosaccharomyces pombe* pyridoxal reductase. A possible additional family in the aldo-keto reductase superfamily. *J Biol Chem* **1999**, *274* (33), 23185-90.
168. McCormack, K.; Connor, J. X.; Zhou, L.; Ho, L. L.; Ganetzky, B.; Chiu, S. Y.; Messing, A., Genetic analysis of the mammalian K⁺ channel beta subunit Kvbeta 2 (Kcnab2). *J Biol Chem* **2002**, *277* (15), 13219-28.
169. McCormack, K.; McCormack, T.; Tanouye, M.; Rudy, B.; Stuhmer, W., Alternative splicing of the human Shaker K⁺ channel beta 1 gene and functional expression of the beta 2 gene product. *FEBS Lett* **1995**, *370* (1-2), 32-6.
170. Clements, J. E.; Anderson, B. B., Pyridoxine (pyridoxamine) phosphate oxidase activity in the red cell. *Biochim Biophys Acta* **1980**, *613* (2), 401-9.

171. DePecol, M. E.; McCormick, D. B., Syntheses, properties, and use of fluorescent N-(5'-phospho-4'-pyridoxyl)amines in assay of pyridoxamine (pyridoxine) 5'-phosphate oxidase. *Anal Biochem* **1980**, *101* (2), 435-41.
172. Bates, C. J.; Powers, H. J., A simple fluorimetric assay for pyridoxamine phosphate oxidase in erythrocyte haemolysates: effects of riboflavin supplementation and of glucose 6-phosphate dehydrogenase deficiency. *Hum Nutr Clin Nutr* **1985**, *39* (2), 107-15.
173. Merrill, A. H., Jr.; Wang, E., Highly sensitive methods for assaying the enzymes of vitamin B6 metabolism. *Methods Enzymol* **1986**, *122*, 110-6.
174. Ubbink, J. B.; Schnell, A. M., High-performance liquid chromatographic assay of erythrocyte enzyme activity levels involved in vitamin B6 metabolism. *J Chromatogr* **1988**, *431* (2), 406-12.
175. Ombrone, D.; Giocaliere, E.; Forni, G.; Malvagia, S.; la Marca, G., Expanded newborn screening by mass spectrometry: New tests, future perspectives. *Mass Spectrom Rev* **2016**, *35* (1), 71-84.
176. Musayev, F. N.; di Salvo, M. L.; Ko, T. P.; Gandhi, A. K.; Goswami, A.; Schirch, V.; Safo, M. K., Crystal Structure of human pyridoxal kinase: structural basis of M(+) and M(2+) activation. *Protein Sci* **2007**, *16* (10), 2184-94.
177. Fonda, M. L., Pyridoxamine (pyridoxine) phosphate oxidase activity in mammalian tissues. *Comp Biochem Physiol B* **1988**, *90* (4), 731-7.
178. Hamfelt, A., Pyridoxal kinase activity in blood cells. *Clin Chim Acta* **1967**, *16* (1), 7-18.
179. Reed, G. F.; Lynn, F.; Meade, B. D., Use of coefficient of variation in assessing variability of quantitative assays. *Clin Diagn Lab Immunol* **2002**, *9* (6), 1235-9.
180. Mitra, J.; Metzler, D. E., Schiff bases of pyridoxal 5'-phosphate with Tris and glycine. *Biochimica et Biophysica Acta (BBA) - General Subjects* **1988**, *965* (1), 93-96.
181. Fernley, H. N.; Walker, P. G., Studies on alkaline phosphatase. Inhibition by phosphate derivatives and the substrate specificity. *Biochem J* **1967**, *104* (3), 1011-8.
182. Martin, S. K.; Miller, L. H.; Kark, J. A.; Hicks, C. U.; Haut, M. J.; Okoye, V. C.; Esan, G. J., Low erythrocyte pyridoxal-kinase activity in Blacks: Its possible relation to falciparum malaria. *Lancet* **1978**, *1* (8062), 466-8.
183. Fonda, M. L.; Trauss, C.; Guempel, U. M., The binding of pyridoxal 5'-phosphate to human serum albumin. *Archives of biochemistry and biophysics* **1991**, *288* (1), 79-86.
184. Zhao, G.; Winkler, M. E., Kinetic limitation and cellular amount of pyridoxine (pyridoxamine) 5'-phosphate oxidase of Escherichia coli K-12. *J Bacteriol* **1995**, *177* (4), 883-91.

185. Choi, J. D.; Bowers-Komro, M.; Davis, M. D.; Edmondson, D. E.; McCormick, D. B., Kinetic properties of pyridoxamine (pyridoxine)-5'-phosphate oxidase from rabbit liver. *J Biol Chem* **1983**, *258* (2), 840-5.
186. Adam, B. W.; Flores, S. R.; Hou, Y.; Allen, T. W.; De Jesus, V. R., Galactose-1-phosphate uridylyltransferase dried blood spot quality control materials for newborn screening tests. *Clin Biochem* **2015**, *48* (6), 437-42.
187. Erandi, H.; Ge, L.; W., J. D.; A., G. R.; S., M. B., Estimation of the Volume of Blood in a Small Disc Punched From a Dried Blood Spot Card. *European Journal of Lipid Science and Technology* **2018**, *120* (3), 1700362.
188. Kadjo, A. F.; Stamos, B. N.; Shelor, C. P.; Berg, J. M.; Blount, B. C.; Dasgupta, P. K., Evaluation of Amount of Blood in Dry Blood Spots: Ring-Disk Electrode Conductometry. *Anal Chem* **2016**, *88* (12), 6531-7.
189. Denniff, P.; Spooner, N., The effect of hematocrit on assay bias when using DBS samples for the quantitative bioanalysis of drugs. *Bioanalysis* **2010**, *2* (8), 1385-95.
190. Li, Y.; Scott, C. R.; Chamoles, N. A.; Ghavami, A.; Pinto, B. M.; Turecek, F.; Gelb, M. H., Direct multiplex assay of lysosomal enzymes in dried blood spots for newborn screening. *Clin Chem* **2004**, *50* (10), 1785-96.
191. Andersen, H. R.; Nielsen, J. B.; Nielsen, F.; Grandjean, P., Antioxidative enzyme activities in human erythrocytes. *Clin Chem* **1997**, *43* (4), 562-8.
192. Cooper, S. C.; Ford, L. T.; Berg, J. D.; Lewis, M. J., Ethnic variation of thiopurine S-methyltransferase activity: a large, prospective population study. *Pharmacogenomics* **2008**, *9* (3), 303-9.
193. Zander, R.; Lang, W.; Wolf, H. U., Alkaline haematin D-575, a new tool for the determination of haemoglobin as an alternative to the cyanhaemoglobin method. I. Description of the method. *Clin Chim Acta* **1984**, *136* (1), 83-93.
194. Desmet, F. O.; Hamroun, D.; Lalande, M.; Collod-Beroud, G.; Claustres, M.; Beroud, C., Human Splicing Finder: an online bioinformatics tool to predict splicing signals. *Nucleic Acids Res* **2009**, *37* (9), e67.
195. Yeo, G.; Holste, D.; Kreiman, G.; Burge, C. B., Variation in alternative splicing across human tissues. *Genome Biol* **2004**, *5* (10), R74.
196. MacLean, B.; Tomazela, D. M.; Shulman, N.; Chambers, M.; Finney, G. L.; Frewen, B.; Kern, R.; Tabb, D. L.; Liebler, D. C.; MacCoss, M. J., Skyline: an open source document editor for creating and analyzing targeted proteomics experiments. *Bioinformatics* **2010**, *26* (7), 966-8.
197. Lear, S.; Cobb, S. L., Pep-Calc.com: a set of web utilities for the calculation of peptide and peptoid properties and automatic mass spectral peak assignment. *J Comput Aided Mol Des* **2016**, *30* (3), 271-7.

198. Anderson, N. L.; Anderson, N. G., The human plasma proteome: history, character, and diagnostic prospects. *Mol Cell Proteomics* **2002**, *1* (11), 845-67.
199. Garcia, M. C., The effect of the mobile phase additives on sensitivity in the analysis of peptides and proteins by high-performance liquid chromatography-electrospray mass spectrometry. *J Chromatogr B Analyt Technol Biomed Life Sci* **2005**, *825* (2), 111-23.
200. Burkhardt, J. M.; Schumbrutzki, C.; Wortelkamp, S.; Sickmann, A.; Zahedi, R. P., Systematic and quantitative comparison of digest efficiency and specificity reveals the impact of trypsin quality on MS-based proteomics. *J Proteomics* **2012**, *75* (4), 1454-62.
201. Harlan, R.; Zhang, H., Targeted proteomics: a bridge between discovery and validation. *Expert Rev Proteomics* **2014**, *11* (6), 657-61.
202. O'Farrell, P. H., High resolution two-dimensional electrophoresis of proteins. *J Biol Chem* **1975**, *250* (10), 4007-21.
203. Braathen, G. J.; Sand, J. C.; Lobato, A.; Hoyer, H.; Russell, M. B., Genetic epidemiology of Charcot-Marie-Tooth in the general population. *Eur J Neurol* **2011**, *18* (1), 39-48.
204. d'Ydewalle, C.; Benoy, V.; Van Den Bosch, L., Charcot-Marie-Tooth disease: emerging mechanisms and therapies. *Int J Biochem Cell Biol* **2012**, *44* (8), 1299-304.
205. Gess, B.; Baets, J.; De Jonghe, P.; Reilly, M. M.; Pareyson, D.; Young, P., Ascorbic acid for the treatment of Charcot-Marie-Tooth disease. *Cochrane Database Syst Rev* **2015**, (12), CD011952.
206. Murphy, S. M.; Laura, M.; Fawcett, K.; Pandraud, A.; Liu, Y. T.; Davidson, G. L.; Rossor, A. M.; Polke, J. M.; Castleman, V.; Manji, H.; Lunn, M. P.; Bull, K.; Ramdharry, G.; Davis, M.; Blake, J. C.; Houlden, H.; Reilly, M. M., Charcot-Marie-Tooth disease: frequency of genetic subtypes and guidelines for genetic testing. *J Neurol Neurosurg Psychiatry* **2012**, *83* (7), 706-10.
207. Zuchner, S.; Vance, J. M., Mechanisms of disease: a molecular genetic update on hereditary axonal neuropathies. *Nat Clin Pract Neurol* **2006**, *2* (1), 45-53.
208. Chalmers, R. M.; Riordan-Eva, P.; Wood, N. W., Autosomal recessive inheritance of hereditary motor and sensory neuropathy with optic atrophy. *J Neurol Neurosurg Psychiatry* **1997**, *62* (4), 385-7.
209. Coburn, S. P., Vitamin B-6 Metabolism and Interactions with TNAP. *Subcell Biochem* **2015**, *76*, 207-38.
210. Wang, P.; Pradhan, K.; Zhong, X. B.; Ma, X., Isoniazid metabolism and hepatotoxicity. *Acta Pharm Sin B* **2016**, *6* (5), 384-392.
211. Kastner, U.; Hallmen, C.; Wiese, M.; Leistner, E.; Drewke, C., The human pyridoxal kinase, a plausible target for ginkgotoxin from *Ginkgo biloba*. *FEBS J* **2007**, *274* (4), 1036-45.
212. Hughes, R., Investigation of peripheral neuropathy. *BMJ* **2010**, *341*, c6100.

213. Ubbink, J. B.; Delport, R.; Bissbort, S.; Vermaak, W. J.; Becker, P. J., Relationship between vitamin B-6 status and elevated pyridoxal kinase levels induced by theophylline therapy in humans. *J Nutr* **1990**, *120* (11), 1352-9.
214. Gandhi, A. K.; Desai, J. V.; Ghatge, M. S.; di Salvo, M. L.; Di Biase, S.; Danso-Danquah, R.; Musayev, F. N.; Contestabile, R.; Schirch, V.; Safo, M. K., Crystal structures of human pyridoxal kinase in complex with the neurotoxins, ginkgotoxin and theophylline: insights into pyridoxal kinase inhibition. *PLoS One* **2012**, *7* (7), e40954.
215. di Salvo, M. L.; Hunt, S.; Schirch, V., Expression, purification, and kinetic constants for human and Escherichia coli pyridoxal kinases. *Protein Expr Purif* **2004**, *36* (2), 300-6.
216. Mildvan, A. S., Role of magnesium and other divalent cations in ATP-utilizing enzymes. *Magnesium* **1987**, *6* (1), 28-33.
217. Wang, Z.; Cole, P. A., Catalytic mechanisms and regulation of protein kinases. *Methods Enzymol* **2014**, *548*, 1-21.
218. Jones, D. C.; Alpey, M. S.; Wyllie, S.; Fairlamb, A. H., Chemical, genetic and structural assessment of pyridoxal kinase as a drug target in the African trypanosome. *Mol Microbiol* **2012**, *86* (1), 51-64.
219. Safo, M. K.; Musayev, F. N.; di Salvo, M. L.; Hunt, S.; Claude, J. B.; Schirch, V., Crystal structure of pyridoxal kinase from the Escherichia coli pdxK gene: implications for the classification of pyridoxal kinases. *J Bacteriol* **2006**, *188* (12), 4542-52.
220. Yoshida, T.; Kakizuka, A.; Imamura, H., BTeam, a Novel BRET-based Biosensor for the Accurate Quantification of ATP Concentration within Living Cells. *Sci Rep* **2016**, *6*, 39618.
221. Chern, C. J.; Beutler, E., Pyridoxal kinase: decreased activity in red blood cells of Afro-Americans. *Science* **1975**, *187* (4181), 1084-6.
222. Kark, J. A.; Haut, M. J.; Hicks, C. U.; McQuilkin, C. T.; Reynolds, R. D., A rapid fluorometric assay for erythrocyte pyridoxal kinase. *Biochem Med* **1982**, *27* (1), 109-20.
223. Contractor, S. F.; Shane, B., Pyridoxal kinase in the human placenta and foetus through gestation. *Clin Chim Acta* **1969**, *25* (3), 465-74.
224. Murphy, W. G., The sex difference in haemoglobin levels in adults - mechanisms, causes, and consequences. *Blood Rev* **2014**, *28* (2), 41-7.
225. Baumforth, K. R.; Nelson, P. N.; Digby, J. E.; O'Neil, J. D.; Murray, P. G., Demystified ... the polymerase chain reaction. *Mol Pathol* **1999**, *52* (1), 1-10.
226. Pomp, D.; Medrano, J. F., Organic solvents as facilitators of polymerase chain reaction. *Biotechniques* **1991**, *10* (1), 58-9.
227. Musso, M.; Bocciardi, R.; Parodi, S.; Ravazzolo, R.; Ceccherini, I., Betaine, dimethyl sulfoxide, and 7-deaza-dGTP, a powerful mixture for amplification of GC-rich DNA sequences. *J Mol Diagn* **2006**, *8* (5), 544-50.

228. Chakrabarti, R.; Schutt, C. E., The enhancement of PCR amplification by low molecular-weight sulfones. *Gene* **2001**, *274* (1-2), 293-8.
229. M'Angale, P. G.; Staveley, B. E., A loss of Pdxk model of Parkinson disease in *Drosophila* can be suppressed by Buffy. *BMC Res Notes* **2017**, *10* (1), 205.
230. Elstner, M.; Morris, C. M.; Heim, K.; Lichtner, P.; Bender, A.; Mehta, D.; Schulte, C.; Sharma, M.; Hudson, G.; Goldwurm, S.; Giovanetti, A.; Zeviani, M.; Burn, D. J.; McKeith, I. G.; Perry, R. H.; Jaros, E.; Kruger, R.; Wichmann, H. E.; Schreiber, S.; Campbell, H.; Wilson, J. F.; Wright, A. F.; Dunlop, M.; Pistis, G.; Toniolo, D.; Chinnery, P. F.; Gasser, T.; Klopstock, T.; Meitinger, T.; Prokisch, H.; Turnbull, D. M., Single-cell expression profiling of dopaminergic neurons combined with association analysis identifies pyridoxal kinase as Parkinson's disease gene. *Ann Neurol* **2009**, *66* (6), 792-8.
231. Meisler, N. T.; Thanassi, J. W., Pyridoxine kinase, pyridoxine phosphate phosphatase and pyridoxine phosphate oxidase activities in control and B-6-deficient rat liver and brain. *J Nutr* **1980**, *110* (10), 1965-75.
232. Gospe, S. M., Jr., Pyridoxine-Dependent Epilepsy. In *GeneReviews((R))*, Adam, M. P.; Ardinger, H. H.; Pagon, R. A.; Wallace, S. E.; Bean, L. J. H.; Stephens, K.; Amemiya, A., Eds. Seattle (WA), 1993.
233. Siren, A.; Polvi, A.; Chahine, L.; Labuda, M.; Bourgoin, S.; Anttonen, A. K.; Kousi, M.; Hirvonen, K.; Simola, K. O.; Andermann, E.; Laiho, A.; Soini, J.; Koivikko, M.; Laaksonen, R.; Pandolfo, M.; Lehesjoki, A. E., Suggestive evidence for a new locus for epilepsy with heterogeneous phenotypes on chromosome 17q. *Epilepsy Res* **2010**, *88* (1), 65-75.
234. Viader, A.; Golden, J. P.; Baloh, R. H.; Schmidt, R. E.; Hunter, D. A.; Milbrandt, J., Schwann cell mitochondrial metabolism supports long-term axonal survival and peripheral nerve function. *J Neurosci* **2011**, *31* (28), 10128-40.
235. Muller, I. B.; Wu, F.; Bergmann, B.; Knockel, J.; Walter, R. D.; Gehring, H.; Wrenger, C., Poisoning pyridoxal 5-phosphate-dependent enzymes: a new strategy to target the malaria parasite *Plasmodium falciparum*. *PLoS One* **2009**, *4* (2), e4406.
236. Kent, W. J.; Sugnet, C. W.; Furey, T. S.; Roskin, K. M.; Pringle, T. H.; Zahler, A. M.; Haussler, D., The human genome browser at UCSC. *Genome Res* **2002**, *12* (6), 996-1006.
237. Suvorova, I. A.; Rodionov, D. A., Comparative genomics of pyridoxal 5'-phosphate-dependent transcription factor regulons in Bacteria. *Microb Genom* **2016**, *2* (1), e000047.
238. Tramonti, A.; Nardella, C.; di Salvo, M. L.; Pascarella, S.; Contestabile, R., The MocR-like transcription factors: pyridoxal 5'-phosphate-dependent regulators of bacterial metabolism. *FEBS J* **2018**.
239. In *Dietary Reference Intakes for Thiamin, Riboflavin, Niacin, Vitamin B6, Folate, Vitamin B12, Pantothenic Acid, Biotin, and Choline*, Washington (DC), 1998.

240. Hunt, A. D., Jr.; Stokes, J., Jr.; Mc, C. W.; Stroud, H. H., Pyridoxine dependency: report of a case of intractable convulsions in an infant controlled by pyridoxine. *Pediatrics* **1954**, *13* (2), 140-5.
241. Coughlin, C. R., 2nd; Swanson, M. A.; Spector, E.; Meeks, N. J. L.; Kronquist, K. E.; Aslamy, M.; Wempe, M. F.; van Karnebeek, C. D. M.; Gospe, S. M., Jr.; Aziz, V. G.; Tsai, B. P.; Gao, H.; Nagy, P. L.; Hyland, K.; van Dooren, S. J. M.; Salomons, G. S.; Van Hove, J. L. K., The genotypic spectrum of ALDH7A1 mutations resulting in pyridoxine dependent epilepsy: a common epileptic encephalopathy. *J Inherit Metab Dis* **2018**.
242. Yoshida, I.; Sakaguchi, Y.; Nakano, M.; Yamashita, F.; Hitoshi, T., Pyridoxal phosphate-induced liver injury in a patient with homocystinuria. *J Inherit Metab Dis* **1985**, *8* (2), 91.
243. Takuma, Y.; Seki, T., Combination therapy of infantile spasms with high-dose pyridoxal phosphate and low-dose corticotropin. *J Child Neurol* **1996**, *11* (1), 35-40.
244. Morrison, A. L.; Long, R. F., The photolysis of pyridoxal phosphate. *Journal of the Chemical Society (Resumed)* **1958**, (0), 211-215.
245. Pantou, K. K.; Farup, P. G.; Sagen, E.; Sirum, U. F.; Asberg, A., Vitamin B6 in plasma - sample stability and the reference limits. *Scand J Clin Lab Invest* **2013**, *73* (6), 476-9.
246. Coman, D.; Lewindon, P.; Clayton, P.; Riney, K., PNPO Deficiency and Cirrhosis: Expanding the Clinical Phenotype? *JIMD Rep* **2015**.
247. Jacobson, K. A.; Costanzi, S.; Joshi, B. V.; Besada, P.; Shin, D. H.; Ko, H.; Ivanov, A. A.; Mamedova, L., Agonists and antagonists for P2 receptors. *Novartis Found Symp* **2006**, *276*, 58-68; discussion 68-72, 107-12, 275-81.
248. Santini, A.; Cammarata, S. M.; Capone, G.; Ianaro, A.; Tenore, G. C.; Pani, L.; Novellino, E., Nutraceuticals: opening the debate for a regulatory framework. *Br J Clin Pharmacol* **2018**, *84* (4), 659-672.
249. McLafferty, F. W.; Gohike, R. S., Mass Spectrometric Analysis. Aromatic Acids and Esters. *Analytical Chemistry* **1959**, *31* (12), 2076-2082.
250. Goodacre, R.; Shann, B.; Gilbert, R. J.; Timmins, E. M.; McGovern, A. C.; Alsberg, B. K.; Kell, D. B.; Logan, N. A., Detection of the dipicolinic acid biomarker in *Bacillus* spores using Curie-point pyrolysis mass spectrometry and Fourier transform infrared spectroscopy. *Anal Chem* **2000**, *72* (1), 119-27.
251. Churchich, J. E., Fluorescence changes induced by binding of 4-pyridoxic acid 5 - phosphate to proteins. *J Biol Chem* **1972**, *247* (21), 6953-9.
252. Gao, G. J.; Fonda, M. L., Kinetic analysis and chemical modification of vitamin B6 phosphatase from human erythrocytes. *J Biol Chem* **1994**, *269* (10), 7163-8.
253. Fouad Mansour, M.; Assefa, M.; El-Khouly, A.; Zhu, P.; Van Schepdael, A.; Adams, E., Development of a reversed phase liquid chromatographic method for analysis of pyridoxal-5'-phosphate and its impurities. *Electrophoresis* **2018**, *39* (20), 2540-2549.

254. Ito, M.; Seki, T.; Takuma, Y., Current therapy for West syndrome in Japan. *J Child Neurol* **2000**, *15* (6), 424-8.
255. Dunn, P.; Albury, C. L.; Maksemous, N.; Benton, M. C.; Sutherland, H. G.; Smith, R. A.; Haupt, L. M.; Griffiths, L. R., Next Generation Sequencing Methods for Diagnosis of Epilepsy Syndromes. *Front Genet* **2018**, *9*, 20.
256. Mefford, H. C., Clinical Genetic Testing in Epilepsy. *Epilepsy Curr* **2015**, *15* (4), 197-201.
257. Ostrander, B. E. P.; Butterfield, R. J.; Pedersen, B. S.; Farrell, A. J.; Layer, R. M.; Ward, A.; Miller, C.; DiSera, T.; Filloux, F. M.; Candee, M. S.; Newcomb, T.; Bonkowsky, J. L.; Marth, G. T.; Quinlan, A. R., Whole-genome analysis for effective clinical diagnosis and gene discovery in early infantile epileptic encephalopathy. *npj Genomic Medicine* **2018**, *3* (1), 22.
258. Soden, S. E.; Saunders, C. J.; Willig, L. K.; Farrow, E. G.; Smith, L. D.; Petrikin, J. E.; LePichon, J. B.; Miller, N. A.; Thiffault, I.; Dinwiddie, D. L.; Twist, G.; Noll, A.; Heese, B. A.; Zellmer, L.; Atherton, A. M.; Abdelmoity, A. T.; Safina, N.; Nyp, S. S.; Zuccarelli, B.; Larson, I. A.; Modrcin, A.; Herd, S.; Creed, M.; Ye, Z.; Yuan, X.; Brodsky, R. A.; Kingsmore, S. F., Effectiveness of exome and genome sequencing guided by acuity of illness for diagnosis of neurodevelopmental disorders. *Sci Transl Med* **2014**, *6* (265), 265ra168.
259. Yubero, D.; Brandi, N.; Ormazabal, A.; Garcia-Cazorla, A.; Perez-Duenas, B.; Campistol, J.; Ribes, A.; Palau, F.; Artuch, R.; Armstrong, J.; Working, G., Targeted Next Generation Sequencing in Patients with Inborn Errors of Metabolism. *PLoS One* **2016**, *11* (5), e0156359.
260. Jaeger, B.; Abeling, N. G.; Salomons, G. S.; Struys, E. A.; Simas-Mendes, M.; Geukers, V. G.; Poll-The, B. T., Pyridoxine responsive epilepsy caused by a novel homozygous PNPO mutation. *Molecular genetics and metabolism reports* **2016**, *6*, 60-3.
261. Du, X.; Chen, Y.; Zhao, Y.; Luo, W.; Cen, Z.; Hao, W., Dramatic response to pyridoxine in a girl with absence epilepsy with ataxia caused by a de novo CACNA1A mutation. *Seizure* **2017**, *45*, 189-191.
262. Spacey, S., Episodic Ataxia Type 2. In *GeneReviews((R))*, Adam, M. P.; Ardinger, H. H.; Pagon, R. A.; Wallace, S. E.; Bean, L. J. H.; Stephens, K.; Amemiya, A., Eds. Seattle (WA), 1993.
263. Sreedharan, S.; Stephansson, O.; Schioth, H. B.; Fredriksson, R., Long evolutionary conservation and considerable tissue specificity of several atypical solute carrier transporters. *Gene* **2011**, *478* (1-2), 11-8.
264. Takenouchi, T.; Hashida, N.; Torii, C.; Kosaki, R.; Takahashi, T.; Kosaki, K., 1p34.3 deletion involving GRIK3: Further clinical implication of GRIK family glutamate receptors in the pathogenesis of developmental delay. *Am J Med Genet A* **2014**, *164A* (2), 456-60.
265. Sakata, K.; Yamashita, T.; Maeda, M.; Moriyama, Y.; Shimada, S.; Tohyama, M., Cloning of a lymphatic peptide/histidine transporter. *Biochem J* **2001**, *356* (Pt 1), 53-60.

266. Aldini, G.; Orioli, M.; Rossoni, G.; Savi, F.; Braidotti, P.; Vistoli, G.; Yeum, K. J.; Negrisoli, G.; Carini, M., The carbonyl scavenger carnosine ameliorates dyslipidaemia and renal function in Zucker obese rats. *J Cell Mol Med* **2011**, *15* (6), 1339-54.
267. Karagiannidis, I.; Dehning, S.; Sandor, P.; Tarnok, Z.; Rizzo, R.; Wolanczyk, T.; Madruga-Garrido, M.; Hebebrand, J.; Nothen, M. M.; Lehmkuhl, G.; Farkas, L.; Nagy, P.; Szymanska, U.; Anastasiou, Z.; Stathias, V.; Androutsos, C.; Tsironi, V.; Koumoula, A.; Barta, C.; Zill, P.; Mir, P.; Muller, N.; Barr, C.; Paschou, P., Support of the histaminergic hypothesis in Tourette syndrome: association of the histamine decarboxylase gene in a large sample of families. *J Med Genet* **2013**, *50* (11), 760-4.
268. Dibbens, L. M.; Feng, H. J.; Richards, M. C.; Harkin, L. A.; Hodgson, B. L.; Scott, D.; Jenkins, M.; Petrou, S.; Sutherland, G. R.; Scheffer, I. E.; Berkovic, S. F.; Macdonald, R. L.; Mulley, J. C., GABRD encoding a protein for extra- or peri-synaptic GABAA receptors is a susceptibility locus for generalized epilepsies. *Hum Mol Genet* **2004**, *13* (13), 1315-9.
269. Wang, L.; Shao, Y. Y.; Ballock, R. T., Carboxypeptidase Z (CPZ) links thyroid hormone and Wnt signaling pathways in growth plate chondrocytes. *J Bone Miner Res* **2009**, *24* (2), 265-73.
270. Shibata, N.; Ohoka, N.; Sugaki, Y.; Onodera, C.; Inoue, M.; Sakuraba, Y.; Takakura, D.; Hashii, N.; Kawasaki, N.; Gondo, Y.; Naito, M., Degradation of Stop Codon Read-through Mutant Proteins via the Ubiquitin-Proteasome System Causes Hereditary Disorders. *J Biol Chem* **2015**, *290* (47), 28428-37.
271. Shamseldin, H. E.; Smith, L. L.; Kentab, A.; Alkhalidi, H.; Summers, B.; Alsedairy, H.; Xiong, Y.; Gupta, V. A.; Alkuraya, F. S., Mutation of the mitochondrial carrier SLC25A42 causes a novel form of mitochondrial myopathy in humans. *Hum Genet* **2016**, *135* (1), 21-30.
272. Yildiz, Y.; Pektas, E.; Tokatli, A.; Haliloglu, G., Hereditary Dopamine Transporter Deficiency Syndrome: Challenges in Diagnosis and Treatment. *Neuropediatrics* **2017**, *48* (1), 49-52.
273. Vilas, G. L.; Johnson, D. E.; Freund, P.; Casey, J. R., Characterization of an epilepsy-associated variant of the human Cl⁻/HCO₃⁻ exchanger AE3. *Am J Physiol Cell Physiol* **2009**, *297* (3), C526-36.
274. Hentschke, M.; Wiemann, M.; Hentschke, S.; Kurth, I.; Hermans-Borgmeyer, I.; Seidenbecher, T.; Jentsch, T. J.; Gal, A.; Hubner, C. A., Mice with a targeted disruption of the Cl⁻/HCO₃⁻ exchanger AE3 display a reduced seizure threshold. *Mol Cell Biol* **2006**, *26* (1), 182-91.
275. Ruffin, V. A.; Salameh, A. I.; Boron, W. F.; Parker, M. D., Intracellular pH regulation by acid-base transporters in mammalian neurons. *Front Physiol* **2014**, *5*, 43.
276. Nijboer, C. H.; Kavelaars, A.; Vroon, A.; Groenendaal, F.; van Bel, F.; Heijnen, C. J., Low endogenous G-protein-coupled receptor kinase 2 sensitizes the immature brain to hypoxia-ischemia-induced gray and white matter damage. *J Neurosci* **2008**, *28* (13), 3324-32.

277. Rockman, H. A.; Chien, K. R.; Choi, D. J.; Iaccarino, G.; Hunter, J. J.; Ross, J., Jr.; Lefkowitz, R. J.; Koch, W. J., Expression of a beta-adrenergic receptor kinase 1 inhibitor prevents the development of myocardial failure in gene-targeted mice. *Proc Natl Acad Sci U S A* **1998**, *95* (12), 7000-5.
278. Yamazawa, K.; Ogata, T.; Ferguson-Smith, A. C., Uniparental disomy and human disease: an overview. *Am J Med Genet C Semin Med Genet* **2010**, *154C* (3), 329-34.
279. Peters, J., The role of genomic imprinting in biology and disease: an expanding view. *Nat Rev Genet* **2014**, *15* (8), 517-30.
280. Disteche, C. M.; Berletch, J. B., X-chromosome inactivation and escape. *J Genet* **2015**, *94* (4), 591-9.
281. Carrel, L.; Willard, H. F., X-inactivation profile reveals extensive variability in X-linked gene expression in females. *Nature* **2005**, *434* (7031), 400-4.
282. Berletch, J. B.; Yang, F.; Xu, J.; Carrel, L.; Disteche, C. M., Genes that escape from X inactivation. *Hum Genet* **2011**, *130* (2), 237-45.
283. Dibbens, L. M.; Tarpey, P. S.; Hynes, K.; Bayly, M. A.; Scheffer, I. E.; Smith, R.; Bomar, J.; Sutton, E.; Vandeleur, L.; Shoubridge, C.; Edkins, S.; Turner, S. J.; Stevens, C.; O'Meara, S.; Tofts, C.; Barthorpe, S.; Buck, G.; Cole, J.; Halliday, K.; Jones, D.; Lee, R.; Madison, M.; Mironenko, T.; Varian, J.; West, S.; Widaa, S.; Wray, P.; Teague, J.; Dicks, E.; Butler, A.; Menzies, A.; Jenkinson, A.; Shepherd, R.; Gusella, J. F.; Afawi, Z.; Mazarib, A.; Neufeld, M. Y.; Kivity, S.; Lev, D.; Lerman-Sagie, T.; Korczyn, A. D.; Derry, C. P.; Sutherland, G. R.; Friend, K.; Shaw, M.; Corbett, M.; Kim, H. G.; Geschwind, D. H.; Thomas, P.; Haan, E.; Ryan, S.; McKee, S.; Berkovic, S. F.; Futreal, P. A.; Stratton, M. R.; Mulley, J. C.; Gecz, J., X-linked protocadherin 19 mutations cause female-limited epilepsy and cognitive impairment. *Nat Genet* **2008**, *40* (6), 776-81.
284. Depienne, C.; Bouteiller, D.; Keren, B.; Cheuret, E.; Poirier, K.; Trouillard, O.; Benyahia, B.; Quelin, C.; Carpentier, W.; Julia, S.; Afenjar, A.; Gautier, A.; Rivier, F.; Meyer, S.; Berquin, P.; Helias, M.; Py, I.; Rivera, S.; Bahi-Buisson, N.; Gourfinkel-An, I.; Cazeneuve, C.; Ruberg, M.; Brice, A.; Nabbout, R.; Leguern, E., Sporadic infantile epileptic encephalopathy caused by mutations in PCDH19 resembles Dravet syndrome but mainly affects females. *PLoS Genet* **2009**, *5* (2), e1000381.
285. Miceli, F.; Soldovieri, M. V.; Joshi, N.; Weckhuysen, S.; Cooper, E.; Taglialetela, M., KCNQ2-Related Disorders. In *GeneReviews(R)*, Pagon, R. A.; Adam, M. P.; Ardinger, H. H.; Wallace, S. E.; Amemiya, A.; Bean, L. J. H.; Bird, T. D.; Ledbetter, N.; Mefford, H. C.; Smith, R. J. H.; Stephens, K., Eds. Seattle (WA), 1993.
286. Mefford, H. C.; Cook, J.; Gospe, S. M., Jr., Epilepsy due to 20q13.33 subtelomere deletion masquerading as pyridoxine-dependent epilepsy. *Am J Med Genet A* **2012**, *158A* (12), 3190-5.
287. Hadley, J. K.; Passmore, G. M.; Tatulian, L.; Al-Qatari, M.; Ye, F.; Wickenden, A. D.; Brown, D. A., Stoichiometry of expressed KCNQ2/KCNQ3 potassium channels and subunit

composition of native ganglionic M channels deduced from block by tetraethylammonium. *J Neurosci* **2003**, 23 (12), 5012-9.

288. Schnee, M. E.; Brown, B. S., Selectivity of linopirdine (DuP 996), a neurotransmitter release enhancer, in blocking voltage-dependent and calcium-activated potassium currents in hippocampal neurons. *J Pharmacol Exp Ther* **1998**, 286 (2), 709-17.

289. Brown, D. A.; Hughes, S. A.; Marsh, S. J.; Tinker, A., Regulation of M(Kv7.2/7.3) channels in neurons by PIP(2) and products of PIP(2) hydrolysis: significance for receptor-mediated inhibition. *J Physiol* **2007**, 582 (Pt 3), 917-25.

290. Hernandez, C. C.; Falkenburger, B.; Shapiro, M. S., Affinity for phosphatidylinositol 4,5-bisphosphate determines muscarinic agonist sensitivity of Kv7 K⁺ channels. *J Gen Physiol* **2009**, 134 (5), 437-48.

291. Oppici, E.; Fargue, S.; Reid, E. S.; Mills, P. B.; Clayton, P. T.; Danpure, C. J.; Cellini, B., Pyridoxamine and pyridoxal are more effective than pyridoxine in rescuing folding-defective variants of human alanine:glyoxylate aminotransferase causing primary hyperoxaluria type I. *Hum Mol Genet* **2015**, 24 (19), 5500-11.

292. Albersen, M.; Groenendaal, F.; van der Ham, M.; de Koning, T. J.; Bosma, M.; Visser, W. F.; Visser, G.; de Sain-van der Velden, M. G.; Verhoeven-Duif, N. M., Vitamin B6 vitamer concentrations in cerebrospinal fluid differ between preterm and term newborn infants. *Pediatrics* **2012**, 130 (1), e191-8.

293. Libbrecht, M. W.; Noble, W. S., Machine learning applications in genetics and genomics. *Nat Rev Genet* **2015**, 16 (6), 321-32.

294. Karczewski, K. J.; Snyder, M. P., Integrative omics for health and disease. *Nat Rev Genet* **2018**, 19 (5), 299-310.

295. Maljevic, S.; Wuttke, T. V.; Lerche, H., Nervous system KV7 disorders: breakdown of a subthreshold brake. *J Physiol* **2008**, 586 (7), 1791-801.

296. Linley, J. E., Perforated whole-cell patch-clamp recording. *Methods Mol Biol* **2013**, 998, 149-57.

297. Michel, A. D.; Chessell, I. P.; Hibell, A. D.; Simon, J.; Humphrey, P. P., Identification and characterization of an endogenous P2X7 (P2Z) receptor in CHO-K1 cells. *Br J Pharmacol* **1998**, 125 (6), 1194-201.